

**RESEARCH ON BERG RIVER WATER
MANAGEMENT**

VOLUME 1

**APPLICATION OF HYDRODYNAMIC RIVER
FLOW AND RESERVOIR WATER QUALITY
MODELS TO THE BERG RIVER SYSTEM**

By

N Nitsche, W Kamish and AHM Görgens

Department of Civil Engineering,
University of Stellenbosch

*Final report to the Water Research Commission on the project A Water
Quality Information System for Integrated Water Resource Management:
The Riviersonderend-Berg River System*

**WRC Report No. 951/1/06
July 2006**

ISBN Set No 1-77005-366-2

ISBN 1-77005-368-9

EXECUTIVE SUMMARY

VOLUME 1

BACKGROUND

Impoundments and associated bulk water supply infrastructure are present in most South African river systems. Because of the disparate natural occurrence of rainfall and runoff, and its mismatch with water demand concentrations, many of these schemes have to incorporate inter-catchment transfers to meet demands in the face of inadequate local availability. Furthermore, water quality deterioration, because of human impacts through a wide range of land-uses and waste discharges, has for some time been recognised as a threat in South Africa, as it diminishes the utilisable part of the runoff in many catchments. These complexities increasingly offer challenges to water resource managers that require a response with integrative management philosophies and innovative management tools.

During 1997, in recognition of the aforementioned needs, the Department of Civil Engineering of the University of Stellenbosch, formulated a research proposal to the Water Research Commission (WRC) whose aim would be to serve the philosophy of Integrated Water Resource Management (IWRM), through the development of an integrated information system specifically for water quality – here abbreviated to “WQIS”. To be useful to IWRM, this WQIS was to provide diagnostic and predictive utilities to serve technical planning and operational decision-making in a river system, but, simultaneously, provide appropriate information to support water managers in communication with technical stakeholders. It was also recognised that the project would need identification of a “prototype” catchment for development of appropriate WQIS approaches and to provide a relevant database.

Simultaneous with the research formulation process described above, the Department of Soil and Water Science¹ (DSWS) at the University of Stellenbosch, formulated a research proposal to the WRC to investigate the causes of and quantification of apparently increasing salinisation of the Berg River, one of the prime water sources to meet growing demands in the Greater Cape Town and West Coast Region. The WRC proposed that the two separate proposals be merged to form a single Terms of Reference and, ultimately, a single contract between the WRC and the University, with Prof Görgens as the Project Leader. It then also made sense to select the Berg River as the prototype for the WQIS development, partly because of the accent that the DSWS research would put on salinisation processes, which is one of the Berg River’s most pressing issues, and partly because the Berg catchment contains all the general water resource management challenges and complexities referred to earlier.

OVERALL PROJECT AIMS

The original aims of the project as specified in the WRC contract are as follows:

- i) To develop Water Quality Information Systems to support both integrated management of a water resources system, and to support communication about water quality management with stakeholders and communities in the catchments of that system.
- ii) To develop an understanding of the primary water quality responses, and their causes, of the Rivieronderend-Berg River (RSE-BR) System, which would serve as a case study for the Water Quality Information System implementation. (The Berg River is connected via a two-way tunnel to the Theewaterskloof Dam on the Rivieronderend River.)
- iii) To evaluate the potential for operation of the future RSE-BR System to meet recently developed salinity guidelines for irrigation.

As the project planning unfolded, it became clear to the Steering Committee that the aims needed adjustment for two sets of reasons: On the one hand, they were too broad for the available budget and time-frame. On the other hand, parallel development of suitable approaches to community participation in IWRM, as part of DWAF’s initiatives to implement the National Water Act (1998), was forcing a change in the focus of the project. The Steering Committee, therefore, agreed that most of the research focus would fall on Aims (i) and (ii), and that (iii) should be seen as a long-term objective of salinity-based research in the Berg River catchment.

¹ Now called the Department of Soil Science.

Furthermore, the Steering Committee agreed that the WQIS would primarily be developed as a technical information tool aimed at supporting water resource managers and stakeholders on the technical domain, and that communication support for community participation in consultative water management processes would fall outside the ambit of the current contract.

TWO RESEARCH THEMES AND TWO SETS OF RESEARCH OUTPUTS

The background described earlier, as well as the stated objectives, imply that two related, but essentially different, research themes underlie this project:

- Theme One: Development and/or application of decision support and information management software for general water quality management in a river system with diverse components and human impacts. This Theme was the responsibility of the Department of Civil Engineering.
- Theme Two: Water quality-related research in the form of field-scale process studies and large-scale soils data interpretation and mapping, with a strong focus on salinisation processes. This Theme was the responsibility of the Department of Soil Science.

Each Theme yielded a separate set of research outputs and Reports. This document deals exclusively with the research methodology, results and findings produced by the Department of Civil Engineering under Theme One.

STUDY OBJECTIVES COVERED BY THIS REPORT

The study objectives covered by this document are as follows:

- i) Application of a one-dimensional hydrodynamic river flow and water quality model, DUFLOW, to the Berg River and illustration of its utilisation to support decision-making for various water quality management scenarios.
- ii) Application of a two-dimensional hydrodynamic reservoir water quality model, CE-QUAL-W2, to the proposed Skuifraam Dam in the Upper-Berg to illustrate its utilisation to support decision-making for various in-dam water quality management scenarios and to provide realistic upstream boundary conditions for DUFLOW scenario runs.
- iii) Development of a WQIS that has a user-friendly GIS-based Graphical User Interface, including interfaces with DUFLOW and CE-QUAL-W2, and illustration of its utilisation in typical decision-support for water quality management in river systems, using the Berg River as prototype.

HYDRODYNAMIC RIVER FLOW AND WATER QUALITY MODEL, DUFLOW

The following steps outline the approach and essence of this component of the Study:

- i) A water quality status assessment of the Berg River main-stem was completed, using readily available data from DWAF and other sources, and both spatial and temporal trends were examined and interpreted. This led to a decision that the water quality variables, Salinity, Phosphates, Oxygen and Temperature, would be a minimum set of concerns for future water resource management in the Berg River.
- ii) A survey of internationally available hydrodynamic river flow and water quality models was done, and, following selection criteria that have been declared important by management-orientated user groups in South Africa and elsewhere, it was decided to select the hydrodynamic water-quality model, DUFLOW, and evaluate its adaptability for representing the Berg River with all its complexities.
- iii) An exhaustive search with local authorities, DWAF and consulting civil engineers, yielded a large database of surveyed cross-sections, while a number of cross-sections were also specially surveyed for this Project. In total, 108 cross-sections were included in the model configuration, which represented a distance of 147 km, from Flow-Gauging Station G1H004 in the Upper-Berg to Misverstand Dam in the Lower-Berg.
- iv) To utilise the open-source code facility in the model, customised water quality modules for Oxygen and Temperature balance in the model were programmed.

- v) After a limited sensitivity study, the model was calibrated for selected hydraulic and water quality parameters using one year of daily hydro-meteorological and water quality data for a period regarded as the most complete from a data availability point of view. As sizeable incremental areas and tributaries of the Berg River had been ungauged, empirical estimates of daily inflows and water quality loads from those areas had to be made.
- vi) The calibrated model was temporally verified for a different period of reasonable data availability, and also spatially verified, by modelling individual incremental areas independently.
- vii) A range of water quality management scenarios were postulated for the Berg River and examined through customised utilities in the WQIS.

DISCUSSION AND CONCLUSIONS: DUFLOW APPLICATIONS

Flow Calculations

The finite difference approach that DUFLOW uses to calculate the St Venant equations of continuity and momentum is advanced and therefore allows the user to model complex systems. The finite difference approach allows varied space steps, which proved to be advantageous; especially in the upper Berg, where steep slopes required very small space steps for stable calculations. The lower Berg River could then be modelled in larger space steps in order to save running time and superfluous cross-sections.

Structures that were included are weirs at the specific gauging stations and bridges that are found along the main stem of the Berg River. Information was available for most of the structures, and where difficulties were experienced with computational stability, the roughness coefficient was adjusted. A trigger function used in DUFLOW for structure flow control allows modelling of multiple notches at a weir, such as is often found in South African rivers.

Water Quality Calculations

An advantage of DUFLOW is the open code structure it uses for the water quality module. This allows the user to either change the water quality algorithms according to the degree of complexity required or add additional water quality processes that need to be simulated. In future use of the configured model, water quality processes can be added or deleted. Thus, the model is very flexible. In this study, TDS, COD and Temperature algorithms were added to the EUTROF1 module, as these are variables of concern specifically in the Berg River catchment. The Phosphate algorithm had to be simplified, as most of the processes could not be modelled due to lack of in-stream data. The results of the Temperature algorithms proved to be satisfactory.

Two-weekly water quality samples were available. As the model was configured on a daily time step, the samples had to be "patched" (infilled) in order to include the variables as time series. DUFLOW has an option of entering the time series at irregular time steps, but DUFLOW linearly interpolates the values for the missing samples, which is not quite correct for the distribution of the water quality variables as they are also dependent on the flow value. A moving regression method was used to infill the TDS and soluble phosphate values, while a simple harmonic function was used for the temperature infilling.

Schematisation points were added at every location where a tributary discharges into the main stem or where a point source had been identified. A considerable number of point sources were not included, due to lack of information. It would be a pre-requisite, if the simulation model will be used as an operational tool, that all primary sources of water quality discharge into the river are identified and included in the model.

A limitation of DUFLOW is that it does not allow incoming loads to be input in a diffuse fashion along the length of the modelling reaches. It is therefore difficult to distinguish between non-point and point sources, if the model is to be used as a scenario tool, because the non-point sources have to be treated as distributed point sources.

Modelling Results

The reliability of the modelling results is mainly determined by the accuracy and availability of the input data. Errors in the water quality simulation are dependent on various factors, such as: accuracy of the infilling-method, availability of grab samples in the river, accuracy of the flow simulation, etc. The flow

simulation is dependent on various factors such as cross-section data, channel roughness information, etc. The errors that are introduced at the beginning of the flow calculations (i.e. in the first reach) are carried all the way downstream to the end boundary.

The estimation of runoff from ungauged sub-catchments for the calibration of the flow module proved to be problematic. Considerable volumes of water were still missing during peak flows for most of the stations. This could be due to under-estimation of the flood at the various gauging stations, which thus also leads to under-estimation for the ungauged runoff. The accuracy of the simulation of the water quality loads is dependent on minimising errors resulting from the flow simulation.

Learning curve

The learning curve time to use the model efficiently is greatly reduced by the user friendly interfaces that DUFLOW offers. This is a major advantage, as it can be operated easily for configuration and scenario analyses by the user. An understanding of the underlying hydraulics and water quality processes is however needed to fully understand the system.

Limitations

- Although the finite difference approach to calculate the St. Venants equations proved to be advantageous due to the stability and the choice of unequal time and space steps, a limitation of this approach is, however, that it is very data intensive compared to other simpler flow calculation methods.
- The different network objects (i.e. weirs, abstraction points, etc.) can only be altered in the network window itself. For adjustments to the objects it would have been easier to change the specific descriptions in an additional textfile or database, especially if numerous objects are configured.
- The results are written in a textfile, which take up considerable space (about 50 Mb for the quality files). For use in other systems, such as the WQIS, a database format would have been more suitable for updating and presenting.
- Like many European or American models, DUFLOW is not able to simulate evaporation losses from the water body. Such losses can be quite significant in South Africa, and are therefore of importance. These losses had to be treated as abstraction flows at schematisation points.
- Non-point sources are not modelled as diffuse inflows by DUFLOW. These are however extremely important when considering the nutrient mass balance. From the water quality results it was evident that the agricultural runoff is significant in floods (all loads are under-simulated).
- Water Quality calculations became unstable when negative water depths were experienced for the different runs. Negative water depths are a physical impossibility, but are sometimes simulated in the low flow period, due to inaccuracies between the calculated water level and the configured cross-section's reference level. Although the process calculations were able to be coded to overcome this problem, the transport mathematical formulations were fixed, and the negative water depths affected the calculations. Much effort went into altering the time and space steps until a stable flow calculation was achieved.

Scenario Analysis

The text files produced by DUFLOW are easily altered for different scenario runs. DUFLOW is capable of simulating different scenarios that are of interest to the user. Three scenarios were looked at: a short term effluent spill scenario, a linkage to the hydrodynamic reservoir model, which is described in Section 3 of this volume, and thirdly, an operational long-term management scenario. Although simulation time was long due to small calculation time steps (a calculation time step of 10 minutes proved to be stable) and the result file is large in terms of computer space, DUFLOW is capable of simulating various water quality related changes and predicting the outcomes of different water management scenarios.

RECOMMENDATIONS: DUFLOW APPLICATION

Although the information for the Berg River Catchment is probably more extensive than for many other catchments in South Africa, there is still considerable need for additional research and data if a realistic representation of the river is desired. This is especially important when the model is not only used as an

analysing tool for historical data, but also used to examine management scenarios. Research into the following areas may produce results that would strengthen the model's capability to represent the Berg River Catchment:

Non-point and point sources

There is considerable need to improve the monitoring system for point and non-point sources along the Berg River catchment. This would make a database available of different sources that contribute to nutrient and salt loads in the river. Although DWAF already monitors point sources that have been issued with a water quality permit, there are numerous sources that contribute to the deteriorating water quality in the Berg River. As most of the phosphorous in the river is due to runoff from agricultural land, it would be of benefit to link the hydrodynamic river model to a catchment model to estimate water quality loads from ungauged areas, rather than the ungauged runoff estimation methods used in this study.

Expansion of data/information on variables of interest in the Berg River

Oxygen is of interest in the river for ecological reasons, therefore it would be important to empirically explore the oxygen mass balance in the Berg River, by taking grab samples over a longer period and incorporating COD discharges of the point sources into the river. Different algorithms relating to oxygen should be studied and adopted according to the specific river.

The scenario analysis showed that the summer temperature in the river would change considerably (-10 degree Celsius change) if Skuifraam Dam were to be built in the upper reaches. This is obviously of concern and there is need to investigate the ecological impact of these temperature changes in the river.

Although earlier studies have been conducted on the phosphorous transport in the Berg River, the DUFLOW model has been activated in only the advection equation to analyse the phosphate concentration, as insufficient data is available on other dependent variables. By including data on the suspended solids and, therefore, the mobilisation of particulates into the river, as well as production of algae, improved results on the simulation and a better understanding of the phosphorous concentration patterns in the river can be expected.

Linkage to other models

As mentioned above, it would be beneficial for management support, if DUFLOW were to be linked to other models as this would also ensure that DUFLOW could be used in catchment-wide applications. In this research, a user-friendly interface environment was developed and implemented as a Water Quality Information System (WQIS) that provides analytical, spatial and graphical information based on the requirements of a wide spectrum of users and which integrates simulation models (river and reservoir) into the WQIS, as described below. It would be important to broaden this study and integrate a catchment model into the WQIS so that it can provide tributary inputs to DUFLOW, as well as further develop the DUFLOW model for scenario analysis to support decision making for integrated water management.

HYDRODYNAMIC RESERVOIR WATER QUALITY MODEL, CE-QUAL-W2

The following steps outline the approach and essence of this component of the Study:

- i) The two-dimensional hydrodynamic water quality reservoir model, CE-QUAL-W2, was configured for the site conditions, dam wall and outlet arrangements and dam basin dimensions of the proposed Skuifraam Dam in the Upper-Berg River catchment.
- ii) A four-year period of daily meteorological data for the Upper-Berg was derived from a collection of weather stations in the region and inflow and water quality data for the Dam was assumed to be similar to that observed at G1H004, just upstream of the Dam site.
- iii) Selected sensitivity studies were performed to improve understanding of the role of critical model parameters.
- iv) Various water quality scenarios were formulated to demonstrate the role that the reservoir model can play in technical water resource management decisions. These range from inflow scenarios for pumping from a downstream supplement scheme, to different scenarios for transfers, and back, to

Theewaterskloof Dam on the Riviersonderend River, to different release patterns for downstream environmental flow requirements.

DISCUSSION AND CONCLUSIONS: CE-QUAL-W2 APPLICATIONS

- i) Two-dimensional hydrodynamic and water quality models can provide useful insight into the mixing of water and water quality variables, as well as bio-chemical processes which occur within reservoirs.
- ii) Outputs from two-dimensional models are useful in assisting decision-makers in the task of determining the water quality component of the ecological reserve.
- iii) Regional meteorological data has proven extremely valuable as input (driving forces) for CE-QUAL-W2 in the absence of site-specific meteorological data.
- iv) Two-dimensional hydrodynamic and water quality models such as CE-QUAL-W2 require various rate constants to accurately model bio-chemical reactions. In this study, it was found that the oxygen profile within dams are particularly sensitive to the Sediment Oxygen Demand (SOD) and that this data is not readily available for this type of modelling. Availability of this type of data will greatly improve the reliability of the model outputs.
- v) Water quality monitoring of inflowing streams is of utmost importance for water quality modelling. This study revealed the lack of stream temperature data, which is an important driving force for heat transfer within the reservoir.
- vi) The Berg River Water Quality Information System (WQIS) is a useful tool for managers and decision-makers, bringing together various modelling tools (DUFLOW and CE-QUAL-W2) and providing post-processing which allows visualization of model outputs.

RECOMMENDATIONS: CE-QUAL-W2 APPLICATIONS

From the above conclusions the following recommendations can be made:

- i) The systematic monitoring of meteorological data throughout the country should be continued and new initiatives should aim to gather site-specific meteorological data specifically for important impoundments and along important river courses, and, specifically, as a foresight undertaking for the proposed Skuifraam Dam.
- ii) The systematic monitoring of water quality constituents should be continued throughout the country and special attention should be given to *temperature and nutrient* data sampling.
- iii) In September 2001, Nico Rossouw and Wageed Kamish of Ninham Shand Consulting Services attended a course on the latest version of CE-QUAL-W2 (v3.1), in Portland (U.S.A) and personal contact was made with the developers and custodians of the model. It is therefore recommended that close relationships and contacts with these scientists be maintained so that modelling of this type remains relevant in South Africa.

TABLE OF CONTENTS

| | |
|-------------------|------|
| EXECUTIVE SUMMARY | i |
| TABLE OF CONTENTS | vii |
| LIST OF TABLES | xii |
| LIST OF FIGURES | xiv |
| ACKNOWLEDGEMENTS | xvi |
| PREFACE | xvii |

SECTION 1

APPLICATION OF A HYDRODYNAMIC RIVER FLOW WATER QUALITY MODEL : DUFLOW :

APPLICATION TO THE BERG RIVER

| | |
|--|------------|
| CHAPTER ONE : BACKGROUND | 1-1 |
| CHAPTER TWO : CONCEPTUAL CONTEXT OF MODEL APPLICATION | 1-1 |
| 2.1 INTRODUCTION | 2-1 |
| 2.2 HISTORY OF RIVER WATER QUALITY MODELLING..... | 2-1 |
| 2.3 CONCEPTS IMPORTANT TO WATER QUALITY MODEL APPLICATIONS..... | 2-2 |
| 2.3.1 Model Elements..... | 2-2 |
| 2.3.2 Model Attributes..... | 2-2 |
| 2.3.3 Model Application Steps..... | 2-3 |
| 2.4 DATA CONSIDERATIONS FOR MODEL USE..... | 2-5 |
| 2.5 REVIEW OF WATER QUALITY MODELS FOR RIVERS..... | 2-6 |
| 2.5.1 American Models..... | 2-6 |
| 2.5.2 European Models..... | 2-7 |
| 2.6 DISCUSSION | 2-9 |
| CHAPTER THREE : DESCRIPTION OF THE BERG RIVER BASIN | 3-1 |
| 3.1 GEOGRAPHY..... | 3-1 |
| 3.2 TOPOGRAPHY, GEOLOGY AND CLIMATE..... | 3-1 |
| 3.3 LAND COVER | 3-1 |
| 3.4 WATER INFRASTRUCTURE DEVELOPMENTS IN THE CATCHMENT | 3-5 |
| 3.4.1 Voëlmei Dam..... | 3-5 |
| 3.4.2 Wemmershoek Dam..... | 3-5 |
| 3.4.3 Misverstand Dam..... | 3-5 |
| 3.4.4 Theewaterskloof Dam..... | 3-5 |
| 3.4.5 Future Developments | 3-6 |
| 3.4.6 Operation of the Berg River-Theewaterskloof Link | 3-6 |
| CHAPTER FOUR : REVIEW OF WATER QUALITY STATUS OF BERG RIVER MAIN STEM | 4-1 |
| 4.1 INTRODUCTION | 4-1 |
| 4.2 STUDIES DONE ON THE WATER QUALITY OF THE BERG RIVER | 4-1 |
| 4.3 VARIABLES OF CONCERN..... | 4-1 |
| 4.4 DELINEATION OF STUDY AREA..... | 4-2 |

| | | |
|--|---|------------|
| 4.5 | WATER USERS | 4-2 |
| 4.6 | ASSESSMENT OF pH..... | 4-2 |
| 4.6.1 | Introduction..... | 4-2 |
| 4.6.2 | Main Stem Sampling Stations | 4-3 |
| 4.6.3 | Municipal Supply..... | 4-3 |
| 4.7 | ASSESSMENT OF EC AND TDS | 4-4 |
| 4.7.1 | Introduction..... | 4-4 |
| 4.7.2 | Main Stem Sampling Stations | 4-4 |
| 4.7.3 | Municipal Supply..... | 4-5 |
| 4.8 | ASSESSMENT OF PHOSPHATES | 4-5 |
| 4.8.1 | Introduction..... | 4-5 |
| 4.8.2 | Main Stem Sampling Stations | 4-5 |
| 4.8.3 | Municipal Supply..... | 4-6 |
| 4.9 | ADDITIONAL WATER QUALITY SAMPLES TAKEN IN THE BERG RIVER MAIN STEM..... | 4-6 |
| 4.10 | CONCLUSIONS | 4-7 |
| CHAPTER FIVE : SOFTWARE STRUCTURE AND MATHEMATICAL BACKGROUND TO DUFLOW WATER QUALITY MODEL | | 5-1 |
| 5.1 | INTRODUCTION | 5-1 |
| 5.2 | DESCRIPTION OF THE DUFLOW MODEL SOFTWARE STRUCTURE | 5-1 |
| 5.2.1 | Features of the Interface | 5-1 |
| 5.2.2 | Calculation Options..... | 5-2 |
| 5.2.3 | Import and Export of Data | 5-3 |
| 5.2.4 | Presentation of Results | 5-3 |
| 5.2.5 | Configuration of the Model | 5-4 |
| 5.3 | HYDRODYNAMIC MATHEMATICAL BACKGROUND..... | 5-5 |
| 5.3.1 | Introduction..... | 5-5 |
| 5.3.2 | Unsteady Flow Equations..... | 5-5 |
| 5.3.3 | Numerical Solutions to Unsteady Flow..... | 5-6 |
| 5.3.4 | Boundary and Initial Conditions..... | 5-7 |
| 5.3.5 | Cross-sections..... | 5-7 |
| 5.3.6 | Structures | 5-8 |
| 5.4 | WATER QUALITY | 5-11 |
| 5.4.1 | Introduction..... | 5-11 |
| 5.4.2 | Transport | 5-11 |
| 5.4.3 | Discretization of Mass Transport Equations..... | 5-13 |
| 5.4.4 | Initial and Boundary Conditions..... | 5-14 |
| 5.4.5 | Water Quality Processes | 5-14 |
| 5.5 | ACCURACY AND STABILITY OF NUMERICAL MODELS | 5-24 |
| 5.6 | TIME AND SPACE STEP | 5-24 |
| 5.7 | CONCLUSION..... | 5-25 |
| CHAPTER SIX : DATA PREPARATION AND CONFIGURATION OF THE MODEL..... | | 6-1 |
| 6.1 | INTRODUCTION | 6-1 |
| 6.2 | HYDRODYNAMIC SCHEMATIZATION | 6-1 |

| | | |
|--|--|------------|
| 6.2.1 | Flow Data Preparation | 6-1 |
| 6.2.2 | Nodes and Boundary Conditions | 6-1 |
| 6.2.3 | Cross-sections | 6-3 |
| 6.2.4 | Structures | 6-4 |
| 6.2.5 | Tributaries | 6-5 |
| 6.2.6 | Roughness Coefficient | 6-5 |
| 6.2.7 | Abstractions and Return Flows | 6-6 |
| 6.2.8 | Evaporation Losses | 6-8 |
| 6.3 | WATER QUALITY CONFIGURATION | 6-9 |
| 6.3.1 | Water Quality Data Preparation | 6-9 |
| 6.3.2 | Water Quality Variables | 6-17 |
| 6.3.3 | Abstractions | 6-17 |
| 6.3.4 | External Variables | 6-17 |
| 6.3.5 | Parameters | 6-19 |
| 6.4 | PROBLEMS ENCOUNTERED | 6-19 |
| CHAPTER SEVEN : FLOW MODEL SENSITIVITY, CALIBRATION AND VERIFICATION | | 7-1 |
| 7.1 | INTRODUCTION | 7-1 |
| 7.2 | OBJECTIVE FUNCTIONS | 7-1 |
| 7.3 | MODEL CALIBRATION AND SENSITIVITY PROCEDURE | 7-2 |
| 7.4 | CALIBRATION PERIOD | 7-2 |
| 7.5 | BOUNDARY CONDITIONS AND INITIAL CONDITIONS | 7-3 |
| 7.6 | ADDITION OF UNGAUGED SUB-CATCHMENT FLOWS | 7-3 |
| 7.7 | SENSITIVITY OF FLOW RESISTANCE | 7-6 |
| 7.8 | RESULTS OF FLOW MODEL CALIBRATION | 7-7 |
| 7.9 | MODEL VERIFICATION | 7-8 |
| 7.9.1 | Verification in Space | 7-9 |
| 7.9.2 | Verification in Time | 7-10 |
| 7.10 | DISCUSSION OF FINAL MODEL RESULTS | 7-11 |
| CHAPTER EIGHT : WATER QUALITY MODEL SENSITIVITY, CALIBRATION AND VERIFICATION | | 8-1 |
| 8.1 | INTRODUCTION | 8-1 |
| 8.2 | MODEL CALIBRATION AND SENSITIVITY PROCEDURE | 8-1 |
| 8.3 | DETERMINATION OF RELIABLE CALIBRATION PROCEDURE | 8-1 |
| 8.4 | BOUNDARY AND INITIAL CONDITIONS | 8-1 |
| 8.5 | ESTIMATION OF UNGAUGED WATER QUALITY SUB-CATCHMENT LOADS | 8-2 |
| 8.6 | SENSITIVITY OF WATER QUALITY PARAMETERS | 8-4 |
| 8.6.1 | Dispersion | 8-4 |
| 8.6.2 | Phosphorous | 8-5 |
| 8.6.3 | Temperature | 8-5 |
| 8.6.4 | Oxygen | 8-7 |
| 8.7 | SENSITIVITY OF GRAB SAMPLES COMPARED TO INFILLED SAMPLES | 8-8 |
| 8.8 | POINT SOURCES | 8-9 |
| 8.9 | RESULTS OF WATER QUALITY MODEL CALIBRATION | 8-12 |
| 8.9.1 | TDS | 8-12 |
| 8.9.2 | Phosphate as PO ₄ | 8-13 |
| 8.9.3 | Temperature | 8-15 |
| 8.9.4 | Oxygen | 8-15 |

| | | |
|--|---|-------------|
| 8.10 | WATER QUALITY MODEL VERIFICATION | 8-15 |
| 8.10.1 | TDS..... | 8-15 |
| 8.10.2 | Phosphate as PO4..... | 8-16 |
| 8.10.3 | Temperature | 8-18 |
| 8.10.4 | Oxygen | 8-18 |
| 8.11 | WATER QUALITY SIMULATION WITHOUT UNGAUGED RUNOFF | 8-18 |
| 8.11.1 | TDS..... | 8-18 |
| 8.11.2 | Phosphate as PO4..... | 8-19 |
| CHAPTER NINE : SCENARIO ANALYSIS | | 9-1 |
| 9.1 | INTRODUCTION | 9-1 |
| 9.2 | OPERATIONAL SHORT-TERM SCENARIO | 9-1 |
| 9.3 | LINKAGE TO RESERVOIR MODEL | 9-5 |
| 9.3.1 | Flow | 9-5 |
| 9.3.2 | TDS..... | 9-6 |
| 9.3.3 | Phosphate as PO4..... | 9-8 |
| 9.3.4 | Temperature | 9-10 |
| 9.3.5 | Oxygen | 9-12 |
| 9.4 | LONG-TERM CONTROL..... | 9-13 |
| 9.5 | DISCUSSION | 9-14 |
| CHAPTER TEN : CONCLUSIONS AND RECOMMENDATIONS | | 10-1 |
| 10.1 | INTRODUCTION | 10-1 |
| 10.2 | CONCLUSIONS | 10-1 |
| 10.2.1 | Flow Calculations..... | 10-1 |
| 10.2.2 | Water Quality Calculations | 10-1 |
| 10.2.3 | Results..... | 10-2 |
| 10.2.4 | Learning Curve | 10-2 |
| 10.2.5 | Limitations..... | 10-2 |
| 10.2.6 | Scenario Analysis | 10-3 |
| 10.3 | RECOMMENDATIONS | 10-3 |
| 10.3.1 | Non-point and Point Sources..... | 10-3 |
| 10.3.2 | Expansion of Data Information on Variables of Interest in the Berg River..... | 10-3 |
| 10.3.3 | Linkage to Other Models | 10-3 |

SECTION 2

**APPLICATION OF A TWO DIMENSIONAL HYDRODYNAMIC RESERVOIR
WATER QUALITY MODEL : CE-QUAL-W2 :**

**APPLICATION TO THE PROPOSED SKUIFRAAM DAM
ON THE BERG RIVER**

| | |
|---|------------|
| CHAPTER ONE : INTRODUCTION | 1-1 |
| 1.1 BACKGROUND | 1-1 |
| 1.2 OVERVIEW OF CE-QUAL-W2 MODEL | 1-1 |
| 1.3 LINKAGE TO RIVER MODEL | 1-2 |
| CHAPTER TWO : PREPARATION OF INPUT PARAMETERS FOR SKUIFRAAM DAM | 21 |
| 2.1 GEOMETRIC DATA | 2-1 |
| 2.2 INITIAL CONDITIONS | 2-5 |
| 2.2.1 Meteorological Data | 2-5 |
| 2.2.2 Upstream Boundary Conditions | 2-7 |
| 2.2.3 Flow Rates and Patterns of Releases | 2-9 |
| CHAPTER THREE : SIMULATION RESULTS | 3-1 |
| 3.1 SELECTION OF METEOROLOGICAL DATA SET | 3-1 |
| 3.2 INTERPRETATION OF SIMULATION RESULTS | 3-1 |
| CHAPTER FOUR : SCENARIO CASE STUDIES | 4-1 |
| 4.1 SCENARIO CASE STUDIES | 4-1 |
| 4.2 PRESENTATION OF RESULTS | 4-1 |
| CHAPTER FIVE : CE-QUAL-W2 : APPLICATION | 5-1 |
| 5.1 APPLICATION OF CE-QUAL-W2 : THE OPERATING LEVELS OF SKUIFRAAM DAM AND THE POTENTIAL USE OF A HIGH LEVEL SLUICE GATE FOR THE ENVIRONMENTAL FLOOD RELEASE | 5-1 |
| 5.2 RE-ASSESS PREVIOUS WORK ON FUTURE OPERATING RULES | 5-1 |
| 5.3 RE-RUN THE YIELD MODEL WITH REALISTIC MAXIMUM DEMANDS PLACED ON THE SKUIFRAAM / THEEWATERSKLOOF SYSTEM | 5-1 |
| 5.4 CONTINUOUS PLOTS AND BOX PLOTS OF MONTHLY WATER LEVELS | 5-2 |
| 5.4.1 Dissolved Oxygen | 5-4 |
| 5.4.2 Temperature | 5-4 |
| 5.4.3 Bottom Inflow from Supplement | 5-5 |
| 5.5 CONCLUSIONS | 5-5 |
| CHAPTER SIX : CONCLUSIONS AND RECOMMENDATIONS | 6-1 |
| 6.1 CONCLUSIONS | 6-1 |
| 6.2 RECOMMENDATION | 6-1 |
| CHAPTER SEVEN : REFERENCES | 7-1 |
| APPENDIX 1 | |
| APPENDIX 2 | |

LIST OF TABLES

SECTION 1

| | | |
|------|--|------|
| 2.1 | Comparison of model attributes..... | 2-8 |
| 3.1 | Percentage of various crops under irrigation in the upper and middle reaches of the Berg River catchment (DWAFC, 1993)..... | 3-5 |
| 4.1 | Summary of water quality samples taken in the Berg River..... | 4-6 |
| 5.1 | Comparison of finite difference schemes..... | 5-6 |
| 5.2 | The quantities that are used for different flow conditions (STOWA, 1998)..... | 5-8 |
| 5.3 | Dispersion Calculation Methods..... | 5-13 |
| 5.4 | Mathematical Models describing reaeration coefficients..... | 5-23 |
| 6.1 | Reaches of the main stem Berg River..... | 6-1 |
| 6.2 | Sources of cross-sections provided in the Berg River..... | 6-3 |
| 6.3 | Details of weirs..... | 6-4 |
| 6.4 | Details of bridges..... | 6-5 |
| 6.5 | Major tributaries in the Berg River catchment..... | 6-5 |
| 6.6 | Abstraction data of Paarl Municipality..... | 6-6 |
| 6.7 | Abstractions in the Berg River for 1993/1994 (Mm3)..... | 6-7 |
| 6.8 | Comparison of Return Flows in years at Paarl STW..... | 6-8 |
| 6.9 | Evaporation Losses (mm/month) at Bien Donne for the year 1993/1994..... | 6-9 |
| 6.10 | Infilling of water quality variables..... | 6-9 |
| 6.11 | Calculation Methods for Flux..... | 6-10 |
| 6.12 | Statistics of TDS Infilling..... | 6-13 |
| 6.13 | Statistics of Phosphorus as PO ₄ Infilling..... | 6-14 |
| 6.14 | Details of Temperature Infilling..... | 6-16 |
| 6.15 | Statistics of Temperature Infilling..... | 6-16 |
| 6.16 | Meteorological stations used and corresponding water gauging stations..... | 6-17 |
| 6.17 | Average monthly air temperature measured at meteorological stations..... | 6-18 |
| 6.18 | Monthly Radiation Averages (MJ/day) at Bien Donne for 1993/1994..... | 6-18 |
| 6.19 | Monthly wind speed (km/month) for 1993/1994..... | 6-19 |
| 6.20 | Evaporation Rate (average mm/day) for the various meteorological stations..... | 6-19 |
| 6.21 | Parameters used in DUFLOW..... | 6-19 |
| 7.1 | Accuracy Rating of Gauging Stations..... | 7-3 |
| 7.2 | Description of Gauged Tributaries..... | 7-4 |
| 7.3 | Areas and Correction Factors of Ungauged Tributaries..... | 7-4 |
| 7.4 | Mass balance of flow corrected and measured for 1993/1994..... | 7-6 |
| 7.5 | Sensitivity of Flow Resistance..... | 7-7 |
| 7.6 | Results of model calibration..... | 7-8 |
| 7.7 | Results of Verification Run using G1H020 as Inflow Hydrograph..... | 7-9 |
| 7.8 | Results of Verification Run using G1H036 as Inflow Hydrograph..... | 7-10 |
| 7.9 | Verification in time (1994/1995)..... | 7-11 |
| 8.1 | Accuracy of water quality boundary conditions..... | 8-1 |
| 8.2 | Correction of Ungauged Concentration..... | 8-3 |
| 8.3 | Statistics of Ungauged TDS Values..... | 8-3 |
| 8.4 | Statistics of Ungauged PO ₄ Values..... | 8-3 |
| 8.5 | Point sources identified in the Berg River Catchment..... | 8-10 |
| 8.6 | COD Loads (tons/month) for 1993/1994..... | 8-11 |
| 8.7 | TDS Loads (tons/month) for 1993/1994..... | 8-11 |
| 8.8 | Absolute % error difference between the simulation without ungauged loads and the simulation with ungauged loads for TDS..... | 8-19 |
| 8.9 | Absolute % error difference between the simulation without ungauged loads and the simulation with ungauged loads for phosphates..... | 8-20 |

VOLUME 1 : TABLE OF CONTENTS

| | | |
|------|---|------|
| 9.1 | Comparison of flows at G1H004 and dam release/spill pattern | 9-5 |
| 9.2 | Comparison of released TDS from Skuifraam Dam and historical TDS at G1H004 | 9-6 |
| 9.3 | TDS Concentration after simulation of dam releases..... | 9-7 |
| 9.4 | TDS Loads after simulation using dam spills and releases as the upstream boundary | 9-8 |
| 9.5 | Comparison of phosphate as P04 released from Skuifraam Dam and historical data at G1H004 | 9-8 |
| 9.6 | Phosphate Concentration after simulation using dam spills and releases as the upstream boundary | 9-9 |
| 9.7 | Phosphate Loads after simulation using dam spills and releases as the upstream boundary | 9-10 |
| 9.8 | Comparison of temperature released from Skuifraam Dam and historical temperature at G1H004 | 9-10 |
| 9.9 | Temperature after simulation using dam spills and releases as the upstream boundary | 9-11 |
| 9.10 | Comparison of oxygen released from Skuifraam Dam and oxygen at G1H004 | 9-12 |
| 9.11 | Oxygen after simulation using dam spills and releases as inflow | 9-13 |

SECTION 2

| | | |
|-----|---|-----|
| 2.1 | lateral cell widths used to describe the bathymetry of the proposed Skuifraam Dam..... | 2-3 |
| 2.2 | Cell volumes obtain from the bathymetry of the proposed Skuifraam Dam..... | 2-4 |
| 2.3 | Positions of major inflows and outflows on the Proposed Skuifraam Dam | 2-5 |
| 2.4 | Flow rates of other inflows into the proposed Skuifraam Dam..... | 2-7 |
| 2.5 | Flow rates of releases and withdrawals from the proposed Skuifraam Dam | 2-9 |
| 3.1 | Calibration coefficients for hydrodynamics and temperature | 3-1 |
| 5.1 | In-stream Flow Requirements Release Pattern (Skuifraam Dam) | 5-1 |
| 5.2 | Frequency of IFR flood releases being made from different levels..... | 5-2 |
| 5.3 | Comparison of the scenarios promoting stratification and mixing | 5-3 |
| 5.4 | Comparing the seasonal temperature of the inflow with the temperatures of the releases at different levels..... | 5-4 |
| 5.5 | The frequency, dissolved oxygen range, and temperature range of IFR releases made from different levels | 5-5 |

LIST OF FIGURES

SECTION 1

| | | |
|------|---|------|
| 3.1 | Gauging stations in the Berg River region..... | 3-2 |
| 3.2 | Geology in the Berg River Catchment..... | 3-3 |
| 3.3 | Land-use in the Berg River Catchment | 3-4 |
| 3.4 | Future developments in the Berg River catchment | 3-7 |
| 5.1 | User interface components..... | 5-2 |
| 5.2 | Network schematisation objects..... | 5-2 |
| 5.3 | Time series property box..... | 5-3 |
| 5.4 | Time related graph | 5-3 |
| 5.5 | Space related graph | 5-3 |
| 5.6 | Cross-section property box..... | 5-4 |
| 5.7 | Calculation settings dialog box..... | 5-4 |
| 5.8 | Four-point Preissmann scheme..... | 5-7 |
| 5.9 | Schematization of cross-sections | 5-8 |
| 5.10 | Schematization of floodplain using lateral flows..... | 5-8 |
| 5.11 | Structure flow conditions, covered by DUFLOW | 5-10 |
| 5.12 | Sinks and sources of temperature model..... | 5-16 |
| 5.13 | Diagram of phosphate constituents..... | 5-20 |
| 6.1 | Incoming high-flow from tributaries..... | 6-2 |
| 6.2 | Incoming low-flow from tributaries..... | 6-2 |
| 6.3 | Inflow hydrograph at G1H004..... | 6-2 |
| 6.4 | Stage-discharge relationship at G1R003 | 6-2 |
| 6.5 | Longitudinal profile from G1H004 to Misverstand | 6-3 |
| 6.6 | Graphical representation of evaporation rates at Bien Donne | 6-9 |
| 6.7 | Radiation (MJ) at Bien Donne | 6-18 |
| 7.1 | Isohyetal map showing gauged and ungauged sub-catchments in the Berg River region | 7-5 |
| 7.2 | Sensitivity of Mannings Roughness value..... | 7-7 |
| 8.1 | Comparison of infilled water quality concentration of areas 1 and 2 with infilled concentration of gauging station G1H020 | 8-2 |
| 8.2 | Comparison of infilled water quality concentration of areas 4 and 5 with infilled concentration of gauging station G1H039 | 8-2 |
| 8.3 | Dispersion sensitivity | 8-4 |
| 8.4 | Concentration using non-decouple dispersion | 8-4 |
| 8.5 | Sensitivity of temperature parameter | 8-5 |
| 8.6 | Sensitivity of temperature parameters at G1H020 | 8-6 |
| 8.7 | Sensitivity of temperature parameters at G1H036 | 8-6 |
| 8.8 | Sensitivity of temperature parameters at G1H013 | 8-6 |
| 8.9 | Sensitivity of temperature parameters at G1R003 | 8-6 |
| 8.10 | Depth influence on solar radiation | 8-7 |
| 8.11 | Influence of θ_{re} on summer oxygen values..... | 8-8 |
| 8.12 | Comparison of TDS simulation at G1H036 | 8-8 |
| 8.13 | Comparison of PO4 simulation at G1H013 | 8-9 |
| 8.14 | TDS concentration of G1H039 and G1H041 | 8-12 |
| 8.15 | Phosphate concentration of tributaries | 8-14 |
| 8.16 | TDS concentration of tributaries for the verification year | 8-16 |
| 8.17 | Phosphate concentration of tributaries for the verification year | 8-17 |
| 9.1 | Post-audit of models | 9-1 |
| 9.2 | Effluent spill hydrograph shapes | 9-2 |
| 9.3 | Results of phosphate spill without release shown in time | 9-3 |
| 9.4 | Results of phosphate spill with release shown in time | 9-3 |
| 9.5 | Results of phosphate spill shown without release for 16 February | 9-4 |

VOLUME 1 : TABLE OF CONTENTS

| | | |
|------|---|------|
| 9.6 | Results of phosphate spill without release for 18 February | 9-4 |
| 9.7 | Results of phosphate spill without release for 24 February | 9-4 |
| 9.8 | Results of phosphate spill with release for 16 February | 9-4 |
| 9.9 | Results of phosphate spill with release for 18 February | 9-4 |
| 9.10 | Results of phosphate spill with release for 24 February | 9-4 |
| 9.11 | Comparison of historical inflow hydrograph and releases of Skuifraam Dam..... | 9-5 |
| 9.12 | Comparison of historical TDS at G1H004 and TDS releases from Skuifraam Dam at G1H004 | 9-7 |
| 9.13 | Comparison of historical phosphate as PO ₄ and releases from Skuifraam Dam | 9-9 |
| 9.14 | Comparison of historical temperature and temperature releases from Skuifraam Dam | 9-11 |
| 9.15 | Comparison of historical oxygen and releases of Skuifraam Dam..... | 9-12 |
| 9.16 | Schematisation of long-term control scenario | 9-13 |

SECTION 2

| | | |
|-----|--|------|
| 2.1 | Segments of proposed Skuifraam Dam | 2-1 |
| 2.2 | Comparison between measured and simulated data for the proposed Skuifraam Dam..... | 2-2 |
| 2.3 | Comparison of temperatures at Jonkershoek and Villiersdorp | 2-6 |
| 2.4 | Comparison of wind speed at Villiersdorp and Paarl..... | 2-6 |
| 2.5 | Simulated and measured TDS data for the Berg River flowing into the proposed Skuifraam Dam..... | 2-7 |
| 2.6 | Simulated and measured phosphate data for the Berg River flowing into the proposed Skuifraam Dam..... | 2-8 |
| 2.7 | Measured and infilled data for the Berg River at gauging station G1H04Q01 | 2-8 |
| 2.8 | Volume balance for the proposed Skuifraam Dam..... | 2-10 |
| 4.1 | Dissolved oxygen profile for Segment 9 in the control scenario (SOD = 0.2 g/m ² /day)..... | 4-1 |
| 4.2 | Dissolved oxygen profile for Segment 9 in Scenario 1 (SOD = 0.5 g/m ² /day) | 4-1 |
| 4.3 | Dissolved oxygen profile for Segment 9 in Scenario 2 (SOD = 0.5 g/m ² /day) | 4-2 |
| 5.1 | Skuifraam Dam's storage under present (1999) and future (2008) agricultural demands | 5-2 |
| 5.2 | Skuifraam Dam - storage under present and future agricultural demands | 5-3 |

ACKNOWLEDGEMENTS

The research in this report emanated from a project funded by the Water Research Commission and entitled :

WATER QUALITY INFORMATION SYSTEMS FOR INTEGRATED WATER RESOURCES MANAGEMENT : THE RIVIERSONDERENDBERG RIVER SYSTEMS

The Steering Committee responsible for this project, consisted of the following persons :

| | |
|-----------------------|--|
| Mr HM du Plessis | Water Research Commission (Chairman) |
| Dr GC Green | Water Research Commission |
| Mr OCE Hempel | Water Research Commission(Committee Secretary) |
| Prof AHM Görgens | University of Stellenbosch |
| Prof A Rooseboom | University of Stellenbosch |
| Prof MV Fey | University of Stellenbosch |
| Dr PA Myburgh | ARC- Infruitec/Nietvoorbij |
| Mr AS Roux | PAWC : Department of Agriculture |
| Mr P van Niekerk | PAWC : Department of Agriculture |
| Mr F Knight | PAWC : Department of Agriculture |
| Prof H Wesso | University of the Western Cape |
| Mr JH Human | Agriculture Western Cape |
| Mr FJD le Roux | Agriculture Western Cape |
| Mr MR Obree | CMC : Head : Catchment Management Department |
| Mr P Viljoen | Department of Water Affairs and Forestry |
| Mr G McConkey | Department of Water Affairs and Forestry |
| Prof HD van Schalkwyk | University of OFS |

The financing of the project by the Water Research Commission and the contribution of the members of the Steering Committee is acknowledged gratefully.

This project was made possible through the co-operation of many individuals and institutions. The authors therefore wish to record their sincere thanks to the following :

1. In the Soil Science Department, Stellenbosch University: Matt Gordon, Ross Campbell, Kamilla Latief, Kenneth Davidse and Judy Smith.
2. Agriculture Western Cape, Elsenburg: Ms Liezl Landman for the GIS work involved in this project.
3. The management and staff of the Broodkraal Farm, especially Mr J. de Kock, Mr Koot and Mrs Nadine Nel, Julian Ellis, Francois Hanekom and Andre Smit.
4. The owner, Mr J D Kirsten, of the Rooihogte Farm and, among the staff, Mr P. van der Merwe, Mr H Esterhuizen and Mr E. Kellerman.
5. The companies Nitrophosca and Kynoch that made valuable information available to this project.

PREFACE

1.1 BACKGROUND

Impoundments and associated bulk water supply infrastructure are present in most South African river systems. Because of the disparate natural occurrence of rainfall and runoff, and its mismatch with water demand concentrations, many of these schemes have to incorporate inter-catchment transfers to meet demands in the face of inadequate local availability. Furthermore, water quality deterioration, because of human impacts through a wide range of land-uses and waste discharges, has for some time been recognised as a threat in South Africa, as it diminishes the utilisable part of the runoff in many catchments. These complexities increasingly offer challenges to water resource managers that require a response with integrative management philosophies and innovative management tools.

In recognition of the aforementioned needs, Prof André Görgens of the Department of Civil Engineering of the University of Stellenbosch, during 1997, engaged water resource managers in the Department of Water Affairs and Forestry in discussions about an appropriate research response to these management challenges. From these discussions a research proposal to the Water Research Commission (WRC) was born, whose aim would be to serve the philosophy of Integrated Water Resource Management (IWRM), through the development of an integrated information system specifically for water quality – here abbreviated to “WQIS”.

To be useful to IWRM, this WQIS was to provide diagnostic and predictive utilities to serve technical planning and operational decision-making in a river system, but, simultaneously, provide appropriate information to support water managers in communication with technical stakeholders. It was also recognised that the project would need identification of a “prototype” catchment for development of appropriate WQIS approaches and to provide a relevant database. Early candidate catchments for this purpose were the Berg River and Breede River in the Western Cape and the inter-connected Fish-Sundays river system in the Eastern Cape

Simultaneous with the research formulation process described above, the late Prof Hulme Moolman of the Department of Soil and Water Science¹ (DSWS) at the University of Stellenbosch, started formulating a research proposal to the WRC to investigate the causes of and quantification of salinisation of the Berg River, one of the prime water sources to meet growing demands in the Greater Cape Town and West Coast Region. Both the Department of Water Affairs and Forestry and agricultural and industrial stakeholders had expressed concern about perceptions that Middle- to Lower-Berg River salt concentrations appeared to be on the increase.

Unfortunately, Prof Moolman, who at the time was engaged in salinity-related research in the neighbouring Breede River catchment and who was the leading salinity-related researcher in South Africa, fell gravely ill before the research proposal approval process was completed. As a strategy to ensure that the research process at the DSWS would continue regardless of the outcome of Prof Moolman's illness, the WRC requested Prof Görgens, who had done salinity-related research in the past, to take over management of both his own Department's research proposal and that of the DSWS. The result was that the two separate proposal formulation processes were merged to form a single Terms of Reference and, ultimately, a single contract between the WRC and the University, with Prof Görgens as the Project Leader. It then also made sense to select the Berg River as the prototype for the WQIS development, partly because of the accent that the DSWS research would put on salinisation processes, which is one the Berg River's most pressing issues, and partly because the Berg contains all the general water resource management challenges and complexities referred to earlier².

¹ Now called the Department of Soil Science.

² The combined impoundments of the Riviersonderend-Berg River (RSE-BR) system currently contribute more than 80% of the total annual water yield of 450 million m³ available to the Greater Cape Town and West Coast Region. The current RSE-BR system comprises Theewaterskloof Dam on the RSE River, linked by tunnels to the Berg and Eerste River catchments, as well as Wemmershoek and Voëlvllei Dams (both of which are off the Berg River main-stem). Sustained growth in the water requirements of the Region necessitates expansion of the RSE-BR system in the near future. The following Berg River schemes have been under investigation for implementation: Skuifraam Dam in the Upper-Berg, Skuifraam Supplement Scheme downstream of Franschoek and Middle-Berg Diversion Scheme to Voëlvllei Dam. Apart from supplying the bulk needs of the Region, these schemes would also serve the Government's rural development strategy in that they will support upliftment of a number of disadvantaged communities in the Berg catchment and will make possible development of irrigation schemes for emergent farmers from these communities. Additionally, irrigation extensions by currently established farmers will be made possible. However, the implementation of these schemes would remove an additional 20% of fresh water from the Berg River main-stem and will lead to a more regulated river system between Skuifraam and the Lower Berg. The likelihood of all these developments has sparked serious concerns relating to future water quality fitness-for-use and maintenance of ecological integrity.

1.2 PROJECT AIMS

The original aims of the project as specified in the WRC contract are as follows:

- i) To develop Water Quality Information Systems to support both integrated management of a water resources system, and to support communication about water quality management with stakeholders and communities in the catchments of that system.
- ii) To develop an understanding of the primary water quality responses, and their causes, of the Riviersonderend-Berg River (RSE-BR) System, which would serve as a case study for the Water Quality Information System implementation.
- iii) To evaluate the potential for operation of the future RSE-BR System to meet recently developed salinity guidelines for irrigation.

As the project planning unfolded, it became clear to the Steering Committee that the aims needed adjustment for two sets of reasons: On the one hand, they were too broad for the available budget and time-frame. On the other hand, parallel development of suitable approaches to community participation in IWRM, as part of DWAF's initiatives to implement the National Water Act, were forcing a change in the focus of the project. The Steering Committee, therefore, agreed that most of the research focus would fall on Aims (i) and (ii), and that (iii) should be seen as a long-term objective of salinity-based research in the Berg River catchment. Furthermore, the Steering Committee agreed that the WQIS would primarily be developed as a technical information tool aimed at supporting water resource managers and stakeholders on the technical domain, and that communication support for community participation in consultative water management processes would fall outside the ambit of the current contract.

1.3 TWO RESEARCH THEMES, TWO RESEARCH TEAMS

The background described earlier, as well as the stated objectives, imply that two related, but essentially different, research themes underlie this project:

- Theme One: Development and/or application of decision support software for general water quality management in a river system with diverse components and human impacts.
- Theme Two: Water quality-related research in the form of field-scale process studies and large-scale soils data interpretation, with a strong focus on salinisation processes.

It follows that, when the project was resourced at its initiation in July 1998, the two Research Themes, and the involvement of two different University Departments, would lead to the establishment of two separate Research Teams.

The Theme One research (water quality management decision support software) was undertaken by the Department of Civil Engineering and comprised the following researchers:

- Prof AHM Görgens – Project Leader
- N Nitsche – Hydrodynamic River Flow and Water Quality Modeller (full-time)
- W Kamish – Reservoir Modeller (part-time)
- J Tukker – Water Quality Information System Software Developer (full-time)
- MP Matji – Support Hydrologist (part-time).

The Theme Two research (field-scale-processes and large-scale mapping) was undertaken by the Department of Soil Science and comprised the following researchers:

- WP de Clercq – Senior Researcher (full-time)
- Prof MV Fey – Specialist Advisor (part-time)
- Dr F Ellis – Specialist Soil Scientist (part-time)
- H Engelbrecht – Junior Researcher (full-time)
- K Latief – Laboratory Assistant (full-time)
- K Davidse – Laboratory Assistant (part-time)
- P Basson – Technikon Internship (full-time for one year)
- M van Meirvenne – Visiting Researcher (part-time)
- G de Smet – Visiting Researcher (part-time)

Mr Willem de Clercq, appointed at the Project initiation as full-time Senior Researcher, took care of the Department of Soil Science component of the research. Prof Martin Fey was appointed as Prof Moolman's successor when about 55% of the project duration had been completed. Given the work load attached to his new position, Prof Fey preferred to act as Specialist Advisor, with Mr de Clercq continuing to lead that Department's research under this Project.

1.4 STRUCTURE OF REPORTS AND SUPPORTING OUTPUTS

Given the essentially different nature of the two sets of Research Themes described earlier, the Steering Committee decided that two free-standing sets of Reports and other deliverables would ensue from the Project – one set per Theme – as described below.

Theme One research (water quality management decision support software):

- i) *Volume 1: Application of hydrodynamic water quality models for river flow and reservoir processes to the Berg River System* by N Nitsche, W Kamish and AHM Görgens.
- ii) *Volume 2: Development of the WQIS (Water Quality Information System): Application to the Berg River System* by MJ Tukker and AHM Görgens.

An Extended Summary version of these two Volumes have been produced as paper documents, while the full versions of these two volumes are presented on CD, lodged inside an envelope inside the back cover of each paper document. The reader should note that the CD also contains a demonstration version of the full WQIS as configured for the Berg River, complete with installation requirements

Theme Two research (field-scale-processes and large-scale mapping):

- iii) *Volume 3: Water and soil quality information for integrated water resource management: The Berg River catchment* by W.P de Clercq, F. Ellis, M.V Fey, M van Meirvenne, H Engelbrecht, G de Smet.

Volume 3 also includes a soils map with legend and Salinity Hazard map of the Berg River catchment as a free-standing program that allows viewing and printing of the maps.

An Executive summary is presented that highlights all aspects of theme two of this research. The full report is, however, presented on the accompanying CD with an interactive Acrobat version of the maps, lodged inside an envelope inside the back cover of each paper document.

1.5 CAPACITY-BUILDING

Department of Civil Engineering, University of Stellenbosch

Human resource development: The Project Team comprised four young professionals who are all members of the so-called "Designated Group" under the Employment Equity Act of 1999. These researchers are:

- Ms Nadia Nitsche (Civil Engineer and River Flow / Water Quality Modeller)
- Ms Jean Tukker (Hydrologist and Software Developer)
- Mr Wageed Kamish (Chemical Engineer and Reservoir Modeller)
- Mr Maselaganye Matji (Hydrologist and Catchment Modeller).

Three of the team members have acquired Master's degrees based on this and related research.

Technology transfer: Demonstrations of an early version of the Water Quality Information System software were given to officials of DWAF (Dept.: Water Quality Management and Dept.: Water Resource Planning) in Pretoria, DWAF Regional Office officials in Bellville and officials of the Department of Agriculture in Elsenburg. Papers on the hydrodynamic modelling of Skuifraam have been read at the SAICE Conference in May 2001 in George and at the SANCIAHS conference in Pietermaritzburg in September 2001.

Department of Soil Science, University of Stellenbosch

Human Resource Development: The following persons from the Designated Group worked on the Project as Laboratory Assistants:

- Ms Kamilla Latief
- Mr Kenneth Davidse

On each of the farms, Rooihoogte and Broodkraal, a local employee from the Designated Group was trained by the Department of Soil Science researchers to do soil moisture readings with both the neutron probe and tensiometers, and also to take and preserve water samples.

Collaboration with Technikon: Mr Pieter Basson, a final year Technikon student in Civil Engineering, worked full-time on this project for a year to meet the Technikon requirements for full-time in-service training.

Technology Transfer: On 28 August 2001 three seminars were held on the farm Rooihoogte:

- *Besproeiingsgronde langs Berg Rivier met klem op Rooihoogte en Broodkraal plase*, by Freddie Ellis.
- *Sout voorkoms in besproeiingsgronde van Broodkraal en Rooihoogte*, by Hendrik Engelbrecht
- *Die omvang van brak, bestuur daarvan en die toekoms*, by Willem de Clercq .

The following papers were presented at the Cartographic Modelling and Land Degradation Workshop, Gent, Belgium, 24-25 September 2001:

- *Mapping soil salinisation in an irrigated vineyard in South Africa*, by W de Clercq, G de Smet and M van Meirvenne.
- *Land degradation on old land surfaces affected by termite activity in arid and semi-arid regions of South Africa*, by F Ellis.

Papers presented at congresses:

- *Contribution of termites to the formation of hardpans in soils of arid and semi-arid regions of South Africa*. Ellis, F., 2002. Paper delivered at the 17th World Congress of Soil Science, Bangkok, Thailand, August 2002.
- *Soils associated with microrelief features ("heuweltjies") occurring on an ancient land surface in the lower Berg River Valley*. Ellis, F., de Clercq, W.P. and Engelbrecht, H. Soil Sci. Soc. South Africa Congress, Pretoria, 2001.

Theses completed and in progress:

- De Smet G. (2001). *Mapping soil salinity in South Africa*. Land and Forest Management, Ghent University, Belgium. (Ing)
- Engelbrecht H. (2002). *Modelling soil salinity in the Berg River Catchment*. Department of Soil Science, University Stellenbosch. (MSc, in progress)
- De Clercq WP (2002). *Defining and mapping soil salinity hazard in irrigated vineyards of S.A.*, Department of Soil Management, Ghent University, Belgium. (PhD, In progress).

Rural Community Interaction: Discussions about this project have been held with representatives of the Saron and Wittewater (at Moravia) communities in the Middle- to Lower-Berg River catchment.

SECTION 1

**APPLICATION OF A HYDRODYNAMIC RIVER FLOW WATER QUALITY
MODEL: DUFLOW :**

APPLICATION TO THE BERG RIVER

CHAPTER ONE BACKGROUND

Impoundments and associated bulk water supply infrastructure are present in most South African river systems. Because of the disparate natural occurrence of rainfall and runoff, and its mismatch with water demand concentrations, many of these schemes have to incorporate inter-catchment transfers to meet demands in the face of inadequate local availability. Furthermore, water quality deterioration, because of human impacts through a wide range of land-uses and waste discharges, has for some time been recognised as a threat in South Africa, as it diminishes the utilisable part of the runoff in many catchments. These complexities increasingly offer challenges to water resource managers that require a response with integrative management philosophies and innovative management tools.

During 1997, in recognition of the aforementioned needs, the Department of Civil Engineering of the University of Stellenbosch, formulated a research proposal to the Water Research Commission (WRC) whose aim would be to serve the philosophy of Integrated Water Resource Management (IWRM), through the development of an integrated information system specifically for water quality - here abbreviated to "WQIS". To be useful to IWRM, this WQIS was to provide diagnostic and predictive utilities to serve technical planning and operational decision-making in a river system, but, simultaneously, provide appropriate information to support water managers in communication with technical stakeholders. It was also recognised that the project would need identification of a "prototype" catchment for development of appropriate WQIS approaches and to provide a relevant database.

One of the aims of this project was to develop Water Quality Information Systems (WQIS) to support both integrated management of a water resources system, and to support communication about water quality management with stakeholders and communities in the catchments of that system - In this study the Riviersonderend-Berg River (RSE-BR) System was used as the prototype catchment. To develop this WQIS, however, it was necessary to combine a suite of water quality models with a user interface so that the results of the modelling could be visually interpreted. **CE-QUAL-W2** (refer to Section 3 of this report), a two-dimensional hydrodynamic and water quality model was used to simulate the flow pattern and constituent profiles in the proposed impoundment in the system while **DUFLOW**, a one-dimensional hydrodynamic river flow and water quality model, was used to simulate the river. The application of the river model, DUFLOW, is discussed in the ensuing chapters.

CHAPTER TWO CONCEPTUAL CONTEXT OF MODEL APPLICATION

2.1 INTRODUCTION

Modelling is a tool that is necessary in water quality management as it "*provides the link between the conceptual understanding of the physical catchment characteristics and the empirical quantification of the hydrological, water quality and ecological responses*" (Pegram *et al*, 1997, pg 17).

The above quotation summarizes the importance of modelling in water quality management, as it is able to describe the interaction between ecology, water quality, hydrology and hydraulics and, most important, allow for *what-if* scenarios which enable the users to attain a clearer understanding of the responses of the system as a whole.

The definition of a model is given by Carstensen *et al* (1997) as: *the abstract representation of a real system by the ideas and constituents and functional relationships*. The term *model* is used in many different ways to describe any representation of the real system, such as a laboratory model, computational model or conceptual model. The term *water quality model* or *simulation model* is used in this study to describe which computational hydraulic and water quality software is being used and either *sub-models* or *algorithms*, describe the mathematical equations that represent the water quality processes.

The aim of hydrodynamic river water quality modelling is to describe and understand interactions between the hydraulics of the river and the chemical and biological water quality river constituents⁴. A model is very effective in assisting in water quality management decisions for different scenarios which would affect the river and the water users. As computers have been becoming more powerful, more complex systems and formulations of the interaction between the water quality variables have been able to be modelled and understood.

The aim of this chapter is to provide the reader with the basic concepts of modelling and to clarify the terminology that will be used in this chapter. Additionally, a review has been carried out on some of the well-known water quality programs that are available and the findings summarized.

2.2 HISTORY OF RIVER WATER QUALITY MODELLING

The history of water quality modelling can be divided roughly into four periods:

- **1925-1960**
The main water quality variables that were studied were Dissolved Oxygen (DO) and Biochemical Oxygen Demand (BOD). The algorithms concentrated on streams and estuaries. The goal was to manage effluent and understand its impact on the water body.
- **1960-1970**
The first available computers made it possible to apply more complex mathematical formulations and thus the first computerized models were developed. One of the first computer models that was developed was for a study on the Delaware Estuary (Thomann, 1963, cited by Orlob, 1992), by using the Streeter and Phelps oxygen sag equation which was developed in 1925 for the Federal Water Pollution Control Administration (now called the US Environmental Protection Agency (EPA)). This model has been used and applied extensively. These first models that were developed concentrated on the temperature, dissolved oxygen and biochemical oxygen demand, as these were the major studies that were done in the beginning.

⁴ A water quality constituent (also called water quality variable) is defined as a biological or chemical (organic or inorganic) substance or physical characteristic that describes the quality of a water body. (DWAf(c), 1993).

- **1970-1980**

In the mid-70s a number of models were developed which also incorporated the various other water quality constituents, as knowledge on the eutrophication of water bodies improved with research. Well-known modellers such as Chen, Orlob, Di Toro and Thomann developed elaborate nutrient/food chain models. (Chapra, 1997). Non-point control of water quality variables also became important during these years⁵. The increasing power of computers made it possible to study and model much more complex reaction processes of all the water quality constituents. Models were developed as decision tools for lakes, rivers and estuaries, some of which are DOSAG and QUAL1 which were developed by the Texas Water Development Board, and later extended to QUAL2E under the auspices of the EPA. (Orlob, 1992). QUAL2E is possibly the most used steady-state water quality model by practitioners in the English speaking world.

- **1980-date**

Since 1980 there has been growing emphasis on fully hydrodynamic modelling of rivers, reservoir and estuary processes, with closely-coupled water quality processes, as well as on the fate and transport of toxic substances. Also, the interactions of water quality constituents with the sediment are more widely researched and modelled (e.g. Chapra and Reckhow, 1983). Some ecosystem models consider several classes of algae, zooplankton, invertebrates, plants and fish. With the advancement in computer technology various models (i.e. reservoir, river and estuary) are incorporated together by interfaces and used as water quality management decision tools. Uncertainty analysis has also been added to water quality computer programs.

2.3 CONCEPTS IMPORTANT TO WATER QUALITY MODEL APPLICATIONS

Concepts important to water quality model applications include model constituents, attributes and concepts used in the actual model construction. There exists a wide range of terminology when describing the various aspects of models and model building, which according to Carstensen *et al.* (1997) is the result of the wide range of different scientific fields of researchers that work within the field of water quality management. Therefore, it is important to clarify the terms that will be used in this study.

2.3.1 Model Elements

In water quality simulations there are normally two primary types of model elements: variables and parameters. Examples of parameters are normally the kinetic coefficients of a chemical equation describing the response of a specific water body to outside or internal forces or stimuli (i.e. influenced by temperature, radiation, sediment, ratio of chemical mass, etc.). The parameters are determined either through field studies or in the calibration process or "transferred" from other comparable applications. Examples of state variables are the water quality variables, such as concentration or loads of phosphates, chlorophyll-a, etc. that are of concern to the modeller.

2.3.2 Model Attributes

Following are defined as model attributes:

Dimensions:

Models may be categorized as **zero dimensional, one dimensional, two dimensional or three dimensional**. Rivers are normally treated as one dimensional models, where the values of flow and quality only change in the longitudinal direction; one dimensional or two dimensional, where both longitudinal and depth-related dynamics are simulated, i.e. the lateral state is regarded as "average", reservoir models simulate the vertical changes. Zero dimensional models are normally only models that are used for reservoirs, these are also known as input-output models, here the assumption is made that the water is well mixed and only the input and output changes. Three dimensional models include the vertical, longitudinal and lateral changes.

Time:

The main distinction that is made among the various water quality models is between **steady state and dynamic models**. Steady state models assume that the variables do not change in time or in space,

5 Non-point pollution sources are distributed or dispersed discharges of pollutants from surface run-off, infiltration or atmospheric sources. (DWAF(c), 1993)

while dynamic models do take the variability of the variables in time and space into account and thus allow for modelling of non-point runoff and sudden increased effluent discharges. The output of the results is normally in the form of time-series.

Data:

Another division that can be made between the different water quality models is that of **deterministic** and **stochastic** models. In deterministic models (also sometimes referred to as mechanistic) a fixed relationship between input and output is assumed. This relationship may be empirical ("black box"), conceptual or mechanistic. Stochastic models allow for random variation in input parameters. The variations are described by statistical distributions. Observed streamflow and water quality data requirements for stochastic models are usually greater than for deterministic models to ensure reliable estimation of statistical parameters.

Purpose of Model:

Water quality models designed for computer solution are either **simulation** or **optimization** models. Simulation models calculate the concentration of the various variables based on the given river flow and the quantity and quality of the waste loading. Optimization models are effective in assisting management, as they include model management variables to test the impacts of certain management decisions.

Mathematical Computation:

The common basis for most water quality models is the principle of continuity or mass balance. The transport as well as the chemical and biological processes are calculated in many models. Transport processes that are usually included are advection, longitudinal and/or lateral dispersion, vertical convection (reservoirs) and eddy diffusion. A distinction in the equations is made between conservative and non-conservative variables. Conservative constituents undergo no chemical and biological changes and thus only the transport equations and geometrical characteristics of the river determine the concentration of the variable (i.e. TDS, Total Dissolved Solids). Non-conservative variables normally undergo biological and chemical changes and thus the water quality processes are more difficult to model.

Simulation models are normally solved either by formal integration of the basic differential equations or by numerical analysis techniques such as finite difference or finite element methods. Each of these approaches is based on a solution of simultaneous sets of linear and non-linear equations.

Input Data:

Another distinction is made between point sources and non-point sources. Point sources refer to the concentrated discharge of contaminants from a known source (i.e. effluent discharge from a sewage treatment works). Non-point sources are spatially distributed or dispersed discharges and export of contaminants derived from the surface and sub-surface drainage as well as from the atmosphere. They are often hydrometeorologically driven. The characteristics of point sources are much more easily understood as they are normally measurable. The difficulty in modelling non-point sources and point sources lies in the randomness with which they happen.

2.3.3 Model Application Steps

The steps that are taken when applying a model are:

- Identification of the problem that needs to be studied
- Model Selection
- Configuration
- Sensitivity Analysis
- Model Calibration
- Model Verification
- Scenario Analysis

Identification of a problem:

The identification of the problem is a very important step in the model building process, as it will determine which model to use and the amount of data that is needed. The objectives of the study normally determine which water quality variables need to be studied, the resolution of the model and the data needs. In South Africa different requirements in a model are usually needed when compared to

European models, as the focus tends to follow salinity and eutrophication and less on toxic substances modelling, which is presently the main concern.

Model Selection:

A choice of model is based on various criteria, of which the most common are:

- *the ability of the model to describe the specific problem*
A model should be selected based on its adequacy for the intended use, for the specific waterbody, and for the critical conditions occurring at that waterbody. An obvious consideration for narrowing the selection of an appropriate model is based on the waterbody type (river, estuary, or lake) and the type of analysis wanted (salinity, nutrients etc.).
- *whether the assumptions made in the model are relevant to the specific study area (i.e. the equations used)*
For some process algorithms, a number of assumptions have been made to decide on certain parameters and equations. Care needs to be taken that the algorithms are flexible enough to allow for alterations or are relevant to the study area, especially when models have been programmed for particular climatic circumstances, but then used in different circumstances.
- *degree of model complexity² and data availability*
The extent of the data that is needed for the model is often dependent on the model complexity. One should consider the data requirements and whether the required historical data is available. The level of analysis has to be appropriate to the problem investigated, i.e. simple models³ or complex models.
- *the resolution required for the specific problem (i.e. space and time step)*
The model has to represent the specific problem studied, i.e. if eutrophication has to be modelled, normally daily time steps are used, although a smaller time step might be more appropriate to accommodate the photosynthesis of the algae which fluctuates during the day.
- *the availability, cost and support of the model*
One should consider model familiarity, technical support and model availability, documentation quality, application ease, and professional recognition and acceptance of a model. There are a number of models available free of charge from the Internet (mainly EPA models such as WASP and Qual2E), while other models are very expensive for South Africa (e.g. Mike 11, ISIS; see section 2.5 for details).

For any specific water quality situation studied, the appropriate model depends largely on the problem investigated and the availability of the data required. Different models place emphasis on different water quality variables or just use different mathematical formulations which could be unsuitable for the specific river studied and the problem investigated. Most importantly, the model needs to be capable of configuration, calibration, verification and simulation within the limits of time and budget. This is difficult to determine at the beginning, as the configuration time is very dependent on the specific study and the prior knowledge of the model.

Sensitivity Analysis:

A sensitivity analysis is important for the calibration process, as it determines which parameters have a significant impact on the model results. The term objective function is used for the statistical functions that are applied to determine the degree of influence the parameters have on the results. A list of objective functions and the approach that should be used in model calibration and sensitivity analysis is given by Görgens (1983) for hydrological modelling, but the same approach applies to calibrating water quality models.

Calibration:

The definition of a model calibration is given in Thomann and Mueller (1987) as: the first stage testing or tuning of a model to a set of field data,...*such tuning to include a consistent and rational set of*

6 Complex is a relative attribute that assesses whether the model contains more than one state variable, parameter and type or there exist multiple solutions of the model equations. (Carstensen et. al., 1997)

7 A simple model is characterized by few parameters and equations. (Carstensen et. al. 1997)

theoretically defensible parameters and input. The value of the parameters can be deduced from field measurements, but normally adjustments are made to the default parameters in the model until an optimal fit is achieved between the simulated data set and the measured prototype data. The >goodness-of-fit= is determined by curve-fitting and applying the objective functions to analyse the goodness-of-fit. Consideration should be given to the realistic range that the parameters can have in the specific model for the specific water body. The process of the calibration includes firstly ensuring the accurateness of the input data, boundary functions and the physical representation of the river and then secondly adjusting the parameters.

Verification:

The terms verification and validation are often both used to describe the confirmation of a model by using a set of data that is totally independent of the data set that has been used to calibrate the model. Carstensen *et al* (1997), Chapra (1997) and Reckhow *et al* (1990) discourage both terms and propose terms such as confirmation, robustness and corroboration for this model step, as "*...it is obvious that a model can never describe reality completely. Therefore, there will always exist experimental conditions for which the model is not valid. Hence, validation of a model is utopian!*" (Carstensen *et al*, 1997, pg. 164). However, in this study the term verification will be used to describe the process of ensuring that the model applied to the specific river for a set of data can be applied to another situation and validation is the examination of the numerical models used to describe the water quality processes and the computer code to ascertain that there are no numerical problems with obtaining a solution. Validation is normally the concern of the algorithm and software developers and the assumption that the model is valid numerically is already made at the beginning of the model building.

Scenario Analysis:

The verified model is then used for different scenario analysis. When using the verified model for different scenarios the uncertainty of the parameter estimation and data errors have to be kept in mind as different scenarios could affect the parameter that has been used to calibrate the model and increase the error. A scenario analysis is also sometimes termed a model postaudit (Thomann and Mueller, 1987; Chapra 1997).

2.4 DATA CONSIDERATIONS FOR MODEL USE

The resolution of data requirements is very dependent on the modelling method. The data requirements depend on the complexity of the model and the make-up of the overall uncertainties present:

"The underlying uncertainty is due to inherent randomness of the natural phenomenon. However, uncertainty arises also from the inaccuracies in the estimation of the parameters and in the choice of distribution. Uncertainties associated with errors of parameter estimation can be reduced by increasing the amount of data, whereas the uncertainty associated with the inherent variability may remain unchanged or may even increase with additional data". (Ang and Tang, 1975)

As can be seen from the quotation, uncertainty in the data result mainly from:

- quality of data
- parameter estimation

Uncertainty of results can be divided into the uncertainty which arises from the deviation in measurements itself, as well as in uncertainty which arises due to errors in estimating the parameters:

Quality of data:

The errors that can occur can result from:

- different laboratory techniques and errors in laboratory measurements
- different sampling times (e.g. in case of constituents such as phytoplankton that is dependent on the light during that specific hour)
- different sampling position (e.g. samples taken in small pools might show higher concentration than in flowing water)
- precision of data needed for river schematization, i.e. river geometry, flow measurements and river bed roughness coefficient

Parameter Estimation:

The confidence of the value of parameters has normally been established in the calibration procedure. A sensitivity analysis should be used to indicate which parameter has a significant influence on the simulation results.

Objective Functions:

Statistical indicators that determine the goodness-of-fit between measured and simulated data are called objective functions. The statistical goodness of fit tests gives the modeller information on the degree of the error between observed and simulated values, as well as the degree of influence a certain parameter might have on the results. There are several different statistical tests that can be performed on the two sets of data and depending on the model, the objectives and the problem studied, appropriate objective functions can be selected. Some statistical methods that can be used are described in Görgens (1983) and Reckhow *et al.* (1990). Görgens (1983) also describes the procedures one should follow when using objective functions in sensitivity analyses and calibration procedures. The statistical objective functions used in this study are explained in Section 7.2.

2.5 REVIEW OF WATER QUALITY MODELS FOR RIVERS

Available models cover a range of purposes, such as combined river and reservoir models, rainfall-runoff models, catchment models, ground water models or only stream hydraulics models. The review of models below reviews hydrodynamic water quality models (except for Qual2E, which is steady state).

Below, a short description is given to various models that are currently available and Table 2.1 summarizes the main features.

2.5.1 American Models

WQRRS

(Hydrologic Engineering Centre, 1978)

The WQRRS (Water Quality for River-Reservoir Systems) package includes SHP (Stream Hydraulics package), WQRRSQ (Stream Water Quality) and WQRRSR (Reservoir water quality model). The three components of the system may also be used independently. The hydraulic computations can be calculated either by hydrological routing, kinematic routing, steady flow equations or by the unsteady flow equations (using St Venant equations). The stream hydraulic module routes down the flow using several different methods (St. Venant equations, Kinematic Wave, Muskingum, Modified Puls) and is able to model both steady and unsteady flow regimes. The river quality module assumes, on the contrary steady flow conditions, and models aerobic degradation as well as simple diffusion of non-reactive pollutants. The water quality models are able to calculate dissolved oxygen, total dissolved solids, the nutrients, alkalinity and carbon, two types of phytoplankton, benthic algae, zooplankton, benthic animals and three types of fish, organic sediment and coliform bacteria.

CE-QUAL-RIV1

(Environmental Laboratory, 1995)

This model is a fully dynamic one dimensional flow and water quality simulation model (US Army Corps of Engineers Waterways Experiment Station 1990). It was developed by the Ohio State University for the Environment Protection Agency (Bedford *et al.*, 1983). This model is developed for highly unsteady flow conditions, and is able to handle various control structures as well as multiple control structures, such as dams and navigation locks. The model also includes two stand-alone programs that can be interfaced or used separately. RIV1H is the hydrodynamic model which uses a numerical solution to the St Venant flow equations, RIV1Q is the water quality program that simulates temperature, dissolved oxygen, biochemical oxygen demand and nutrients.

QUAL-2E

(Brown, L. And T.O. Barnwell, 1995)

QUAL2E has a long history with its first model being QUAL1 which was developed by the Texas Water Development Board (Orlob, 1992). The early and widespread use of QUAL2E makes it a standard against which other models are normally compared (Shanhan *et al.*, 1998), but it also has a particular limitation in that it cannot simulate unsteady flow.

The Enhanced Stream Water Quality Model (QUAL2E) is applicable to well mixed, dendritic streams. It simulates the major processes of nutrient cycles, algae production, benthic and carbonaceous demand, atmospheric re-aeration and their effects on the dissolved oxygen balance. It can predict up to 15 water quality constituent concentrations. It is intended as a water quality planning tool for developing total maximum daily loads (TMDLs) and can also be used in conjunction with field sampling for identifying the magnitude and quality characteristics of non-point sources. By operating the model dynamically, the user can study dissolved oxygen variations and algal growth. However, the effects of dynamic forcing functions, such as headwater flows or point source loads, cannot be modelled with QUAL2E. QUAL2EU allows users to perform three types of uncertainty analyses: sensitivity analysis, first order error analysis, and Monte Carlo simulation.

WASP

(Ambrose *et al*, 1993)

The Water Quality Analysis Simulation Program (WASP) was developed and is maintained by the Environmental Protection Agency (EPA). It includes simulation for rivers, reservoirs and estuaries. It simulates time varying responses, the equations used are dispersion and advection. Point and non-point loading can be modelled and the water quality processes are modelled in special sub-routines which allow the user to supply his own processes that are specific for the problem studied. It allows, by representing the water body as different segments, for one dimensional, two dimensional and three dimensional modelling. WASP consists of the hydrodynamic model DYNHYD and the water quality model WASP. WASP includes two different groups of water quality models, firstly EUTRO which is used to simulate dissolved oxygen, biochemical oxygen demand, nutrients and eutrophication., secondly TOXI, which simulates toxic pollution, comprising organic chemicals, metals and sediment. DYNHYD and WASP are able to stand-alone, i.e. be used without the other model.

2.5.2 European Models

DUFLOW

(STOWA/EDS, 1998)

DUFLOW (Dutch Flow) is the joint ownership of the Faculty of Civil Engineering at Delft University of Technology and the Public Works Department (Rijkswaterstaat), International Institute for Hydraulic and Environmental Engineering (IHE), the Delft University of Technology, the Agricultural University of Wageningen and STOWA. It includes three models, DUFLOW the hydrodynamic water quantity and water quality model, RAM, the precipitation runoff module and MODUFLOW, which incorporates Duflow with the ground water module MODFLOW. DUFLOW comes with two predefined water quality models, EUTROF1 and EUTROF2. Similar to WASP, the water quality processes can be modelled in special sub-routines which allows the user to supply his own processes that are specific for the problem studied. The flow model is a one dimensional and uses the St Venant equations with numerical solution to calculate the flow. EUTROF1 includes the cycling of nitrogen, phosphorous and oxygen, as well as the growth of one phytoplankton species. In EUTROF2 the sediment water interaction is included as well as three algae species.

ISIS

(HR Wallingford, 1997)

ISIS contains various separate modules: the ISIS Flow, the ISIS Quality and ISIS Routing.

ISIS Flow is a full hydrodynamic simulator using 4 point implicit finite difference scheme as numerical solution for modelling flows and levels in open channels and estuaries. ISIS Flow is able to model complex looped and branched networks, and flood plain flows. ISIS Flow has options that include simple backwaters, flow routing and full unsteady simulation. Common types of bridges, culverts, sluices and weirs can be modelled.

ISIS Quality simulates water quality and includes advection / diffusion of conservative and non-conservative water quality variables, as well as water temperature, sediment transport, interaction of quality variables with sediments, phytoplankton and pH. The user is able to specify the processes included in the simulation.

MIKE-11

(DHI, 1992)

MIKE11 includes basic modules for rainfall-runoff, hydrodynamics, advection-dispersion and cohesive, as well as non-cohesive sediments and water quality simulations.

The hydrodynamic module provides an implicit, finite difference computation of unsteady flows in rivers and estuaries. Both sub-critical and supercritical flow can be described by means of a numerical scheme which adapts according to the local flow conditions. The computational scheme is applicable to vertically homogeneous flow conditions ranging from steep river flows to tidally influenced estuaries. In addition to the fully dynamic description, a choice of other flow descriptions is available, such as diffusive wave, kinematic wave and quasi-steady state.

The water quality module requires output from the hydrodynamic module, in space and time, of discharge and water level, cross-sectional area and hydraulic radius. Conservative constituents can be modelled with the advection-dispersion module. For non-conservative constituents the user needs an additional module, the water quality module, which simulates degradation of organic matter, the photosynthesis and respiration of plants, nitrification and the exchange of oxygen with the atmosphere. Two add-on modules are available for the Water Quality Module : the Water Quality Heavy Metals Module (WQHM) and the Eutrophication Module (EU).

Table 2.1 Comparison of model attributes

| | CE-QUAL-RIV1 | QUAL2E | WASP | WQRRS | DUFLOW | ISIS | MIKE-11 |
|-----------------------------|--|---|---|--|---|---|---|
| Distributors | US Army Corps of Engineers Waterways Experiment Station | EPA | EPA | US Army Corps of Engineers Hydrologic Engineering Center. | Delft, IHE, Agricultural University of Wageningen and STOWA | HR Wallingford | Danish Hydraulic Institute DHI |
| Dimensional Characteristics | one | one | one, two and three for quality module, one dim. for river module, 2,3 for lakes and estuary | one | one | one | one |
| Hydraulics | unsteady flow | steady flow | dynamic, unsteady flow | hydrological routing, kinematic routing, steady and unsteady flow | fully dynamic | kinematic routing, steady and fully dynamic | kinematic routing, diffusive wave approx. and fully dynamic |
| Equations used | St Venant | steady flow | St Venant | St Venant | St Venant | St Venant | St Venant |
| Numerical solution | finite difference, 4 point Preissmann scheme | N/A | finite difference | finite elements | finite difference, 4 point Preissmann scheme | finite difference, 4 point Preissmann scheme | finite difference, 6 point Abbot scheme |
| Water Quality Transport | advection, dispersion | advection/ dispersion | advection, dispersion | advection/ dispersion | dispersion | advection/ diffusion | advection/ diffusion |
| Water Quality Variables | temperature, DO, BOD and nutrients, Chi-1, algae | temperature, salinity, BOD-DO, Nitrogen, Phosphates, Chi-a, conservative and non-conservative variables | open structure, two predefined models : TOX15 and EUTRO5 | DO, BOD, nutrients, TDS, alkalinity, 2 types of phytoplankton, benthic algae + animals, zooplankton, 3 types of fish, organic sediment and chl-a | open structure, 2 predefined models EUTROF1 and EUTROF2 | open structure, predefined quality model; conservative and non-conservative pollutants, water temperature, sediment transport | conservative and non-conservative; phosphates, eutrophication, heavy metals and sediments |
| Point/ Non-point sources | Point Sources | Point sources | point and diffuse mass loading | Point loading | point loading, diffuse loading only with prec., runoff module | point loading | point loading |
| Cost (at time of 1999) | Available from US Army Corps of Engineers Waterways Experiment Station | available from EPA through the internet, QUAL2E US\$ 330 | available from EPA through the internet, WASP5/ DYNHD5 US\$ 330 | available from US Army Corps of Engineers Hydrologic Engineering Center. | R 12 000 (DFL 4000) | R 50 000 (+ R10000 per module) | R 100 000+ |

2.6 DISCUSSION

In the case of the current Berg River study the following selection criteria have been declared important by the potential management-orientated user group surveyed by the Project Team (DWAF, pers. comm., 1999):

- user friendliness of model, availability and support of model
- cost of model
- ability to model water quality variables identified as variables of concern: salinity, oxygen, temperature and phosphates
- applicability, or ability to adjust to South African situation
- fine time resolution (daily)
- should be a hydrodynamic model for modelling flow variations during floods, low flows and in tributaries in time and space
- cost, availability and support in South Africa

With the introduction of the new Water Act in South Africa, water resource management and planning involves various users and goals. In order to be able to execute decisions the user often does not want to rely on a complex model where extensive user expertise is necessary; but that is rather fast and reliable. If the model should be used as a management "tool", continuous support and availability is necessary. It is desirable to have a model that is flexible and can be changed according to the specific problems studied and encountered. The model should be able to cope with different time steps and also with sudden and fast releases of the proposed dam or sudden effluent spills that occur at a point source.

Using the selection criteria as a guide, it has been decided to use the DUFLOW model for this particular study. Although DUFLOW has the same limitations as say ISIS (no evaporation modelling), it is still much cheaper and has the advantage of comprising an open water quality structure where the water quality processes can either be simplified or added/removed, the model therefore is flexible to change to different water quality situations. The model allows the user to create a user-friendly way through windows based interfaces and a graphical editor. As it is a hydrodynamic water quality model, the time and space steps can be entered as desired by the user; thus allowing fine time resolution if needed. By inserting options for scenarios, the model could be used for management purposes.

CHAPTER THREE DESCRIPTION OF THE BERG RIVER BASIN

3.1 GEOGRAPHY

The Berg River lies in the Western Cape and its catchment lies between latitude 23° 45' and 33° 50' south and longitude 18° 45' and 18° 55' east. The Berg River rises in the Jonkershoek and Franschhoek mountains and flows in a north-westerly direction where it eventually discharges into the sea at Laaiplek. The major tributaries are the Franschhoek, Wemmers, Krom, Kompagnies, Klein Berg, Vier-en-Twintig Rivieren, Matjies, Platkloof, Boesmans and Sout Rivers. The river is about 270 km long and has a catchment of some 9 000 km² (DWAf(c), 1993).

Figure 3.1 shows the gauging stations situated in the Berg River main stem, as well as the tributaries.

3.2 TOPOGRAPHY, GEOLOGY AND CLIMATE

The mainstem river is about 160 km long from the headwaters to the sea and its width varies from 1 to 5 km near its headwaters to between 30 to 40 km long at the coast (Bath, 1989). The lower reach of the river is extremely flat so that sea water intrusion pushes up nearly 100 km from the river mouth under high tide conditions (Bath, 1989).

The Berg River is geologically an old river system. This can be seen firstly from the rapid fall in profile from headwaters which then flattens out in the Paarl area, secondly from the degree of meandering of the main river channel and thirdly the existence of multiple channels separated by low lying islands in the lower reaches and the great width of the river valley (Bath, 1989).

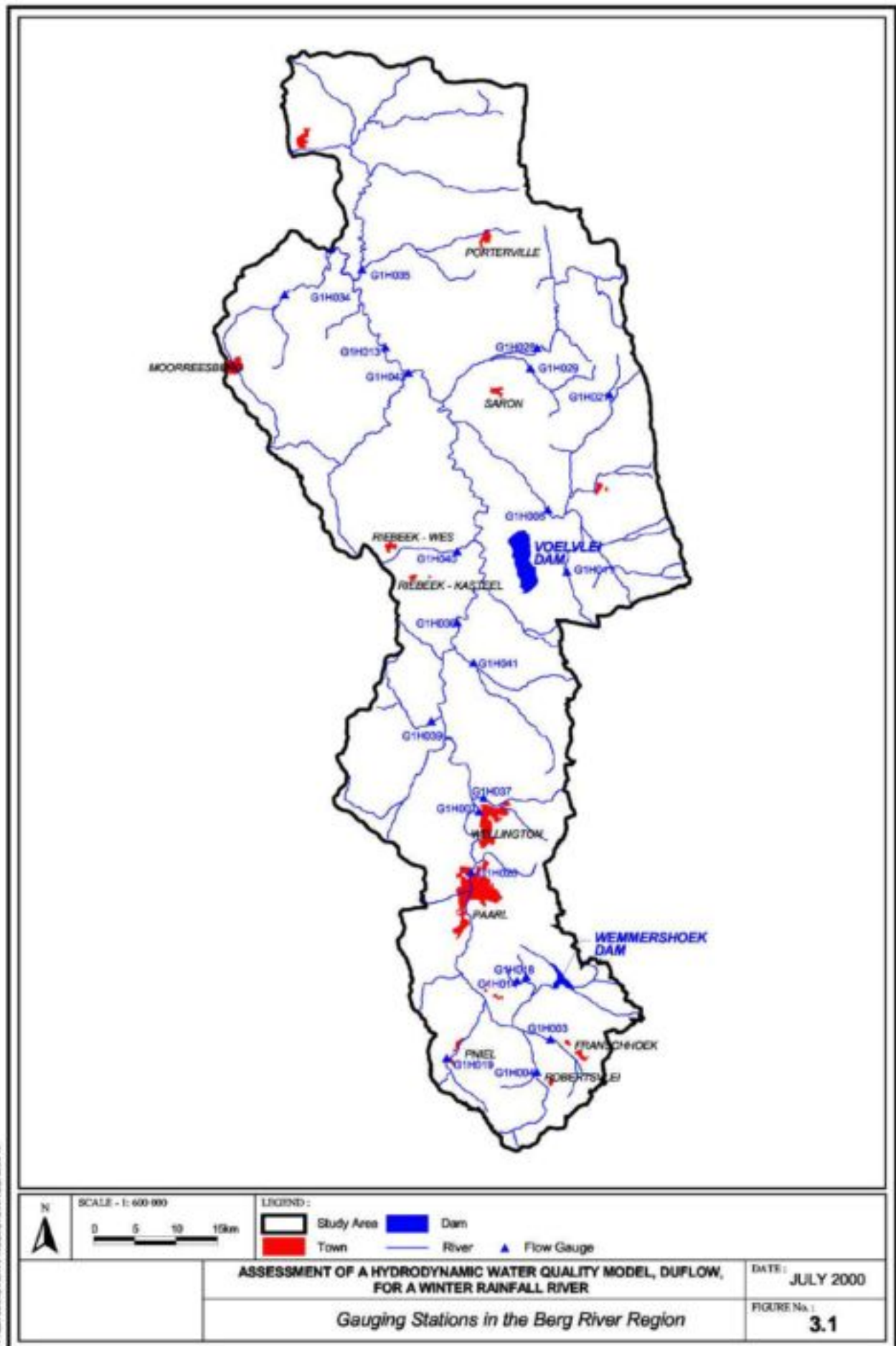
The basin of the Berg River is bounded on the eastern side by a range of mountains (RL 1500m), on the western side the basin flattens out to a hilly plain. Downstream of Paarl/Wellington sandstone formations give way to Malmesbury shales, thereafter tributaries on the eastern bank of the Berg River drain areas with Table Mountain Sandstone, while the western bank drains areas with the saline Malmesbury Shale as dominant geological formation (DWAf(e), 1993). Figure 3.2 shows the different geological formations found in the Berg River Catchment.

The Berg River catchment lies in the winter rainfall area of the south-western Cape, about 80% of the rainfall falls in the months of April to September. Rainfall in the mountains is about 3000mm per year (Midgley *et al.*, 1994). The snow that falls on the peaks and upper slopes of the mountains during intermittent cold spells in the winter also contributes to the flows. In the adjoining valleys, rainfall varies from 900 to 1200 mm annually, but drops to between 400 and 500 mm in the hilly plain through which the river flows most of its length, and to even less when it approaches the sea (Midgley *et al.*, 1994). The tributaries are perennial on the eastern side and semi-perennial on the western side.

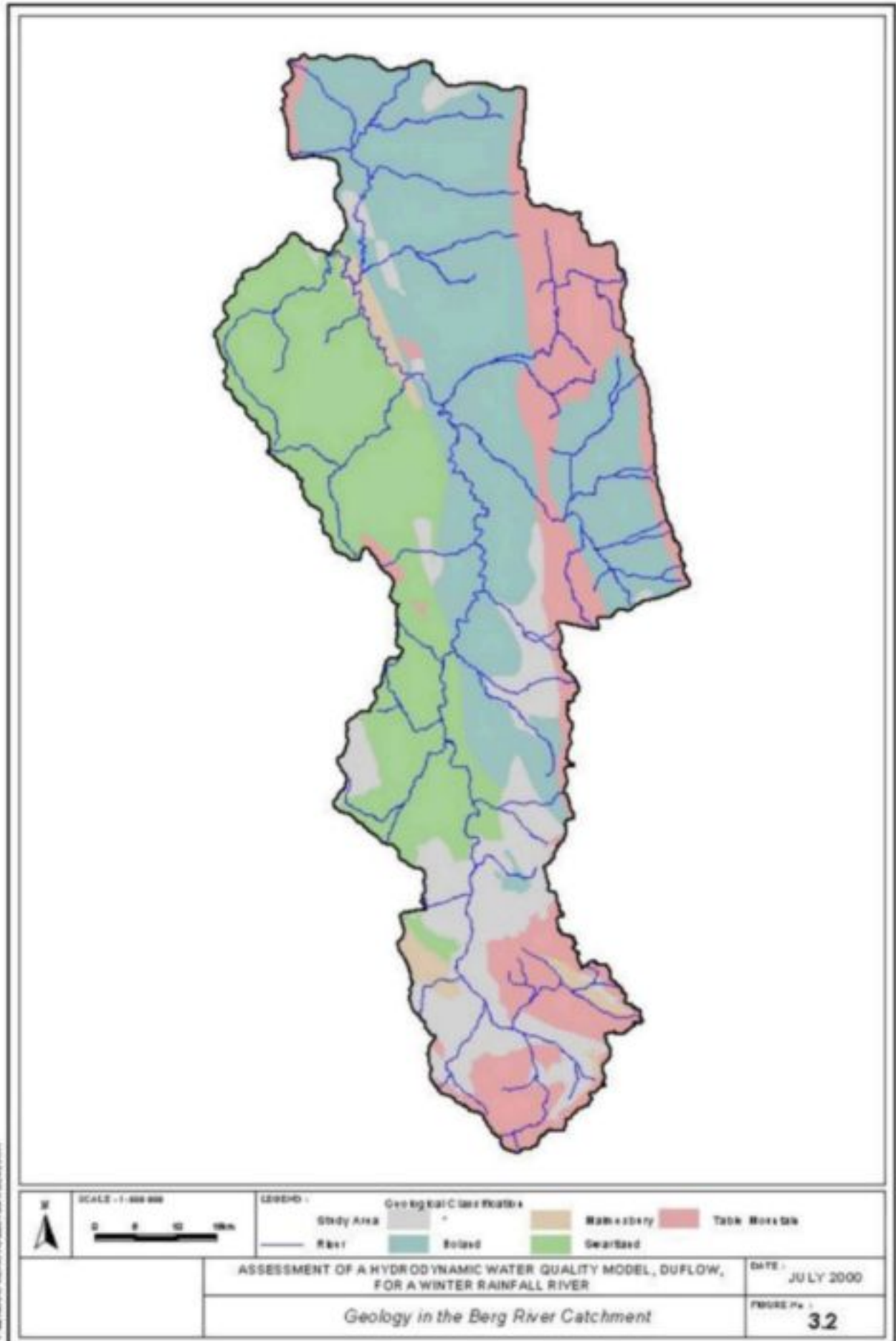
3.3 LAND COVER

Present land covers in the Berg River catchment fall primarily into three types: agricultural, forestry and urban. Agricultural land use is further divided into irrigated, and dry land farming activities. The latter of these make up the largest proportion of the catchment (DWAf(e), 1993).

There are 9 irrigation boards in the Berg River catchment area. These are: Perdeberg, Suid Agter Paarl, Noord Agter Paarl, Riebeekkasteel, Riebeek Wes and the Berg River under the Upper Berg River Irrigation Board, Twenty Four Rivers, Klein Berg River and Lower Berg River. From the allocated amount of water, Upper Berg River Irrigation Board uses about 41%, the Twenty Four Rivers Irrigation Board and Klein Berg River area about 27% and 24% respectively, while the lower Berg River Irrigation Board uses only about 8% of the water used for irrigation (DWAf(e), 1993). A summary has been given in the Situation Analysis of the Berg River (DWAf(e), 1993) of the areas of the various crops under irrigation in the upper and middle reaches of the Berg River. The data was obtained from the irrigation boards in the Berg River catchment and from Burger *et al.*, 1971. Although the data from Burger *et al.*, 1971, is old and possibly outdated, information from the irrigation boards still supported the recent data and the percentages of irrigation crops used has not changed much. Figure 3.3 shows the land use in the Berg River catchment, the lower reaches of the Berg River dry land farming is the predominant agricultural land use. Table 3.1 shows the percentage of crops irrigated in the upper and middle reaches (DWAf(e), 1993).



P:\BIRMAC\VIEW\PROJECTS\BIRTSCH\BIRTSCH.AWB



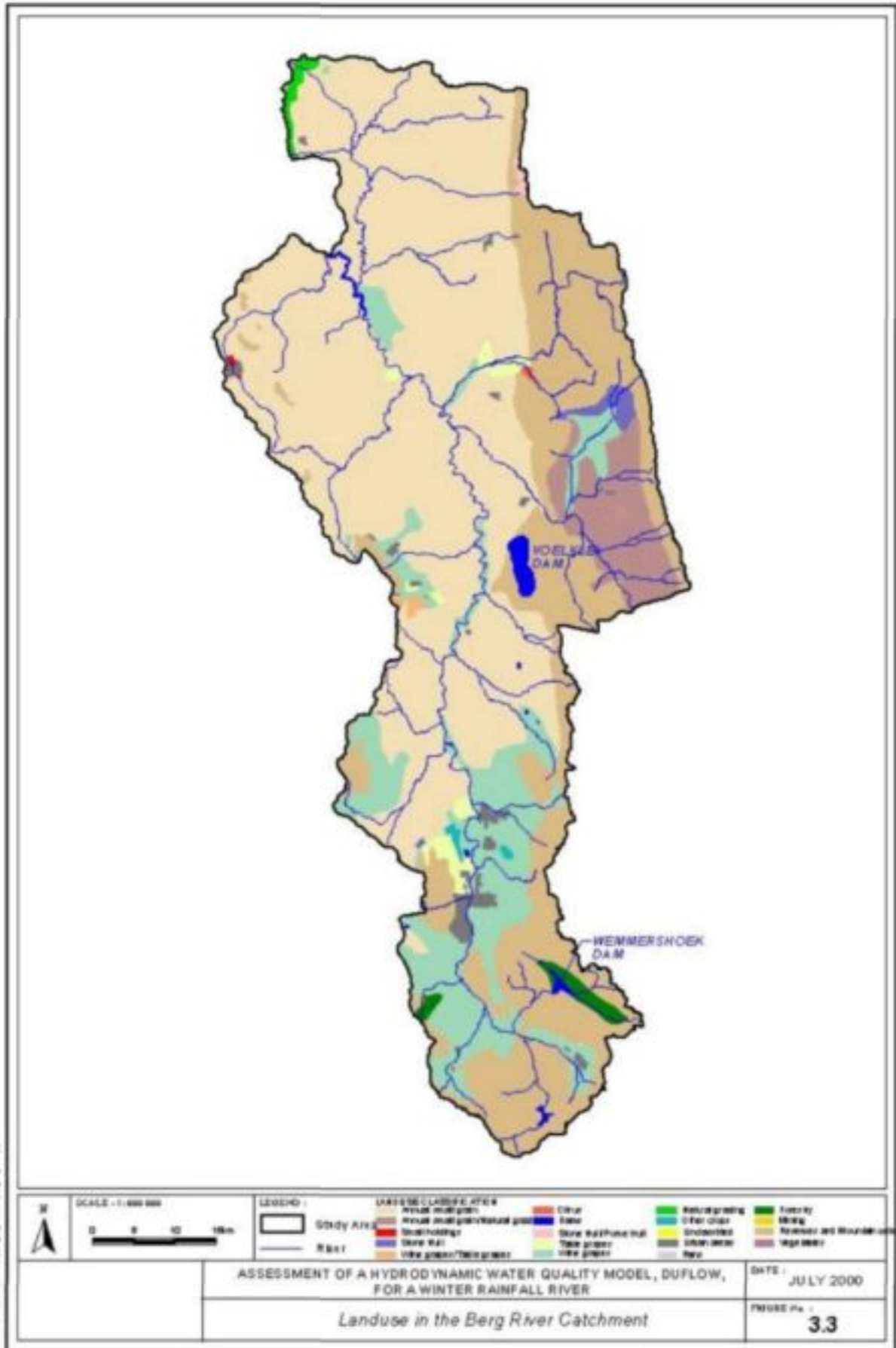


Table 3.1 Percentage of various crops under irrigation in the upper and middle reaches of the Berg River catchment (DWAFc, 1993)

| Crop | % Area irrigated in the upper and middle Berg River reaches |
|--|---|
| Soft Fruits (Apricots, Pears, Peaches etc.) | 7.7 |
| Sub Tropical Fruits (Oranges, lemon etc.) | 3.2 |
| Vineyards | 51.6 |
| Vegetables | 1.7 |
| Tobacco | 0.5 |
| Artificial pasture | 10.6 |
| Other (Almonds, Apples, Olives, Cherries etc.) | 24.7 |

3.4 WATER INFRASTRUCTURE DEVELOPMENTS IN THE CATCHMENT

3.4.1 Voëlvlei Dam

The Voëlvlei Dam was the first large water supply scheme that was developed in the Berg River. The first Voëlvlei scheme was completed in 1953. The natural Vogelvlei lake was impounded by building a small wall structure. As the natural vlei had a catchment of only 40 km², additional water was diverted from the Klein Berg River, where a small weir was built, into a canal to the dam. In 1971 the dam was raised to its present full supply capacity of 172 Mm³ (DWAF(c), 1994). The dam is currently supplied by diverted runoff from the Klein Berg River, and additionally Twenty-four Rivers and Leeu River catchments through canals. The dam supplies water to Cape Town, the Swartland Scheme and irrigation water for downstream users. The water for the Swartland Scheme supplies Riebeeckkasteel, Riebeeck Wes and Malmesbury, while the Voëlvlei water treatment works supplies Cape Town (DWAF(a), 1992). The irrigation water is released into the Berg River along with water for the Withoogte Scheme which is then abstracted from Misverstand Weir further downstream (DWAF(c), 1994).

3.4.2 Wemmershoek Dam

The Wemmers River was impounded in 1957 and supplies part of Cape Town's urban demand (DWAF(a), 1992). The Dam is owned by the City of Cape Town. The water from the Wemmershoek water treatment works supplies Cape Town, Paarl and Wellington (DWAF(a), 1992). The full supply capacity is 58.8 Mm³ and a yield of 56 Mm³/a (DWAF(a), 1992). During low flow in the Berg River this scheme releases compensation water to supply irrigation demands as far as the Voëlvlei canal. Since the completion of the Theewaterskloof-Riviersonderend (RSE) scheme the releases have been made from a tunnel into the upper Berg River at Robertsvlei.

3.4.3 Misverstand Dam

At Misverstand, in the lower Berg River, a weir was built across the river in 1975 to enable water to be abstracted (DWAF(c), 1994). The dam is linked to the Withoogte water treatment works via a 12.5 km pipeline, which supplies water to Moorreesburg, Vredenburg, Saldanha Bay and Langebaan. The capacity is about 6 Mm³ (DWAF(c), 1994).

3.4.4 Theewaterskloof Dam

Although the Theewaterskloof Dam and the Riviersonderend scheme do not lie in the Berg River, it does supply water into the Berg River. The Theewaterskloof Dam has a capacity of about 480 Mm³, and the system has a yield of 207 Mm³/a (DWAF(a), 1992). The dam was built in 1980 and is used to supply the Cape Town Municipality and irrigation in the Riviersonderend, Eerste and Berg River valleys (DWAF(b), 1994).

3.4.5 Future Developments

Due to mainly increasing population, a solution had to be found to meet Cape Town's increasing water demand. The following schemes are being investigated for imminent implementation in the Berg River: Skuifraam Dam in the Upper Berg, Skuifraam Supplement Pump Scheme downstream of Franschoek and Lorelei Diversions to an enlarged Voëlvei Dam in the Middle Berg (see Figure 3.4).

Skuifraam Dam:

Skuifraam Dam is proposed for the upper reaches of the upper Berg River just downstream of the confluence of the Berg and Wolwekloof Rivers. The dam would capture flood flows and transfer water to the Theewaterskloof Dam. The full supply capacity is supposed to be 168 Mm³ and the naturalised inflow is estimated to be 115 Mm³ (DWAF(d), 1994), the yield has been calculated to be 56 Mm³/a. Detailed operation rules and use of the Skuifraam Scheme is described in the report *Development of the Upper Berg River (Skuifraam Scheme)* (DWAF(e), 1994).

Skuifraam Supplement Scheme:

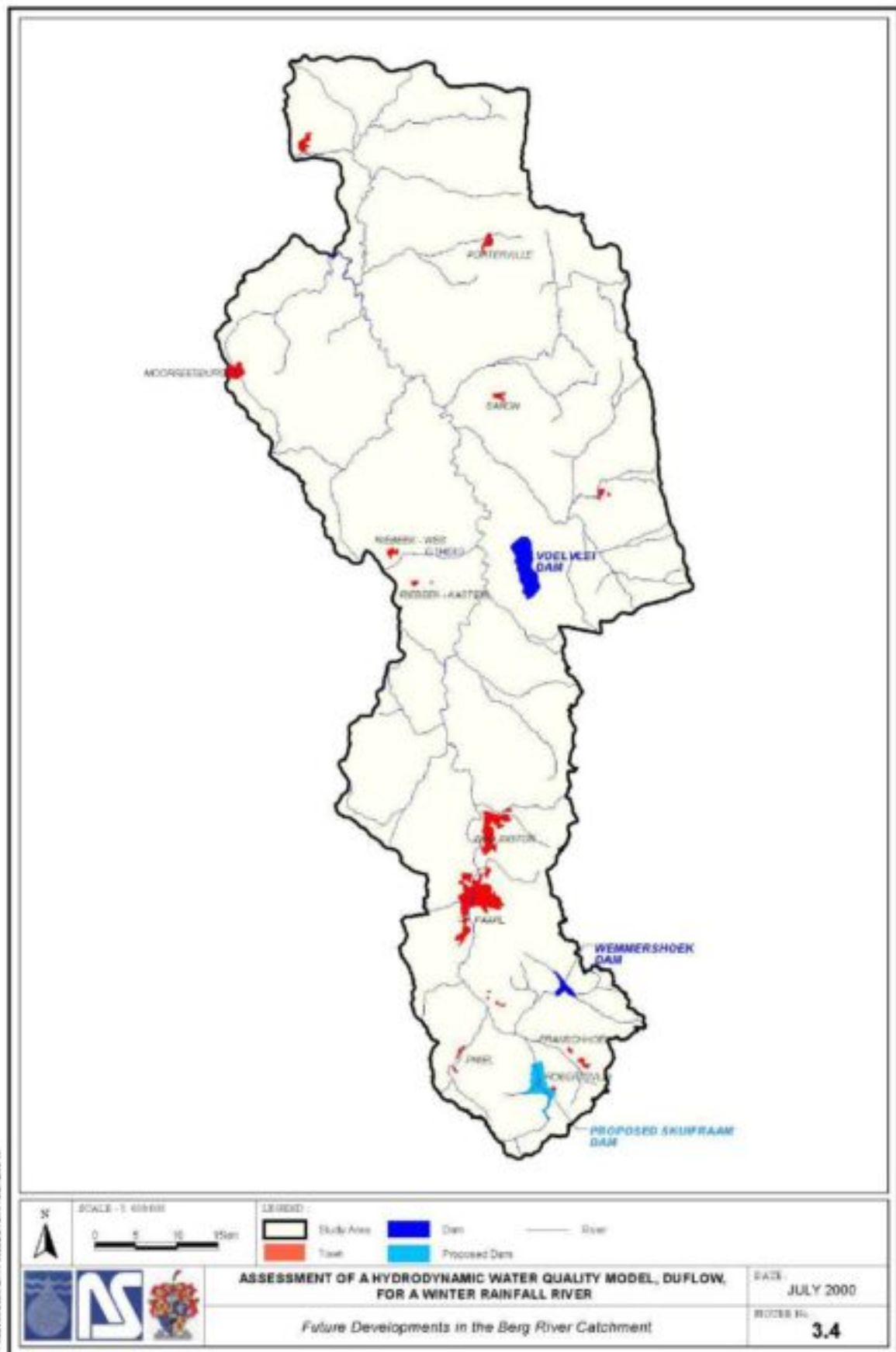
The MAR between Skuifraam and Paarl increases by about 150 Mm³/a (DWAF(d), 1994). Skuifraam Supplement Pumping Scheme has been proposed to abstract this potential water. The Skuifraam Supplement Scheme will have an off-channel balancing dam of about 4 ha and the height of the diversion weir will be about 5m (DWAF(d), 1994). The water will be pumped at a capacity of 4m³/s into a raised Voëlvei Dam.

Concerns have been raised that the salinity might increase after building the Skuifraam Dam, as the winter flow downstream of Skuifraam Dam would be reduced. A study done by Ninham Shand for the Western Cape System Analysis has however shown that this will have little effect on the salinity in the lower reaches (DWAF(b), 1993).

3.4.6 Operation of the Berg River-Theewaterskloof Link

The RSE scheme includes the Theewaterskloof Dam on the Sonderend River, a tunnel through the Franschoek mountains and an outlet in the upper Berg River which releases compensation water to supply irrigation demands in the Berg River, an tunnel in the Upper Berg River that passes under the Klein Drakenstein Mountains to a balancing dam at Kleinplaas on the Jonkershoek tributary of the Eerste River; a tunnel from the Kleinplaas Dam to an outlet near to Stellenbosch (DWAF(a), 1992). The four tunnels of the system are called the Franschoek tunnel/Jonkershoek Tunnel, the Stellenboschberg tunnel and the Dasbos tunnel which branches off the Jonkershoek tunnel. A pipeline connects the Franschoek/Jonkershoek Tunnel to the Wemmershoek Dam, while another pipeline connects the Kleinplaas Dam, which is situated on the Eerste River, to the Stellenboschberg Tunnel and an additional pipeline to the Blackheath water treatment works near Cape Town. Diversion works on the Banhoek and Wolwekloof Rivers (tributaries of the Berg River), allow surplus winter flows to be diverted and conveyed through the tunnel system into Theewaterskloof Dam where the water is stored. In summer it can then be released back through the tunnel system to the various outlets (DWAF(b), 1992). The releases into the Berg River include the 10 Mm³/a which have been previously made by Wemmershoek Dam and additional releases to supply allocation made from the RSE scheme to irrigators in the Berg River. The maximum capacity of the tunnel outlet is 6.6 m³/s (DWAF(b), 1994).

The proposed Skuifraam Dam would transfer water to the Theewaterskloof Dam or supply water direct to Cape Town via the Jonkershoek tunnel. The transfer will be achieved by pumping water through a pipeline into the Dasbos Tunnel and from there into the Franschoek/Jonkershoek Tunnel (DWAF(b), 1994).



CHAPTER FOUR

REVIEW OF WATER QUALITY STATUS OF BERG RIVER MAIN STEM

4.1 INTRODUCTION

To provide insight into the role a hydrodynamic model can play in the Berg River systems operations, it is necessary to assess the water quality status of the main stem of the Berg River and how it has changed through time.

To give a brief background to the studies that have been done in the past of the water quality situation in the Berg River, the most important findings are summarized in the first section of this chapter. These studies have been initiated due to concerns that water users have expressed about certain water quality variables.

From these studies, a minimum group of water quality variables of concern was identified, the relevant data assembled for the period of best availability; October 1992 to September 1998, and analysed for trends in comparison with the most recent source of information, i.e. the report '*Water Quality in the Berg River: A Situation Analysis*' (DWAF(g), 1993) which analysed samples taken until end of 1991. These results are discussed below in detail, showing the results in table format.

The study area was divided into four reaches and the data of the gauging station in the particular reach has been analysed and treated as "typical" values for the specific reach. Additionally, results are shown of gauging stations representing tributaries draining Table Mountain Sandstone, and a tributary draining saline Malmesbury shales as dominant geological formation. The quality of the water was also analysed by dividing the quality criteria into municipal and raw water users.

4.2 STUDIES DONE ON THE WATER QUALITY OF THE BERG RIVER

Concerns of salinity increase in the Berg River main stem and eutrophication at the Misverstand weir has led to various research investigations in the past.

One of the first studies was in the 1950s by Harrison and Elsworth (DWAF(g), 1993). This study was initiated to determine the degree of pollution of the river. Fourie and Steer (as cited by DWAF(g), 1993) and Fourie and Görgens (1977) investigated the mineralisation of the river. It was found that the salinity increases of the river could be the result of increasing irrigation along the river. Bath (1989) studied the phosphate transport of the river and concluded that 80% of the annual phosphorous was contributed by diffuse sources. The implementation of the 1 mg/l special standard for phosphate was postponed, as it was shown that it would have an minimal effect on the phosphorous loading in the river (DWAF(g), 1993). A phosphorous transport module was developed which should assess the fate and transport of phosphorous along the river in order to be able to control it (Bath and Marais, 1991).

Due to concerns that the salinity in the Berg River would increase if Skuifraam Dam would be built in the upper reaches where the good quality water would be impounded, a salinity modelling study was undertaken by Ninham Shand (DWAF(b), 1993). This study showed that the Skuifraam Dam would have relatively small effects on the salinity of the lower reaches in the river.

4.3 VARIABLES OF CONCERN

In line with the Situation Analysis by DWAF, which identified 12 variables of concern, the following variables of concern were considered:

- pH
- Salinity : Total Dissolved Salts (TDS) and EC
- Phosphate
- Temperature
- Oxygen

4.4 DELINEATION OF STUDY AREA

For ease of comparison we used the same division of the Berg River System as DWAF used in the Situation Analysis (DWAF(g), 1993). Water quality variables have been analysed and separated according to the river reach, one gauging station per reach representing the average expected water quality values. Additionally, the water quality data of gauging stations representing a tributary draining the Table Mountain Sandstone, and a tributary draining the Malmesbury Shales as dominant geological formation, have been analysed and evaluated. Figure 3.1 already showed the gauging stations in the Berg River Catchment.

The river reaches have been divided into:

River Reach 1

The river reach 1 includes the Berg River and all the tributaries upstream of Paarl (G1H020). No large urban or industrial sites occur in this region. The river and tributaries drain areas with Table Mountain Sandstone as dominant geological formation. The water quality data of G1H004 illustrates the quality of the water one can expect in the Upper Berg River.

River Reach 2

This reach covers the part of the catchment from Dal Josafat (G1H020) to Hermon (G1H036). Paarl and Wellington lie along this reach. Tributaries on the eastern bank of the Berg River drain areas with Table Mountain Sandstone, while the western bank drains areas with the saline Malmesbury Shale as dominant geological formation (DWAF(g), 1993). The reach stops just before the Voëlvelei canal where better quality water is released to supply downstream users. Summer irrigation demands are supplied by releases from the Theewaterskloof tunnel.

River Reach 3

This reach lies from G1H036 to the old Berg River pump station (G1H023). Only Klein Berg River and Twenty-Four Rivers drain the Table Mountain Sandstone. The water quality is improved by the releases of the Voëlvelei Dam to supply summer irrigation demands. This reach includes the impoundment at Miverstand from where the Withoogte WTW abstracts water.

River Reach 4

This reach marks the section that is influenced by the tidal effects and is consequently characterised by higher salinity. The water quality data of G1H023 is indicative of the water quality in this reach.

4.5 WATER USERS

In the comparison of trends that follow below the division of users into municipal and raw water users in the Situation Analysis (DWAF(g),1993) was accepted for this study.

4.6 ASSESSMENT OF pH

4.6.1 Introduction

The pH of water is determined by the concentration of the hydrogen ion (H⁺). A pH below 7 indicates that the water is acidic in nature, while above 7 it is alkaline. Most fresh waters are more or less neutral with pH ranges around 6-8 (Dallas, Day, 1993). The pH of natural waters influences physical, chemical and biological processes in the system. The surface waters in the upper Berg River Catchment tend to be acidic.

N.B.: In all the samples taken one can see a step of about +1 pH after 1989/1990. It should be noted that in 1989 DWAF improved the preservation of samples through a more efficient preservation method, as well as improving laboratory procedures, that prevented microbiological acidification in the sample (Dr P. Kempster, IWQS: pers.comm., 1998).

4.6.2 Main Stem Sampling Stations

Spatial Pattern

It can be seen from Table 1.1.3 (Appendix 1.1) that the tributaries on the eastern bank of the river tend to be more acidic than the waters of the western bank tributaries. This is because the tributaries on the eastern bank drain areas with Table Mountain Sandstone as main geological formation, which weather to acidic soils and are also low in salts. The water of the Berg River becomes more alkaline downstream with the more acidic water at the origin of the river. Refer to Table 1.1.1 (Appendix 1.1) for intervals of pH that were used by DWAF to analyse the quality of the water.

Temporal Pattern

| Findings in <i>Water Quality in the Berg River : A Situation Analysis (DWAF (g), 1993)</i> | Trends during 1992-1998 |
|--|--|
| The pH does not seem to indicate a seasonal trend, although unusual long-term changes were observed at river reach 3. In the early 1970's the pH varied between 7 and 8 while in the term 1970 to 1980 the pH declined and ranged from 5.5 to 7 in 1980. The pH increased again, especially in 1989, 1990 and reached values ranging from 7 and 8 in 1991. | The means of the different sampling stations seem to stay constant after the increase in pH in 1989/90. Only few samples fall above a pH 8.5 and thus no actual problems should be encountered with irrigation (refer to Table 1.1.1 and 1.1.2.4 in Appendix 1.1). At all the sampling stations (Figures 1.1.1 to 1.1.10, also Table 1.1.2 and Table 1.1.9 (Appendix 1.1)) the range of the pH's seems to deviate less from the median than was the case in the previous years and the values are concentrated more around the median. |

4.6.3 Municipal Supply

Many of the problems that are encountered by the municipal supplies occur due to the acidic nature of the water of the upper Berg River Catchment. The raw water tends to dissolve the cement lining of the water distribution networks (aggression) and thus the water needs to be treated in order to raise the pH. This increases the cost of the water treatment. The pH also influences the solubility of iron and aluminium. The concentration of these elements is quite high in waters with low pH, but as aluminium and iron are removed in the treatment process, problems would not be expected of the treated water. (DWAF(f), 1993). The intervals that were used by DWAF to assess the pH of the water can be seen in Table 1.1.3 (Appendix 1.1).

| Sampling Station | Findings in <i>Water Quality in the Berg River: A Situation Analysis (DWAF (g), 1993)</i> | Trends during 1992-1998 |
|---|---|---|
| Wemmershoek water treatment works G1R002 | At Wemmershoek water treatment works the pH lies mostly below the value of 6.5. This means that 'for most of the time the water is potentially aggressive to cement structures, and that the water would require a high lime dosage to condition the final water to pH 9'. It has been observed that the alkalinity of the water is mostly low (<5mg/l as CaCO ₃) and will thus react readily to lime addition. The pH of the water is nevertheless not considered to be a problem within the treatment works. pH does not seem to be seasonal. | Only 46 samples were taken during the period 1991 to 1998, with only 3 samples during 1993. The pH values seem to stay constant since the increase in 1989. The majority of the pH values of the samples lie between 6 and 7 (refer to Tables 1.1.4 and 1.1.12 and Figures 1.1.9 of Appendix 1.1). |
| Swartland water treatment works G1R001 | For 35% of the time the pH of the water is below 6.5, when excess lime needs to be used. The alkalinity is low and pH conditioning should not be a problem. The pH varies from 8.9 to 4.2 with a median of about 6.7. | The pH values deviate less from their mean in the years 1993 to 1998. From 1989 to 1993 more occasional high pH values (over pH 8.5) were measured. Most values are between 6.5 and 8.5 (refer to Tables 1.1.4 and 1.1.12 and Figure 1.1.8 of Appendix 1.1). |
| Withoogte water treatment works G1R003 | The pH seems to be seasonal, peaking in the summer months. The pH also seems to have increased over the years. The range, including the increase from 1989 to 1990, is from 5.3 to 8.8 with a median of 6.9. As most of the values lie between 6.5 and 8.5, there should not be any problems for municipal supplies. | The pH values lie mainly between pH 7 and 8. No values over pH 8.5 were observed. In the summer of 1992 some values were very low at pH 4 to 5, but thereafter the values were all above pH 6 again. The pH values seem to be seasonal but the seasonality seems not apparent in the years 1996, 1997. Here also, the deviation from the mean seems to be less than in the previous years (refer to Tables 1.1.4 and 1.1.12 and Figure 1.1.10 of Appendix 1.1). |

4.7 ASSESSMENT OF EC AND TDS

4.7.1 Introduction

Electrical Conductivity represents the ability of the water to conduct an electrical current. It is a measure of the concentration of dissolved salts and hence the salinity and total dissolved salts (TDS) contents of the water. Taste, hardness and corrosion are affected by the components of TDS, including chlorides, sulphates, magnesium, calcium and carbonates.

The South African Water Quality Guidelines expresses the target range in conductivity (mS/m) and lists the corresponding value for total dissolved solids in milligrams per litre (mg/l). Since the majority of material dissolved in most water is ionic, TDS and conductivity usually correlate closely for a particular type of water. (Dallas, Day, 1993) In the South African Guidelines the relationship between Total Dissolved Salts (TDS) and Electrical Conductivity (EC) is specified as:

$$EC \text{ (mS/m)} * 6.5 = TDS \text{ (mg/l)},$$

but in reality it varies, depending on the nature and concentration of the solutes present, their degree of dissociation into ions, the amount of electrical charge on each ion, the mobility of the ions and the temperature of the solution (DWAF (e), 1993).

To be able to compare the samples of the period 1980-1990 that were analysed for the Situation Analysis (DWAF(g), 1993) with the samples of 1991-1998, EC was taken as the measure of salinity.

4.7.2 Main Stem Sampling Stations

Spatial Pattern

High salinity occurs in the rivers draining the Malmesbury Shales (Doring, Fish, Sand, Matjies, Sout and Morreesburg Rivers). This makes the water of these rivers highly unsuitable for irrigation and yield losses should be expected. The tributaries draining the Table Mountain series as dominant geological formation show a low TDS concentration.

The water of the Berg River becomes more saline further downstream due to the runoff from the Malmesbury Shales.

Temporal Pattern

Refer to Table 1.1.5 (Appendix 1.1) for intervals of EC that were used by DWAF to assess the quality of the water for irrigation.

| Findings in <i>Water Quality in the Berg River: A Situation Analysis (DWAF (g), 1993)</i> | <i>Trends during 1992-1998</i> |
|--|--|
| It was detected in the analysis by DWAF that positive trends exist in the years 1980 to 1992 at all the points analysed for EC. It was implied that this increase in salinity is because of increases predominantly in the sodium and chloride concentrations. | Comparing the percentage of values falling in a certain range (see Table 1.1.6) one could say that the salinity has increased slightly over the years in the lower reaches, although this increase is not very high. From the Figures 1.1.11-1.1.16 one can see clearly that the EC has a seasonal pattern. The seasonal variation in conductivity for G1H020 (Figure 1.1.12) and G1H036 (Figure 1.1.13) is probably caused by saline irrigation return flow entering the river during the low flow summer months. (DWAF (d), 1993). Refer to Table 1.1.6 and Table 1.1.10 for statistics of salinity and percentages falling into th intervals specified. (All tables and figures in Appendix 1.1). |

4.7.3 Municipal Supply

The intervals that were used by DWAF to assess the quality of the water with respect to salinity can be seen in Table 1.1.7 (Appendix 1.1).

| Sampling Station | Findings in <i>Water Quality in the Berg River: A Situation Analysis</i> (DWAF (g), 1993) | Trends during 1992-1998 |
|---|---|---|
| Wemmershoek water treatment works G1R002 | The EC of the water supplied to Wemmershoek water treatment works remains steadily below 4 mS/m, except for an outlier on the 7 th August 1986: EC = 88mS/m, TDS value is 595 mg/l. | There does not seem to be an increase in EC values. Most of the samples taken fall below 5 mS/m. (refer to Tables 1.1.8 and 1.1.13 and Figure 1.1.19) |
| Swartland water treatment works G1R001 | The EC of the water ranges from 8 to 14 mS/m and problems should not be encountered. | All samples taken are below 25mS/m. There seemed to be an increase in salinity from the years 1992 to 1994, but thereafter it seems to decrease again and most samples are just above 11 mS/m. (refer to Tables 1.1.8 and 1.1.13 and Figure 1.1.18) |
| Withoogte water treatment works G1R003 | At Misverstand Weir the EC does not seem to be seasonal, but it has been perceived that the EC is higher in the wetter months in the year. It has been suggested that rainfall washoff is responsible for the higher salt concentrations and that long-term trends in the salinity are likely to follow the trends of the rainfall cycles. The range is from 13 to 95 mS/m with a median at about 37.2 mS/m. | There does not seem to be an increase in EC values at Misverstand weir. (refer to Table 1.1.8 and 1.1.13 and Figure 1.1.20) |

4.8 ASSESSMENT OF PHOSPHATES

4.8.1 Introduction

Eutrophication refers to water, particularly in lakes and reservoirs, which is high in nutrients and hence has excessive plant and algae growth, rendering the water less fit for use.

DWAF assessed the trophic status of the Berg River by examining the chlorophyll a concentration. For economy of efficiency it was decided to focus in this study on phosphates as indicator of the nutrient status.

4.8.2 Main Stem Sampling Stations

| Findings in <i>Water Quality in the Berg River : A Situation Analysis</i> (DWAF(g), 1993) | Trends during 1992-1998 |
|---|--|
| It has been observed by studying the chlorophyll a concentrations that the concentrations still fall within the South African target guideline range. It has been concluded that chlorophyll related problems for recreation or irrigation is unlikely. | An increase in phosphate concentrations at all stations (refer to Figures 1.1.31 to 1.1.37 and Table 1.1.11 in Appendix 1.1) can be clearly seen. In the years 1980-1990 there seems to be more occasional outliers in the concentrations. |

4.8.3 Municipal Supply

| Sampling Station | Findings in <i>Water Quality in the Berg River: A Situation Analysis</i> (DWAF(g), 1993) | Trends during 1992-1998 |
|--|--|---|
| Wemmershoek water treatment works G1R002 | From the analysis of the chlorophyll-a concentrations it was suggested that at Wemmershoek WTW, Voëlvei and Swartland WTWs no serious problems are expected with regard to the chlorophyll a concentrations. | At Wemmershoek water treatment works (G1R002) only few samples were taken and it is difficult to see any pattern to be able to compare it to the previous years. The samples taken show still a low phosphate concentration and thus there should be minimum algal growth (see also Figure 1.1.39 and Table 1.1.14 (Appendix 1.1)) |
| Swartland water treatment works G1R001 | From the analysis of the chlorophyll a concentrations it was suggested that at Wemmershoek WTW, Voëlvei and Swartland WTWs no serious problems are expected with regard to the chlorophyll a concentrations. | At the Swartland water treatment works the range of phosphorus lies between 0 to 0.04 with most values between 0.01 and 0.03, where previously the values mostly fell below 0.02 mg/l. Here also the concentration of phosphate is still relatively low (see Figure 1.1.38 and Table 1.1.14 (Appendix 1.1)) |
| Withoogte water treatment works G1R003 | "Nutrient concentrations in Misverstand weir are more than sufficient to sustain a large algae population, but the number of algae in this water body are held in check by the high turbidity of the system. Elevated turbidity reduces the amount of light available to the algae and hence inhibits their growth. However in the Misverstand weir the physical and chemical conditions are such that they promote the development of a type of algae which creates taste and odour problems at very low concentrations." (DWAF(g), 1993). At Misverstand weir the chlorophyll-a concentrations are much higher and the water needs to be treated accordingly. The chlorophyll a concentrations seem strongly seasonal with peak concentrations in summer. | From the graphs of Withoogte (Misverstand weir) and at Swartland water treatment works one can very clearly see that the phosphate concentrations have increased from 1991 onwards. The phosphate concentration ranges from 0.01 to 0.06 with most values at 0.025 mg/l as PO ₄ (refer to Figure 1.1.40 and Table 1.1.14(Appendix 1.1)). |

4.9 ADDITIONAL WATER QUALITY SAMPLES TAKEN IN THE BERG RIVER MAIN STEM

Additional water quality samples have been taken in the Berg River main stem weekly over a two month period. The water quality variables sampled were EC, pH, Oxygen and Temperature. The location the samples were taken are at:

- Bien Donne : lies upstream of Paarl, wine and fruit farm
- Picardi: lies in Paarl just upstream of railway bridge, samples were taken at the effluent discharge and just downstream of effluent discharge
- Wellington: samples were taken downstream of Krom River confluence at Sanddrift downstream of leather factory in Wellington

Table 4.1: Summary of water quality samples taken in the Berg River

| | pH | EC (mS/m) | O ₂ (mg/l) | Temp (°C) |
|-----------------------|-----|-----------|-----------------------|-----------|
| Bien Donne | 6.7 | 7.2 | 9.6 | 19.3 |
| Picardi (ds of effl.) | 6.8 | 8.4 | / | / |
| Picardi (at effl.) | 6.7 | 24.4 | / | / |
| Wellington | 6.9 | 17.2 | 7.7 | 18.4 |

Comparing the EC results (Table 4.1) with Table 1.1.10 (Appendix 1.1), it can be seen that the EC values measured upstream of Dal Josafat (G1H020) are below the mean of 10.6 mS/m at G1H020. At Wellington the EC value measured is 6.6 mS/m higher than the mean measured at G1H020. These measured values indicate that the EC in the river increases rapidly downstream of Paarl, which could be the result of the industrial effluent discharging into the river.

Comparing the pH results with Table 1.1.9, it can be seen that the pH samples measured just upstream of G1H020 (Bien Donne and Picardi) are below the average pH of 7.3 calculated for the historical grab samples taken at G1H020. The pH measurements taken at Wellington are also below the average at G1H020.

As no other oxygen samples have been taken in the Berg River no comparison to other samples can be made.

The temperature samples lie below 20°C. The samples have been taken between March and end of May, and comparing the results to Table 1.1.14 of section 6.3.1, these averages are to be expected.

4.10 CONCLUSIONS

Assessment of pH

After the change in preservation of samples (1989,1990) the pH concentration seems to be more consistent and deviates less around the mean. Problems that could occur for the municipal water users stem from the low pH of the upper Berg River and the acidic runoff from the Table Mountain Sandstone areas.

Assessment of salinity

No significant increase in salinity during the period 1992-1998 is evident and should therefore at this time not be necessarily a cause of concern. The lower part of the Berg River is much more saline than the upper reaches (which could create problems for the municipal supply and irrigation) and care should be taken that these reaches do not increase in salinity over the years.

Assessment of phosphate

At all stations a definite increasing trend in phosphates over the years can be seen. At the water treatment works the phosphate concentrations have increased during the years, although they still show low concentrations. It can therefore be assumed that most of the increase in phosphate is due to increasing land use and irrigation. In the years 1980 - 1990 there seems to be more occasional outliers in the concentrations.

CHAPTER FIVE SOFTWARE STRUCTURE AND MATHEMATICAL BACKGROUND TO DUFLOW WATER QUALITY MODEL

5.1 INTRODUCTION

On the basis of the review of available water quality models presented in Chapter 2, it was decided to use DUFLOW to model the Berg River because of the appropriateness of its scientific content, its user friendliness, the graphical interface and inexpensiveness compared to the various other packages that are on the market.

DUFLOW is jointly owned by the Faculty of Civil Engineering at Delft University of Technology and the Public Works Department (Rijkswaterstaat), International Institute for Hydraulic and Environmental Engineering (IHE), the Agricultural University of Wageningen and STOWA. For academic use, the cost for DUFLOW for Windows (version 3.0) and RAM (Precipitation runoff module) was 1000 Dutch Gulden. An additional 900 Dutch Gulden was paid for maintenance and service for a year. The delivery cost by DHL was an additional R92-00.

PC system requirements for using the DUFLOW Modelling Studio are :

- minimal 486, suggested is a Pentium
- minimal 16 Mb internal memory, a minimum of 24 Mb is recommended
- minimal 50 Mb external memory

Operating system requirements for running the DUFLOW Modelling Study is :

- Windows 95 or WindowsNT (4.00 or higher)

The DUFLOW package that was received late in October 1998 comprised an installation CD-ROM with a User's Guide and Reference Manual. For installing a component of the DUFLOW Modelling Studio (DUFLOW, RAM or Moduflow) a password is needed.

In this Chapter a short description is given of the software structure of DUFLOW.

Additionally an outline is given, firstly, to the basic hydrodynamic equations and, secondly, to the water quality processes, as well as the numerical method that DUFLOW uses to solve these equations. A numerical method which is used to determine the solution of complex equations is defined as mathematical expressions quantifying fundamental physical principles (Koutitas, 1983).

In this chapter emphasis is placed on the approach DUFLOW uses to quantify unsteady flow and to describe water quality processes. These approaches are common to most one dimensional hydrodynamic water quality models that use some form of an implicit scheme as numerical solution.

5.2 DESCRIPTION OF THE DUFLOW MODEL SOFTWARE STRUCTURE

5.2.1 Features of the Interface

The user interface consists of the following components:

- Menus
- Toolbars
- Status Bar
- Scenario Manager window
- Working space with the Network window and Results windows
- Output windows

The Network editor is a graphical editor that enables the user to draw the network schematization in a very user-friendly way. The mouse is used to place selected objects, such as nodes, sections and structures in the network window.

- *Nodes* are points at which one or more sections arise or end
- A *section* connects two nodes
- *Objects* that can be defined on sections are: structures, cross-sections, discharge points, etc.

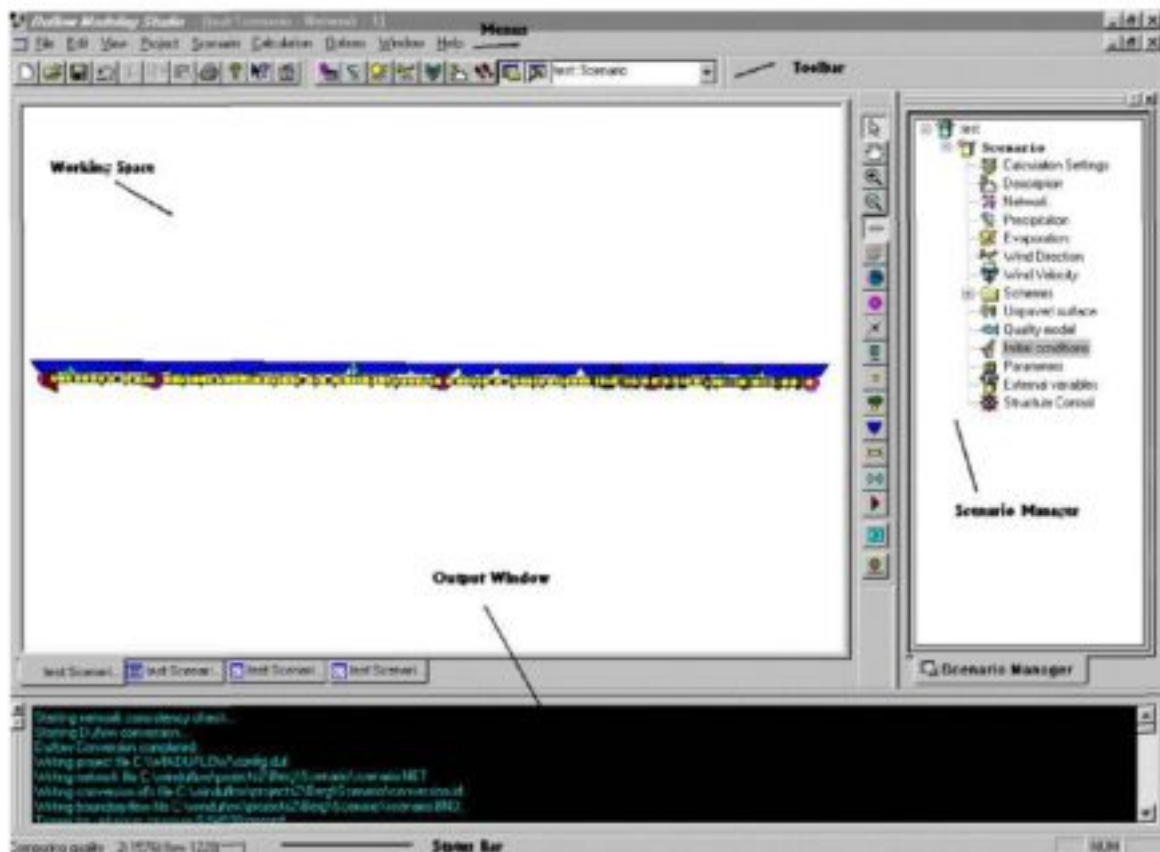


Figure 5.1 : User interface components

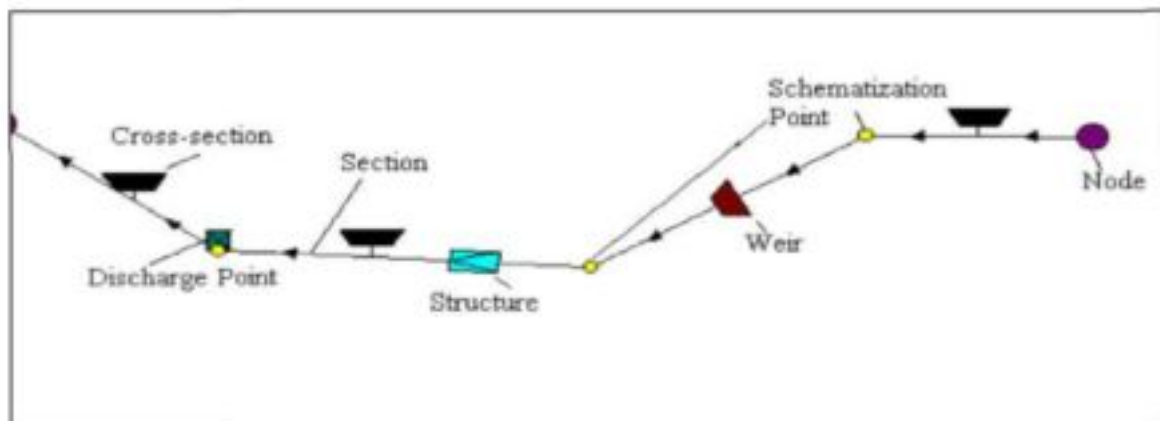


Figure 5.2 : Network Schematisation Objects

The properties of these objects can be modified in their property boxes. Cross-sections can be applied on miscellaneous places on the section. The cross-sectional profile over the entire section is interpolated between the different cross-sections given by the user.

5.2.2 Calculation Options

Type of calculations possible:

- *Flow* : Only flow can be calculated
- *Flow and Quality*: Flow and quality are calculated simultaneously

- **Quality :** (This option can only be used if an intermediate flow result file was generated in a flow calculation. In this case the necessary flow information for the mass transport is read from the intermediate flow result file.)
- **Box :** The use of this option enables the examination of the relative importance of the transport processes in comparison with the chemical and biological processes involved. Transport is not calculated, i.e. a steady flow is used where the parameters have been defined in the quality file. The calculations for the water quality thus only takes the processes into consideration (i.e. only the sinks and sources of the quality variable, the equations/processes are described in Section 5.4.5)

5.2.3 Import and Export of Data

Time Series that are used as boundary conditions and discharge points can be imported from and exported to external files in ASCII format. Results in text form can also be exported in the text form to be used in spreadsheets for statistical analyses.

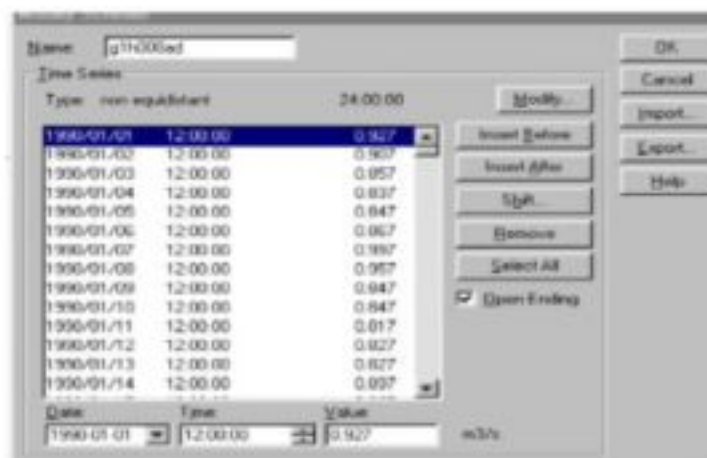


Figure 5.3 : Time Series Property Box

5.2.4 Presentation of Results

The results of a calculation can be displayed in three different ways:

- A Time Related Graph,
- A Space Related Graph (the user can define the route that should be plotted)
- Results as Text in a table as a function of time (makes it possible to export the results into spreadsheets).

Both text and graphs are displayed in windows. These windows appear in the working space. A result window can contain the output of more than one variable or the output from different scenarios.

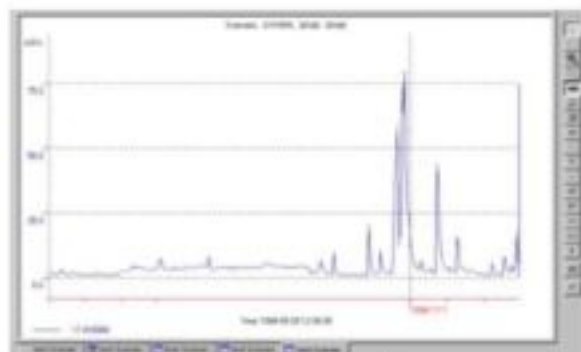


Figure 5.4: Time Related Graph



Figure 5.5: Space Related Graph

5.2.5 Configuration of the Model

Network Schematization

The configuration of the model occurs through the network window. One can create the model easily by dragging and dropping elements (such as nodes, sections, weirs, etc.) from the Network Palette into the Network window by using the mouse, one can easily modify the schematization with schematization or bending points.

Cross-sections are also first added by using a toolbutton from the palette. Cross-sections are defined by schemes and at every cross-section a scheme has to be connected to the cross-section. A scheme is created in the cross-section dialog box and the data is entered here for the cross-section. The same scheme could be added for every cross-section.

To add a structure such as a weir, the same procedure is followed. First, the user can click the weir toolbar from the palette and drag it into the network window. The position of the weir can be changed in the Object Properties box by changing the distance from the last node. The needed data for the weir needs to be entered into this box.

Discharge points are added at schematization points and here the user can define a time series of discharged water, wasted load or concentration.

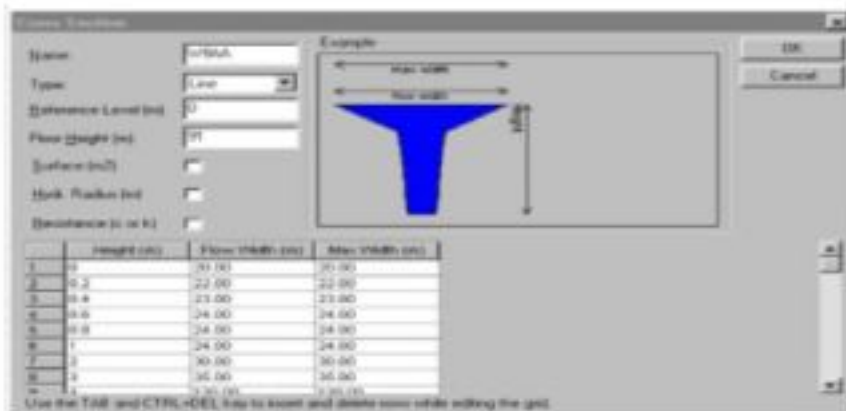


Figure 5.6 : Cross-section Property Box

Calculation Settings

In the calculation settings dialog box the start calculation time and time step need to be selected. The type of calculation also needs to be specified. When the flow calculation is verified, a quality model can be added.



Figure 5.7 : Calculation Settings Dialog Box

Scenarios

The programme consists of a Scenario Manager with which the user can define several different scenarios, without changing the base scenario. This gives the user the ability to see the result of different scenarios, such as pollution spills or sudden rainfall storms.

5.3 HYDRODYNAMIC MATHEMATICAL BACKGROUND

5.3.1 Introduction

DUFLOW can represent riverflow as non-uniform and unsteady. This is the most complex flow type as it requires the solution of the St. Venant equations through time and distance. A short description is given below to the mathematical approach to calculate unsteady non-uniform flow.

5.3.2 Unsteady Flow Equations

The equations used to analyse unsteady flow in an open channel are the continuity equation and the momentum equation, known as the St. Venant equations. The assumptions made in order to be able to apply the St Venant equations are, firstly, that the density of the water does not vary (incompressible); secondly, the slope of the river bed is small; and thirdly, that wave lengths are large compared to the water depth and thus vertical accelerations can be neglected.

Resistance

The channel friction can be calculated using De Chezy or Manning. Default in DUFLOW is the De Chezy coefficient.

Velocity Correction Factor

The correction factor for non-uniformity of the velocity distribution in the advection term, which is defined as:

$$a = \frac{A}{Q^2} \int v(y,z)^2 dydz \tag{5.4}$$

where the integral is taken over the cross-section A.

In the case of complex cross-sections, such as cross-sections including floodplains, $a = 1.05$ with v the velocity in the main stream. The value may be indicated as greater, but the v is then defined as the average velocity for the total section (Rooseboom *et al*, 1986).

Advection Term

$$\frac{\delta (aQv)}{\delta x} \tag{5.5}$$

can be broken into

$$a \left(2 \frac{Q\delta Q}{A \delta x} - \frac{Q^2 \delta A}{A^2 \delta x} \right) \tag{5.6}$$

The first item in equation 5.6 represents the impact of change in discharge, while the second term expresses the effect of change in the cross-sectional flow area and is called the Froude term. In cases of abrupt changes in cross-section this Froude term may lead to computational instabilities. DUFLOW allows the user in the calculation settings to choose between three ways of calculating the advection term (STOWA, 1998) :

- a) Total Froude : includes the Froude term
- b) Damped Froude : the absolute value of the Froude term will not exceed the friction term
- c) Neglected Froude : the entire Froude term is neglected.

The solution to the St. Venant equations is complex and therefore a number of numerical methods have been developed to get a solution to the equations. It has to be recognized that although the St. Venant

equations are capable of calculating supercritical flow, the numerical solution is not able to do so. Therefore, DUFLOW is unable to calculate supercritical flow.

5.3.3 Numerical Solutions to Unsteady Flow

Three principal types of numerical methods can be used to calculate open channel flow: method of characteristics, finite differences and finite elements.

Method of Characteristics

This method solves the unsteady flow equations by transforming the partial differential equations into normal differential equations and then solving them by numerical techniques. There are then two compatibility equations that are valid along two sets of characteristic lines. These methods can be divided into the way they are discretised (i.e. grid or rectangular methods). (Some of the researchers that have investigated this numerical scheme are : Lai, 1976; Ghidaoui and Karney, 1994.

Finite Element Methods

Finite element methods assume that the solution has a simple form over small elements. This leads to a system of simultaneous equations in matrices for each element, the equation is then solved inside each element by using the method of weighted residuals. This method is normally used in multi-dimensional modelling (Katopodes, 1984; Koutitas, 1983).

Finite Difference Methods

The finite difference methods, which are more commonly used than finite element methods, can be further classified as implicit and explicit methods. Explicit schemes provide the solution for Q and H at every next time step for each point on the distance grid, while implicit schemes provide the solution for Q and H at the next time step for all the points on the grid simultaneously, which makes it more complex, as it requires the solution of a number of simultaneous equations. Explicit schemes are easier to use but must conform to the Courant stability criteria in order to be stable ($c\Delta t/\Delta x < 1$, where c is the wave speed) (Koutitas, 1983), whereas the implicit scheme are conditionally stable for all time steps; this is the main difference between the implicit and explicit scheme. The implicit method is said to be more efficient than the explicit method as computation time is much less; larger time steps can be used without influencing the stability of the equations, nor the acceptable accuracy of the solution.

Table 5.1 : Comparison of finite difference schemes

| Scheme | Description | References |
|---|--|---|
| <i>Explicit finite difference schemes</i> | These schemes were the first to be applied to the St Venant equations and were widely used because of their simplicity in programming and execution. (Dooge, 1989). Explicit finite difference approximations that have been applied to flood routing include : The simple explicit scheme The diffusive scheme The leapfrog scheme The Lax-Wendroff scheme | Dooge (1989) Grijzen (1986) |
| <i>Implicit finite difference scheme</i> | In implicit methods the solution is obtained by applying the implicit scheme at each of the nodes along the channel simultaneously, combining the difference equations obtained in this way with the boundary conditions at each end and solving the whole set of equations simultaneously. Some of the implicit schemes are : 4 point Preissmann scheme Crank Nicholson scheme Linear implicit schemes | Amein (1968) Amein and Fang (1970) Fread (1973) Amein and Chu (1975) |

The 4 Point Implicit Preissmann Scheme

DUFLOW discretises the St Venant equations by using the four-point implicit Preissmann scheme, which is discussed below. Preissmann proposed a general four point implicit scheme with a weighting of θ in 1960 (Grisjen, 1986). The discretization is done in space and time, i.e. in a two dimensional grid (see Figure 5.8). The weighting $\theta = dt'/dt$ (refer to Figure 5.8). Therefore, the four point implicit schemes are unconditionally stable at $\theta=0.5$ as the point P, which lies between the time lines and space lines in Figure 5.8, lies exactly halfway between the time line n and $(n+1)$. For $\theta=1$ the solution scheme becomes fully implicit, as the point P is exactly on the time line $(n+1)$, while for a weighting of 0 the point P will lie on the current time line n and the scheme is then fully explicit (refer also to previous definitions of explicit and implicit schemes).

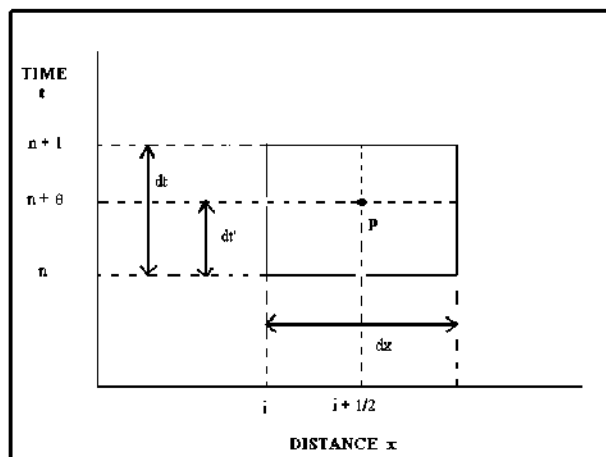


Figure 5.8 : Four-point Preissmann scheme

5.3.4 Boundary and Initial Conditions

A unique solution to the St. Venant equations requires two initial and two boundary conditions.

In DUFLOW the boundary conditions are user defined and may be specified as levels, discharges or a relation between the two. The best choice of what type of boundary to use, is the quantity or relation that is the least sensitive to the state of the model itself. Therefore, the upstream boundary condition in a river is preferably a discharge whereas the downstream boundary condition should be a water level, if the river flows into a lake or sea, or a level-discharge relation based on uniform flow, if the downstream boundary is somewhere along the river (STOWA, 1998). The accuracy of the boundary condition's readings are of great importance as they determine a realistic solution to the calculations.

The initial conditions are specified at every node and schematization point as flow conditions at the initial time step. In DUFLOW the initial conditions are defined as a discharge and a water level. Care needs to be taken at very low flow (i.e. discharge and depth near to a value of 0), as the numerical calculations could become unstable. Any inaccuracies in the initial conditions are cancelled out after a reasonable number of time steps.

5.3.5 Cross-sections

Information about the geometry of the river is needed for solving the set of equations. Information of the cross-sectional shape can be found from topographical maps or from surveys conducted in the area. For modelling purposes, cross-sections are often assumed trapezoidal, rectangular or of parabolic shape. DUFLOW gives the option to enter the cross-section as any of the three. The cross-section is entered as a function of depth, as can be seen in Figure 5.9. Therefore, storage areas and flow areas can be entered at different depths. When including the floodplain, a decision needs to be made whether to model the cross-section as a complex cross-section, or a number of parallel branches with the different

schematisations, introducing the flow from the floodplain as lateral flows into and from the main channel, as in Figure 5.10.

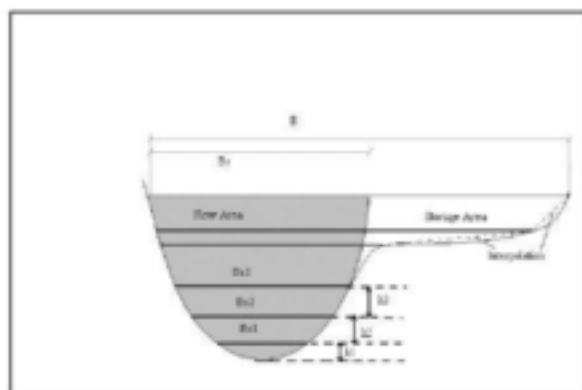


Figure 5.9 : Schematization of cross-sections

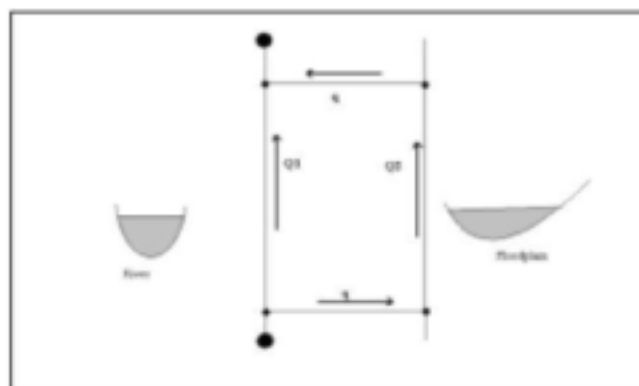


Figure 5.10 : Schematization of floodplain using lateral flows

5.3.6 Structures

Various types of control structures can be defined in DUFLOW such as weirs, culverts, pumps and siphons. Below is a description about general structures and weirs that were used in modelling the bridges and weirs in the Berg River. For a description on pumping systems, siphons and culverts the reader is referred to the DUFLOW Manual (STOWA, 1998). At weirs and other structures, discharges and levels can be modified and controlled by so-called trigger conditions, depending on flow conditions at specified locations in the network, parameters such as the width of a weir, the level of the sill, etc. can be adjusted during the computation to reflect for instance structural modifications during this period.

Weirs

The discharge over a weir depends on the water level on both sides, the level of the sill, type of structures and the flow conditions (free surface flow or submerged conditions). A structure is defined between two nodes, i and j and the discharge in the structure is denoted as Q . Figure 5.11 shows the flow conditions that can occur over a weir, where it is assumed that $H_i > H_j$. Under submerged conditions, if $H_i < H_j$, the conditions of flow are symmetrical with Figure 5.11 except for the loss coefficient. Table 5.2 should be read in conjunction with Figure 5.11. The general equation for the discharge over a weir is

$$Q_{n+1} = \mu B H \sqrt{2g\Delta H} \quad 5.14$$

Table 5.2 : The quantities that are used for different flow conditions (STOWA, 1998)

| Flow condition | DMS-object | μ | H | ΔH | Description |
|----------------|-------------------|---------|-------------------------|-------------------------|--|
| I | General structure | μ_0 | H_0 | $H_i^{n+1} - H_0$ | Vertical gate |
| II | General structure | μ_k | $\frac{2}{3} H_i^{n+1}$ | $\frac{1}{3} H_i^n$ | Vertical gate |
| III | Weir | μ_v | $\frac{2}{3} H_i^{n+1}$ | $\frac{1}{3} H_i^n$ | Flow over weir |
| IV | Weir | μ_v | H_i^n | $H_i^{n+1} - H_j^{n+1}$ | Flow over weir |
| V | General structure | μ_k | H_i^n | $H_i^{n+1} - H_j^{n+1}$ | Vertical gate |
| VI | General structure | μ_k | H_0 | $H_i^{n+1} - H_j^{n+1}$ | Submerged flow through underflow sluice gate |
| VII | General structure | μ_0 | H_0 | $H_i^{n+1} - H_j^{n+1}$ | Submerged flow through underflow sluice gate |

The parameters are defined as :

| | |
|------------|---|
| B | width of the weir, multiple notch handled by so-called trigger functions (refer to definition at end of this section) |
| μ | the loss coefficient |
| H | depth over the sill |
| ΔH | difference in head between upstream and downstream head |
| H_i, H_j | water depth over the sill respectively at the beginning and at the end of the section |
| HO | height of opening |
| μ_o | loss coefficient, gate flow |
| μ_v | loss coefficient, free surface flow |
| μ_t | loss coefficient, transition between μ_o and μ_v |

$$\mu_t = \mu_v + 2 \left(\frac{H_i}{HO} - 1 \right) (\mu_o - \mu_v) \quad 5.15$$

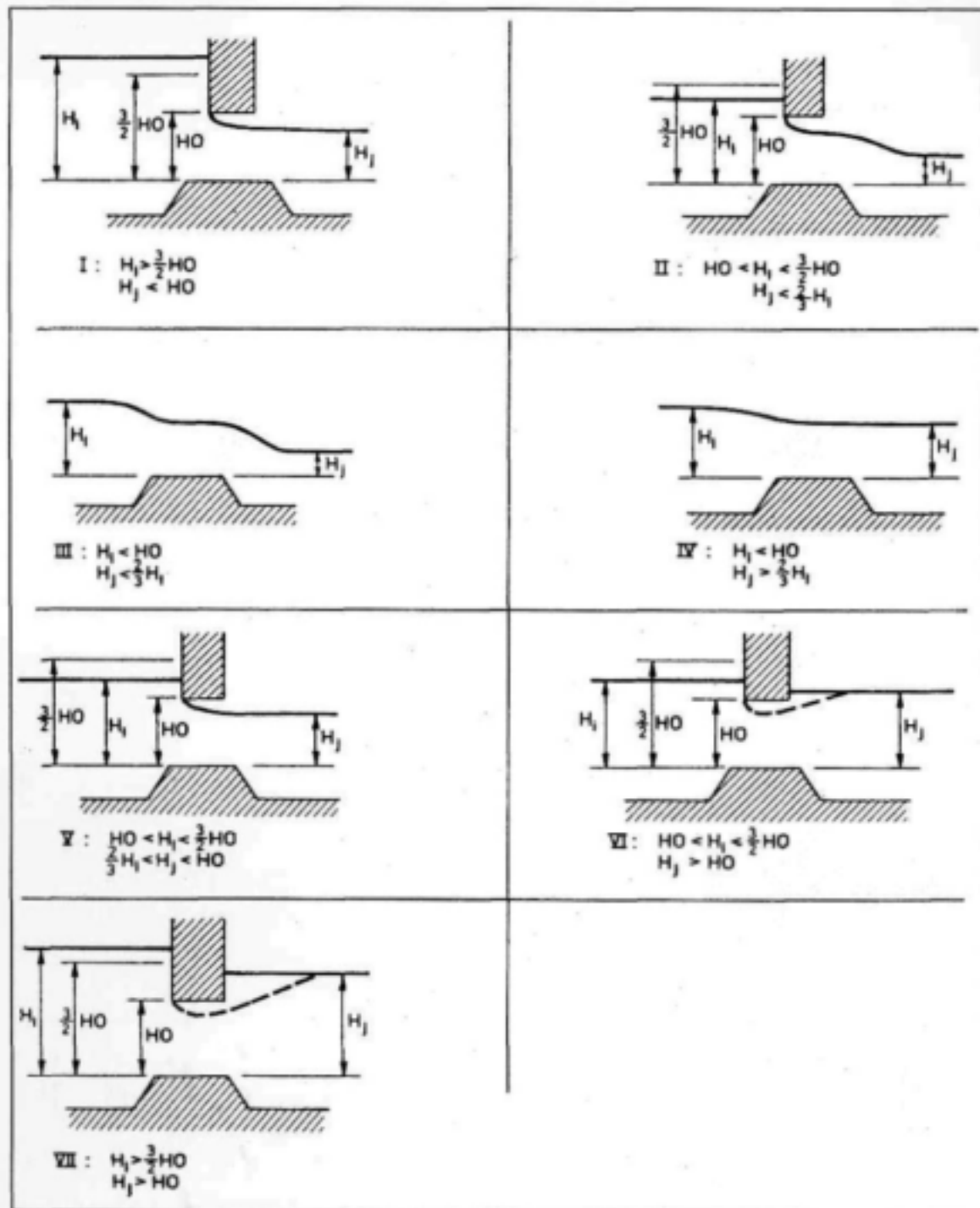


Figure 5.11 : Structure Flow Conditions, covered by DUFLOW

Bridges

Bridges are defined as General Structures. Required Data for the structures are the width of the flow opening of the structure, the height of the flow opening of the structure and the level of the upper side of the flow opening above the reference level.

Trigger Functions

If a parameter of the structure varies according to hydraulic conditions (i.e. multiple notch of weir, or raising of gates at certain water levels), the specifications for the control of these structures can be defined in DUFLOW as *trigger series*. The operational parameter is defined, as well as which type of

trigger (i.e. H node>H trigger, H>H+dH, etc.), the operational parameter (sill level, gate level, etc.) will change according to the entered conditions.

5.4 WATER QUALITY

5.4.1 Introduction

Water quality models predict changes in water quality variables due to loading, transport and reactions within the water body. The basic theory describing these changes is the conservation of mass. The water quality mass balance in a volume of water can be expressed as :

accumulation = loadings +- reactions
(Chapra and Reckhow, 1983)

where :

- loadings - external loadings added to substances, mass of a material discharged per unit time into a volume of water
- transport - the movement of matter through a volume
- reactions - mass is gained or lost by chemical or biological reactions in the water body
- accumulation - either positive (mass increases, as sources are greater than sinks) or negative (mass decreases, sinks are greater than sources)

If water quality variable changes its mass due to chemical or biochemical reactions it is called a *non-conservative* constituent, while where a variable is just dependent on the transport it is a *conservative* constituent. *Sources* specify all the chemical reactions that contribute to an increase of mass of the constituent, while the *sinks* are responsible for the decrease of mass.

In the next sections, the terms will be explained and formulated mathematically, with emphasis on the approach DUFLOW takes to formulate the mass balance in a certain water volume.

5.4.2 Transport

Transport is the movement of matter through a certain volume along with water flow. The mathematical equation describing the transport of a variable in a one dimensional system is the advection-dispersion equation:

$$\frac{\delta(BC)}{\delta t} = \frac{\delta(QC)}{\delta x} + \frac{\delta}{\delta x} (AD \frac{\delta C}{\delta Y}) + P \tag{1} \tag{2} \tag{3} \tag{4} \tag{5.16}$$

where :

- C constituent concentration (g/m³)
- Q flow (m³/s)
- A cross-sectional flow area (m²)
- D dispersion coefficient (m²/s)
- B cross-sectional storage area (m²)
- x x co-ordinate
- t time (s)
- P production of the constituent per unit length (g/m.s)

Term (1) and (2) of the equation represents both the advection processes, while term (3) represents the longitudinal mixing in a water body, which is known as diffusion. With the advection, the particle is swept along (advected) with a velocity comparable to that of a flow as well as molecular diffusion. Diffusion and advection are not always independent and mixing in a water body can occur as a result of both, the combination of advection and diffusion is therefore termed dispersion (Chadwick and Morfett, 1993).

The term (4) of equation 5.16 is called the production term P and it includes all physical, chemical and biological process to which a specific constituent is subject to and will be described in Section 5.4.5. A

differentiation needs to be made between a conservative and a non-conservative constituent, a non-conservative quantity has a continuously decaying mass due to the biological or chemical reactions, even if no transport or diffusion takes place. A conservative constituent does not undergo any changing processes except for being transported and diffused. Therefore, the production term P would only apply to non-conservative variables.

The mass transport equation 5.16 is simplified to :

$$\frac{\delta S}{\delta x} = \frac{\delta(BC)}{\delta t} - P = 0 \quad 5.17$$

in which S is the transport (quantity passing a cross-section per unit time).

This equation is the mass balance equation, which states that the accumulation of a water quality variable is equal to the production rate minus the transport gradient.

The transport by advection and dispersion is described as :

$$S = QC - AD \frac{\delta C}{\delta x} \quad 5.18$$

The relation between the advective and diffusive transport is expressed by the Peclet number (Koutitas, 1983).

The Peclet number is defined as :

$$Pe = v \frac{\Delta x}{D} \quad 5.19$$

High Peclet numbers show that the advective transport prevails over the diffusive one. Small numbers mean that the diffusion predominates. Instability of equations can occur if the Peclet number becomes too large ($Pe > 2$), and could be controlled by increasing the dispersion in the calibration procedure.

One Dimensional Dispersion

The value of D (longitudinal dispersion coefficient) will vary along the channel, depending on the geometry of the channel.

The dispersion coefficient can be determined by either performing tracer studies in the river, or by estimating the dispersion from equations that have been developed which relate dispersion to the shear stress. Much research has been done on the dispersion coefficient and equations have been developed. Various approximations of determining the dispersion coefficient have evolved. The equations are normally based on Fischer's one-dimensional approximation flow (assuming that the flow is fully mixed) and Taylor's prediction of dispersion in a fully developed pipe (Fischer, 1968; Taylor, 1957).

A number of studies have shown that one-dimensional theory does not adequately describe longitudinal dispersion in many rivers, especially at low flow (Seo, 1990). Typically the time series of the measured concentration are positively skewed when compared to the actual calculated time series using the one-dimensional equation (i.e. the concentration time series calculated increases faster than the measured tracer time series). This could be due to temporary storage in 'dead zones' (slowly moving parts of the flow along the channel beds and banks) (Day, 1975; Nordin and Troutman, 1980; Valentine and Wood, 1977; Seo, 1990). Equations have been formulated to adapt the one dimensional equation to data from tracer studies by various methods. Some of the methods to determine the dispersion coefficient are summarized in Table 5.3.

Table 5.3: Dispersion Calculation Methods

| Method | Author |
|--|----------------------------|
| Method of moments to estimate the skewness coefficient | Nordin and Troutman (1980) |
| Numerical Routing to estimate the longitudinal coefficient | Jobson (1987) |
| Differential equations incl. longitudinal advection in mainstream, regions of vortex in storage zones with mass interchange at the interface. | Il Won Seo (1990) |
| Taking the natural log from concentrations between two points and solving as a log-linear relationship. The dispersion coefficient can be estimated from the slope of the linear regression and the mean velocity. | Thomann and Mueller (1987) |

DUFLOW gives the option to "Decouple"; i.e. only dispersion in forward direction is taken into account. Decoupling only takes place at those nodes where a discharge is located. Otherwise the dispersion is considered on both sides of a node. A dispersion coefficient needs to be specified at every node and discharge point, this allows the user to model the influence of different coefficients, as the dispersion coefficient varies along the river stretch.

The dispersion coefficient can range from $150 \cdot 10^5 \text{ cm}^2 \text{ sec}^{-1}$ (Missouri River) to only $0.96 \text{ cm}^2 \text{ sec}^{-1}$ (Coachella Canal in California), depending on the river (Chapra, 1997).

5.4.3 Discretization of Mass Transport Equations

In the flow calculations the discharges were expressed as a set of linear equations as functions of water levels. For the water quality the transport (S) is expressed as functions of concentration (c). The Galerkin method is applied to obtain these expressions :

The mass conservation equation is integrated over a section and multiplied with a weighting function Ψ :

$$\int_0^{\Delta x} \Psi_i \left[\frac{\partial S_i}{\partial x} + \frac{\partial(B_i C)}{\partial t} - P_i \right] dx = 0 \quad 5.20$$

This results in :

$$\Psi_i S_i \Big|_0^{\Delta x} + \int_0^{\Delta x} \Psi_i \left[\frac{\partial(B_i C)}{\partial t} - \frac{\partial \Psi_i}{\partial x} \left(QC - A_i D \frac{\partial C}{\partial x} \right) - \Psi_i P_i \right] dx = 0 \quad 5.21$$

Two weighting functions are distinguished for every section :

$$\Psi_1 = 1 - \frac{x}{\Delta x} \quad 5.22$$

$$\Psi_2 = \frac{x}{\Delta x} \quad 5.23$$

C is assumed to vary linearly with each section, i.e.

$$C = \Psi_1 c_1 + \Psi_2 c_2 \quad 5.24$$

in which c_1 and c_2 are the concentrations at the beginning and at the end of each section.

The solution then becomes :

For the beginning of the section :

$$-S_1 + \frac{\Delta x}{3} \frac{\partial B_1 c_1}{\partial t} + \frac{\Delta x}{6} \frac{\partial B_2 c_2}{\partial t} + \frac{Q_1 c_1 + Q_2 c_2}{2} - A_1 D \frac{c_2 - c_1}{\Delta x} - \frac{\Delta x}{3} P_1 - \frac{\Delta x}{6} P_2 = 0 \quad 5.25$$

and at the end of the specific section :

$$S_2 + \frac{\Delta x}{6} \frac{\partial B_1 c_1}{\partial t} + \frac{\Delta x}{3} \frac{\partial B_2 c_2}{\partial t} - \frac{Q_1 c_1 + Q_2 c_2}{2} - A_2 D \frac{c_2 - c_1}{\Delta x} - \frac{\Delta x}{6} P_1 - \frac{\Delta x}{3} P_2 = 0 \quad 5.26$$

These equations are also discretised with respect of time and give :

$$S_2^+ + \frac{(1-\theta)}{\theta} S_2^- + \frac{\Delta x}{6\theta} \left(\frac{B_1^+ c_1^+ - B_1^- c_1^-}{\Delta t} \right) + \frac{\Delta x}{3\theta} \left(\frac{B_2^+ c_2^+ - B_2^- c_2^-}{\Delta t} \right) + \frac{\theta Q_1^+ c_1^+ + \theta Q_2^+ c_2^+ + (1-\theta) Q_1^- c_1^- + (1-\theta) Q_2^- c_2^-}{2\theta} - A_2 D \frac{\theta c_2^+ - \theta c_1^+ + (1-\theta) c_2^- - (1-\theta) c_1^-}{\Delta x \theta} + \frac{\Delta x}{6\theta} P_1 + \frac{\Delta x}{3\theta} P_2 = 0 \quad 5.27$$

$$S_1^+ = -\frac{(1-\theta)}{\theta} S_1^- + \frac{\Delta x}{3\theta} \left[\frac{B_1^+ c_1^+ - B_1^- c_1^-}{\Delta t} \right] + \frac{\Delta x}{6\theta} \left[\frac{B_2^+ c_2^+ - B_2^- c_2^-}{\Delta t} \right] + \frac{\theta Q_1^+ c_1^+ + \theta Q_2^+ c_2^+ + (1-\theta) Q_1^- c_1^- + (1-\theta) Q_2^- c_2^-}{2\theta} - 5.28$$

$$A_1 D \frac{\theta c_2^+ - \theta c_1^+ + (1-\theta) c_2^- - (1-\theta) c_1^-}{\Delta x \theta} - \frac{\Delta x}{3\theta} P_1 - \frac{\Delta x}{6\theta} P_2 = 0 \quad 5.28$$

The indices + and - refer to present and last time step respectively. The weighting factor with respect to time is θ . Using a value $\theta=1$ results into a fully implicit method (refer also to Section 5.3.3). Unknowns are c_1 , c_2 , S_1 and S_2 .

Using these equations together with the mass balance over the nodes, a set of linear equations is set up. with a system of matrix, as in the flow equations (equation 5.18), the solution to the various unknowns can be found by using the LUD decomposition.

5.4.4 Initial and Boundary Conditions

When simulating quality, if a flow boundary is defined at the upstream boundary of the network, a concentration boundary condition has to be defined as well. The user has the option of entering the water quality data as loads or as concentration. If evaporation is modelled, the concentration will then not be defined, and it is treated as 0. At the physical boundaries, a concentration boundary for every defined dissolved substance is compulsory.

5.4.5 Water Quality Processes

As explained in Section 5.4.2, the mass of water quality variables can be changed by a variety of chemical and biochemical reactions.

In DUFLOW the mathematical formulations describing the processes can be supplied by the user. These are supplied in a file which can be created or modified by using the user interface. A special description language DUPROL has been developed to allow this. DUFLOW comes with EUTROF1 and EUTROF2,

which are two predefined eutrophication models. EUTROF1 includes the cycling of nitrogen, phosphorous and oxygen. The growth of one phytoplankton, chlorophyll-a, is simulated. EUTROF 2 describes the same as EUTROF1 but allows for the water-sediment exchange and has 3 different phytoplankton species which can be studied. EUTROF1 was used in the Berg River study, as it contains simpler algorithms describing the water quality processes, therefore less data and parameter intensive than EUTROF2. For this study alterations have been made to the model to allow additional modelling of TDS and temperature, as these variables are of great concern in the Berg River study (refer to Section 5.4.5.1 for a description on the addition of the temperature processes; as well as Section 5.4.5.3 for a description of the addition of COD in the oxygen algorithms).

In the computational part the process descriptions are combined with the transport equations. The lumped variable P (refer to equation 5.17) contains the certain processes of each water quality constituent.

The differential equations for the variables have normally the following form:

$$\frac{\delta C}{\delta t} = k_1 C + k_0 \quad 5.29$$

The kinetic coefficients k_1 and k_0 are then written in the DUPROL interface, separately for each variable. If the kinetic coefficients are not defined, they are automatically set to zero.

In the following section certain processes are described for each of the constituents that are studied in the Berg River, which are TDS, Dissolved Oxygen, Nutrients (in the form of Phosphates) and Temperature.

5.4.5.1 Temperature

The temperature of a water body is of particular significance as :

- (a) temperature influences all biological and most chemical reactions,
- (b) the discharge of municipal or industrial effluent may affect the aquatic ecosystem due to different temperatures than the receiving water, and
- (c) variations in temperature affect the density of water and hence the transport of water (the transport algorithm assumes density to be constant).

In the following section, the mathematical equation of the influence of temperature on the chemical and biological reactions is considered. The mathematical model of the heat balance of a water body, with sinks and sources, is also described.

Temperature Dependence of chemical Reactions :

The mass of water quality constituent is influenced by a variety of chemical reactions. The rates of most reactions increase when the water temperature increases. As kinetic description of most biological reactions are based on a standard temperature of 20 degrees Celsius, the reaction rates needs to be adjusted according to the surrounding water temperature.

To compute the reaction rate at another temperature, the following equation is used :

$$k_T = k_{20^{\circ}C} \theta^{T-20^{\circ}C} \quad 5.30$$

where :

- T - temperature in degrees Celsius
- k - reaction rate at 20 degrees Celsius
- θ - constant

This has been derived from the van't Hoff-Arrhenius equation, for more information on the derivation the reader is referred to Chapra and Reckhow (1983).

This equation is commonly used to depict the change in reaction rate due to the change in temperature. In DUFLOW the temperature coefficients for algal growth, mineralisation, nitrification, respiration and reaeration, as well as oxidation do need to be supplied by the user.

Temperature Model developed for this study:

The temperature of a given water body depends on the sources and losses of heat in a water body. These have to be therefore estimated as accurately as possible in order to assess the heat balance. Thomann and Mueller (1987) summarize the sources and sinks as follows:

Sources:

- Shortwave solar radiation
- Longwave atmospheric radiation
- Conduction of heat from atmosphere to water
- Direct heat inputs from municipal and industrial activities.

Sinks (losses):

- Longwave radiation emitted by water.
- Evaporation
- Conduction from water to atmosphere.

The heat balance in a small volume of the river will be:

Rate of change of temperature = heat in - heat out + net heat exchange

The EUTROF1 and the EUTROF2 model do not allow the user to model the temperature in the particular water body, but only take the effect of temperature on the kinetic reactions into account. Thus, for this study, a temperature sub-model has been developed and incorporated into the EUTROF1 model by using the Compiler.

The components of the net heat exchange are (refer also to Figure 5.12):

$$J = J_s + J_a - (J_b + J_c + J_e)$$

5.31

where :

- J - total surface heat flux
- J_s - net solar shortwave radiation
- J_a - atmospheric longwave radiation
- J_b - longwave back radiation from the water
- J_c - conduction
- J_e - evaporation

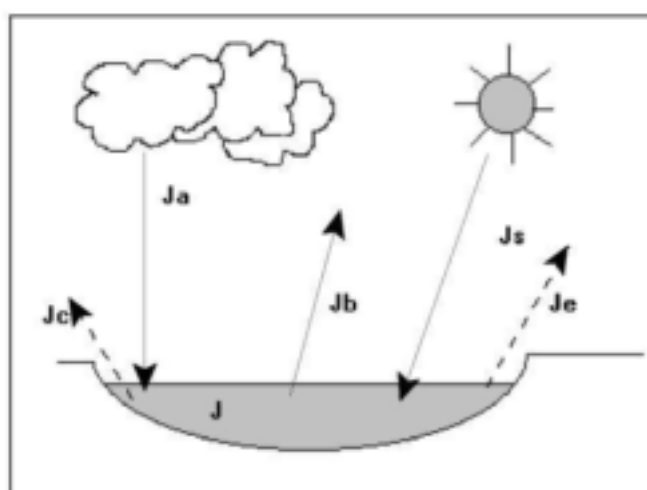


Figure 5.12 : Sinks and Sources of Temperature Model

Net solar shortwave radiation (Js)

Solar radiation is dependent on various factors such as the solar altitude (depending on date, time of day, location), scattering of radiation by clouds and adsorption by atmospheric gases, reflection (dependent on condition of sky and water surface), as well as shading of the streams. Many algorithms have been developed to calculate the solar radiation and some water quality models allow the user to use these algorithms (CE-QUALI, RIV1, etc.). The reader is referred to Schulze (1995) for detailed explanations on developments of these algorithms especially with regard to South African conditions. These equations determining the solar radiation in Southern Africa have been developed by Drummond and Vonwinckel in 1957, Schulze and Mcgee in 1978 and Reid in 1981 (Schulze, 1995). The Southern African Atlas of Agrohydrology and -Climatology (Schulze *et al*, 1997) uses an equation developed by Clemence in 1992 for mapping the solar radiation for different months in the whole of the country. Solar radiation is often measured by meteorological stations around the country and these measurements can be used directly in the equation. As radiation data is available at different stations near to the Berg River, these algorithms have not been used to calculate the solar radiation, but rather the actual measurements have been taken as input data.

Atmospheric longwave radiation (Ja)

Atmospheric longwave radiation is normally expressed as:

$$J_a = \sigma (T_{air} + 273)^4 * \left(A + 0.031\sqrt{e_{air}} \right) (1 - R_L) \tag{5.32}$$

(1) (2) (3)

where

- Ja - Atmospheric Longwave Radiation (J/(m²day))
- σ - Stefan Boltzmann constant (4.9 * 10⁻³ J/(m²day.K⁴))
- T_{air} - air temperature (°C)
- A - a coefficient (0.5 to 0.7 (Chapra, 1997), or Schulze (1995) defines it as 0.56)
- e_{air} - air vapour pressure (Pa)
- R_L - reflection coefficient (generally small, about 0.03 (Chapra, 1997))

The first term takes the Steffann Boltzmann law into account, the second term calculates the atmospheric attenuation which represents the difference between the emittance value for the earth's surface and the effective emittance for the atmosphere, and the third term represents the reflection of the water body. These terms are explained below :

Stefan Boltzmann Law

The Stefan Boltzmann law states that the higher the temperature of an object, the shorter is the wavelength of its emission and the greater the quantity of energy emitted per unit of surface area. This is expressed as :

$$J_{rad} = \epsilon \sigma T_a^4 \tag{5.32}$$

where

- J_{rad} - Radiation (J/m²day)
- T_a - absolute temperature (K)
- σ - Stefan Boltzmann constant (J/(m²dayK⁴))
- ε - emissivity of a body

The emissivity is a correction factor which takes into account that a body is not a perfect radiation emitter (Chapra, 1997).

Atmospheric Attenuation

The air vapour pressure can be calculated using :

$$e_{air} = 4.596_e \frac{17.27T_{aveair}}{273.3 + T_{aveair}} \tag{5.33}$$

where

- e_{air} - air vapour pressure (Pa)

The assumptions are made that :

- air temperature cools down to dew temperature at night
 - the variation of actual vapour density is small
- (Schulze *et al*, 1997)

Reflection

R_L is a coefficient that takes into account the back scattering of radiation by the cloud cover. Schulze (1995) calculates the effect of cloud cover by also taking the ratio of actual sunshine hours to maximum possible sunshine hours into account which will depend on latitude and time. As no data is available on the sunshine hours, this has not been modelled, but just kept as a parameter.

Back Radiation of water (J_b):

The back radiation ($J/m^2/day$) from the water surface can also be represented by the Stefann Boltzmann law : T_s is the surface water temperature ($^{\circ}C$); the other terms, emissivity and the Stefann Boltzmann constant have already been explained above.

$$J_b = \epsilon \sigma (T_s + 273)^4 \tag{5.34}$$

Conduction (J_c):

With conduction the heat transfer is dependent on the water, as the heat is transferred from one molecule to another when the molecules of different temperatures come into contact. This occurs normally at the air-water interface. Conduction plays a more substantial role in the heat transfer in lakes than rivers as the air-water interface is larger. The algorithm representing conduction is dependent on the wind velocity and the difference between the temperatures of the water body and the air.

$$J_c = c_1 f(U_w)(T_s - T_{air}) \tag{5.35}$$

where

- J_c - heat transfer due to conduction ($J/m^2/day$)
- c_1 - Bowen's coefficient (about 0.47 mmHg/ $^{\circ}C$)
- T_s - water temperature
- T_{air} - air temperature
- $f(U_w)$ - dependence of the transfer on wind velocity. Chapra (1997) recommends a relationship proposed by Brady, graves and Geyer in 1969 :

$$f(U_w) = 19 + 0.95U_w^2 \tag{5.36}$$

Where U_w is the wind speed measured in m/s at 4 metres above water surface.

Evaporation (J_e):

The heat lost due to evaporation is determined by the rate of mass transfer from the water to the atmosphere times the latent heat of vaporization. This is then :

$$J_e = \rho_w LE \tag{5.37}$$

where

- J_e - heat transfer due to evaporation ($J/m^2/day$)
- ρ_w - density of water (998.2 kg/m^3)
- L - latent heat (J/kg)
- E - evaporation in m/day

The latent heat is calculated as :

$$(5971.1 - 0.57 T_s) * (4.1868 * 10^{-3}) \tag{Jørgensen and Gromiec, 1989} \tag{5.38}$$

the second term converts cal/g to J/kg.

All terms

All above terms (equations 5.32 to 5.38) describe the change of heat in a water body. All the terms have been adjusted to give the units of J/(m²d) and can then be inserted into equation 5.31. To convert change of heat (J/m²day) to change in temperature (°C/day), following conversion is made :

$$\Delta T = \frac{J}{\rho_w C_p z} C_p z \quad 5.39$$

where

| | | |
|------------|---|---|
| ΔT | - | rate of change in temperature (°C/time) |
| ρ_w | - | density of water (998.2 kg/m ³) |
| C_p | - | specific heat of water (4182 J/(kg °C)) |
| z | - | depth of water (m) |
| J | - | heat (J/m ² time) |

This conversion is based on the relationship of concentration to mass: $c = \text{mass}/\text{volume}$. This allows us to model temperature as a concentration and to use the equation 5.19 that is used for the transport of a concentration. Similar conversion equations are used by Qual-2E and CE-QUAL-RIV1.

5.4.5.2 *Nutrients as Phosphorous*

The major nutrients that contribute to eutrophication are phosphorus as phosphate ions (PO₄³⁻) and nitrogen as nitrate (NO₃⁻), nitrite (NO₂⁻) and ammonium (NH₄⁺) ions. Plants normally use the nutrients in inorganic form. The reduction of algal growth rate depends on the most limiting factor, which means that the growth of a phytoplankton is limited by the nutrient that is available in low levels in the water body. Several studies show that phosphorus is often the limiting nutrient to phytoplankton growth in rivers (Chapra, 1997). Although DUFLOW can simulate changes in nitrates, ammonia and phosphates, only the impact of phosphates will be modelled in the Berg River.

Chapra (1997) attributes the scarcity of phosphorous to following reasons :

- Phosphorous is not very abundant in the earth's crust
- Phosphate minerals are not very soluble
- It does not exist in gaseous form
- Phosphate adsorbs strongly to fine-grained particles. Settling and sedimentation serves to remove phosphate from the water to the bottom sediments.

The main sources of phosphate are human activities, in the form of non-point sources from agricultural and urban land and point sources as wastewater effluents. There are many ways to characterise phosphates. Two forms are used in DUFLOW to characterise phosphorous : organic and inorganic phosphorous.

- *Soluble reactive phosphorous* (H₂PO₄⁻, HPO₄²⁻, PO₄³⁻)
This form of phosphorous is available for plants. It is also called orthophosphates.
- *Particulate organic phosphorous*
This form consists of living plants, bacteria as well as organic detritus.
- *Non-particulate organic phosphorous*
Dissolved or colloidal organic compounds containing phosphorous. Primary origin is decomposition of particulate organic P.
- *Particulate inorganic phosphorous*
These are the phosphate minerals sorbed onto sediment such as clays or complexed with solid matter (e.g. calcium carbonates or iron hydroxydes).
- *Non-particulate inorganic phosphorous*
These are condensed phosphates.

Chapra (1997) summarised these forms of phosphate found in a body of water as follows :

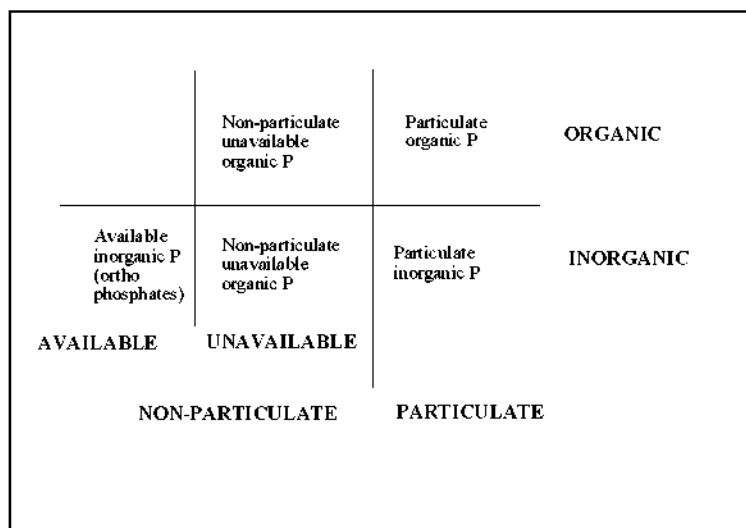


Figure 5.13 : Diagram of Phosphate Constituents

The differentiation into particulate and non-particulate is classified for measurement purposes. The particulate is removed by settlement and can then be measured. The division into available phosphorous is created especially for modelling purposes as this is the only form of phosphorus that is available for phytoplankton growth. The inorganic and organic form is often not mentioned in the literature or in water quality models but rather lumped into particulate and non-particulate unavailable phosphates. In DUFLOW a distinction is only made between organic phosphorous and inorganic phosphorous, the organic particulate phosphates are modelled separately as the phytoplankton group.

The inorganic dissolved phosphorous (orthophosphate) is only available for algae growth and thus normally of interest. To calculate for the orthophosphates in the waterbody, DUFLOW calculates the amount by multiplying it by a factor which allows for the fraction of inorganic phosphates that have been sorbed onto sediments.

$$P_{ortho} = f_{dpano} * P_{inorg} \quad 5.40$$

The dissolved fraction is calculated as :

$$f_{dpano} = \frac{1}{1 + K_{pip} SS} \quad 5.41$$

- K_{pip} - Partition constant phosphorous (about 0.01 l/mgSS)
- SS - Suspended Solids Concentration
- P_{inorg} - Inorganic Phosphate Concentration
- P_{ortho} - Orthophosphate Concentration

No suspended solids data was available for the years that have been studied, thus the assumption has been made that SS=0. This means that all the inorganic phosphate is measurable as orthophosphates.

DUFLOW models the organic and inorganic phosphate as :

Organic Phosphorous :

$$\frac{dP_{org}}{dt} = -k_{min}\theta_{min}^{(T-20)}P_{org} - \frac{y_{so}}{z}(1 - f_{dporg})P_{org} + F_{porg} [k_{res}\theta_{ra}^{(T-20)} - k_{die}]a_{pc}A \quad 5.42$$

Inorganic Phosphorous :

$$\frac{dP_{inorg}}{dt} = -\frac{V_{ss}}{z} (1 - f_{dpano}) + k_{min} \theta_{min}^{(T-20)} P_{org} - \mu_{max} F_T F_N F_I a_{pc} A + (1 - f_{porg}) [k_{res} \theta_{ra}^{(T-20)} + k_{die}] a_{pc} A + \frac{Pflux}{z} \quad 5.43$$

where :

| | | |
|----------------|---|--|
| P_{org} | - | organic Phosphate Concentration |
| P_{inorg} | - | inorganic Phosphate Concentration |
| k_{min} | - | Mineralisation rate constant (l/day) |
| k_{res} | - | Respiration rate constant (l/day) |
| k_{die} | - | Die rate constant (l/day) |
| θ_{min} | - | Temperature coefficient for mineralization |
| θ_{ra} | - | Temperature coefficient reaeration |
| T | - | Temperature (°C) |
| v_{so} | - | Nett settling velocity organic matter (m/day) |
| v_{ss} | - | Settling velocity suspended solids (m/day) |
| f_{dporg} | - | Fraction dissolved organic phosphorous |
| f_{porg} | - | Fraction algal phosphorous released as organic phosphorous |
| f_{dpano} | - | Fraction dissolved inorganic phosphorous |
| a_{pc} | - | Phosphorous to carbon ratio |
| A | - | Algal Biomass (mg C/l) |
| z | - | water depth (m) |
| F_T | - | Temperature dependency of algal growth rate |
| F_N | - | Nutrient limitation of algal growth rate |
| F_I | - | Light limitation of algal growth rate |
| μ_{max} | - | maximum specific growth rate algae |

Equations 5.42 and 5.43 take into account the

- gain of organic P due to die-off of phytoplankton
- gain of inorganic P due to die-off of phytoplankton
- mineralization of organic P to inorganic P (temperature dependent)
- settling of P
- release of inorganic P due to algal respiration
- adsorption of P to suspended solids

For more detail, the reader is referred to Thomann and Mueller (1987). As no algae, sediment or total phosphate data is available for the Berg River, equation 5.43 only remains with :

$$\frac{dP_{inorg}}{dt} = k_{min} \theta_{min}^{(T-20)} P_{org}$$

The transport of the inorganic phosphate concentration (P_{inorg}) is the main influence on the simulation of the concentration, and not the process calculations.

5.4.5.3 Dissolved Oxygen (DO)

Dissolved Oxygen in the water body shows clearly the impact effluent has on the water and thus is ecologically of much interest. In an unpolluted river, the oxygen level will normally be near to the saturation level. The dissolved oxygen becomes depleted when effluents enter the river, because heterotrophic organisms (organisms that live on organic matter) deplete the oxygen in the process of breaking down the organic matter.

As the dissolved oxygen drops, reaeration from the temperature will become higher in order to reach the saturation concentration again. Reaeration is the process of oxygen adsorption from atmosphere to water. A critical level of oxygen is reached when the reaeration rate is equal to the depletion. Reaeration dominates over the decomposition after this critical point. The time series describing this process shows a 'sag' in the series before oxygen is recovered to its initial value. The equation formulated to describe the process leading to this critical oxygen value is therefore known as the dissolved oxygen "sag" equation of Streeter and Phelps (Thomann and Mueller, 1987).

In the water body, the sources of oxygen are:

- Re-aeration from the atmosphere
- Photosynthetic oxygen production
- DO in incoming tributaries or effluents.

The sinks of DO are:

- Oxidation of carbonaceous waste material.
- Oxidation of nitrogenous waste material
- Oxygen demands of sediments.
- Use of oxygen for respiration for aquatic plants.

Oxygen in DUFLOW is modelled as :

$$\frac{dO_2}{dt} = k_{re}\theta_{re}^{(T-20)}(c_s - O_2) \quad 5.44$$

where :

- | | | |
|---------------|---|--|
| O_2 | - | dissolved oxygen concentration (mg/l) |
| k_{re} | - | reaeration rate constant |
| θ_{re} | - | temperature coefficient reaeration |
| T | - | Temperature (°C) |
| c_s | - | saturation oxygen concentration (mg/l) |

Equation 5.44 only models the reaeration.

Additional terms are included in DUFLOW in the equation describing oxygen, but have been omitted here as they will not be modelled in this particular study. The additional terms in the algorithm are :

- oxidation of carbon BOD,
- sediment oxygen demand
- algal respiration
- nitrification

Oxygen saturation concentration

The oxygen saturation concentration is a fixed level of oxygen that is reached in the water body for a given temperature (Thomann and Mueller, 1987).

The oxygen saturation concentration is calculated using the following formulation (Hua, 1990) :

$$C_s = 14.562 - 0.41022T + 0.0079910T^2 - 0.000077774T^3 \quad 5.45$$

This oxygen saturation level is dependent on the temperature, salinity and pressure due to elevation. The above formulation makes no provision for the effects of salinity and pressure. If rivers are modelled to the estuary mouth or at high altitudes, these effects should be taken into consideration. Formulations of the saturated oxygen concentration taking altitude and pressure into account can be read in Chapra (1997), Thomann and Mueller (1987).

Dissolved oxygen deficit :

$$k_{re}\theta_{re}^{(T-20)}(c_s - O_2) \quad 5.46$$

The DO deficit is introduced as the difference between oxygen saturation concentration (c_s) and oxygen. The reaeration coefficient k_{re} determines the time it takes for the DO in the water body to recover to the equilibrium value. A high reaeration coefficient indicates rapid recovery, and lower reaeration coefficients slower recovery of the DO levels. The coefficient is influenced by internal mixing and turbulence due to velocity gradients and fluctuations and by temperature.

Reaeration Rate

Re-aeration is the process of oxygen absorption from the atmosphere to the water. This is one of the main sources of oxygen in water. Much research has been performed on stream reaeration. The most commonly used formulations are summarised in Chapra (1997) and Thomann and Mueller (1987).

Table 5.4 : Mathematical Models describing reaeration coefficients

| Name | Year | Mathematical Model | Velocity used to develop equation (m/s) | Depth used to develop equation (m) | Comment |
|------------------|------|------------------------------------|---|------------------------------------|--|
| O'Connor-Dobbins | 1956 | $k_{re} = 3.93 U^{0.5} H^{-1.5}$ | 0.15 - 0.49 | 36189 | Can be applied to moderate to deep streams with moderate to low velocities (Chapra, 1997). The range of values obtained from measurements were 0.05/day to 12.2/day (Thomann and Mueller, 1987). |
| Churchill | 1962 | $k_{re} = 5.026 U H^{-1.67}$ | 0.55 - 1.52 | 36465 | This formula applies to faster streams. |
| Owens and Gibbs | 1964 | $k_{re} = 5.32 U^{0.67} H^{-1.85}$ | 0.03 - 0.55 | 0.4 - 2.4 | Used for shallower and fast moving streams. |

The O'Connor formulation is normally used in practice, but it can under-estimate the reaeration coefficient for small streams. The mass transfer coefficient for oxygen (m/day) is calculated in DUFLOW using the O'Connor equation. As the depth increases, the reaeration coefficient approaches zero in the algorithm; this is in reality not the case and therefore an additional minimum value of oxygen transfer coefficient is introduced. This minimum value is normally in the range of 0.6-1 m/day. DUFLOW takes this minimum coefficient into consideration by introducing a minimum oxygen transfer coefficient (equations 5.47 and 5.48).

$$k_{re} = \frac{k_{max}}{H} \tag{5.47}$$

$$k_{max} = 3.93U^{0.5}H^{-1.5} \tag{5.48}$$

or if $k_{max} < k_{min}$: $k_{max} = k_{min}$

k_{min} is the minimum oxygen transfer coefficient (m/d) which is defined by the user.

COD

At most South African wastewater treatment plants the effluent will be tested for the Chemical Oxygen Demand (COD) rather than that the Bio-chemical Oxygen Demand (BOD) as in Europe. As DUFLOW only measures BOD₅ (5 day carbon BOD), another adjustment had to be made to allow the user to enter the COD data obtained and then converting it to oxygen. In the COD test the electron donor capacity of carbonaceous material is measured by oxidising the material by a strong oxidant in which the electron acceptor is oxygen. It is known that stoichiometrically when the equivalent of 1 g O₂ is used in the COD test, then the mass of COD oxidised is also 1 g.

$$1g \text{ COD} = 1g \text{ O}_2 \quad (\text{UCT, 1984})$$

Thus, the COD value indicates how much oxygen is being used in the effluent. The term that has been introduced additionally to the oxygen algorithm is :

$$DO = DO - COD \tag{5.49}$$

If the effluent has a higher COD value than oxygen in the receiving water, it has been coded that a zero oxygen concentration will show instead of negative oxygen levels.

5.4.5.4 Total Dissolved Salts

EUTROF1 models no conservative substances, thus as with the additional coding of temperature and COD, TDS has been included as an additional variable. TDS is only dependent on the mass transport in the river and thus the term P of equation 5.17 is treated as 0. In the quality model k_0 and k_1 , for the TDS are thus included as 0 (refer to equation 5.30), and only the transport is calculated.

5.4.5.5 Parameters used in water quality reactions

The parameters used in the reaction processes are the parameters that can also be adjusted by calibration. Table 6.21 in the next chapter represents the default values that DUFLOW uses.

5.5 ACCURACY AND STABILITY OF NUMERICAL MODELS

An accumulation of errors in the finite difference scheme is called *instability* (Grisjen, 1986). An implicit scheme is much more stable than an explicit scheme, because all the equations occur simultaneously and errors are not brought forward from one point to the following and then accumulate, such as is the case in an explicit scheme. Grisjen *et al* (1976) gives a comprehensive analysis of numerical errors resulting from explicit and implicit schemes and summarises them for dynamic waves in 1986.

The *accuracy* of the finite difference solution depends on the differential equation. *Accuracy* refers to the difference between the exact solution to the algorithms and the finite difference solution.

The stability and accuracy in implicit schemes depend largely on the implicit factor θ (refer to Section 5.3.3), the time step Δt and section width Δx .

If a finite difference solution approaches the exact solution as the finite difference increment Δx approaches zero, the method is said to be *convergent* (Grisjen *et al*, 1976).

Instabilities that do occur when calculating the flow and water quality can result from :

- Large differences in boundary values during the computational time step
- Errors in the initial conditions
- Large differences in the channel discretization

These instabilities can be controlled by changing the time or distance steps, or "smoothing" differences in the boundary values and cross-sectional schematization.

5.6 TIME AND SPACE STEP

The space step can be defined by the user as a maximum length. The section between two nodes will then automatically be sub-divided into equal space steps which are just smaller or equal than the maximum length specified by the user. The hydraulic characteristics between the space steps are interpolated. The time step is also defined by the user. It is not necessary to use the same time step for the hydrodynamic calculations as for the water quality concentrations. The results can be written at a higher time step than those specified for the calculation process. As mentioned in Section 5.5, if instabilities do occur in the calculations they can be altered by changing the space and time steps. Normally, smaller values are used as the solution then becomes more accurate.

The selection of space and time step also influences the numerical dispersion and hence the stability in the computation. The numerical dispersion is introduced by discretization of the mass transport equation in the water quality calculations is expressed by STOWA (1998) :

$$E_{num} = \frac{u}{2} (1 - 2\theta) u \Delta t$$

where :

- E_{num} - numerical dispersion
- u - velocity (m/s)
- Δt - time step (s)
- θ - weighting used in 4 point Preissmann scheme (refer to Section 5.3.3)

5.7 CONCLUSION

Hydrodynamic Model:

It has to be remembered that DUFLOW is unable to calculate supercritical flow, although the St Venant equations are able to do so. The implicit scheme shows some advantages to the explicit scheme especially with regard to schematization and calculation time. The implicit scheme is advantageous for this particular study, as it is unconditionally stable. This was of value when configuring the upper Berg River (as is explained in Chapter 6), where the slope of the river is very steep and small calculation steps are necessary.

Water Quality Model:

A limitation to the predefined eutrophication model EUTROF1 is, that no temperature, nor conservative variables such as TDS are not modelled. Nevertheless, DUFLOW allows (by having an open structure) that the user can adjust the water quality model corresponding to the particular problem that needs to be studied. The water quality model should be altered to adjust the various algorithms for South African situations.

Time and Space:

As the hydrodynamic and water quality model do not necessarily need to have the same time step, the computation time can be greatly reduced by allowing the water quality time step to be higher than the hydrodynamic model. The benefit of allowing the user to define a time step is to analyse the water quality variables in the required time the chemical and biochemical processes take place. If at a later stage more data should become available, the model could run at an even finer resolution. As the numerical scheme is implicit it has major advantages regarding the space step. The user can define unequal space steps according to the problem and the output required. Also, the stability of the calculations is improved by using an implicit scheme.

CHAPTER SIX DATA PREPARATION AND CONFIGURATION OF THE MODEL

6.1 INTRODUCTION

This chapter presents the preparation of data and the configuration of the Berg River in the DUFLOW Modelling System (DMS). Referring to Section 2.3.3 the configuration of the model is dependent on the complexity and the degree of resolution as well as accuracy required.

The first stage of developing the model was the data gathering and the preparation of the data according to the format that DUFLOW requires, these include the geometrical profile of the river, the boundary conditions (i.e. the flow hydrographs), the data for the various structures and also the water quality data that will be used in the model.

The chapter is divided into two main sections, the first section describing the configuration and data preparation for the hydraulic calculations, while the second section reports on the water quality data preparation and configuration.

6.2 HYDRODYNAMIC SCHEMATIZATION

6.2.1 Flow Data Preparation

The daily flow data was obtained from DWAF and modified into a format which is required by DUFLOW. Only the recent flow data was considered, i.e. measurements made from 1990 to 1998. Additional years could be added to the files, but the recent flow data set can be regarded as very representative. This would also slow down the model, due to extensive data output files. For more information on flow data prior to this period, an extensive review can be found in the Western Cape System Analysis (WCSA) report on the hydrology of the Berg River (DWAF(b), 1992).

Figures 6.1 and 6.2 show the inflow hydrographs of the major flow-contributing tributaries, for low flow period and also for the high flow period of the configuration years. Figure 3.1 already represented the gauging stations in the Berg River catchment.

6.2.2 Nodes and Boundary Conditions

The two external nodes are upstream at upper Berg (G1H004) and downstream at Misverstand Dam (G1R003). Three internal nodes were also included in the schematization at the gauging stations G1H020 (Dal Josafat), G1H036 (Hermon) and G1H013 (Drie Heuwels). The total length of the river is approximately 149 km. The river length between the two external boundaries was divided into four reaches, which can be seen in Table 6.1.

Table 6.1 : Reaches of the main stem Berg River

| Reach | Beginning node | End node | Length (km) | Average Slope (%) |
|-------|----------------|----------|-------------|-------------------|
| 1 | G1H004 | G1H020 | 31 | 0.35 |
| 2 | G1H020 | G1H036 | 41 | 0.095 |
| 3 | G1H036 | G1H013 | 57 | 0.055 |
| 4 | G1H013 | G1R003 | 20.5 | 0.05 |

One boundary condition is needed at each end point of the network schematization (refer to Section 5.3.4). The upstream boundary condition at G1H004 is the inflow hydrograph (see Figure 6.3), while at G1R003 a stage-discharge rating curve has been specified as the end boundary condition (see Figure 6.4). The rating curves for all the weirs were obtained from DWAF.

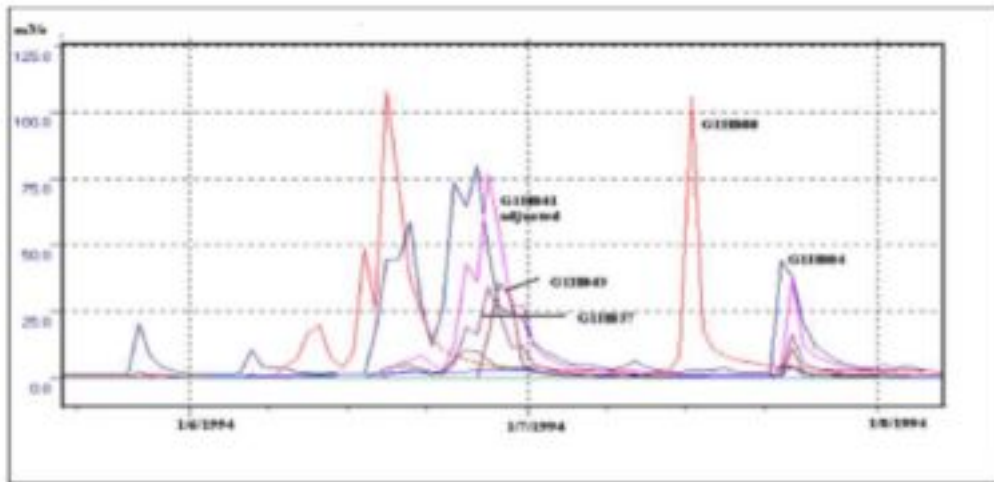


Figure 6.1: Incoming high-flow from tributaries

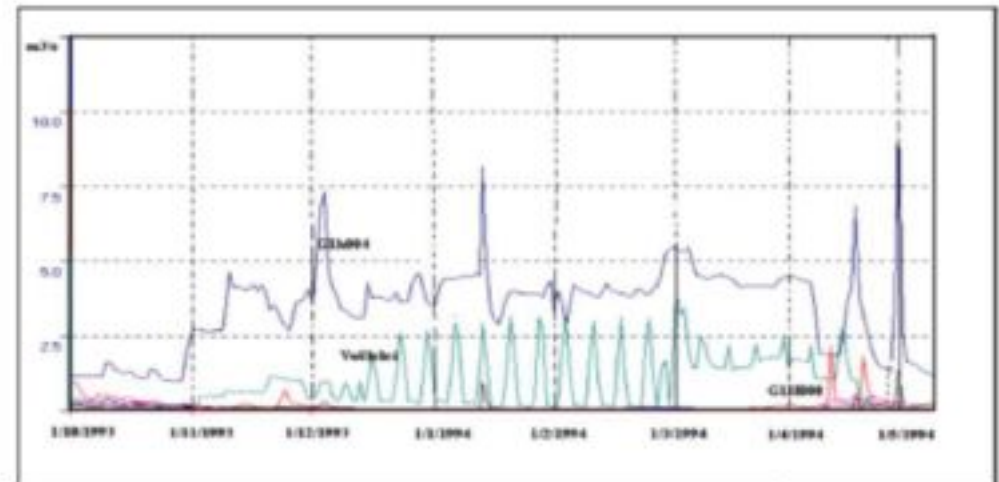


Figure 6.2: Incoming low-flow from tributaries

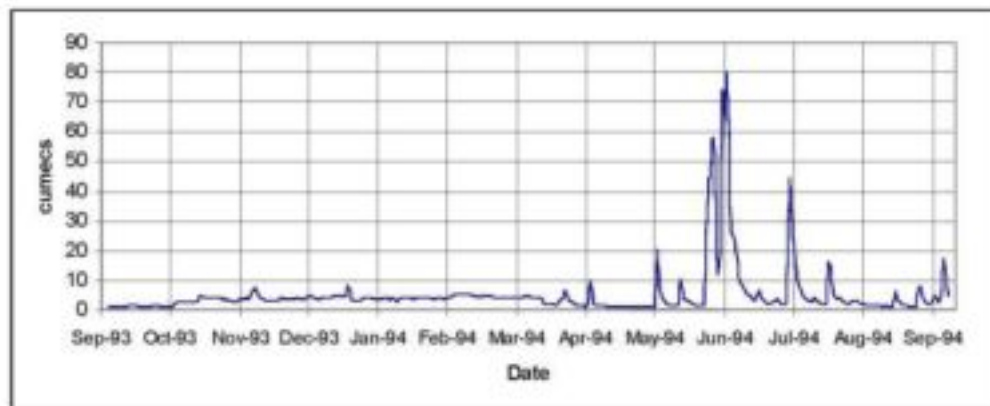


Figure 6.3: Inflow Hydrograph at G1H004

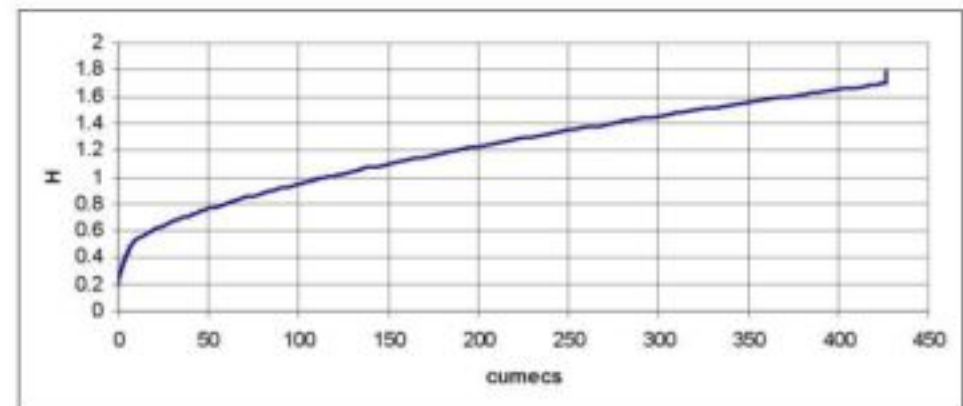


Figure 6.4: Stage-Discharge Relationship at G1R003

6.2.3 Cross-sections

The sources in Table 6.2 were able to provide detailed cross-sections for the Berg River.

Table 6.2: Sources of cross-sections provided in the Berg River

| | | Source | Comments |
|---|--|--|---|
| 1 | Skuifraam Dam Tailwater Cross-sections | DWAF | 17 sections at 300m interval |
| 2 | Skuifraam Dam Supplement Scheme | Ninham Shand | 1:2000m coverage |
| 3 | Paarl Cross-sections | Paarl Municipality | 23 cross sections taken through Paarl |
| 4 | 1:50 year Wellington Flood Study | Ninham Shand | 1:2000m coverage |
| 5 | detailed Surveys | Robin Pharaoh & Associates/ Satmap Solutions CC | 26 detailed surveys from G1H004 to Miverstand at selected sites |
| 6 | Photosurveys | Photosurveys | 67 photosurveys from G1H004 to Miverstand at selected sites |
| 7 | Main River Gauging Stations | DWAF | Local datum |

A total of 108 cross-sections were used for configuration of the model. Some of the cross-sections were not surveyed beyond the banks and information on the characteristics of the flood plain were obtained from orthophotos (1:10 000). The cross-sections were represented in DUFLOW with the width as a function of height (see Section 5.3.5). Enough points had to be defined in order to represent the cross section as accurately as possible. The cross-sections are entered as symmetrical sections, but it appears that making non-symmetrical profiles symmetric only causes a small error in the calculations (Grijzen, 1986). Most of the parameters used in the calculation of the water surface are dependent on the geometric parameters (surface area, roughness, width) etc. Therefore, it should be important to define the cross-sections with sufficient accuracy, and thus the widths were entered at height differences of 0.2m.

A minimum of one cross-section has to be defined per reach and an unlimited number of cross-sections may be inserted between two nodes. If the space step defined is smaller than the distance between two cross -sections then the hydraulic parameters, i.e. hydraulic radius, surface area which are calculated from the cross-sections, are interpolated linearly at the various points defined by the space step. Traver and Miller (1994) reviewed the effect interpolation has on the calculated water surface profile, as it is the most common practice in computer models, and concluded that the error introduced when interpolating the hydraulic parameters is insignificant compared with errors introduced from surveys. Information of the cross-sections had to be provided manually, unfortunately there was no option to import or export the data as text files.

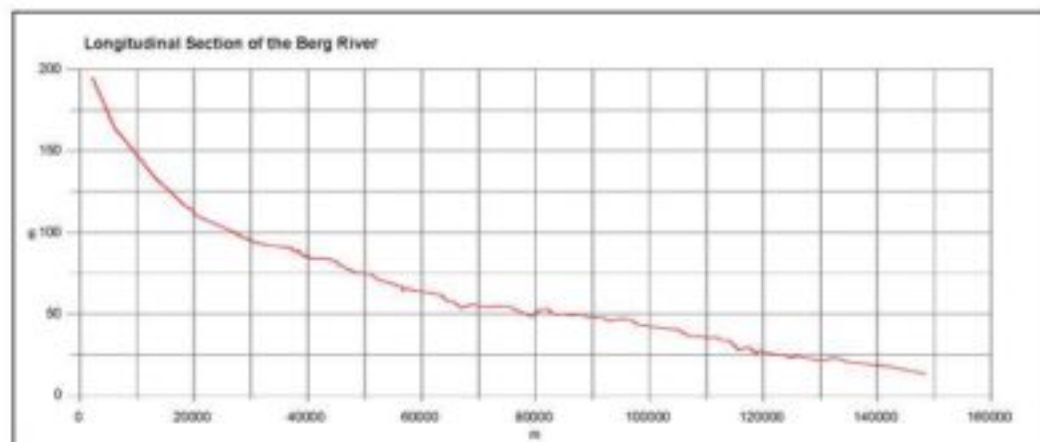


Figure 6.5: Longitudinal profile from G1H004 to Miverstand

6.2.4 Structures

6.2.4.1 Weirs

Details for the weirs were obtained from plans which were made available by DWAF (Western Cape Regional Office). The height and the width of the weir were entered into the weir dialog box of DUFLOW. Trigger Levels have been specified for the different weirs, to take the multiple notches with increasing level into account (refer to 5.3.6 for details about trigger levels).

Table 6.3: Details of weirs

| Gauging Station No | Weir Name | Latitude | Longitude | Description |
|--------------------|---------------|-------------|-------------|--|
| G1H004 | Driefontein | 33° 55' 36" | 19° 03' 41" | Crump weir was constructed 1980 (DWAF(a),1994); was originally a sharp crested weir. |
| G1H020 | Noorder Paarl | 33° 42' 29" | 18° 56' 29" | The weir is situated just upstream of the Dal Josafat Bridge in Paarl. G1H020 consists of two sharp crested weirs and a hydro flume. |
| G1H036 | Vleesbank | 33° 26' 06" | 18° 57' 25" | G1H036 has been built below Hermon Bridge, it consists of stepped crump weirs. |
| G1H013 | Drieheuwels | 33° 07' 57" | 18° 51' 45" | Stepped crump weirs with a hydro flume. |

6.2.4.2 Bridges

A total of 13 bridges were identified along the main stem of the Berg River for the river reach modelled. The information on the various bridges was available from Dept of Road Transport and Paarl Municipality. Table 6.4 describes the details of the bridges modelled. Information about the bridges needed for DUFLOW are: width of the bridge, the vertical clearance and the reduced level of the top of the bridge. For more complex cross-sections at the bridges, the structure control was used (Section 5.3.6), by changing the width for various trigger levels. The information was entered into the DUFLOW dialog box manually.

From the 13 bridges identified, only 7 could be modelled. For some of the bridges no information was available, while the Dal Josafat, Hermon and Jim Fouche Bridge the following reasons applied:

- The numerical scheme becomes easily unstable when the distance between two structures is too small. This was the case for Dal Josafat and G1H020 weir. Similarly, for Hermon Bridge the decision had to be made to either model the weir G1H036 or the bridge as the model becomes unstable when calculating for both structures simultaneously.
- In the upper reaches the slope is quite steep (approximately 0.35%) and Jim Fouche Bridge lies exactly between two incoming tributaries, Franschoek River and Wemmers River, which lie only about 800 km from each other. The model experienced problems when this bridge was configured. In other circumstances this should not have been a problem (i.e. much shorter reach where even smaller space steps could be defined).

Bridges caused persistent numerical instabilities in the model. The effect of these problematic bridges was approximately retained by increasing the roughness coefficient in the specific reach.

Table 6.4: Details of Bridges

| Name | Nr | Approximate Distance from G1H004 (km) |
|-------------------------|----------------|---------------------------------------|
| Jim Fouche Bridge | B5919, MR 191 | 6.5 |
| N1 | B4334 | 24.0 |
| Market Street Bridge | B2994 | 26.9 |
| Lady Grey Street Bridge | B0981 | 27.8 |
| Rembrandt Bridge | N/A | 28.0 |
| Osbosch Street Bridge | N/A | 29.6 |
| Dal Josafat | N/A | 30.5 |
| Oudebrug | B4902, MR 27 | 38.1 |
| Lady Loch Bridge | B3007, MR 222 | 41.7 |
| Vogelgesang | N/A | 48.2 |
| Vleesbank | B4545A | 72.0 |
| Sonkwasdrift | B5792, DR 1154 | 92.2 |
| Skoenmakersfontein | B5730, DR1161 | 107.3 |

6.2.5 Tributaries

The tributaries were entered at schematization points (see Section 5.2.1 for definition on schematization points) that allow the user to insert the hydrographs as time series. The inflowing hydrographs were depicted in Figures 6.1 and 6.2, while Figure 3.1 showed the gauging stations in the Berg River catchment.

Table 6.5: Major Tributaries in the Berg River Catchment

| Flow Gauge | River | Place name |
|------------|-------------|---------------|
| G1H003 | Franschhoek | La Provence |
| G1H019 | Banhoek | Bosmanshoek |
| G1R002 | Wemmers | Wemmershoek |
| G1H041 | Kompagnjies | De Eikeboomen |
| G1H039 | Doring | / |
| G1H043 | Sandspruit | Visgewaagd |
| G1H008 | Klein Berg | Mountain View |
| G1H035 | Matjies | / |
| G1H034 | Holle | / |

6.2.6 Roughness Coefficient

The roughness can be expressed as the inverse of the Manning roughness coefficient n or by the Chezy coefficient C . DUFLOW gives the user the option to change the roughness at every cross-section and

also at every point defined in the cross-section at the relevant sides of the section. This allows the section to have a different roughness at 0.5 m depth than the roughness at 1m. The sensitivity of the roughness coefficient has been investigated for calibration purposes; this is discussed in Section 7.7. The initial roughness coefficients were based on Figure 3.8 in the NTC Road Drainage Manual (Rooseboom *et. al*, 1983).

6.2.7 Abstractions and Return Flows

6.2.7.1 Paarl Abstractions

The municipality of Paarl receives water mainly from the Wemmershoek Dam, but additional water is abstracted from the river as the water from Wemmershoek Dam is costly (Pers. Com. A. Kowalewski, Paarl Municipality).

The abstraction data were made available as monthly average flows. Table 6.6 indicates that there is a 100% decrease in the winter months from the period before 1990 to 1999, while abstractions in the summer months has increased (310% in November). It has been assumed that the abstractions have increased linearly in the years and the calculated figures for 1993/1994 have been inserted into the model.

Table 6.6: Abstraction data of Paarl Municipality

| | 1980 to 1988 (DWAf(b), 1992) | Recent 1998/1999 | % increase |
|--------------|------------------------------------|------------------------------------|------------|
| | Monthly Average (Mm ³) | Monthly Average (Mm ³) | |
| October | 0.04 | 0.088 | 120 |
| November | 0.03 | 0.096 | 310 |
| December | 0.04 | 0.11 | 175 |
| January | 0.07 | 0.086 | 23 |
| February | 0.06 | 0.164 | 173 |
| March | 0.07 | 0.19 | 171 |
| April | 0.07 | 0.13 | 86 |
| May | 0.04 | 0.017 | -57 |
| June | 0.06 | 0 | -100 |
| July | 0.05 | 0 | -100 |
| August | 0.06 | 0.034 | -43 |
| September | 0.06 | 0.125 | 108 |
| Total | 0.6 | 1.04 | 73 |

6.2.7.2 Other Industrial Abstractions

Water Quality in the Berg River: A Situation Analysis (DWAf(g), 1993) describes industries which utilise water from the Berg River with little or no pre-treatment. None of these industries reported, occur in the reach considered for this study and therefore the industrial abstractions have no effect on the flow modelled. The industries mentioned are : PPC De Hoek factory, which abstracts just below Misverstand weir; the Chempos factory, which abstracts water at the Old Berg River pumping station (G1H023) and the Dewdale Trout Farm, which abstracts just upstream of G1H004 (approximately 2.5 km).

6.2.7.3 Irrigation

There are currently eight irrigation boards which are permitted to abstract water from the river. These are:

- Simondium
- Simonsberg
- Noord Agter Paarl
- Suid Agter Paarl
- Perdeberg
- Riebeek Wes
- Riebeekkasteel
- West Coast District, Misverstand

Information was made available by some of the irrigation boards:

- West Coast District Council - 10 Mm³/annum
- Perdeberg Irrigation Board - 6.25 Mm³/annum
- Simondium Irrigation Board - 1.04 Mm³/annum
- Simonsberg Irrigation Board - only after 1997

For the irrigation boards where no information was available, a rate of 7500m³/ha/annum was applied to the scheduled areas. The monthly distribution of water abstracted was adjusted by following the seasonal distribution of the evaporation rate. The irrigation demand was calculated as follows:

$$\text{monthly crop factor} * \text{mean monthly A-Pan evaporation} - \text{effective rain/total rain ratio (0.7)} * \text{mean monthly precipitation}$$

Following abovementioned calculation procedure, the water demands calculated for the irrigation boards are:

- Riebeek Kasteel - 1.1 Mm³/annum
- Suid Agter Paarl - 2.7 Mm³/annum
- Noord Agter Paarl - 2.0 Mm³/annum

The total volume of abstractions was calculated to be 42 Mm³/a. This present figure shows a rising trend when compared to the abstraction value of 35 Mm³/a calculated for the WCSA in 1995 (DWAF(b), 1995). This rising trend is further illustrated by the *Water Quality in the Berg River: A Situation Analysis* (DWAF(g), 1993) that calculated abstractions to be 21.7 Mm³/a from G1H004 to Sonkwasdrift.

Table 6.7: Abstractions in the Berg River for 1993/1994 (Mm³)

| | Oct | Nov | Dec | Jan | Feb | Mar | Apr | May | June | July | Aug | Sept |
|-----------------|------|------|-----|-----|-----|-----|-----|-----|------|------|------|------|
| Mm ³ | 0.94 | 4.64 | 8.3 | 8.6 | 7.6 | 6.4 | 2.5 | 0.8 | 0.65 | 0.45 | 0.64 | 0.62 |

6.2.7.4 Return Flows

Sewage return flows from Paarl are monitored by the Paarl Municipality. The Paarl Sewage Treatment Works (STW) is the most significant effluent producer in the whole of the Berg River catchment. Table 6.8 shows a comparison of the volume discharged into the river at the time of the WCSA (DWAF(b), 1992) and the most recent discharges which have been made available by Paarl Municipality.

Table 6.8: Comparison of Return Flows in years at Paarl STW

| | WCSA (DWAf(b), 1992) | Recent 1997/1998 | % increase |
|--------------|------------------------|------------------------|-------------|
| | Ave (Mm ³) | Ave (Mm ³) | |
| October | 0.6 | 0.885 | 47.5 |
| November | 0.5 | 0.897 | 79.4 |
| December | 0.5 | 0.695 | 39 |
| January | 0.5 | 0.751 | 50 |
| February | 0.5 | 0.62 | 24 |
| March | 0.6 | 0.739 | 23 |
| April | 0.5 | 0.795 | 59 |
| May | 0.6 | 0.974 | 62 |
| June | 0.7 | 1.03 | 43 |
| July | 0.8 | 1.4 | 75 |
| August | 0.8 | 1.15 | 44 |
| September | 0.7 | 0.9 | 28.6 |
| Total | 7.3 | 10.84 | 48.5 |

Sewage return flows from Wellington are not monitored, as the water is discharged into evaporation pans.

6.2.8 Evaporation Losses

Records of average daily evaporation were made available by Western Cape Department of Agriculture, Elsenburg.

As no function is incorporated in the DUFLOW model to calculate the evaporation loss rate relative to the function of surface area at each time increment, the average evaporation loss was modelled as abstraction points.

The loss rate was calculated as:

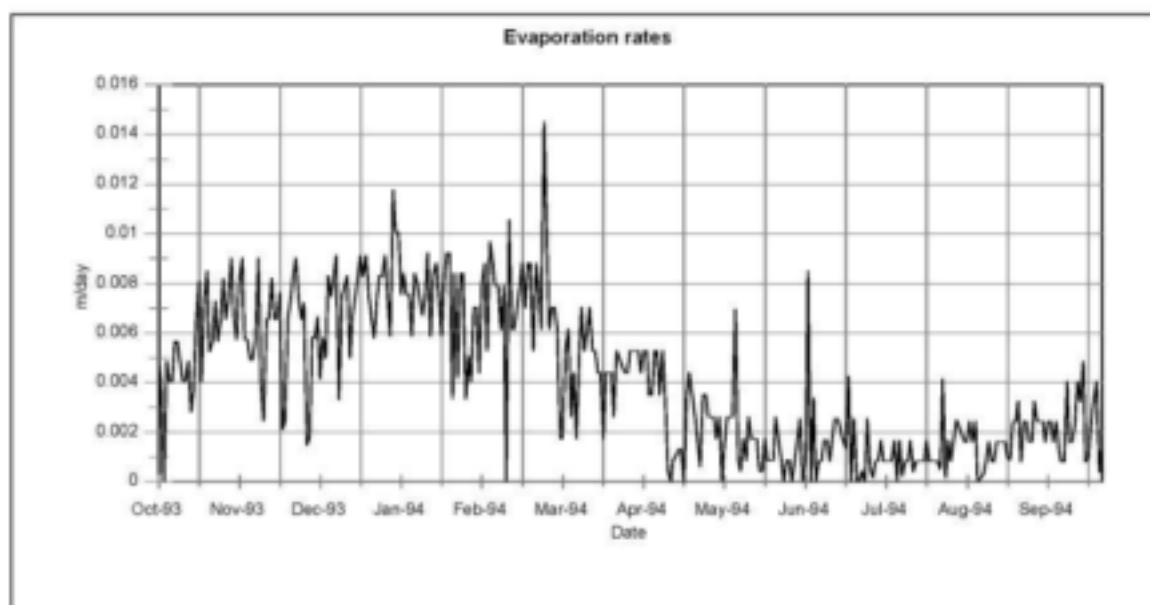
$$\text{Loss (m}^3\text{/s)} = \text{average width (m)} * \text{length between sections (m)} * \text{evaporation loss rate (m/s)}$$

The evaporation rate was divided into several abstraction points in relative proportion to the surface areas that each abstraction/schematization point represented, in order to achieve even distribution of the evaporation along the river. This also ensured that a smoother concentration profile was calculated; thus the impact of the evaporation on the water quality was shown fairly realistically.

The evaporation rates of four meteorological stations were applied to the Berg River model. Table 6.9 indicates average evaporation losses in mm/month for Bien Donne, while the average evaporation rates are summarized for the different meteorological stations in Table 6.20 of Section 6.3.4.

Table 6.9: Evaporation Losses (mm/month) at Bien Donne for the year 1993/1994

| | Oct | Nov | Dec | Jan | Feb | Mar | Apr | May | June | July | Aug | Sept |
|-----------------|-----|-----|-----|-----|-----|-----|-----|-----|------|------|-----|------|
| Mm ³ | 193 | 250 | 300 | 327 | 286 | 207 | 142 | 56 | 32 | 47 | 83 | 101 |

**Figure 6.6: Graphical Representation of Evaporation Rates at Bien Donne**

6.3 WATER QUALITY CONFIGURATION

6.3.1 Water Quality Data Preparation

DUFLOW needs daily concentrations for the variables of concern in the form of continuous time series. As the water quality data obtained by DWAF is measured mostly on a one- or two weekly basis, the daily sequences have to be developed by 'infilling'. Table 6.10 shows the infilling techniques that have finally been used to turn the grab-sample water quality time series into a daily series.

Table 6.10: Infilling of water quality variables

| Parameter with missing data | Parameter used for infilling | Infilling technique |
|-----------------------------|------------------------------|---------------------|
| Log TDS | Log Flow | Moving-Regression |
| Log PO ₄ | Log Flow | Moving-Regression |
| Water Temperature | Date | Harmonic Function |

6.3.1.1 TDS and PO₄ Infilling

Two methods were investigated for this study, before deciding on a certain infilling method:

- The program **FLUX** (Walker, 1987)
- A **moving-regression** method (DWAF, 1998)

These two methods are described in this section along with the results obtained from the infilling method.

Flux

Description

Flux interprets water quality information and flow information from grab samples over the complete flow record between two dates.

There are five different equations that can be used to calculate the concentrations (refer to Table 6.11). Flux has an option to divide the flow and concentration data into different data groups (stratification) and calculate loadings for the different groups using the calculation method chosen. The groups can be defined based upon flow, time or any other variable that seems to influence the load dynamics.

Discussion

Flux seemed suitable for calculating monthly and yearly loads. For filling in daily concentration values the model-selected two regression functions were used (refer to Table 6.11). The results were not satisfactory as the daily concentrations would remain consistent over a certain period, as it is stratified according to flow. The method seemed to calculate a single concentration for the range of flows entered and thus the concentrations do not differ for every single value of flow, but rather displayed five different concentration values for the five ranges of flow stratified. The method could work well if very short periods of samples are entered and the flow does not vary as much.

Table 6.11: Calculation Methods for Flux

| METHOD | DESCRIPTION | EQUATION |
|--|---|--|
| Direct Loading | The loading does not vary with flow, as the flux is only dependent on the mean of the grab samples. This method is suitable if the concentration tends to be inversely related to the flow. | $W1 = \text{Mean}(w)$ |
| Flow Weighted Concentration (Ratio Estimate) | The loading is estimated on the flow weighted average concentration times the mean flow over the averaging period. This method performs best when flow and concentration are unrelated. | $W2 = \frac{\text{Mean}(w)\text{Mean}(Q)}{\text{Mean}(q)}$ |
| Modified Ratio Estimate | Multiplying it by a factor to adjust to situations where concentration does vary with flow modifies the flow-weighted concentration. | $W3 = W2 \frac{(1+F_w/n)}{(1+F_q/n)}$ |
| Regression, First Order | The regression works well for log(c) versus log (q) slopes. The relationship between flow and concentration should be linear. | $W4 = \text{Mean}(w) \left[\frac{\text{Mean}(Q)}{\text{Mean}(q)} \right]^{b+1}$ |
| Regression, Second Order | The regression of first order is modified by a factor that is designed to account for differences in variance between the sampled and the total flow distributions. | $W5 = W4 \frac{(1+r F_Q)}{(1+r F_q)}$ |

Where

- c_i = measured concentration in sample i (mg/m³)
- q_i = measured flow during sample i (hm³/yr)
- b = slope of log (c) versus log (q) regression
- w_i = measured flux during sample i = $q_i c_i$ (kg/yr)
- wq_i = product of flux and flow for sample i (kg * hm³/yr²)
- F_wq = $\text{Var}(wq)/[\text{Mean}(w)\text{Mean}(q)]$
- F_q = $\text{Var}(q)/[\text{Mean}(q) \text{Mean}(q)]$
- F_Q = $\text{Var}(Q)/[\text{Mean}(Q)\text{Mean}(Q)]$
- Q_j = mean flow on day j (hm³/yr)
- n = number of samples (i)
- N = number of daily flows (j)
- W_m = estimated mean flux over N days, method m (kg/yr)
- V_m = variance of estimated mean flux, method m (kg/yr)²
- r = $0.5 b(b+1)$
- $\text{Mean}(x)$ = mean of vector x
- $\text{Var}(x)$ = variance of vector x

(Walker, 1987)

Moving Regression

Description:

The relationship between concentration and flow can be described as:

$$C = aQ^b$$

$$\text{Log } C = \text{log } a + b \text{ log } Q$$

where

C concentration of the water quality variable

Q daily flow

a,b regression coefficients

Studies of the relationship between flow and the concentration constituent have revealed that a single prescribed value for each of the regression coefficients a and b does not adequately describe the relationship between concentration and flow over the full range of most flow regimes in South Africa (DWAF, 1998). The regression coefficients vary because of different factors that influence the relationship between flow and the concentration such as variable loadings from point sources, or whether the sample has been taken during a rising (more surface runoff) or a falling hydrograph (more groundwater). A moving regression method was developed for the Amatole Water Resource System Analysis (DWAF, 1998), which takes these variations into account. The method looks at 5 to 9 sequential concentration values at a time (set by the user), calculates the corresponding regression coefficient a and b, predicts the intermediate values, and then takes the next block of values by moving one sample forward; thus allowing the variation in flow conditions to change the regression coefficients at every single value. It has been found that for most variables about 8 values at a time are adequate to describe the relationship between flow and the concentration. This represents about two months of weekly grab-samples. By increasing the number of values the calculated values show a more average trend and do not take sudden changes accurately into account. Less than six values are too few to provide an adequate regression fit. The numbers of variables were adjusted for the various stations to obtain the best correlation possible.

Discussion

When the intervals between observed values are long (>14 days), the regression does not show satisfactory results. This is due to the strong seasonality of the concentration variables. The various results of this method for total dissolved salts (TDS) and phosphates are described in the next section.

These water quality variables were infilled for all the catchments where flow and water quality data was available. Complications were experienced at following stations:

- G1R002 Wemmershoek Dam sub-catchment

The water quality grab samples are taken at the dam wall, and are therefore affected by the storage in the Wemmershoek Dam. The observed flow, used for the regression infilling method, is measured at the inflow into the dam. As there is no water quality data taken at the same location as the flow is measured, the water quality grab samples taken in the dam are the only indication of the expected water quality.

- G1H028/G1H029

Only intermittent flow data was available, as portions of the flows are diverted to Voëlvllei Dam.

Results of Infilling Method

TDS

The moving regression works well for the TDS infilling as can be seen from the figures at the end of this chapter (Figures 1.2.1 to 1.2.11 in Appendix 1.2). For zero flows the regression is interrupted and produces zero concentrations. From the statistics (refer to Table 6.12) it is illustrated that the difference in means of the observed and calculated values are low (all below 10%).

Phosphate as PO₄

Table 6.13 shows that a similar pattern occurs at low flow as for PO₄ as for TDS infilling. Some stations show a better relationship between flow and phosphates (refer to Table 6.13 and Figures 1.2.12 -1.2.23 in Appendix 1.2). The errors between the measured and calculated values are very varied but after 1990 it seems that the differences are all below 20%, except for G1H003.

It has to be borne in mind that only about 8 grab samples values are included in the regression at a time. If the variance is higher between the grab samples, the difference between the estimated values and the grab sample will be greater. As the method is based on a regression equation, the concentration maxima and minima may be over or underestimated. This is illustrated in Table 6.12 and 6.13, where the percentage difference in means show systematically negative values for all stations. Referring to the Figures (e.g. Figure 1.2.9 in Appendix 1.2) it is further illustrated that the infilling method is unable to reproduce the lower and upper extreme water quality values that have been sampled.

NOTE:

Certain statistical equations have been used to determine the accuracy of fit between the infilled and the measured data. These equations are described along with the calibration description in Section 7.1, as the statistical equations (also known as objective functions) are used extensively in the calibration process.

Table 6.12: Statistics of TDS Infilling

| Gauging Station | No of Samples | Mean Concentration (infilled) | Mean Concentration (Grab Samples) | % error in mean | Std. Dev (infilled) | Std. Dev (grab samples) | % differ. in std deviation | R ² (Loads) |
|--------------------|---------------|-------------------------------|-----------------------------------|-----------------|---------------------|-------------------------|----------------------------|------------------------|
| Main Stream | | | | | | | | |
| G1H004 | 174 | 32 | 33 | -2.8 | 6.9 | 10.3 | -33 | 0.93 |
| G1H020 | 303 | 59 | 61 | -4 | 9.54 | 18.6 | -49 | 0.98 |
| G1H036 | 251 | 127 | 128 | -1.1 | 23.4 | 35 | -33 | 0.87 |
| G1H013 | 271 | 151 | 153 | -1 | 34.7 | 48.5 | -28 | 0.89 |
| G1R003 | 333 | 211 | 217 | -2.8 | 65.2 | 78.5 | -17 | 0.93 |
| Tributaries | | | | | | | | |
| G1H003 | 163 | 82 | 83 | -1 | 24.9 | 28.54 | -13 | 0.98 |
| G1R002 | 34 | 25 | 25 | -1.4 | 1.59 | 4.14 | -62 | 0.99 |
| G1H019 | 277 | 39 | 40 | -2.3 | 7.8 | 10.5 | -26 | 0.93 |
| G1H037 | 65 | 95 | 101 | -5.5 | 26.4 | 31.4 | -16 | 0.95 |
| G1H039 | 130 | 2648 | 2712 | -2.4 | 735 | 897.5 | -18 | 0.97 |
| G1H041 | 234 | 160 | 175 | -8.5 | 51.5 | 88 | -41 | 0.97 |
| G1H008 | 300 | 113 | 118 | -4 | 29.4 | 40.4 | -27 | 0.99 |
| G1H065 | 491 | 67 | 67 | -0.2 | 8.4 | 10.2 | -18 | 0.99 |
| G1H043 | 106 | 4639 | 4665 | -0.57 | 1263 | 1341 | -6 | 0.99 |
| G1H035 | 168 | 1637 | 1681 | -2.6 | 648.7 | 840.5 | -23 | 0.91 |
| G1H034 | 315 | 6310 | 6253 | 0.9 | 2220 | 2297 | -3 | 0.91 |

Table 6.13: Statistics of Phosphate as PO₄ Infilling

| Gauging Station | No of Samples | Mean Concentration (infilled) | Mean Concentration (Grab Samples) | % error in mean | Std. Dev (infilled) | Std. Dev (grab samples) | % differ. in std deviation | R ² (Loads) |
|--------------------|---------------|-------------------------------|-----------------------------------|-----------------|---------------------|-------------------------|----------------------------|------------------------|
| Main Stream | | | | | | | | |
| G1H004 | 174 | 0.019 | 0.02 | -9 | 0.0077 | 0.012 | -35.8 | 0.80 |
| G1H020 | 302 | 0.023 | 0.027 | -16 | 0.013 | 0.047 | -72.3 | 0.84 |
| G1H036 | 252 | 0.053 | 0.059 | -10 | 0.03 | 0.049 | -38.8 | 0.88 |
| G1H013 | 297 | 0.023 | 0.025 | -7 | 0.016 | 0.021 | -23.8 | 0.89 |
| G1R003 | 354 | 0.024 | 0.025 | -5.5 | 0.012 | 0.017 | -29.4 | 0.92 |
| Tributaries | | | | | | | | |
| G1H003 | 160 | 0.025 | 0.034 | -25 | 0.0164 | 0.071 | -77.0 | 0.79 |
| G1R002 | 34 | 0.009 | 0.01 | -10.8 | 0.003 | 0.008 | -62.5 | 0.97 |
| G1H019 | 267 | 0.012 | 0.013 | -8.3 | 0.005 | 0.008 | -37.5 | 0.9 |
| G1H037 | 72 | 0.027 | 0.0277 | -3.5 | 0.01 | 0.015 | -33.3 | 0.87 |
| G1H039 | 128 | 0.3 | 0.33 | -9.7 | 0.16 | 0.212 | -24.5 | 0.96 |
| G1H041 | 234 | 0.02 | 0.024 | -15 | 0.0099 | 0.023 | -56.9 | 0.91 |
| G1H008 | 294 | 0.016 | 0.017 | -6.8 | 0.0087 | 0.011 | -20.9 | 0.96 |
| G1H065 | 506 | 0.013 | 0.014 | -5.4 | 0.0057 | 0.0078 | -26.9 | 0.86 |
| G1H043 | 101 | 0.033 | 0.036 | -7.8 | 0.012 | 0.019 | -36.8 | 0.84 |
| G1H035 | 164 | 0.038 | 0.046 | -17 | 0.026 | 0.043 | -39.5 | 0.95 |
| G1H034 | 317 | 0.147 | 0.176 | -16.5 | 0.15 | 0.18 | -16.6 | 0.62 |

6.3.1.2 Temperature Infilling

Temperature was also measured on a two weekly basis. The air temperature was made available by Western Cape Department of Agriculture, Elsenburg, while the water temperature data was available from DWAF. Some stations (e.g. G1H004, G1H003 and G1H019) have only temperature measurements up to 1990, it was assumed that the missing temperature will follow the same function as in the years prior to 1990.

Three methods were examined in order to determine the best suited function for the infilling of temperature:

1) Regression with the Air Temperature

Air Temperature Data was obtained by Western Cape Department of Agriculture, Elsenburg. The air temperature measurements of the catchment at stations near to the gauging stations of the river were compared to the water temperature and both follow similar harmonic functions. However, at most of the stations the measurements of the two temperature stations did not correspond in years, and therefore a regression between the air temperature and water temperature could not be performed for the majority of the stations.

For station G1H020 and Nederburg the sampling years coincided and a regression of grab sample values was attempted. A correlation coefficient of 0.81 was achieved.

2) Fourier Series

Forecasting and prediction of water temperature is often completed by approximating the daily average water temperature using a regression fit, based on the Fourier series approximation (Long, 1976; Thomann 1967).

The regression analysis uses observation of a time series $X(t_i)$, $i = 1, 2, \dots, n$ and assumes

$$F(t_i) = A_0 + 2 \sum_{k=1}^{M} C_k \sin(2\pi k t_i + \Phi_k)$$

where

$$C_k = (A_k^2 + B_k^2)^{1/2}$$

and

$$\Phi_k = \arctan \frac{A_k}{B_k}$$

and the Fourier coefficients A_k and B_k are obtained by a least squares fit of the data to the k th harmonic component (which in our case is 0.5 to obtain the annual cycle of temperature variations):

$$A_0 = 1/n \sum_{i=1}^n X(t_i)$$

$$A_k = 1/n \sum_{i=1}^n X(t_i) \cos(2\pi k t_i)$$

and

$$B_k = 1/n \sum_{i=1}^n X(t_i) \sin(2\pi k t_i)$$

3) Simple Harmonic Function

For most practical purposes a simple harmonic function is sufficient to describe the seasonal variation for temperature (Sanders et al, 1980). The function applied is:

$$y_t = A (\cos \omega t + B)$$

- yt = value of function at time t
- ω = 360 degree/nr of samples per year
- A,B = least squares fitted constants (see above)

Figures 1.2.24 to 1.2.34 in Appendix 1.2 displays the comparison of infilled and measured temperature values. This prediction of temperatures is a simplification of the abovementioned Fourier series, yet it seems to be sufficient to predict the temperatures reasonably accurately. Table 6.15 summarizes the coefficient of determination (R2) and the errors for every year infilled for the various stations.

Table 6.14: Details of Temperature Infilling

| Station | Years of Data | Nr of Samples | Function |
|---------|---------------|---------------|---------------------------|
| G1H004 | 1987-1990 | 167 | 6.2 cos (x-31450) + 16.5 |
| G1H003 | 1985-1990 | 167 | 6.25 cos (x-31450) + 18.3 |
| G1H019 | 1980-1990 | 315 | 4.15 cos (x-31428) + 15 |
| G1H036 | 1983-1998 | 570 | 6.5 cos (x-32897) + 18.8 |
| G1H008 | 1993-1997 | 173 | 7 cos (x-32890) + 18 |
| G1H039 | 1983-1997 | 274 | 7 cos (x-32175) + 18.8 |
| G1H041 | 1980-1994 | 350 | 7 cos (x-32890) + 18 |
| G1H013 | 1980-1997 | 627 | 7.5 cos (x-31450) + 19.3 |

Table 6.15: Statistics of Temperature Infilling

| Station | Summer Mean Infilled (Oct-March) | Winter Mean Infilled (Apr-Sept) | Summer Mean Measured (Oct-March) | Winter Mean Measured (Apr-Sept) | Summer Mean Error | Winter Mean Error | (R ²) |
|---------|----------------------------------|---------------------------------|----------------------------------|---------------------------------|-------------------|-------------------|-------------------|
| G1H004 | 20.19 | 12.87 | 20.23 | 13.33 | -0.19 | -3.45 | 0.75 |
| G1H003 | 21.67 | 14.52 | 20.58 | 14.1 | 5.3 | 2.98 | 0.67 |
| G1H019 | 17.21 | 14.17 | 17.17 | 14.24 | 0.2 | -0.5 | 0.7 |
| G1H036 | 23.31 | 13.66 | 22.48 | 14.55 | 3.7 | -6.1 | 0.63 |
| G1H008 | 21.13 | 12.78 | 20.57 | 13.77 | 2.7 | -7.2 | 0.00 |
| G1H039 | 22.3 | 15.17 | 23.04 | 15.24 | -3.2 | -0.5 | 0.75 |
| G1H041 | 22.23 | 14.15 | 21.69 | 14.44 | 2.5 | -2 | 0.75 |
| G1H013 | 23.4 | 15.3 | 23.6 | 14.6 | -0.85 | 4.8 | 0.72 |

6.3.1.3 Oxygen Infilling

No oxygen data is available for the Berg River, but as oxygen is also temperature-dependent, the saturated oxygen concentration may be used as upper limit reference value, assuming that no oxygen has been lost for any chemical process. The oxygen concentration was approximated by the following equation (Hua, 1990):

$$DO = 14.562 - 0.41022T_s + 0.0079910T_s^2 - 0.000077774T_s^3$$

- where DO = saturated dissolved oxygen concentration (mg/l)
- Ts = surface water temperature (°C)

6.3.1.4 Incorporation of observed grab samples in infilled time series

As one can see from Figures 1.2.1 to 1.2.23 in Appendix 1.2, the measured grab samples are not included in the generated time series. The infilled time series were used initially in the configuration, as it follows a "smoother" trend without the measured data. In Section 8.6.5, however, a sensitivity analysis was completed with and without the grab samples incorporated into the infilled time series. The grab sample was included in the time series by interpolating the two values before and after each grab sample in order to smoothen the impact it might have on the time series.

6.3.2 Water Quality Variables

The state variables that are not modelled (e.g. chl-a) for this study, but specified in the predefined water quality model, EUTROF1, have been assigned a zero value. The water quality concentrations of interest have been entered as non-uniform time series, which has been infilled according to Section 6.3.1.

6.3.3 Abstractions

There are two possibilities for DUFLOW to calculate water quality loads at points where the water flows out of the system.

- If no water quality boundary condition is specified at a point, the concentration of the outflowing water volume is treated as zero concentration. This option has been used at the evaporation points.
- At irrigation and water abstraction points, a water quality boundary condition had to be defined. The outflowing concentration is then calculated relative to the volume of the outflowing water.

6.3.4 External Variables

External variables, such as solar radiation, evaporation rates and air temperature have been imported into the DUFLOW dialog box as time series. External variables are required for the process calculations. Refer to Section 5.4.5 for a description of the various water quality processes. The meteorological information was obtained from the Department of Agriculture, Elsenburg and the Weather Bureau.

External parameters can be defined at every schematization point or node. This allows for more flexibility, as the external variables can be adjusted corresponding to their location. A limitation of DUFLOW is, that the time series at every schematization point are written to file and therefore the size of the external variables is quite high (51Mb).

Table 6.16 summarizes the meteorological stations which have been used for predicting the influence of the meteorological input data required by DUFLOW, and the corresponding water gauging stations. Unfortunately, not all stations have measurements during the calibration period 1993-1994. The most complete data set for the whole range of years was for Bien Donne. For all stations downstream of G1H037 insufficient information was available for the meteorological stations situated in this area and data of Landau had to be used.

Table 6.16: Meteorological stations used and corresponding water gauging stations

| Meteorological Station | Latitude | Longitude | Water Gauging Station | Latitude | Longitude |
|------------------------|----------|-----------|-----------------------|------------|------------|
| La Motte | 33°•53' | 19°•05' | G1H004 | 33°•55' 36 | 19°•03' 41 |
| Bien Donne | 33°•50' | 18°•59' | G1H019 | 33°•54' 44 | 18°•56' 36 |
| Nederburg | 33°•43' | 19°•01' | G1H020 | 33°•42' 29 | 18°•56' 29 |
| Landau | 33°•36' | 18°•58' | G1H037 | 33°•37' 39 | 18°•59' 29 |

6.3.4.1 Air Temperature

Table 6.17 lists the average air temperature for the different stations. It can be observed from the table, that the difference in temperature between the different stations is minimal. La Motte experiences the highest summer temperatures.

Table 6.17: Average monthly air temperature measured at meteorological stations

| | Oct | Nov | Dec | Jan | Feb | Mar | Apr | May | June | Jul | Aug | Sep |
|------------|------|------|------|------|------|------|------|------|------|------|------|------|
| La Motte | 25.1 | 25 | 28.2 | 23.7 | 23.8 | 21.7 | 20.1 | 14.4 | 12.2 | 11.8 | 13.4 | 15.5 |
| Bien Donne | 18.1 | 20.9 | 22.1 | 23.7 | 23.8 | 22 | 20 | 13.5 | 11.9 | 11.3 | 12.8 | 15.2 |
| Nederburg | 20.3 | 22.4 | 23.4 | 25.3 | 25.9 | 23.6 | 21.3 | 15.1 | 12.5 | 12.3 | 13.7 | 16.1 |
| Landau | 19.8 | 22.5 | 23.3 | 25.5 | 26.1 | 23.6 | 21.6 | 15 | 12.5 | 11.8 | 13.4 | 15.9 |

6.3.4.2 Solar radiation

Solar radiation was provided by the Department of Agriculture, Elsenburg at various weather stations along the river. Similar to the meteorological stations, most of the weather stations do not consist of uninterrupted periods of measurements, except for Bien Donne. It was therefore decided to use the radiation data of this station for the whole catchment. Radiation is required for the calculation of the temperature in the river (refer to Section 5.4.5.1). Referring to Figure 1.2.1 in Appendix 1.2, a slight change in phase is perceived. The lowest recorded measurements are generally equal; while the December/January values are at a maximum in 1990 and 1996. Table 6.18 tabulates the monthly averages (MJ) at Bien Donne for the configuration period.

Table 6.18: Monthly Radiation Averages (MJ/day) at Bien Donne for 1993/1994

| | Oct | Nov | Dec | Jan | Feb | Mar | Apr | May | June | Jul | Aug | Sep |
|------------|------|------|------|------|------|------|------|-----|------|-----|------|------|
| Bien Donne | 17.9 | 24.4 | 24.5 | 26.3 | 23.5 | 19.5 | 14.3 | 9.9 | 6.9 | 9.4 | 10.3 | 12.2 |

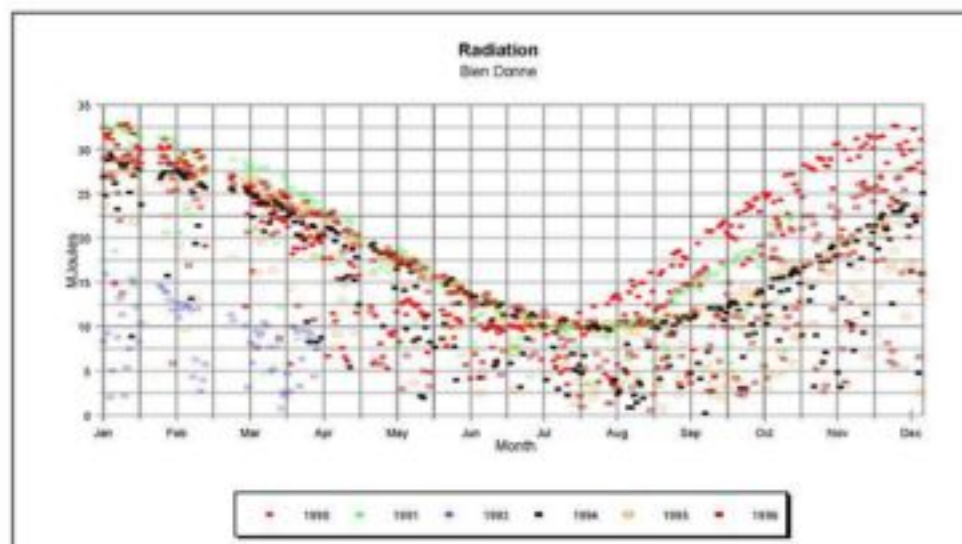


Figure 6.7: Radiation (MJ) at Bien Donne

6.3.4.3 Wind data

The wind data is a meteorological variable that is required for the water temperature computations (refer to Section 5.4.5.1). Table 6.19 summarizes the monthly wind speed at the specific stations. Bien Donne experiences the highest wind nearly all year. The wind data was converted to m/s for the process calculations.

Table 6.19: Monthly wind speed (km/month) for 1993/1994

| | Oct | Nov | Dec | Jan | Feb | Mar | Apr | May | June | Jul | Aug | Sep |
|------------|-------|-----|-----|-----|-----|-----|-----|-----|------|-----|-----|-----|
| La Motte | 114 | 131 | 125 | 125 | 133 | 87 | 86 | 56 | 124 | 74 | 63 | 115 |
| Bien Donne | 207.9 | 237 | 274 | 271 | 285 | 209 | 154 | 66 | 155 | 90 | 154 | 184 |
| Nederburg | 196.8 | 224 | 254 | 240 | 280 | 194 | 166 | 87 | 156 | 92 | 146 | 169 |
| Landau | 113.8 | 115 | 128 | 129 | 121 | 94 | 82 | 62 | 91 | 70 | 85 | 96 |

6.3.4.4 Evaporation Rates

Evaporation rates are needed for the temperature process calculations (refer to Section 5.4.5.1 for the process calculations and their specific algorithms). It can be observed from Table 6.20 that the highest evaporation rate is experienced in January. It is interesting to note that although Landau lies downstream of Nederburg, it experiences higher evaporation rates.

Table 6.20: Evaporation Rate (average mm/day) for the various meteorological stations

| | Oct | Nov | Dec | Jan | Feb | Mar | Apr | May | June | Jul | Aug | Sep |
|------------|-----|-----|------|------|------|-----|-----|-----|------|-----|-----|-----|
| La Motte | 6.3 | 7.9 | 8.2 | 9 | 8.4 | 5.4 | 3.7 | 1.8 | 1.8 | 1.4 | 2.1 | 3.1 |
| Bien Donne | 6.2 | 8.3 | 9.7 | 10.6 | 10.2 | 6.7 | 4.9 | 1.8 | 1.3 | 1.5 | 2.7 | 3.4 |
| Nederburg | 8.3 | 10 | 11.5 | 12.1 | 12.8 | 8.5 | 6.1 | 2.4 | 1.1 | 1.6 | 3.2 | 4.2 |
| Landau | 6.4 | 8.3 | 8.6 | 9.6 | 9.5 | 5.9 | 3.8 | 1.9 | 1.1 | 1.1 | 2.2 | 3.1 |

6.3.5 Parameters

Default values for the parameters are used in the first simulation runs and are then adjusted at the calibration (refer to Section 8.6 for a description of the sensitivity of the parameters). Table 6.21 lists the parameters that are used in the process calculations. All the other parameters that are predefined in the EUTROF1 model have been set to zero.

Table 6.21: Parameters used in DUFLOW

| Parameter | Default Value | Description |
|------------|---------------|--|
| A | 0.56 | Coefficient used in atmospheric longwave radiation (0.5-0.7) |
| •• | 0.97 | emissivity of a body |
| kr_{min} | 0.1 | Minimum oxygen transfer coefficient |
| rl | 0.03 | Reflection coefficient, usually small |
| t_{min} | 1.047 | minimum temperature reaction rate for PO_4 |
| t_{rea} | 1.024 | reaction rate for PO_4 |

6.4 PROBLEMS ENCOUNTERED

The accuracy and stability of the calculations depend on the implicit factor θ , as well as the time step and the space step (refer to Section 5.6). Most of the stability problems encountered during the test runs were due to these factors, especially in the upper reach as the slope is very steep (0.35%) and "negative" water depths resulted at some sections. It took great effort to achieve a fairly stable flow condition which would be stable for calculating the correct water quality concentrations.

- Difficulties were experienced especially in the first reach from G1H004 to G1H020. Downstream of G1H020, the flow calculations were fairly stable. This is because the slope of the river is quite steep in the first reach and DUFLOW does not handle supercritical flow or near supercritical flow well.
- Negative water depths were calculated at some sections in the river. The water quality calculations were unable to calculate any concentration values because of these negative water depths, as the process descriptions occasionally need to take the square root of the water depth.
- In a longitudinal graph the concentrations would be shown as very strong "toothed" graphs. This is due to instability in the transport, which occurs when the Peclet number becomes too high ($Pe > 2$) (see equation 5.19 for definition of the Peclet number).
- As initial conditions are user defined, a constant flow corresponding to the first date of simulation was taken as the upstream boundary value. The simulation was run until the longitudinal graph as well as the time series showed a stable calculation. The levels and the discharge calculated were then used as the initial value. Normally, the initial values should not create any problems as any error would cancel out after a few time steps, but as the calculations start at a very steep slope (average slope of 0.35% in reach 1, G1H004 to G1H020), negative water depths are calculated from the very beginning and the errors then accumulate. The schematization points inserted forced the calculations to begin with positive water depths and also minimal space steps and therefore the calculations would not become unstable right at the start of the calculations.

All the above problems mentioned have been overcome by implementing very small space steps and by adding schematization points (points where a level and discharge can be defined as initial values (refer also to Figure 5.2)) at very small distances. These distances depend on the problem area for the first reach the schematization points were spaced at about 100m, while further downstream, where the slope is milder, the space steps were increased to about 2 km. This lets the computation proceed, but still does not change the fact that the configuration is unstable and any change like an additional discharge point or cross-section will affect the stability. Also, because of the very small space steps, the time taken for the simulation increases and the output file for a year grows to about 12 Mb for the flow and about 50 Mb for the quality constituents.

CHAPTER SEVEN

FLOW MODEL SENSITIVITY, CALIBRATION AND VERIFICATION

7.1 INTRODUCTION

As explained in Section 2.3.3, important steps in any conventional modelling process (following the configuration of the model with a specific data set) are: *calibration*, *sensitivity analysis* and *verification*. These steps have also been taken for the Berg River model. As the water quality part of the model is dependent on the calibrated hydraulic component, and every error introduced in the flow module will influence the water quality calculations, it has been decided to separate the calibration and verification of the hydraulic and water quality modules into two distinct processes reported in two Chapters. This chapter deals therefore with the calibration and verification of the hydraulic component of the model, while Chapter 8 follows with the calibration and verification of the water quality module.

The 'goodness-of-fit' between the simulated values and the measured data set is determined by *objective functions*. The first section of this chapter describes the objective functions used in the following two chapters to analyse the results of the simulation.

The process of adjusting parameters by running the model at different parameter values until a satisfactory result is obtained is called *calibration* (Grijsen, 1986). A close correspondence between observed data and simulated data is required, as the model is supposed to represent the situation in reality. A *sensitivity analysis* is therefore important for the calibration process, as it determines which parameters have a significant impact on the model results. In the second section of this chapter the calibration of the flow simulation, by introducing ungauged runoff, and the sensitivity and adjustment of Manning's roughness value are discussed.

Lastly, the results of the model verification are presented. The term *verification* will be used to describe the process of ensuring that the model applied to the specific river for a set of data can be applied to another situation. The model was first verified in *space*, by using measured downstream hydrographs (G1H020 and G1H036) as boundary inflow hydrographs, to determine the errors introduced in the model during the different reaches. Finally, the model was verified for a *time* period not used during the calibration.

7.2 OBJECTIVE FUNCTIONS

"The term *objective function* is now widely used to describe any specific fitting criterion employed in the parameter estimation process." (Görgens, 1983, pg 141). Therefore, the term **objective function** is used to describe the correspondence of simulated and observed values by several specific statistical procedures (goodness-of-fit criteria). These statistical tests are used to quantify the agreement between predictions and observations. The mathematical description of the objective functions needs to be introduced before progressing to the actual calibration procedure and sensitivity analysis description. It was decided to divide the results into three categories to analyse how the goodness-of-fit changes seasonally:

- overall yearly values
- low-flow period (October to April)
- high-flow period (May to September)

The objective functions used are:

- % error in mean

$$\%e = 100 * \frac{(X_{si} (mean) - X_{ob} (mean))}{X_{ob} (mean)} \quad 7.1$$

- % error in volume or load

$$\%e = 100 * \frac{(X_{si} (vol) - X_{ob} (vol))}{X_{ob} (vol)} \quad 7.2$$

- % error in std deviation

••

$$\frac{0}{0\ell} = 100 * \frac{(X_{si} (std) - X_{ob} (std))}{X_{ob} (std)} \quad 7.3$$

••

- Coefficient of determination (correlation coefficient)²

$$\text{correlation coefficient} = \frac{(n(\sum X_{si} * X_{ob}))}{\sqrt{((n * \sum X_{si}^2 - (\sum X_{si})^2) * (n * \sum X_{ob}^2 - (\sum X_{ob})^2))}} \quad 7.4$$

- Coefficient of efficiency

$$= 1 - \frac{\sum (X_{si} * X_{ob})^2}{\sum (X_{ob} - X_{ob}(\text{mean}))^2} \quad 7.5$$

The *percentage error* in mean, volume and standard deviation (eqn. 7.1-7.3) represents the difference between the predicted and the observed values. This measure is a good indication of the under- or over-simulation. It can however counterbalance discrepancies in the values. Therefore, additional functions are needed to assess the accuracy of the simulated values. The *coefficient of determination* (eqn. 7.4) indicates the degree of correlation between observed and simulated values. It approaches 1 when a high degree of correlation between the two values exists. The *coefficient of efficiency* (eqn. 7.5) is also a dimensionless measure of the correlation of the two values, it is however sensitive to systematic errors. Therefore, the difference between the coefficient of determination and the coefficient of efficiency is a function of the systematic error in the model simulation. The reader is referred to Görgens (1983) for various other valuable objective functions and a step by step approach leading to objective function selection. Reckhow *et al* (1990) also describes useful statistical functions that can be used in the analysis.

7.3 MODEL CALIBRATION AND SENSITIVITY PROCEDURE

The process of adjusting parameters by running the model at different parameter values until a satisfactory result is obtained, is called *calibration* (Grijzen, 1986). A close correspondence between observed data and simulated data is required. Calibration and the sensitivity analysis of the Manning's resistance coefficient were completed simultaneously, as the sensitivity of the Manning's resistance coefficient indicates the degree of adjustment necessary for the parameter. The *sensitivity* of parameters means the relative significance of each parameter in the performance of the whole model (Görgens, 1983; pg. 194).

The calibration procedure consisted of following steps:

- Determination of reliable calibration period
- Determining accuracy of boundary conditions
- Introducing flows of ungauged tributaries
- Calibrating the flow model by adjusting the resistance in the model, which is portrayed by the Manning's roughness coefficient

7.4 CALIBRATION PERIOD

The calibration period October 1993 to October 1994 was chosen, for the following reasons:

Firstly, this period is a whole annual cycle and thus includes low as well as high flow. Wemmershoek inflow information was readily available from July 1993 onwards and in the interest of economy of time to

it was decided to calibrate from this year onwards. There is adequate daily flow information for most of the gauging stations compared to other years.

Secondly, the daily flows at station G1H037 (Krom River tributary) were not measured anymore from 1993 onwards. To be able to use the model in the time period when Skuilfraam Dam would have been built, this influence on the mass balance of the flows needs to be taken into consideration and thus it is treated as an ungauged tributary. Also, this year chosen is after the change of preservation of water quality samples which took place in 1989 (see Section 4.6.1).

7.5 BOUNDARY CONDITIONS AND INITIAL CONDITIONS

The accuracy of the inflow hydrograph and the downstream rating curve is important when considering calibration, especially for the numerical accuracy of the model. Accuracy ratings of the gauging stations were given at a re-rating survey (DWAf, 1994), rating curves were also established by taking the various conditions at the weirs into account (e.g. sedimentation). The accuracy ratings of these stations (0=lowest and 5= highest) are listed in Table 7.1.

The inflow hydrograph at G1H004 has a high rating and therefore it can be expected to be about 80% accurate. G1H003, G1H039 and G1H035 have a very low accuracy rating and this needs to be remembered when analysing the results of the model.

An error in the initial values does have an effect on the calculations, but any errors resulting from inaccuracies of the initial values are soon cancelled out after a few time steps. Therefore, enough "warm up" time has been allowed for in the simulation run for the flow to stabilise before any results are written to a file.

Table 7.1 Accuracy Rating of Gauging Stations

| Station Number | River Name | Accuracy Rating |
|----------------|-------------|-----------------|
| G1H004 | Berg | 4 |
| G1H003 | Franschhoek | 1 |
| G1H019 | Banhoek | 4 |
| G1H020 | Berg | 4 |
| G1H039 | Doring | 0 |
| G1H041 | Kompagnjies | 5 |
| G1H036 | Berg | 4 |
| G1H008 | Klein Berg | 4 |
| G1H043 | Holle | 3 |
| G1H013 | Berg | 4 |
| G1H035 | Matjies | poor |
| G1H034 | Sandspruit | 3 |

7.6 ADDITION OF UNGAUGED SUB-CATCHMENT FLOWS

The lack of flow data for certain tributaries causes difficulties in the comparison between measured flows and simulated values. The winter flow is underestimated due to ungauged inflow, which then has an impact on the simulated water quality loads. The ungauged tributaries runoff therefore had to be estimated as follows:

In the absence of a rainfall-runoff catchment model, a pragmatic adjustment, based on hydrological response pattern was undertaken. The Berg River catchment was subdivided into sub-catchments according to the MAP and also west and east, as the tributaries are perennial on the eastern side and semi-perennial on the western side. A further consideration was that runoff from the Malmesbury shales areas is much higher in TDS than the Table Mountain sandstone areas. The ungauged areas in the Berg River catchment were marked out on topographical maps and the area sizes were determined. The ungauged hydrographs for the river were then estimated by multiplying the nearest or most suitable

gauged daily hydrograph by the ratio of the ungauged runoff area to the gauged area. Additionally, a MAP-MAR (mean annual precipitation-mean annual runoff) weighting derived from the *Surface Water Resources of South Africa, 1990* (Midgley *et al*, 1994) was applied. Table 7.2 summarizes the various correction factors which have been applied to correct for the ungauged inflow and the catchment area as well as the MAP of the gauged areas. The location of the corresponding areas are illustrated in Figure 7.1.

Table 7.2 Description of Gauged Tributaries

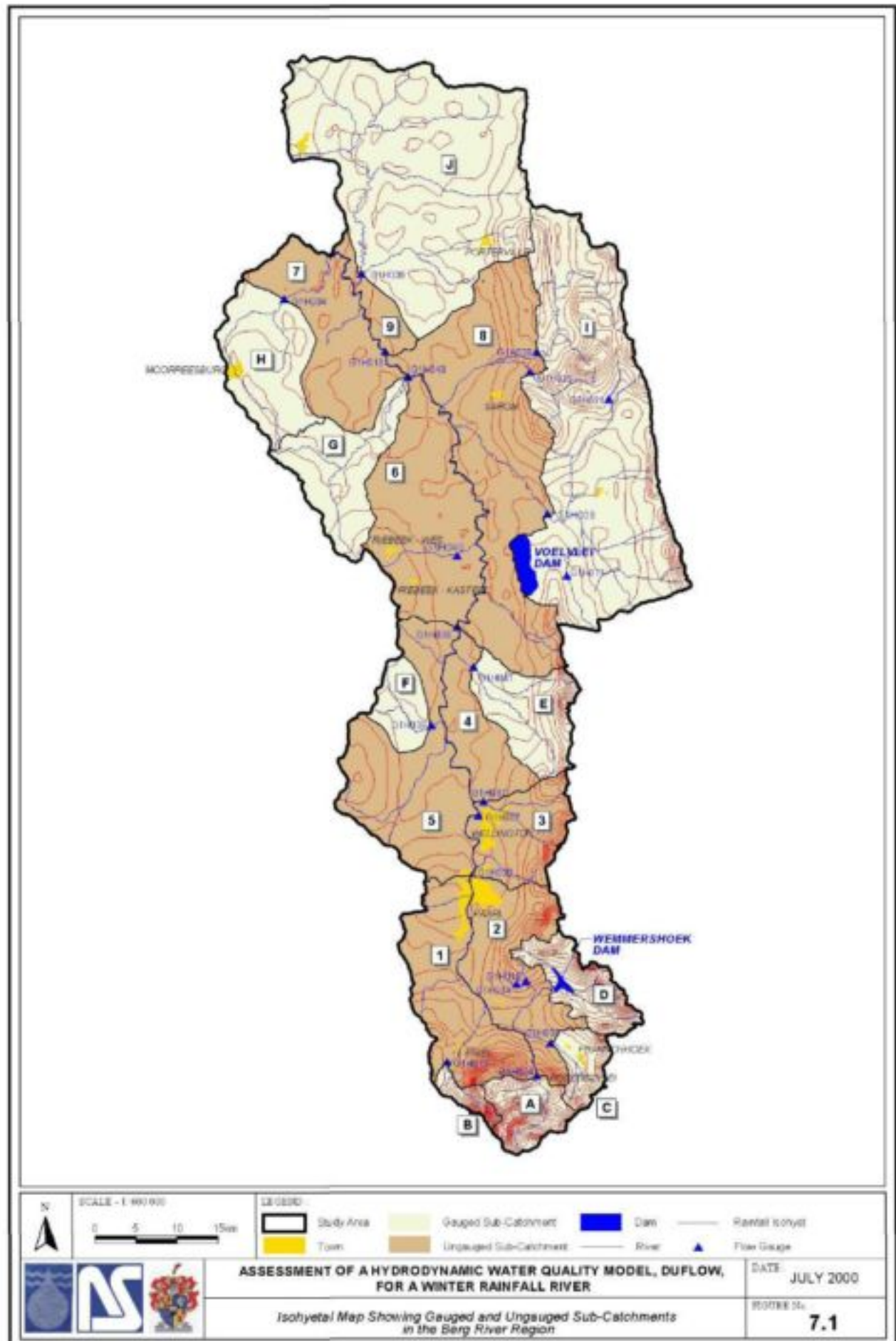
| Catchment Number (Figure 7.1) | Flow Gauge | River | Gauge Name | Catchment Area | MAP |
|----------------------------------|------------|-------------|--------------------|-----------------|------|
| | | | | km ² | mm |
| A | G1H004 | Berg | Driefontein | 72 | 2600 |
| B | G1H019 | Banhoek | Bosmanshoek | 22 | 1804 |
| C | G1H003 | Franschhoek | La Provence | 46 | 1005 |
| D | G1R002 | Wemmers | Wemmershoek | 88 | 1302 |
| E | G1H041 | Kompagnjies | De Eikeboomen | 122 | 707 |
| F | G1H039 | Doring | Grensplaas | 42 | 433 |
| G | G1H043 | Sandspruit | Vrsgewaagd | 150 | 437 |
| H | G1H034 | Holle | Moorreesburgspruit | 160 | 410 |
| I | G1H008 | Klein Berg | Mountain View | 615 | 624 |
| J | G1H035 | Matjies | Matjiesfontein | 671 | 410 |

Table 7.3 Areas and Correction Factors of Ungauged Tributaries

| Catchment Number (Figure 7.1) | Ungauged Area | Area | MAP | MAP/MAR Factor (WR90) | Ungauged Area/ Gauged Area | Flow | Comments |
|----------------------------------|------------------------------|-----------------|-----|-----------------------------|-------------------------------|-------------------|-------------------------------------|
| | | km ² | mm | | | m ³ /s | |
| 1 | west area upstream of G1H020 | 222 | 978 | 0.56 | 222 / 22 | 5.65*G1H019 | |
| 2 | east area upstream of G1H020 | 188.5 | 900 | 0.58 | 188.5 / 88 | 1.2*G1R002 | |
| 3 | G1H037 | 130 | 939 | 1.8 | 130 / 122 | 1.9*G1H041 | No data available from 1993 onwards |
| 4 | area at G1H041 | 164 | 574 | 0.64 | 164 / 122 | 0.86*G1H041 | |
| 5 | area surrounding G1H039 | 225 | 574 | 0.5 | 225 / 42 | 2.7*G1H039 | |
| 6 | G1H040 and surrounding area | 260 | 547 | 2.5 | 260 / 150 | 4.3*G1H043 | No data available for G1H040 |
| 7 and 9 | G1H034 and surrounding area | 170 | 400 | 0.63 | 170 / 160 | 0.64*G1H034 | |
| 8 | G1H008 surrounding area | 400 | 450 | 0.18 | 400 / 615 | 0.12*G1H008 | |

Discussion:

The sub-catchment of G1H039 is used as gauged sub-catchment although it has an accuracy rating of 0 (refer to Table 7.1); the usage of this flow record is still necessary as there is no other gauged sub-catchment on the western side of the Berg River downstream of G1H020 and thus had to be used as an estimate of the runoff from the western tributaries into the main stem of the river.



Prior to the addition of the ungauged sub-catchments, a mass balance of all the incoming flow, gauged and ungauged, was completed. Table 7.4 displays the results of the difference between the mass balance and the measured values at the gauging stations before and after the addition of the sub-catchments. Flow volume which is still lacking between the measured and the flow added in the mass balance, could possibly be due to:

- higher ungauged runoff than estimated
- inaccuracy in the high flow measurements at the various gauging stations.

Most of the ungauged flow occurs in the reach between G1H036 and G1H013 (Table 7.4). G1H020 and G1H036 are slightly overestimated after addition of the ungauged inflow.

Table 7.4 Mass balance of flow corrected and measured for 1993/1994

| | | G1H020 | G1H036 | G1H013 | G1R003 |
|---|---------------------------|--------|--------|--------|--------|
| Difference in Volume (Mm ³) before addition of ungauged sub-catchments | low flow period (Oct-Mar) | 24 | 15 | -13 | 19 |
| | high flow (April-Sept) | -65 | -36 | -130 | 91 |
| Difference in Volume (Mm ³) after addition of ungauged sub-catchments | low flow period (Oct-Mar) | 32 | 17 | -12 | 18.7 |
| | high flow (April-Sept) | 11 | 9 | -88 | 92 |

7.7 SENSITIVITY OF FLOW RESISTANCE

The hydrodynamic model was calibrated against the observed daily flow data for G1H020, G1H036, G1H013 and G1R003. Calibration was achieved by adapting the Manning's roughness coefficient until a satisfactory fit was achieved between the observed daily flow values and the model results.

Table 7.6 shows the sensitivity of the Manning's n value with respect to the mean and the standard deviation calculated. A run with n=0.06 was completed, followed by two runs with n=0.04 and n=0.08, and compared with the n=0.06 simulation, which was treated as "observed" data. The % difference was calculated by:

$$\%diff = (sim_{n_i} - sim_{n_{obs}}) / (sim_{n_{obs}}) * 100\%$$

Change in mean:

It can be seen from the results (Table 7.6) that by increasing the Manning's value by an amount of 0.02 the change in mean is more significant than decreasing the Manning's resistance. The difference in Manning's roughness coefficient has the most effect at stations G1H020 and G1R003. For G1H020 and G1H036 a higher mean is simulated for both a negative and a positive change in the Manning's resistance coefficient. At station G1H013 a lower resistance coefficient simulates a lower mean, while for station G1R003 the mean is simulated lower for higher and lower resistances. The percentage changes are however very low (mostly below 1%), which indicates that the flow simulation is influenced minimal by the resistance. Figure 7.2 illustrates the sensitivity of the resistance.

Table 7.5 : Sensitivity of Flow Resistance

| | Diff. in mean (m ³ /s) n=-0.02 | Diff. in mean (m ³ /s) n=0.02 | Diff. in std deviation (m ³ /s) n=-0.02 | Diff. in std deviation (m ³ /s) n=0.02 | Diff. in R ² n=-0.02 | Diff. in R ² n=0.02 |
|-------------------------|---|--|---|--|------------------------------------|-----------------------------------|
| Low flow period | | | | | | |
| G1H020 | 0.1 | 0.13 | 0.97 | 1.46 | -0.25 | -2.39 |
| G1H036 | 0.04 | 0.1 | 2.34 | -0.78 | -1.48 | -1.67 |
| G1H013 | -0.02 | 0.07 | 1.38 | 2.76 | 0.08 | -4.97 |
| G1R003 | -0.18 | -0.13 | 1 | 0.67 | -1.96 | -5.76 |
| High flow period | | | | | | |
| G1H020 | 0.08 | 0.1 | 0.31 | 1.23 | -0.07 | -0.45 |
| G1H036 | -0.24 | 0.44 | -0.46 | -0.19 | -0.32 | -1.4 |
| G1H013 | 0.03 | 0.37 | 0.16 | 1.04 | -0.55 | -1.3 |
| G1R003 | 0.1 | 0.51 | -9.04 | 0.38 | -0.09 | -1.51 |

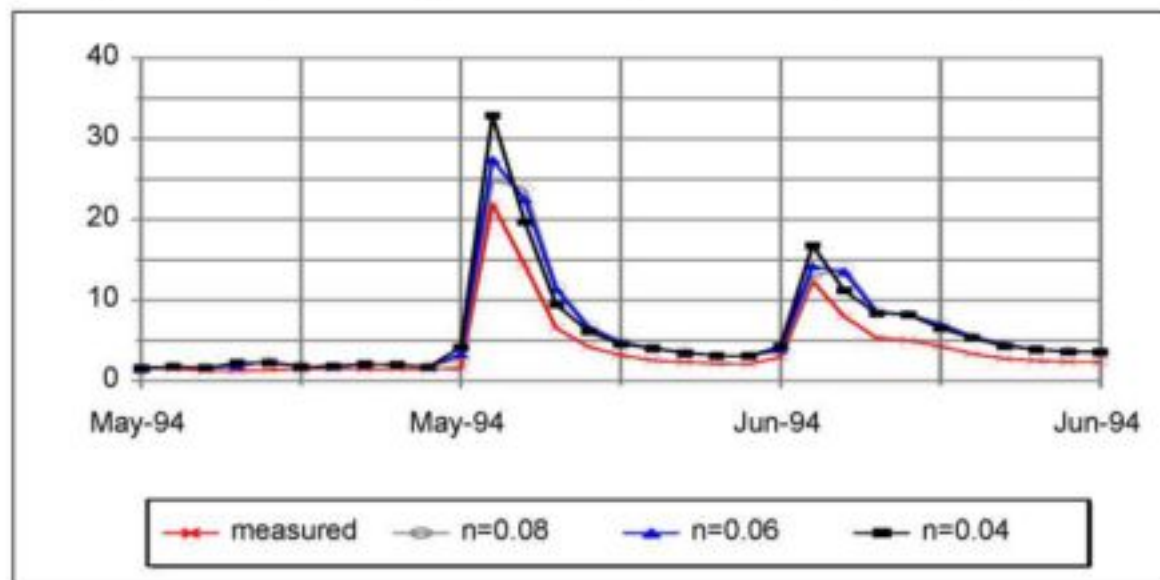


Figure 7.2: Sensitivity of Mannings Roughness Value

7.8 RESULTS OF FLOW MODEL CALIBRATION

For the final model a Manning's value of 0.06 was obtained by a trial and error approach as described in Section 7.7. This value reproduced the observed values fairly accurately. The % error between the resistance factors is relatively small when compared to the error introduced by the missing flow in the peaks from the inflowing hydrographs, and the missing abstractions in the low flow period.

Summer Flow:

It is evident from the large positive error in the low flow period (summer), that more abstractions take place than those registered/permitted (i.e. recognized by our configuration). For calibration purposes an additional "lump" value could be added as additional unaccounted abstractions. It was however decided against it, as in certain time periods the low flow is very near to the measured data and additional abstractions could result in negative depths, which create instabilities when calculating the water quality (refer for example to Figure 1.3.5 in Appendix 1.3, where the simulated low flow follows the measured

data quite comparably). The hydrograph of G1R003 (Figure 1.3.7 in Appendix 1.3) shows well-defined short-lived increases in the simulated low flow, which is only slightly apparent in the measured data. These are due to the irrigation releases made from Voëlveit Dam into the Berg River (refer also to Figure 6.2, where the inflow hydrograph of Voëlveit releases can be seen). For G1H020 and G1H036 (Figures 1.3.2 and 1.3.3 respectively) the low flow pattern does not follow the measured data as consistently as for G1H013 (Figure 1.3.5 in Appendix 1.3) and the correlation coefficient is very low. For all gauging stations, March, April, October and November are clearly over-simulated. Refer to Figures 1.3.1, 1.3.3, 1.3.5 and 1.3.7 in Appendix 1.3 for the graphical representation of the results for the simulated low flow. Table 7.6 shows the statistical results of the comparison between the measured data and the simulated flow.

Winter Flow:

The simulated winter (high) flow follows the pattern of the measured high flow hydrograph for all stations, although the peaks are underestimated at especially G1H013 (Figure 1.3.5) and G1R003 (Figure 1.3.7). G1H013 and G1R003 have an additional simulated peak in July, which is the result of the inflowing hydrograph of G1H008 (refer also to Figure 6.1), and the additional runoff from the ungauged sub-catchment 8 that has been corrected with the flows of G1H008. The correctness of this adjustment may be suspect. The under-simulated flood peaks could be the result of errors in the correction of ungauged sub-catchments or errors in the measurement of the water level at tributary gauging stations, when flooded. The correlation coefficient at all stations for the high flow is acceptable. The volume and the mean are over-simulated although the actual peaks are under-simulated. This is due to the short period when the actual peak occurs, and the volume during the "high flow" winter months for the lower discharges is over-simulated.

Refer to Figures 1.3.1, 1.3.2, 1.3.4 and 1.3.6 in Appendix 1.3 for the graphical representation of the results for the simulated low flow. Table 7.6 shows the statistical results of the comparison between the measured data and the simulated flow.

Table 7.6 : Results of model calibration

| | G1H020 | G1H036 | G1H013 | G1R003 |
|--------------------------------|--------|--------|--------|--------|
| % diff in mean | | | | |
| Total | 5.6 | 17.6 | -8 | 10 |
| Summer | 13.4 | 54 | 26 | 88 |
| Winter | 4.5 | 14.8 | -10 | 6 |
| R2 | | | | |
| Total | 0.98 | 0.98 | 0.92 | 0.94 |
| Summer | 0.83 | 0.71 | 0.73 | 0.64 |
| Winter | 0.97 | 0.98 | 0.92 | 0.93 |
| MCE | | | | |
| Total | 0.95 | 0.95 | 0.81 | 0.87 |
| Summer | 0.41 | 0.54 | 0.47 | 0.22 |
| Winter | 0.94 | 0.96 | 0.82 | 0.88 |
| % diff in std deviation | | | | |
| Total | -2.4 | 9.6 | -29 | -13.7 |
| Summer | 18.8 | -5.7 | -12 | 1.47 |
| Winter | -3.5 | 9.5 | -30 | -15 |

7.9 MODEL VERIFICATION

The term *verification* will be used to describe the process of ensuring that the configuration of the model applied to the specific river for a particular set of calibration data can be applied to another period of data; this is to ensure that the calibration errors in the simulated values are acceptable. The configured and

calibrated model was verified in space and time. Verification in time shows whether the errors are consistent for a totally independent set of data in time; and whether the correction factors of the addition of ungauged runoff are reasonable. Verification in space indicates the degree of accumulation of errors along the four river reaches and whether the correction of the ungauged runoff is reasonable.

7.9.1 Verification in Space

To verify the model in space, two model runs were completed. Firstly, the recorded flow at G1H020 was used as inflow hydrograph at G1H020 in the model to verify the results obtained in the reach of G1H020 to G1H036, and secondly, the flow recorded at G1H036 was used as inflow hydrograph at G1H036 to verify the model results from G1H036 to G1R003.

It was clear after a verification run, using the G1H020 hydrograph as input at G1H020, that most of the errors downstream of this gauging stations occurred due to addition of ungauged inflow in this reach. Table 7.4 summarizes the results of the verification run, the measured data and the original model run. The correlation coefficient of the verification run is higher than the configured model and this could be due to less error introduced in the run. The systematic error (R^2 - MCE) is much less than in the calibration run. Most of the errors that take place at G1R003 could be the result of incorrect estimates of flow from the ungauged catchments between G1H020 and G1H036. This is portrayed by the improvements in the errors when using G1H036 as inflow hydrograph. Ungauged abstractions may also occur in this reach.

Table 7.7 Results of Verification Run using G1H020 as Inflow Hydrograph

| | | G1H036 | G1H013 | G1R003 |
|---------------------------|--------|--------|--------|--------|
| % diff in mean | | | | |
| original model run | Summer | 54 | 26 | 88 |
| | Winter | 14.8 | -10 | 6 |
| verification run | Summer | 37 | 16 | 68 |
| | Winter | 7 | -15 | 0.5 |
| R² | | | | |
| original model run | Summer | 0.71 | 0.73 | 0.64 |
| | Winter | 0.98 | 0.92 | 0.93 |
| verification run | Summer | 0.96 | 0.85 | 0.77 |
| | Winter | 0.97 | 0.91 | 0.93 |
| MCE | | | | |
| original model run | Summer | 0.54 | 0.7 | 0.22 |
| | Winter | 0.96 | 0.82 | 0.88 |
| verification run | Summer | 0.64 | 0.65 | 0.08 |
| | Winter | 0.93 | 0.79 | 0.86 |

Table 7.8 Results of Verification Run using G1H036 as Inflow Hydrograph

| | | G1H013 | G1R003 |
|---------------------------|--------|--------|--------|
| % diff in mean | | | |
| original model run | Summer | 26 | 88 |
| | Winter | -10 | 6 |
| verification run | Summer | -7 | 27 |
| | Winter | -20.5 | -5 |
| R² | | | |
| original model run | Summer | 0.73 | 0.64 |
| | Winter | 0.92 | 0.93 |
| verification run | Summer | 0.94 | 0.85 |
| | Winter | 0.94 | 0.95 |
| MCE | | | |
| original model run | Summer | 0.77 | 0.22 |
| | Winter | 0.82 | 0.88 |
| verification run | Summer | 0.87 | 0.71 |
| | Winter | 0.77 | 0.87 |

7.9.2 Verification in Time

Verification in time was completed by using a totally independent set of flow data and comparing the errors with the errors resulting from the configuration model. The year 1994/1995 was chosen for verification in time, as it had relatively complete flow data sets. Unfortunately, for the station G1H036, the flow measurements are also incomplete from 3 July onwards. It therefore should be noted that the statistical comparison for the high flows have only been included up to that date and are thus not a complete reflection of the correspondence with the measured data. This year experienced much higher flows and also more high peaks (three larger peaks and smaller peaks before July) than the calibration year's data (one defined peak). Figures 1.3.8 to 1.3.15 in Appendix 1.3 show the verification simulated values graphically.

Comparing Tables 7.9 and 7.6, it can be seen that the simulation errors for the verification data are less than for the calibration data. This indicates that the correction factors applied to the ungauged runoff are reasonable. G1R003 is again over-simulated by a high percentage for the summer period. This would be the result of unknown abstractions, given that the contribution of flow from the corrected ungauged areas 7 and 9 (refer to Figure 7.1) is minimal in this period, as the tributary G1H034 is semi-perennial. The simulated low flow displays a better degree of correspondence than the configured data (refer to Table 7.7), and all coefficients of determinations are above 0.8. Again, it can be concluded that the correction factors applied to the ungauged runoff and the information obtained about the abstractions prove to be satisfactory for the low flow, except for the reach G1H013 to G1R003.

Table 7.9: Verification in time (1994/1995)

| | G1H020 | G1H036 | G1H013 | G1R003 |
|--------------------------------|--------|--------|--------|--------|
| % diff in mean | | | | |
| Total | -27 | 12 | -30 | -8 |
| Summer | 5.8 | 31.3 | 15.1 | 72 |
| Winter | -34.6 | -0.4 | -36 | -16.7 |
| R² | | | | |
| Total | 0.91 | 0.86 | 0.82 | 0.88 |
| Summer | 0.8 | 0.82 | 0.86 | 0.81 |
| Winter | 0.9 | 0.86 | 0.8 | 0.87 |
| MCE | | | | |
| Total | 0.63 | 0.72 | 0.5 | 0.76 |
| Summer | 0.91 | 0.78 | 0.82 | 0.6 |
| Winter | 0.69 | 0.79 | 0.57 | 0.8 |
| % diff in std deviation | | | | |
| Total | -51 | 0.3 | -55 | -28.2 |
| Summer | -7.5 | -11 | 14 | 9.8 |
| Winter | -52 | 3.8 | -58 | -29 |

7.10 DISCUSSION OF FINAL MODEL RESULTS

The objective in this chapter was to develop a flow model capable of predicting the hydrograph at any point in the main river channel. It can be concluded from the statistics mentioned for the various calibration and verification runs, that the model has the ability to predict, with sufficient accuracy, the hydrograph at any downstream section in the river. The accuracy is mainly dependent on the accuracy of the inflowing measured hydrographs and also the estimated runoff of ungauged sub-catchments. Other factors such as the accuracy of the boundary conditions also contribute to the errors. The model reliably simulates the mass balance in the system, but the errors resulting from underestimation of the high flow peaks and overestimation of the low flow, are mainly the result of inaccurate estimation of the ungauged flow. This can be seen from the verification simulation in space (Section 7.9). To be able to simulate a flow hydrograph reliably, the upstream input flows and all the information about abstractions and return flows need to be known. Unfortunately, for most situations, this information is either inaccurate, incomplete or non-existent. The verification in time proved that the correction factors applied to the low flow are satisfactory. The results of the verification in time proved to be better than the configured data results. The correction factors for the high flow are however not acceptable, as the peak flows which are higher than the configured peaks are about 125 m³/s less. Either the actual peak flows measured at the gauging stations are unacceptable or additional correction factors should be applied to the ungauged runoff, although this should have been covered by the MAP/MAR correction factor.

CHAPTER EIGHT WATER QUALITY MODEL SENSITIVITY, CALIBRATION AND VERIFICATION

8.1 INTRODUCTION

The focus of this chapter is on the sensitivity of the water quality parameters used in the various water quality processes in DUFLOW and the calibration and verification of the water quality simulation. The reliability of the water quality parameters is largely dependent on the reliability of the flow simulation; therefore, the errors of the flow simulation have to be borne in mind when analysing the result of the water quality simulation. The sensitivity analysis of the water quality parameters determines the adjustments of these parameters in order to obtain a satisfactory fit that compares reasonably well with the observed data.

8.2 MODEL CALIBRATION AND SENSITIVITY PROCEDURE

Following a similar calibration procedure to that of the flow calibration (refer to Section 7.3) was followed; the following steps were taken in the calibration of the water quality processes :

- Determination of a reliable calibration period with respect to water quality data, bearing in mind the objectives and decision on an optimum calibration period for the flow simulation
- Determine accuracy of boundary conditions
- Introducing water quality of ungauged tributaries
- Calibrating water quality by adjusting the parameters
- Introducing point sources.

8.3 DETERMINATION OF RELIABLE CALIBRATION PROCEDURE

The calibration period was based on the years after the change of preservation of water quality samples that took place in 1989 (refer to Section 4.6.1). The period October 1993 to September 1994 is optimal for the flow calibration, as it occurs after the critical year.

8.4 BOUNDARY AND INITIAL CONDITIONS

The only known measure of error that can express the accuracy of the boundary conditions, is the error calculated in the infilling method (refer to Section 6.3.1). These errors are summarized in Table 8.1.

Table 8.1 : Accuracy of water quality boundary conditions

| Water Quality Variable | G1H004 |
|------------------------|--|
| TDS | -2.8% error in mean concentration $R^2 = 0.93$ for load |
| Phosphates | -5.5% error in mean concentration $R^2 = 0.92$ for load |
| Temperature | Summer mean error -0.19% Winter mean error -3.5% $R^2 = 0.75$ |
| Oxygen | The accuracy of oxygen could not be analysed as no data is available. The oxygen is however dependent on the temperature data and thus as a rough estimate the same measure of error exists for the oxygen as for the temperature. |

As water flows out of the system at Misverstand (G1R003), DUFLOW calculates the corresponding outflowing quality for the specific outflowing volume. Therefore, the downstream water quality boundary accuracy is dependent on the accuracy of the downstream flow boundary. An error in the initial values does not have an effect on the calculations, as any errors occurring due to inaccuracies of the initial values are soon cancelled after a few time steps. Enough time has been given in the simulation run for the flow to stabilise before an results are written to a file.

8.5 ESTIMATION OF UNGAUGED WATER QUALITY SUB-CATCHMENT LOADS

The water quality load contributions from areas that were ungauged had to be estimated. The same ungauged areas are applied for estimating the ungauged water quality loads as was used for ungauged flows (Table 7.3 and Figure 7.1). It was assumed that the ungauged runoff has similar water quality characteristics as the neighbouring gauged tributaries. As a moving regression is suitable to describe the water quality-flow relationship, the same 'infilling' method, as has been described in Section 6.3.1, has been used to approximate the daily water quality of ungauged runoff. The ungauged runoff that has been calculated according to Table 7.3 has been matched with the water quality grab samples of a gauged tributary that is surmised to have similar characteristics. A time series was generated via the moving regression infilling method. Table 8.2 shows the gauged and ungauged areas that have been linked, and has to be read in conjunction with Table 7.2 and Figure 7.1. The summary of the statistics of the infilled values can be read in Tables 8.3 and 8.4.

Figure 8.1 compares the infilled water quality concentration of areas 1 and 2 with infilled concentration of gauging station G1H020, while Figure 8.2 compares areas 4 and 5 with the original infilled concentration time series of G1H039. From the Figures 8.1 and 8.2 one can see that the infilling method does follow the characteristics of the water quality concentration of the corresponding 'linked' gauged area. Most of the ungauged areas experience higher runoff than the gauged areas, primarily due to area size, and this is reflected in the negative "error" in the TDS infilling. Areas 1 and 2 receive less runoff than G1H020 and therefore a positive error in mean concentration is calculated. Interestingly, the infilled phosphate values show all negative errors in mean to the original grab sample.

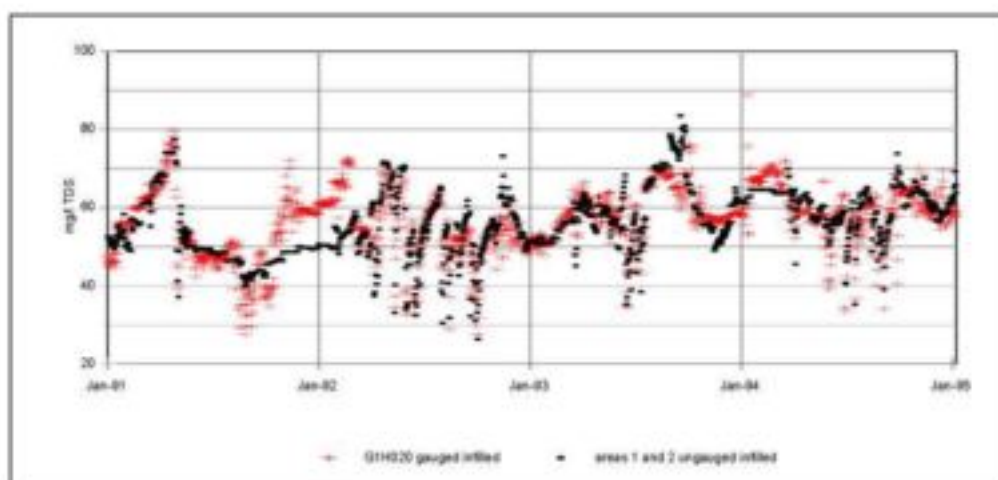


Figure 8.1 : Comparison of infilled water quality concentration of areas 1 and 2 with infilled concentration of gauging station G1H020

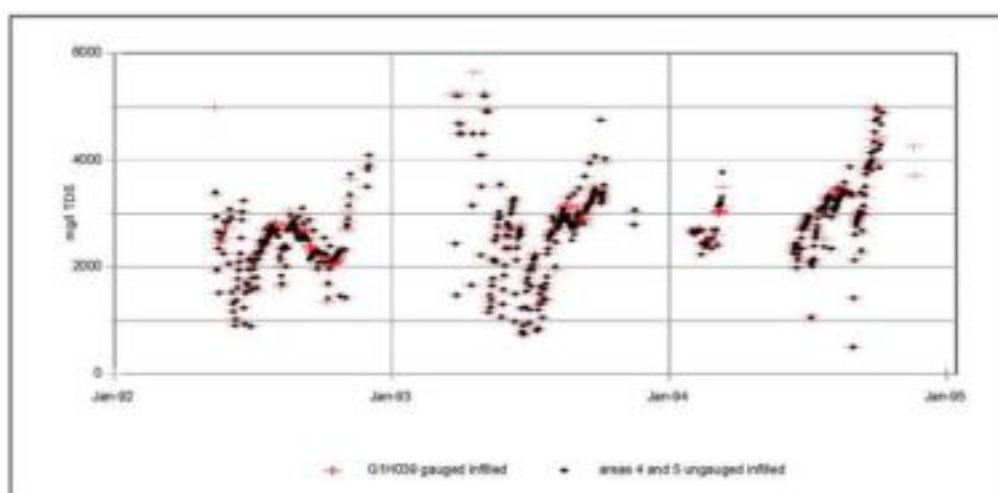


Figure 8.2 : Comparison of infilled water quality concentration of areas 4 and 5 with infilled concentration of gauging station G1H039

Table 8.2: Correction of Ungauged Concentration

| Ungauged Catchment Runoff of Area Number: | Infilled with water quality grab samples of station: | Comment |
|---|--|--|
| 1 and 2 | G1H020 | The water quality samples of the upstream gauged Table Mountain Sandstone areas (A, B, C, D) are of better quality, than from the areas 1 and 2. It has therefore been assumed that the water quality concentration of areas 1+ 2 would follow a similar pattern to the data that has been sampled at G1H020. |
| 3 | G1H041 (E) | It has been assumed that the water quality from area 3 would be similar to the water quality at G1H041, as both sub-catchments drain Table Mountain Sandstone soil, which is of better quality than the water quality of the runoff from the Malmesbury Shales. |
| 4 and 5 | G1H039 (F) | As sub-catchments 4 and 5 experience similar rainfall-runoff patterns to sub-catchment F and also drain Malmesbury Shales, it has been assumed that the corrected runoff from 4 and 5 could be linked to the water quality samples of G1H039. |
| 6 | G1H043 (G) | Sub-catchment 6 has been linked with gauged sub-catchment G, because of similar rainfall-runoff and soils. |
| 8 | G1H008 (I) | It has been assumed that the water quality from area 8 will be similar to the water quality at G1H008, as both sub-catchments drain primarily Table Mountain sandstone soil. The rainfall experienced in sub-catchment 8 is however less than sub-catchment H, and portions of the flow is diverted to Voelvlei Dam. |
| 7 and 9 | G1H034 (J) | The water quality sampled at G1H034 has been assumed to have similar characteristics to the water quality that can be expected at sub-catchments 7 and 9, given similarity in soils and geology. |

Table 8.3 : Statistic of ungauged TDS values

| Sub-catchment No. | No. of Samples | Mean Conc (infilled) (mg/l) | Mean Conc (Grab Samples) (mg/l) | % error in mean | Std. Dev (infilled) | Std. Dev (grab samples) | R ² |
|-------------------|----------------|-----------------------------|---------------------------------|-----------------|---------------------|-------------------------|----------------|
| 1 and 2 | 319 | 60.4 | 60.2 | 3 | 9.7 | 12.1 | 0.97 |
| 3 | 234 | 159.7 | 174 | -8 | 51 | 88 | 0.78 |
| 4 and 5 | 130 | 2636 | 2712 | -3 | 710 | 897 | 0.81 |
| 6 | 110 | 4693 | 4718 | -0.5 | 1293 | 1356 | 0.77 |
| 8 | 300 | 113 | 117 | -4 | 29.4 | 40.4 | 0.72 |
| 7 and 9 | 315 | 6304 | 6253 | 8 | 2214 | 2297 | 0.91 |

Table 8.4 : Statistic of ungauged PO₄ Values

| Sub-catchment No. | No. of Samples | Mean Conc (infilled) (mg/l) | Mean Conc (Grab Samples) (mg/l) | % error in mean | Std. Dev (infilled) | Std. Dev (grab samples) | R ² |
|-------------------|----------------|-----------------------------|---------------------------------|-----------------|---------------------|-------------------------|----------------|
| 1 and 2 | 326 | 0.024 | 0.028 | -14 | 0.013 | 0.05 | 0.75 |
| 3 | 231 | 0.02 | 0.024 | -15 | 0.01 | 0.02 | 0.57 |
| 4 and 5 | 128 | 0.29 | 0.33 | -10 | 0.15 | 0.21 | 0.71 |
| 6 | 110 | 0.03 | 0.036 | -17 | 0.01 | 13560.02 | 0.60 |
| 8 | 294 | 0.016 | 0.017 | -7 | 0.01 | 0.01 | 0.75 |
| 7 and 9 | 317 | 0.15 | 0.176 | -17 | 0.15 | 0.18 | 0.74 |

8.6 SENSITIVITY OF WATER QUALITY PARAMETERS

8.6.1 Dispersion

The calibration of the transport dispersion was attempted by adjusting the dispersion for the conservative constituent, TDS. TDS is only dependant on the dispersion and therefore is a good indicator of the influence of the dispersion parameter. As can be seen from the Figure 8.1, dispersion has a minimal effect on the simulated results.

DUFLOW has an additional option known as 'decouple'. If this option is chosen, dispersion is only considered in a downstream direction. Decoupling only takes place at nodes with a discharge. The DUFLOW manual suggests using the decouple option to prevent flattening of steep concentration gradients at nodes where a discharge is located (STOWA, 1998). A simulation run was completed with dispersion set at 30 m²/s for both options. The non-decouple option shows a difference of -0.062% in both mean and variance. The non-decouple option however indicates slightly more unstable calculations just before the discharge points (tributaries entering the system), as can be seen in Figure 8.4.

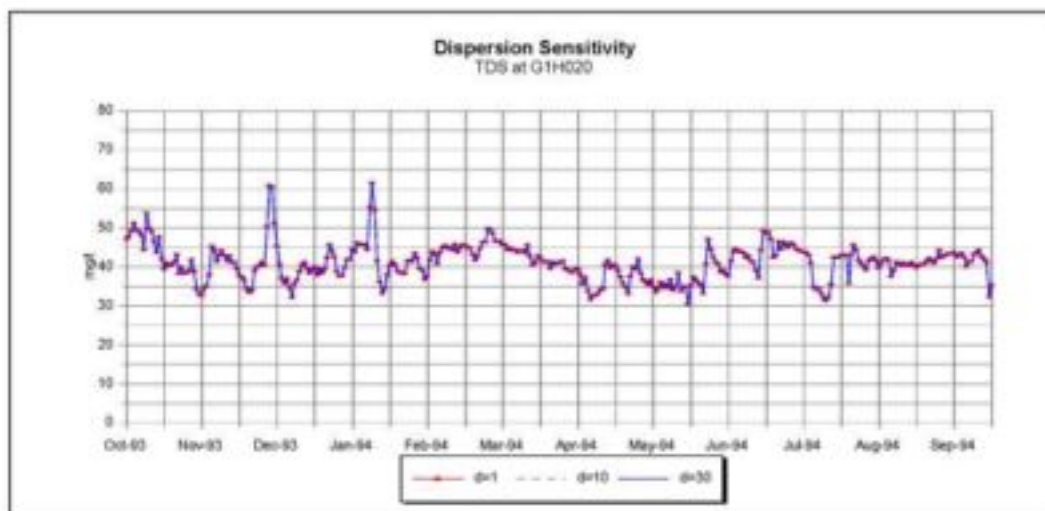


Figure 8.3: Dispersion Sensitivity

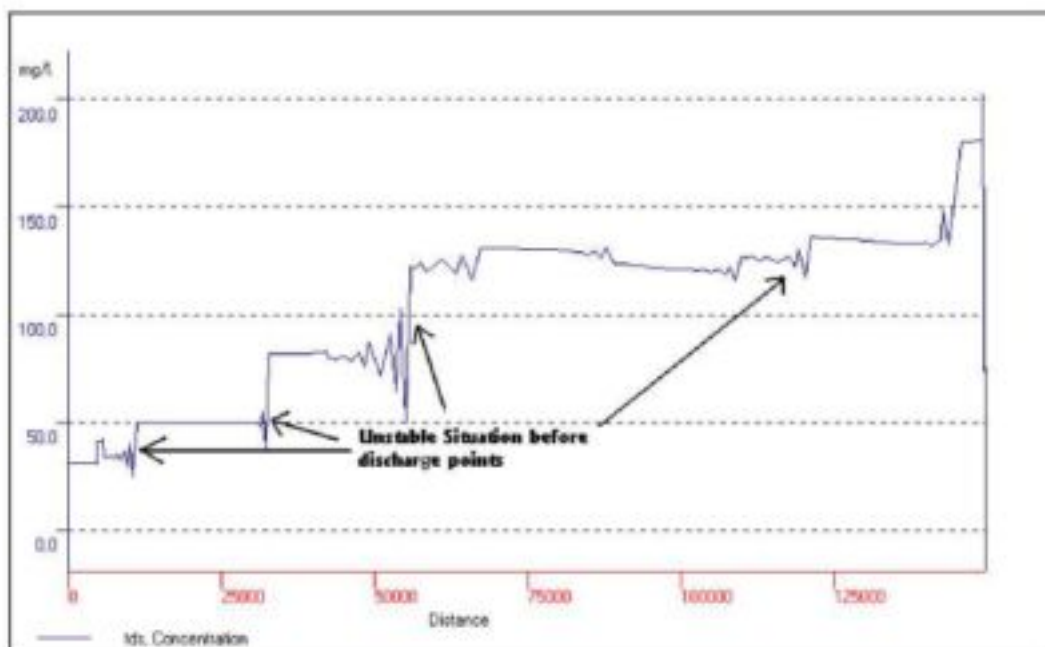


Figure 8.4 : Concentration using non-decouple dispersion

8.6.2 Phosphorous

Sensitivity analyses were performed for the parameters that affect the phosphorous concentration (refer to Section 5.4.5.2), which are Θ_{min} and k_{min} . The sensitivity runs show that these parameters have insignificant influence on the concentration, and therefore the phosphorous concentration is only dependent on the transport calculations.

8.6.3 Temperature

The parameters that can be changed for calibration purposes occur in atmospheric longwave radiation and water longwave back radiation.

Parameters:

Recalling the equation from Section 5.4.5.1, the parameters that have an influence on the atmospheric longwave radiation are A, a constant, and R_L , the cloud cover. The Stefan Boltzmann constant cannot be varied. The term describing the back radiation of the water surface contains the parameter ϵ (emissivity of a body), as it is represented by Stefan Boltzmann's law.

Figures 8.6 to 8.9 summarize the results for the summer temperatures of the different sensitivity runs completed for the parameters A and R_L . The summer temperatures are more sensitive to changes in the parameters (due to the low flow water depth, refer to equation 5.39). It was decided after the sensitivity runs that a R_L value of 0.03 and an A value of 0.55 seemed to depict an acceptable maximum summer temperature when compared with the maximum summer temperatures of the observed data. The average values calculated are, however, all lower than the measured data when using these parameters. The reasonable overall averages and visual comparisons of the trends however, allowed acceptance of these parameters.

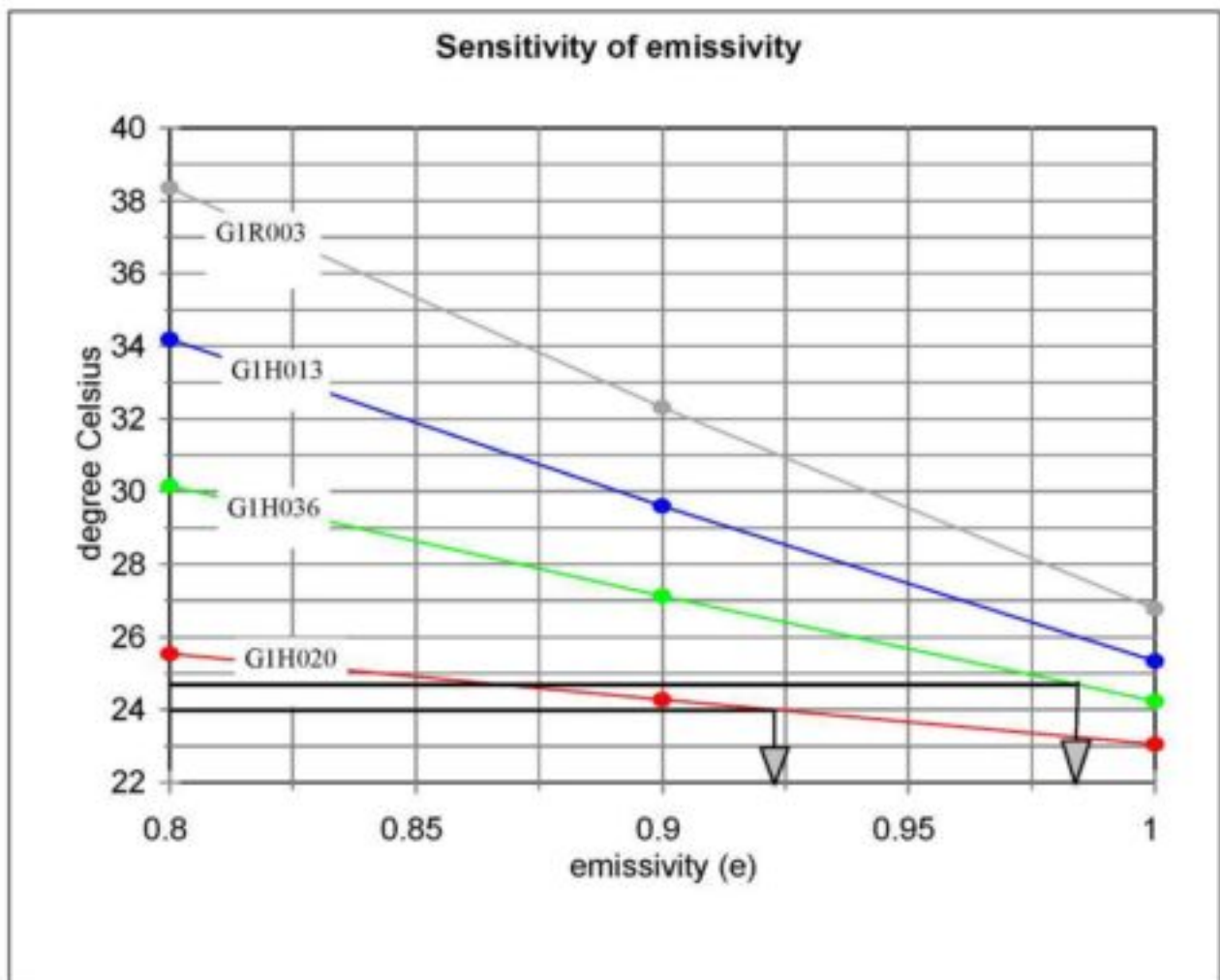


Figure 8.5: Sensitivity of temperature parameter ϵ

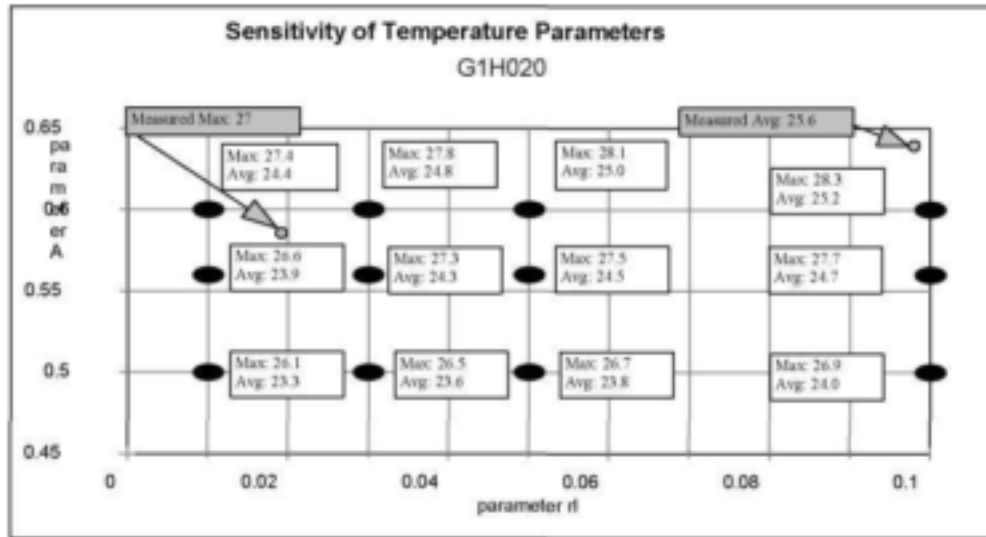


Figure 8.6: Sensitivity of temperature parameters at G1H020

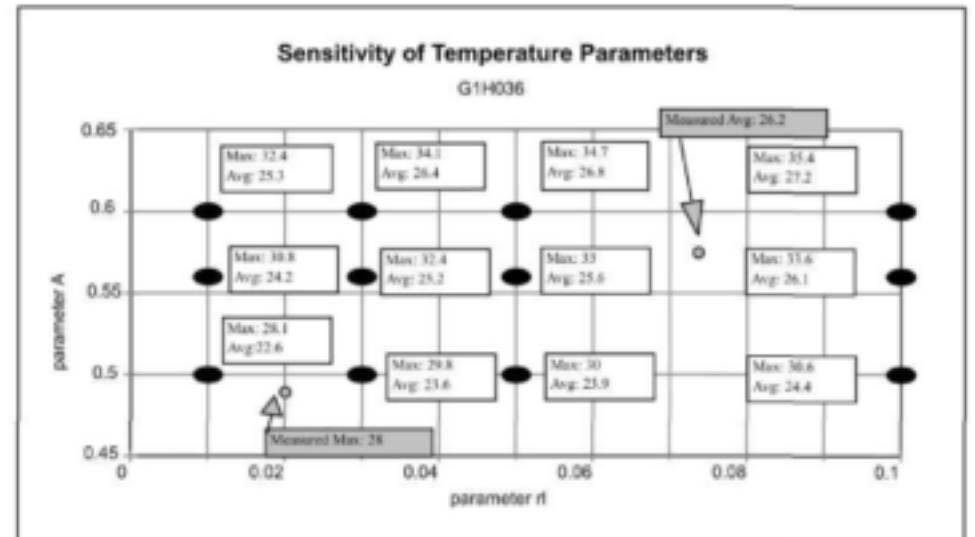


Figure 8.7: Sensitivity of temperature parameters at G1H036

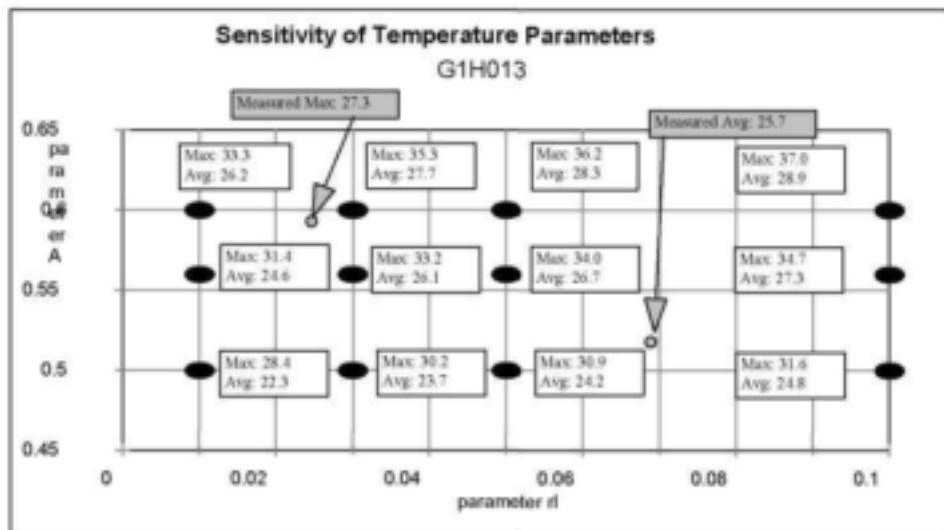


Figure 8.8: Sensitivity of temperature parameters at G1H013

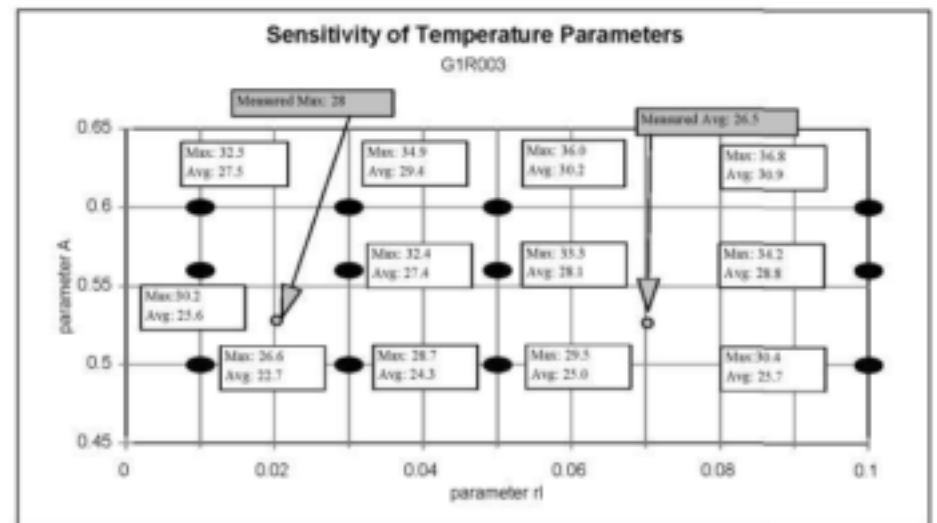


Figure 8.9: Sensitivity of temperature parameters at G1R003

Figure 8.5 shows the sensitivity of the emissivity parameter on temperature. The figure shows the summer temperature averages that were calculated from three runs of emissivity factors of 0.8, 0.9 and 1 for all the stations in the main stem river. For G1H020 an emissivity of 0.92 would simulate an average of 24°C as was measured (refer also to Table 1.4.3 in Appendix 1.4). An emissivity factor of 0.98 would simulate an average of 24.6°C for G1H036, while for G1H013 and G1R003 an emissivity factor of 1 would simulate their average temperature measured (refer to Table 1.4.3). The average emissivity of all four factors simulated is 0.975; this value was used for the Berg River model simulation runs. This value is close to the default value of 0.97.

External variables :

The atmospheric longwave radiation and the back radiation are both influenced by the air temperature, while conduction and evaporation terms are affected by the wind and the evaporation respectively. For a river, the evaporation and conduction will have less effect on the water temperature when compared to the addition of heat through the atmosphere.

Depth:

All the terms are dependent on the depth of the water (refer to equation 5.39). It is evident from the equations that the influence of the water depth on the temperature is much stronger than the influence of the various calibration parameters. Figure 8.10 illustrates an example of how the temperature term is influenced by the depth of the water. Below a depth of 0.5m the temperature term increases exponentially. Therefore, for a water depth below 0.5 m the temperature equations predict the water body to become exponentially warmer as the water depth decreases. This will occur in the summer months when there is low water depth and the solar radiation and air temperature are at their maximum and therefore contribute additional heat.

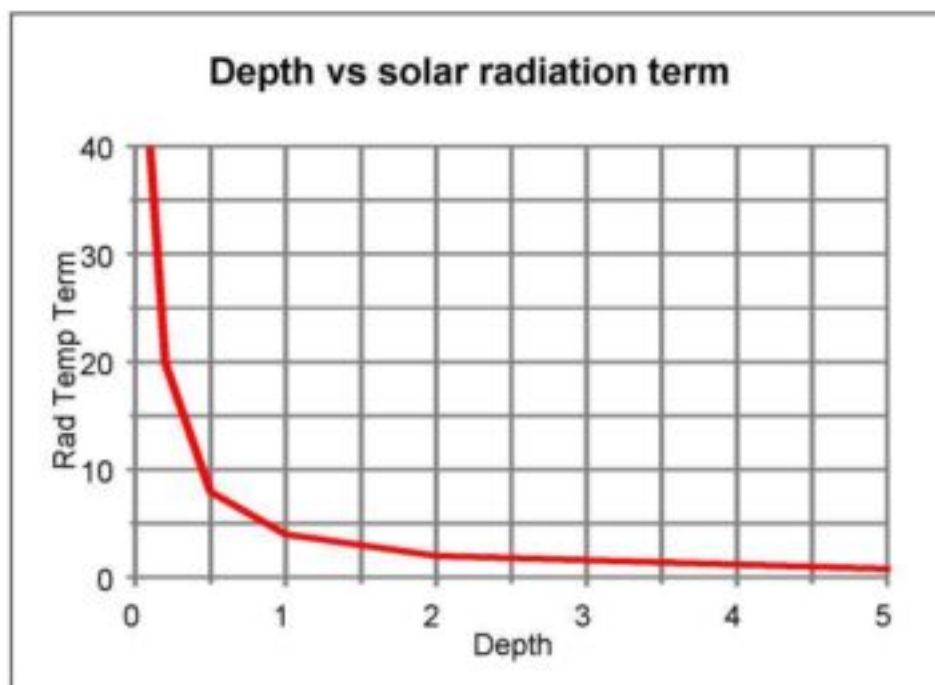


Figure 8.10: Depth influence on solar radiation

8.6.4 Oxygen

As only the water quality variables TDS, PO_4 and Temperature are modelled additional to the oxygen, the effect of the essential influences on the oxygen concentration is not modelled. These are the influences of plant growth and therefore photosynthetic oxygen production; and the oxidation of carbonaceous and nitrogenous waste material, respiration of plants and oxygen demand of the sediments. In this model only two variables influence the modelling of oxygen: k_{re} and α_{re} (refer to equation 5.44) and the effect of temperature on the reaeration. The effect of temperature is seen as an external variable and although the sensitivity of the oxygen to the temperature can be assessed, it cannot be altered in the calibration process.

Figure 8.11 presents the influence of θ_{re} on the oxygen values for the different gauging stations. As no data is available for the oxygen concentration, estimating the correct value for this parameter is therefore difficult. The default value of θ_{re} in DUFLOW is 1.024, which has been accepted for the Berg River.

The parameter k_{re} is calculated according to equations 5.47 and 5.48. The parameter k_{re} is dependent on the k_{max} parameter and the k_{min} parameter. The minimum oxygen transfer coefficient (k_{min}) is defined by the user, and the DUFLOW default value of 0.1 m/d has been applied. The k_{min} parameter has however never been used, as the calculated mass transfer coefficient (k_{max} in equation 5.47) has always been larger than the minimum oxygen transfer coefficient.

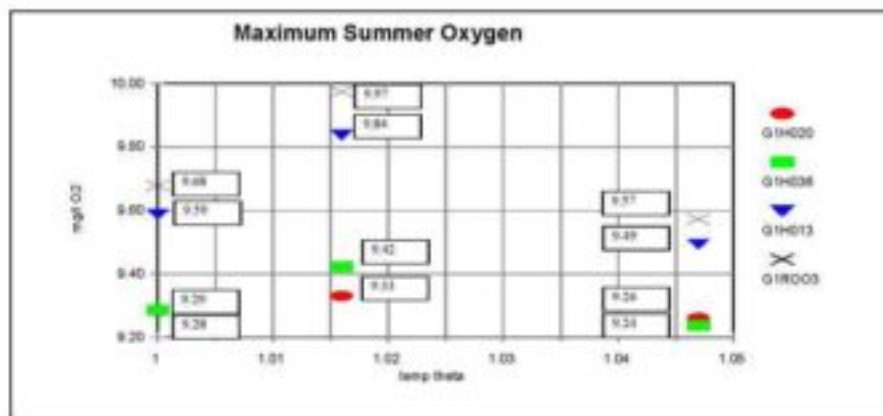


Figure 8.11 : Influence of θ_{re} on summer oxygen values

8.7 SENSITIVITY OF GRAB SAMPLES COMPARED TO INFILLED SAMPLES

Referring back to Section 6.3.1, the water quality data was 'infilled' by means of a moving regression. In order to investigate the sensitivity of incorporating the actual grab samples back into the infilled time series, a sensitivity run was completed with grab samples included in the infilled time series and the results were compared to the results of the simulation runs, using only 'infilled' concentration values.

It can be seen from Figures 8.12 and 8.13 that incorporating grab samples in the infilled series does not show significant difference when compared to the runs that were completed with only 'infilled' values.

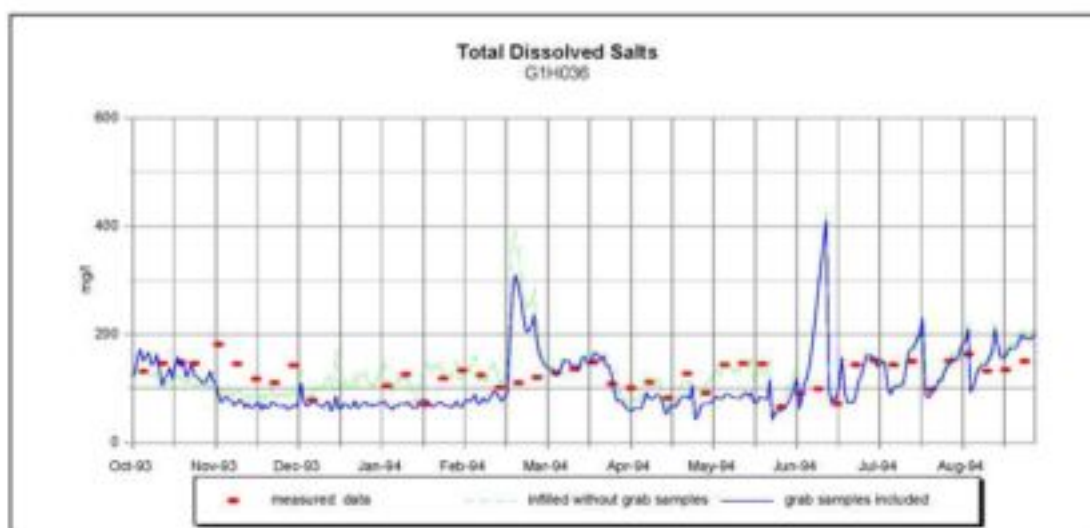


Figure 8.12 : Comparison of TDS simulation at G1H036

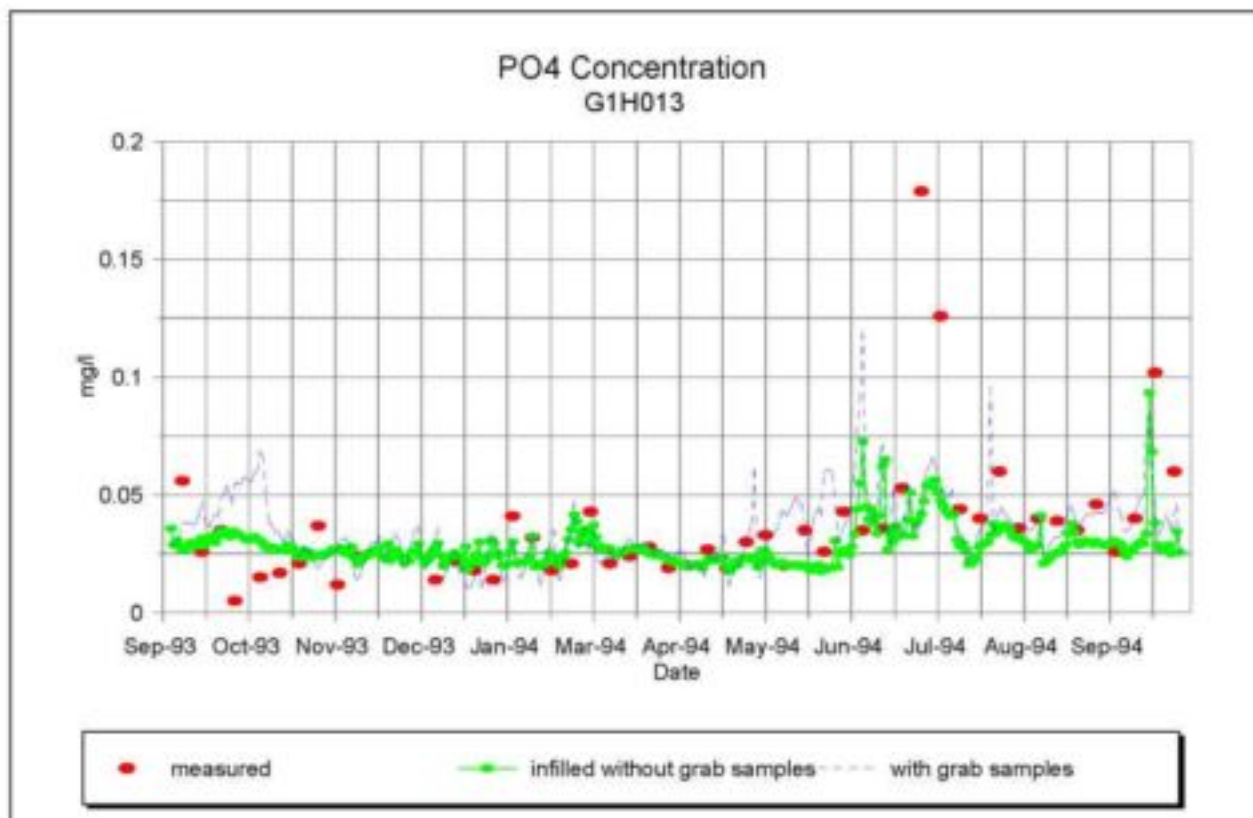


Figure 8.13: Comparison of PO_4 simulation at G1H013

8.8 POINT SOURCES

The Water Quality Situation Analysis (DWAF(g), 1993) identifies the major point sources in the Berg River catchment. Much of the industrial activity in the Berg River catchment is associated with the agricultural sector, and therefore many of the effluent producers are also associated with this sector. For the DUFLOW model only point sources that have been issued with a permit have been considered. This data was available from the Polmon database from DWAF as monthly measurements. Unfortunately, effluent data was only available for the major sewage treatment plants and only a few point sources that irrigate their effluent. There are, however, a number of piggeries and wineries in the Berg River catchment that also produce effluents, which are high in oxygen demand and organic loading. The Berg River Situation Analysis (DWAF(g), 1993) has identified the following point sources :

- 1 Trout Farm
- 1 Fruit and Vegetable processing plants
- 22 Wineries
- 10 Piggeries
- 21 Sewage Treatment Works
- 1 chicken abattoir
- 5 industrial sources

From these only 12 are authorised to discharge into the Berg River or nearby tributaries, which are Franschoek STW, Bien Donne STW, Pniel STW, Wemmershoek STW, PPC cement factory at Riebeeck Wes, Paarl STW, Moorreesburg STW, Piketberg STW, Porterville STW and Tulbach STW and PPC De Hoek STW. Many of the point sources do not have quality requirements as they all irrigate their effluent. Effluent quality is not specified on their permits. The majority of the point sources identified have not been issued with permits. Lack of data makes it difficult to evaluate the volume of effluent that gets irrigated, but it has been estimated in the Berg River Situation Analysis (DWAF(g), 1993) that between G1H004 and G1H020 about 40% of the total annual effluent produced in this reach is irrigated, 21% between G1H020 and G1H036 and about 25% between G1H036 and G1H013.

The point sources that do have permits, and measured water quality and flow volume, have been included in the model. It has been assumed for the point sources (where flow and quality data is available) which do not discharge directly into the Berg River and irrigate their effluent or discharge far up in a tributary that about 25% of the effluent flow reaches the Berg River. Only one authorised point source, Paarl sewage treatment works, discharges effluent directly into the Berg River.

The variables that have been tested by DWAF are COD, EC, SS and pH. Only Franschoek STW had occasional phosphate readings, which were of an average of 5.3 mg/l P as PO₄. The variables that are of interest to us are the COD and TDS values. Tables 8.6 and 8.7 summarise the various loads that have been measured.

It can be seen from Tables 8.6 and 8.7 that Paarl Municipality discharges about 65% COD and 70% of TDS of the overall point source totals. It is clear, that for a water quality simulation model, if ever used for management and control purposes, a more extensive database is needed to evaluate the impact of point sources and non-point sources more exactly.

Table 8.5 : Point sources identified in the Berg River Catchment

| NAME | PERMIT | MANNER OF DISPOSAL | STANDARD (DWAF(g), 1993) | COMMENT |
|----------------------------------|--------|---|---|---|
| Franschoek Municipality STW | yes | irrigation of sportsfield, discharge into river | General Standard, for Residual Chloride the Special Standard | assumed 25% of flow reaches Berg River main stem |
| Pniel STW | yes | discharge into Dwars River | General Standard | assumed 25% of flow reaches Berg River main stem |
| Bien Donne Winery | no | effluent to vineyard, discharge into stormwater drain | none specified | Samples have been taken during study period, have been analysed in Chapter 4 |
| La Motte STW | no | evaporation ponds and seepage | none specified | No data available |
| Victor Vester STW | no | irrigation, in winter discharge of effluent into the Berg River | none specified | No data available |
| Wemmershoek Forestry Station STW | no | discharge into Wemmers River | none specified | |
| King Western Leathers Tannery | yes | evaporation | none specified | no quality standard specified |
| Paarl Municipality | yes | discharge to Berg River | General Standard, PO ₄ -P less than 4 mg/l 90% of the time | |
| Stellenbosch Farmers Winery | yes | discharge of effluent to Berg River | none specified | no water quality data available |
| Wellington Municipality STW | yes | irrigation, evaporation | General standard | assumed 25% of flow reaches Berg River main stem |
| Morreensburg Municipality STW | yes | discharge to Sand River | General standard | COD data assumed 25% reaches Berg River main stem, phosphate and TDS data measured at G1H034 readings |
| Piketburg Municipality STW | yes | irrigation, winter balance to stream | General standard | COD data assumed 25% reaches Berg River main stem, phosphate and TDS data measured at G1H035 readings |
| Porterville Municipality STW | yes | discharge to Jakkalskloof River | General standard | COD data assumed 25% reaches Berg River main stem, phosphate and TDS data measured at G1H035 readings |
| Tulbach Municipality STW | yes | discharge to Klip River | General standard | discharge into Voëlvllei Dam |

Table 8.6 : COD Loads (tons/month) for 1993/1994

| | Franschhoek STW | Pniel STW | Paarl STW | Wellington STW | Moorresburg STW |
|---------------------|-----------------|-------------|------------|----------------|-----------------|
| October | 0.44 | 0.48 | 17.4 | 16.28 | 1.2 |
| November | 0.5 | 0.7 | 11.4 | 13.9 | 0.73 |
| December | 0.52 | 1.18 | 13.8 | 9 | 1.52 |
| January | 0.5 | 1.05 | 20.4 | 16 | 0.89 |
| February | 0.911 | 0.5 | 27.2 | 12.4 | 0.96 |
| March | 1 | 0.97 | 85.2 | 20 | 1.16 |
| April | 1.66 | 1.15 | 26 | 6.9 | 0.96 |
| May | 0.78 | 0.55 | 43.6 | 7 | 0.83 |
| June | 0.66 | 1.21 | 34 | 19.3 | 0.85 |
| July | 0.46 | 0.96 | 20.7 | 9.6 | 1.09 |
| August | 0.41 | 0.5 | 11.3 | 5.1 | 1.09 |
| September | 0.36 | 0.3 | 14 | 9.7 | 1.06 |
| TOTAL (tons) | 8.2 | 9.55 | 325 | 145.2 | 12.34 |

Table 8.7 : TDS Loads (tons/month) for 1993/1994

| | Franschhoek STW | Pniel STW | Paarl STW | Wellington STW | Moorresburg STW |
|---------------------|-----------------|-------------|-------------|----------------|-----------------|
| October | 0.058 | 0.28 | 4.4 | 1.69 | 0.06 |
| November | 0.059 | 0.26 | 4.1 | 1.6 | 0.58 |
| December | 0.079 | 0.21 | 4.6 | 1.45 | 0.57 |
| January | 0.096 | 0.23 | 4.6 | 1.31 | 0.55 |
| February | 0.08 | 0.15 | 4.9 | 1.33 | 0.49 |
| March | 0.1 | 0.18 | 6.1 | 0.84 | 0.47 |
| April | 0.092 | 0.24 | 5.9 | 1 | 0.42 |
| May | 0.087 | 0.24 | 5.8 | 0.78 | 0.45 |
| June | 0.1 | 0.39 | 7.1 | 1.95 | 0.49 |
| July | 0.065 | 0.31 | 4.2 | 1.35 | 0.46 |
| August | 0.06 | 0.14 | 3.3 | 1.1 | 0.49 |
| September | 0.057 | 0 | 4 | 1.46 | 0.59 |
| TOTAL (tons) | 0.933 | 2.63 | 58.9 | 15.86 | 5.62 |

8.9 RESULTS OF WATER QUALITY MODEL CALIBRATION

8.9.1 TDS

The simulated values were compared with the measured data and 'infilled values' for low flows (October to March) and high flows (April to September) and overall. The contribution to the salt load in the Berg River from the point sources with a permit seems to be insignificant when compared to the total salt load contributed by the tributaries. Paarl sewage treatment works adds a yearly load of 145.2 tons, while the total load measured at G1H020 already consists of 15798 tons of TDS in the year. Of concern, however, is all the non-point sources and point sources that are not controlled, which have an additional impact on the overall TDS load.

Irrigation return flows, which are high in salts and nutrients, have not been included in the model, due to insufficient knowledge of the volumes and concentrations. The irrigation return flows have a significant impact on the TDS and phosphate concentrations, particular in the summer months, and the absence of these concentrations should be borne in mind when analysing the results.

- **TDS Concentration results:**

(Table 1.4.2, Figures 1.4.9-1.4.12 in Appendix 1.4)

The coefficient of determination is low for the concentration analysis (Table 1.4.2), between 0.3 and 0.67 for the high flow period and only between 0.03 and 0.47 for the low flows.

High TDS Concentration is discharged into the river in the reach between G1H020 and G1H036. This can be seen from Figures 1.4.9 and 1.4.10, and also from Table 8.11, where the % error increases from -31% to 14%. This is the result of additional TDS concentration from sub-catchments 4 and 5 that have been infilled by using grab samples of G1H039. Figure 8.14 shows the TDS concentration of G1H039 and also of G1H041, which also discharges into the river in this reach (refer to Figure 7.1). Sub-catchments 4 and 5 follow the same pattern as the TDS concentration of G1H039. The high concentration peaks shown in February and also in the winter months at G1H036 and the stations downstream are also a result of the high TDS discharging into the river from sub-catchments 4 and 5. Unfortunately, the accuracy of the gauging station G1H039 was rated 0 (Table 7.1), but it was the only estimate of gauged TDS loads (refer to Section 7.6 and 8.5). The actual effect of incoming TDS concentration from G1H039 is little, due to low flows. As sub-catchments 4 and 5 have however a higher runoff, the loads discharging into the river do have an impact on the concentration. It can therefore be concluded that the TDS concentration of sub-catchments 4 and 5 is considerably less than was assumed.

Low TDS concentration is discharged into the river during the summer months. The concentration shows high under-simulation at all stations (Figures 1.4.9 to 1.4.12 in Appendix 1.4), especially at G1R003, while the phosphate simulation shows hardly any under-simulation during the summer months (Figures 1.4.21-1.4.24 in Appendix 1.4). The under-simulated TDS concentration could therefore be due to a missing TDS point source.

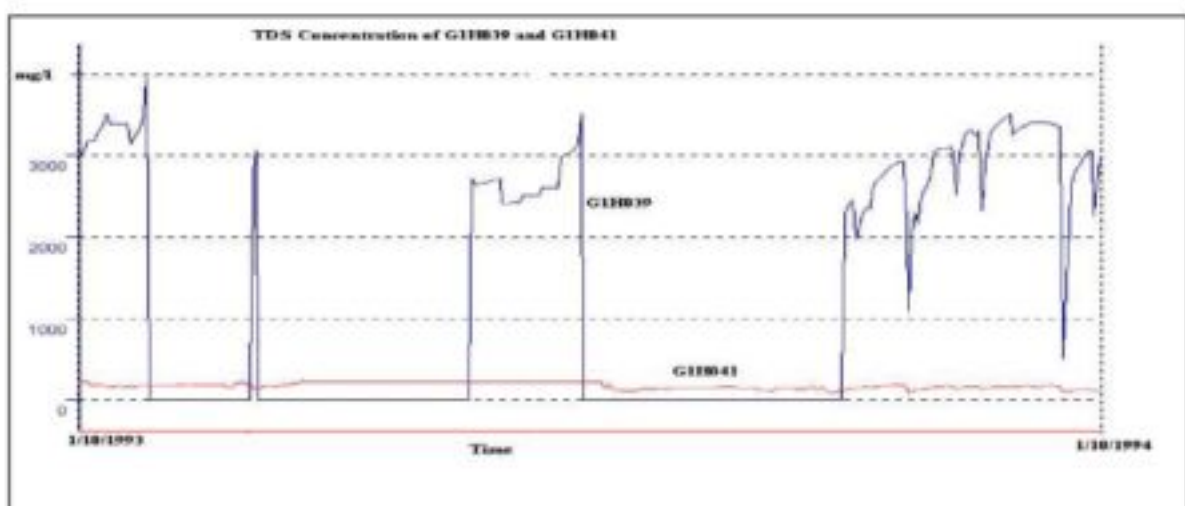


Figure 8.14: TDS Concentration of G1H039 and G1H041

- **TDS Loads Results:**

- Low Flow :

- (Table 1.4.1, Figures 1.4.1-1.4.4 in Appendix 1.4)

- The coefficient of determination for the loads is higher than for the concentration (Table 8.8), this is because the load is dependent on the flow simulated. For the low flow period the load follows the trend of the measured data less accurately than the high flow (refer to Figures 1.4.1 to 1.4.8 in Appendix 1.4). Referring to Table 7.6, it can be seen that the discharge in the low flow period is over-simulated by 54% at G1H036, and this explains the 68% error in the TDS loads at G1H036, as this could be the result of the flow over-simulated for the periods March and April. The other stations also show similar errors in the load simulation when compared to the flow simulation (Tables 1.4.1 in Appendix 1.4 and Table 7.6). Interestingly, the TDS load shows however a smaller error in the loads for the low flow period than the flow simulated (88% error in the flow and only 35% error in the TDS load simulation), which could be the result of addition of ungauged TDS loads of the ungauged areas 7 and 9 (Figure 7.1). These areas contribute minimal runoff to the main stem, but significant TDS loads (as these areas drain the Malmesbury shales, which produce high salinity concentration). Referring to Figures 1.4.1 to 1.4.4 in Appendix 1.4, one can see that the short lived peaks introduced by releases from Voëlvele Dam are clearly defined in the load simulation at G1H013 and G1R003.

- High Flow:

- (Table 1.4.1, Figures 1.4.5-1.8 in Appendix 1.4)

- The overall TDS loads for the high flow months are over-simulated at all stations, except at G1H020. The TDS peak shows a difference of - 50000 g/s at station G1R003 (Figure 1.4.8), -30000 g/s at G1H013 (Figure 1.4.7) and a over-simulation of 25000 g/s at G1H036 (Figure 1.4.6). The error introduced therefore occurs mainly in the reach from G1H036 to G1H013, and could be the result of additional non-point salinity runoff.

8.9.2 Phosphate as PO₄

The phosphate modelling is influenced by advection only (the biological and chemical processes have been omitted due to lack of data on other dependent variables). This has to be borne in mind when analysing the results, as phosphate concentration is in reality not only influenced by advection, although it is often the most influential.

Irrigation return flows, which are high in salts and nutrients, have not been included in the model, due to insufficient knowledge of the volumes and concentrations. The irrigation return flows have a significant impact on the TDS and phosphate concentrations, particularly in the summer months.

..

- **PO₄ Concentration results:**

- (Table 1.4.4, Figures 1.4.21-1.4.24 in Appendix 1.4)

- The coefficient of determination is low for the concentration analysis (Table 1.4.4), between 0 and 0.68 for the high flow period and only between 0.15 and 0.57 for the low flows. Station G1H036 shows a 0% coefficient of determination and referring to Figure 1.4.20, it can clearly be seen that the concentration is greatly under-simulated between March and June, the error in the simulation decreases from -1% to -32% (Table 1.4.4) from G1H020 to G1H036. This under-simulation is not evident at the downstream stations (Figures 1.4.21 and 1.4.22). The measured phosphate concentration has decreased from 0.04 mg/l to 0.024 mg/l (low flow) and from 0.08 mg/l to 0.05 mg/l (high flow) from station G1H020 to G1H036. The errors in concentration mean are also the highest for station G1H036 (-32% at low flow and -55% for high flow). From the verification runs it can also be seen that although the values are under-simulated at G1H036, the measured phosphate values decrease at the downstream stations and the % error between the measured and the simulated phosphate is less. This error could be due to a missing point source in the reach of G1H020 and G1H036, as the flow is not under-simulated during these months (refer to Figure 7.4); the TDS concentration is under-simulated in these months, but not to such a high degree as for the phosphate simulation.

The simulated mean phosphate concentration does not differ between G1H013 and G1R003 for low and high flows. The measured phosphate mean concentration does however decrease from G1H013 to G1R003 for the high flows; this could be due to missing ungauged flows in this reach.

One can see from Figures 1.4.22 to 1.4.24 that small phosphate concentration peaks are simulated in June and end September at all three stations: G1H036, G1H013 and G1R003. Figure 8.15 shows the phosphate concentrations of the gauged tributaries discharging into the Berg River main stem. As one can see from Figure 8.15, the small peaks simulated in the winter months are mainly a result of phosphate inflow from the sub-catchments 4 and 5 that have been estimated with grab samples of G1H039.

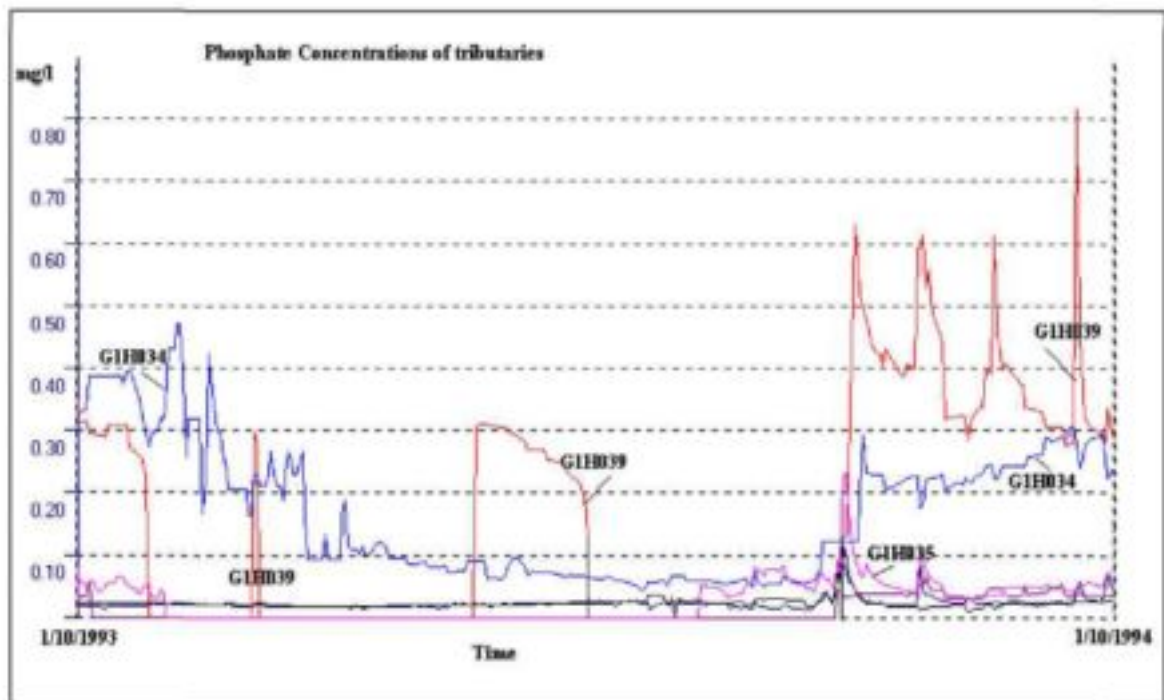


Figure 8.15: Phosphate Concentrations of Tributaries

- ***PO₄ Loads Results:***

Low Flow :

(Table 1.4.3, Figures 1.4.13-1.4.16 in Appendix 1.4)

The coefficient of determination for the loads is higher than for the concentration (Table 1.4.1 and 1.4.3), this is because the load is dependent on the flow simulated. For the low flow period the load follows the trend of the measured data less accurately than the high flow. As for the TDS loads, the phosphate loads are over-simulated in the months March/April, due to the flow over-simulated in these months. At all stations the phosphate loads are over-simulated, especially at G1R003 where the simulated values show a 103% over-simulation. This over-simulation is mainly due to 88% over-simulation of flow at G1R003 (Table 7.6). The other stations also show similar errors in the load simulation when compared to the flow simulation (Tables 1.4.3 and 7.6). Referring to the figures, one can see that the short lived peaks introduced by releases from Voëlvelei Dam are clearly defined in the load simulation at G1H013 and G1R003, this explains also the improvement of the coefficient of determination downstream of G1H036.

High Flow:

(Table 1.4.3, Figures 1.4.17-1.4.20 in Appendix 1.4)

The phosphate peak in the summer was measured to be approximately 60 g/s at G1H013 and 40 g/s at G1R003. For all stations the phosphate peak is under-simulated. This could be the result of additional non-point runoff occurring during a flood. The high flow phosphate loads show high coefficient of determinations (0.95 to 0.98). At G1H020 the total load in the summer period is already under-simulated by 42%. The model adds phosphate loads from the tributaries and ungauged sub-catchments in the reach from G1H013 to G1R003, where in reality the phosphate mass has reduced from 48.2 tons to 25.6 tons.

8.9.3 Temperature

(Figures 1.4.25 to 1.4.28 and Table 1.4.5 in Appendix 1.4)

It can be perceived from the results, that the temperature model predicts the winter months better than the summer months. This could be the result of the algorithm, as the temperature increases exponentially when the water depth decreases (equation 5.39 and Figure 8.10). The water depth is simulated very low (0.2-0.6m) in the summer months. The model follows the seasonal trend quite accurately (R^2 between 0.8 and 0.98). At station G1R003 the temperature is over-simulated for the summer months and under-simulated for the winter months. The occasional outliers in the simulation are due to outliers in the radiation and evaporation rates (refer to Figures 6.6 and 6.7).

8.9.4 Oxygen

(Table 1.4.6, Figures 1.4.29-1.4.31)

The calibration of the oxygen model concentrated on the temperature simulation, as oxygen is dependent on the values of temperature in the river. Many factors affect the concentration of oxygen, such as plant photosynthesis and point sources. The error of the simulated data is also very dependent on the accuracy of the meteorological influences on the oxygen. There are outliers simulated for the May and June months, and this is due to occasional peaks from the radiation data and minor instabilities in the simulation calculation, due to higher velocities in the winter months.

8.10 WATER QUALITY MODEL VERIFICATION

Unfortunately, for the station G1H036 the flow measurements are incomplete from the 3rd of July onwards. It therefore should be noted that the statistical comparison for the high flows are not included for this station. The simulated values were compared with the measured data and '*infilled values*' for low flows (October to March) and high flows (April to May) and overall, as well as to the errors that were experienced in the calibration simulation.

8.10.1 TDS

In the year October 1994 to October 1995, several peaks are experienced during the high flow months instead of one defined peak, as was the case for the calibration year. The maximum peak occurs mid-July and reaches only a value of approximately 40000 g/s at G1H013 and G1R003, compared to the maximum peak of 120000 g/s (at G1R003) for the calibration year (refer to Figure 8.25 and 8.57). The measured data for the low flow period nevertheless has more or less the same pattern as for the calibration period.

- **TDS Concentration results:**

(Table 1.4.8, Figures 1.4.43 -1.4.46 on Appendix 1.4)

The coefficient of determination is low for the concentration analysis, between 0.04 and 0.58 for the high flow period and between 0.23 and 0.30 for the low flows. Although the concentration shows high over-simulation in March and April for the calibrated TDS simulation (Figures 1.4.9 to 1.4.12), this is not evident in the verification simulation. The concentration is over-simulated downstream from G1H036 for the high flow period in the calibration year, while the verified run shows under-simulated concentration at all stations. G1H020 shows similar errors to the calibration simulation, while for G1H013 and G1R003 the yearly errors are higher than the errors of the calibration run. This could be the result of different point sources and non-point sources that have occurred in this year.

The simulation of the concentration during the winter months shows an erratic pattern, which is the result of high inflowing TDS from G1H043 (Figure 8.16). For the calibration year, sub-catchments 4 and 5 (due to pattern of G1H039) contributed most of the salts in the winter months. As one can see from Figure 8.16 high TDS concentration is discharged from G1H034; the flow however is an average of 0.006 m³/s for G1H034 during these months and therefore the load contribution to the river is minimal. Similar to the calibration results, there exists under-simulation in the summer months at all stations. At G1R003 the simulated and measured TDS values are about 125 mg/l different (Figure 1.4.44). This could be the result of the same missing point sources or also due to unknown abstractions.

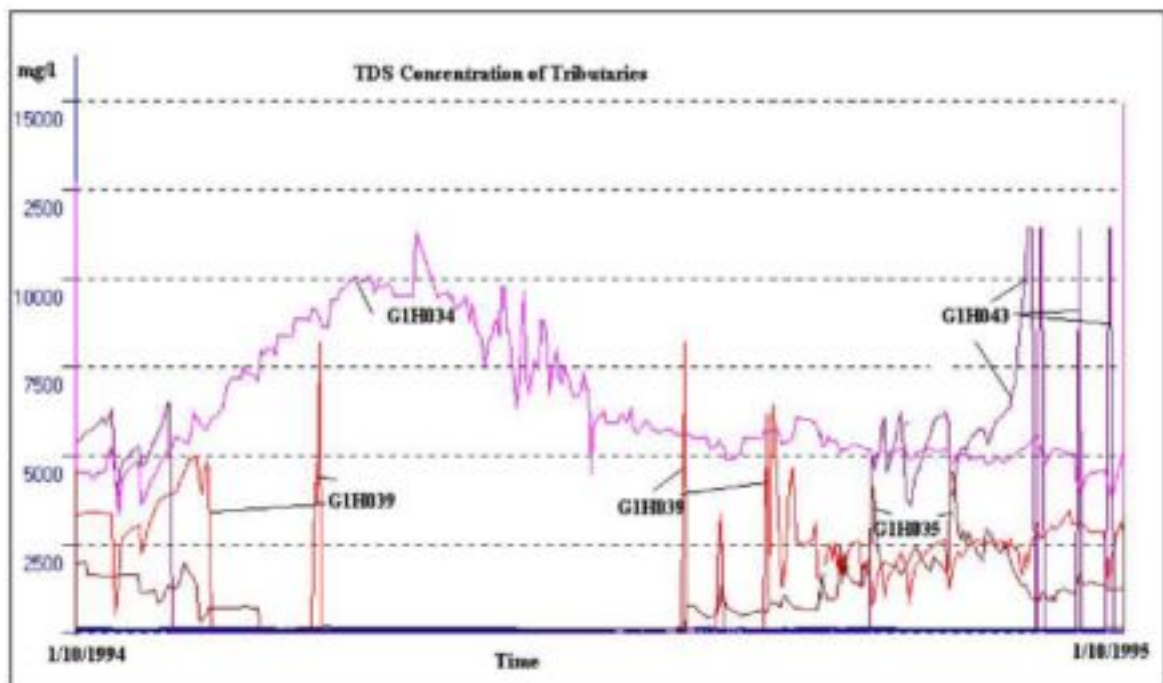


Figure 8.16: TDS Concentration of tributaries for the verification year

- **TDS Loads Results:**

Low Flow :

(Table 1.4.7, Figures 1.4.33 - 1.4.36 in Appendix 1.4)

As for the calibrated run, the coefficient of determination for the loads is higher than for the concentration. This is because the load is dependent on the flow simulated. One can see from the figures that the short lived peaks introduced by releases from Voëlvlei Dam are clearly defined in the load simulation at G1H013 and G1R003, but that the model is unable to simulate these loads to near zero load, as was measured. This is because the model gets unstable for zero water depths, and for modelling purposes a minimum water depth has been provided for in the coding. Interestingly, just as for the concentration, the loads are under-simulated for all stations for the verification run and over-simulated downstream from G1H020 for the calibration run. This could be the result of the definite over-simulation of loads in March/April for the calibration values, which does not occur in the verification run. The verification values show a higher coefficient of determination than for the calibration values (compare Tables 1.4.1 and 1.4.7).

High Flow:

(Table 1.4.7, Figures 1.4.37 - 1.4.40 in Appendix 1.4)

It can be seen from Figures 8.56 and 8.57 that the infilled salt loads stay consistent for the main peak in mid-July downstream from G1H013. In the model, however, salt loads are added from the ungauged sub-catchments and the tributaries, which can be seen by the increased simulated values for this peak. In the calibrated year the infilled TDS values do however increase in the peak (Figures 1.4.6 and 1.4.7), and this could mean that in reality most of the salts have already been discharged into the river by the previous flow peaks in the verification period, whereas in the calibration period only one major peak occurs. The overall TDS mass for the high flow months is under-simulated at all stations, except at G1R003.

8.10.2 Phosphate as PO_4

In the year October 1994 to October 1995, several peaks are experienced during the high flow months instead of one defined peak, as was the case for the calibration year. The maximum peak occurs mid-July and reaches only a value of approximately 15 g/s at G1H013 and G1R003, compared to the maximum peak of 40 g/s (at G1R003) for the calibration year (refer to Figure 8.37 and 8.69). The measured data for the low flow period nevertheless has more or less the same pattern and the same mass as for the calibration period.

- ***PO₄ Concentration results:***

(Table 1.4.10, Figures 1.4.53-1.4.56 in Appendix 1.4)

The coefficient of determination is low for the concentration analysis; the verified model shows however a better correlation to the measured data than the values for the verification simulation (Tables 1.4.10 and 1.4.4). Both the verification values and the calibrated values show a high over-simulation at G1H036 (Figures 1.4.54 and 1.4.22), this error therefore could be the result of an unknown point or non-point source between the reach G1H020 and G1H036, and is not only the result of a sudden high concentration measurement. The concentration is under-simulated most of the time at all stations (except at G1R003). This is also the case for the calibration year, except that G1R003 shows a 6% under-simulation for the low flow for the calibrated values and a 3% over-simulation for the verified values (Table 1.4.10 and 1.4.4). The simulation of the concentration during the winter months shows an erratic pattern, which is a result of the phosphate concentration discharging from G1H039 (refer to Figure 8.17).

- ***PO₄ Loads Results:***

Low Flow:

(Table 1.4.9, Figures 1.4.45-1.4.48 in Appendix 1.4)

At all stations the phosphate loads are over-simulated, especially at G1R003 where the simulated values show a 159% over-simulation. The calibrated values show an over-simulation of 103% (Table 1.4.3), and it can therefore be concluded that the flows (88% over-simulation, Table 7.6) and the loads are over-corrected in the reach from G1H013 and G1R003. The other stations also show similar errors in the load simulation when compared to the flow simulation (Tables 1.4.9 and 7.6), and it is evident that the mass errors are dependent on the errors of the flow simulation. Referring to the figures, one can see that the short lived peaks introduced by releases from Voëlvelei Dam are clearly defined in the load simulation at G1H013 and G1R003, just as for the calibrated values and the coefficients of determinations, as well as the errors, are similar.

High Flow:

(Table 1.9, Figures 1.4.49-1.4.52)

The phosphate peak in the summer was measured to be approximately 19 g/s at G1H013 and 15 g/s at G1R003. At all stations the phosphate peak is under-simulated, except for G1R003 where the phosphate peak is over-simulated as additional loads are introduced between reach G1H013 and G1R003 (compare also to Figures 1.4.17 and 1.4.18). This could be the result of additional non-point runoff occurring during a flood. The high flow phosphate loads show high coefficients of determination (0.92). The errors are less at G1H013, with only -18% under-simulated compared to -55% under-simulation for calibrated values.

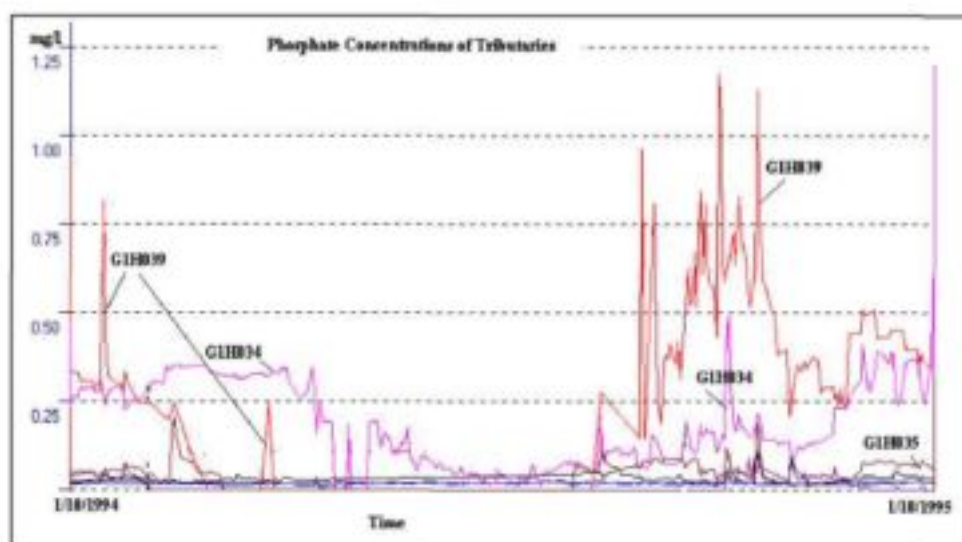


Figure 8.17: Phosphate Concentration of tributaries for verification year

8.10.3 Temperature

(Table 1.4.11, Figures 1.4.57-1.4.60 in Appendix 1.4)

The temperatures are simulated higher for the summer period for the verification run than for the calibrated model. The verification results show higher temperature values than the actual measured temperature, while the calibrated simulation results produced lower temperature values. The overall errors are less for the verified model than for the calibrated model, except for the reach from G1H013 to G1R003, where the error in the low flow period has increased to about 18%. The standard deviations have all increased (refer to Table 1.4.11).

From Figure 1.4.60 it can be seen that the summer temperatures are over-simulated at G1R003, and this could indicate that the parameters, that were acceptable for the calibration year, might not be acceptable for the verification year.

8.10.4 Oxygen

(Table 1.4.12, Figures 1.4.61-1.4.64 in Appendix 1.4)

The verification run showed small variation to the calibrated run. Table 1.4.12 summarizes the results and the percentage difference from the measured data. The percentage errors should be compared with the errors obtained from the calibration simulation (Table 1.4.6). Both runs are influenced by the saturation oxygen concentration, as little information is available on the oxygen in the Berg River. Only the flow and the meteorological data influence the oxygen concentration in this study. The low flow period shows a 1% over-simulation, while the high flow shows a 1% under-simulation. The standard deviations do not differ significantly. From the slight differences between the calibrated and the verified oxygen simulations it can be perceived that the parameters applied in the oxygen simulation are acceptable for another time period. The outliers seen in Figures 1.4.61 to 1.4.64 are due to under-simulation of temperature in the winter months.

8.11 WATER QUALITY SIMULATION WITHOUT UNGAUGED RUNOFF

The addition of ungauged runoff and loads was based on the conclusion that a considerable volume of flow and therefore also loads are missing in the mass balance (refer to Table 7.4). To assess whether the method (of adding ungauged loads and runoff) applied was successful, a simulation run without ungauged sub-catchments was completed. The results, compared to the actual measured data, were compared to the simulation results of Section 8.9.

8.11.1 TDS

- **TDS Concentration Results:**

(Table 1.4.14, Figures 1.4.73 -1.4.76 in Appendix 1.4)

Comparing Figures 1.4.73 to 1.4.76 to Figures 1.4.9 to 1.4.12, it can be seen (as already mentioned in section 8.9.1) sub-catchments 4 and 5 overcorrect the concentration in March and April. The peaks simulated in the winter months, which have also been added by sub-catchments 4 and 5, are also missing. The addition of the ungauged flow improved the concentration for September, October and November; but it had little improvement in the summer months. This can be seen especially at G1R003 (Figures 1.4.76 and 1.4.12), where considerable concentration is still missing. The concentration at G1H036 has been overcorrected the most, as the % error in concentration shifted from -32% to 14% for the low flow and -36% to 44% in the high flow. The overall concentration at high flow is always under-simulated without the addition of ungauged concentration, and over-simulated with ungauged runoff (except at G1H020).

- **TDS Loads Results:**

- Low Flow :

(Table 1.4.13, Figures 1.4.65 - 1.4.68 in Appendix 1.4)

With the low flow load results it can be seen again that the estimation of the ungauged TDS has been overcorrected in March and April with the addition of sub-catchments 4 and 5. The TDS loads have improved considerably, when including the ungauged loads, for the months October and November (Figures 1.4.65 to 1.4.68 and 1.4.1 to 1.4.6). The short-lived peaks occurring from

releases of Voëlvele Dam are already slightly over-simulated without any additional loads. The loads simulated in the three months December, January and February show little change.

High Flow :

(Table 1.4.13, Figures 1.4.69 - 1.4.72 in Appendix 1.4)

Referring to Figure 1.4.69 and 1.4.70 the peak simulated in high flow has improved with the addition of ungauged TDS loads for G1H020 and G1H036. A TDS load peak of 2090 g/s has been simulated with addition of ungauged loads at G1H036, while 888 g/s has been simulated without the addition of ungauged loads. The measured peak was 2529 g/s, thus the % error improved from -65% to -17%. Interestingly, the peak measured at G1H013 and G1R003 is already higher simulated with only gauged loads (G1R003 is 79% and G1H013 26% higher) than the measured peak. This could be due to unknown abstractions of winter floods.

It can be concluded that the addition of ungauged sub-catchments does improve the TDS concentrations and loads for the months of October and November, and in the winter months. Little change has been found during the months December, January and February. Sub-catchments 4 and 5 however over-correct the TDS concentrations and loads, especially in the months March and April. This can also be seen in Table 8.8 which shows that a 57% improvement in errors occurred for the TDS concentration in the second reach (G1H020 to G1H036). The estimated TDS loads for sub-catchments 4 and 5 seem incorrect (also refer to Figure 8.16). The TDS loads have been estimated with grab samples of station G1H039. Unfortunately, the station has a accuracy rating of 0 (refer to Table 7.1), but due to no additional choice of tributary, these grab samples were the only estimate.

Table 8.8: Absolute % error difference between the simulation without ungauged loads and the simulation with ungauged loads for TDS

| Yearly % error difference | G1H020 | G1H036 | G1H013 | G1R003 |
|---------------------------|--------|--------|--------|--------|
| TDS Loads | 28 | 96 | 64 | 68 |
| TDS Concentration | 7 | 57 | 38 | 26 |

8.11.2 Phosphate as PO₄

- **PO₄ Concentration results:**

(Table 1.4.16, Figures 1.4.85-1.4.88 in Appendix 1.4)

Comparing the errors in concentrations between the simulation with ungauged phosphate loads and the simulation run without ungauged phosphate loads (Table 1.4.4 and Table 1.4.16), one can see that the % error has improved for all the stations for low and high flow, when including the ungauged phosphates. The % error has improved about 10% for the low flow and about 20% for the concentrations at high flow. One can see in Figures 1.4.85 to 1.4.88 and Figures 1.4.21 to 1.4.24, that the addition of ungauged phosphates does correct the concentration peaks especially in the winter months.

- **PO₄ Loads Results:**

Low Flow :

(Table 1.4.15, Figures 1.4.77-1.4.80 in Appendix 1.4)

One can see from Figures 1.4.77 to 1.4.80 that the PO₄ loads have improved in the months October and November (as also the TDS loads). There is little change in the low flow loads, except for the small peaks occurring in November and December at station G1H036 (compare Figure 1.4.78 to 1.4.14), that are improved. The overall % error is less for stations G1H020 and G1H036, but have been over-corrected for stations G1H013 and G1R003. This is because, without any ungauged phosphate loads, the loads are already over-simulated at these stations.

High Flow:

(Table 1.4.15, Figures 1.4.81-1.4.84 in Appendix 1.4)

One can see from the figures that the PO₄ load peaks are very under-simulated for all stations, if additional loads from the ungauged sub-catchments are missing. The % error in the simulation run without the ungauged phosphates shows about 80% under-simulation. This error has been improved to about 40% under-simulation when the ungauged loads are added to the model.

It can be concluded that the addition of ungauged phosphate loads has proved to be successful for the high flows, as the error has been halved in the high flows. This proves that a considerable percentage of phosphate load is discharged into the river in a flood. Table 8.9 shows the % error improvements from the run without ungauged loads and the simulation run with ungauged loads for the overall yearly values.

Table 8.9: Absolute % error difference between the simulation without ungauged loads and the simulation with ungauged loads for phosphates

| Yearly % error difference | G1H020 | G1H036 | G1H013 | G1R003 |
|-------------------------------|--------|--------|--------|--------|
| PO ₄ Loads | 38 | 41 | 28 | 52 |
| PO ₄ Concentration | 14 | 17 | 21 | 28 |

CHAPTER NINE SCENARIO ANALYSIS

9.1 INTRODUCTION

A simulation model such as DUFLOW allows a user to understand the behaviour of a river system as a whole, or any of its parts, in space and time. Application of DUFLOW allows analysis of different scenarios that can illustrate the potential outcome of certain 'what if' situations. Figure 9.1 shows how a model can be used after verification, by implementing various water quality control actions and examining how the water system reacts to different scenarios and what the model's capability is to predict the outcome of these various scenarios.

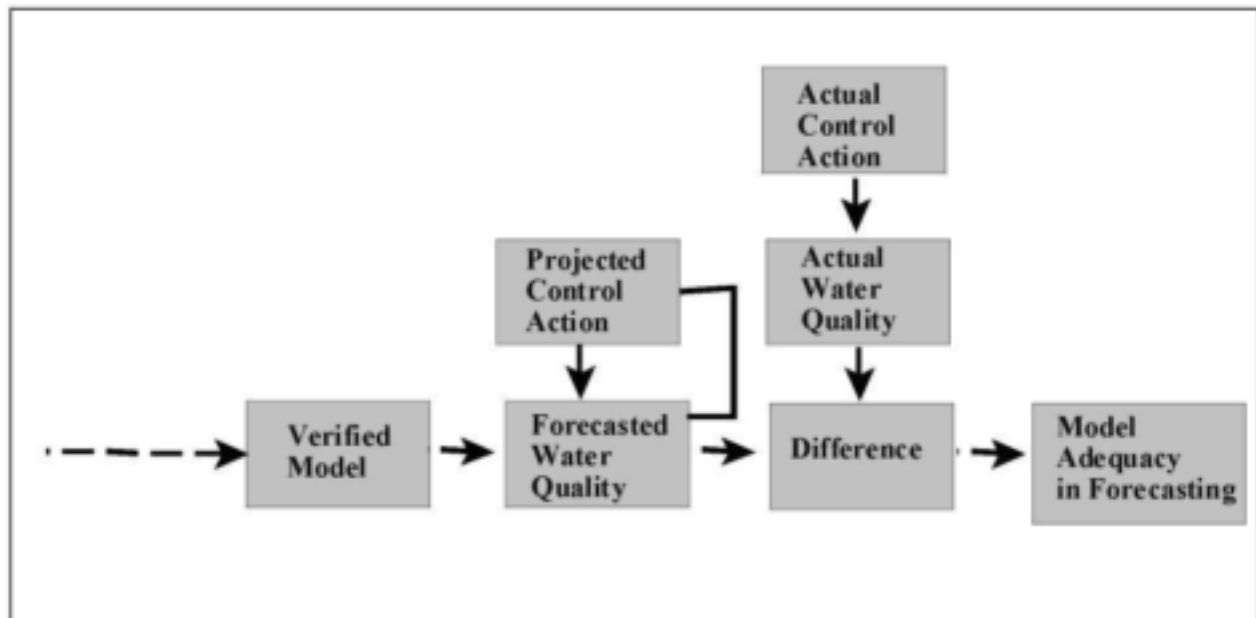


Figure 9.1: Post-audit of models (after Thomann and Mueller, 1987; pg. 8)

In this chapter the use of DUFLOW in different scenarios are examined, in order to determine the model's ability to predict the outcome of different situations that would be important in a water quality control programme. The scenarios that are studied have been divided into three categories:

- Short-term scenarios, such as a pollution spill discharging into the river.
- Long-term alteration of flow and water quality by linking the river simulation model to releases from a reservoir model.
- Long-term control management of concentrations and loads.

These scenarios and the ability of the model to predict the outcome, will be discussed in this chapter.

9.2 OPERATIONAL SHORT-TERM SCENARIO

The magnitude of a sudden spill of an effluent can be examined in a short-term scenario. The questions that are normally of interest to the river system manager if a sudden spill occurs, are:

- What is the time of travel of the effluent ?
- At what rate does the effluent attenuate ?

It was decided to divide the short-term scenario into two different scenarios that could occur:

- *spill without option of release of fresh water:*
If no option of fresh water release is available, the question will be what degree of impact the spill will have on the river and how far, as well as how long, the increased water quality constituent concentration will travel downstream.
- *spill with option of releasing fresh water downstream*
If fresh water can be released, the question will be what volume and duration of water releases from an upstream source would then be required.

The DUFLOW model was linked to the Water Quality Information System (WQIS), discussed in Volume 2, in which the user is prompted to enter the following:

- Location of an effluent spill
- Peak value of concentration of a spill, either for COD, TDS or PO_4
- Start and end times and dates of an effluent spill
- The spill hydrograph shape (Figure 9.2)
- If the user decides to increase the release water, the user is prompted to enter the discharge value and whether the discharge is from Skuifraam (the proposed future dam upstream in the Berg River, refer to Section 3.4.5), or from the Voëlvele Dam (if an effluent spill occurred downstream of the release point of Voëlvele, refer to Section 3.4.1 on details of Voëlvele Dam).

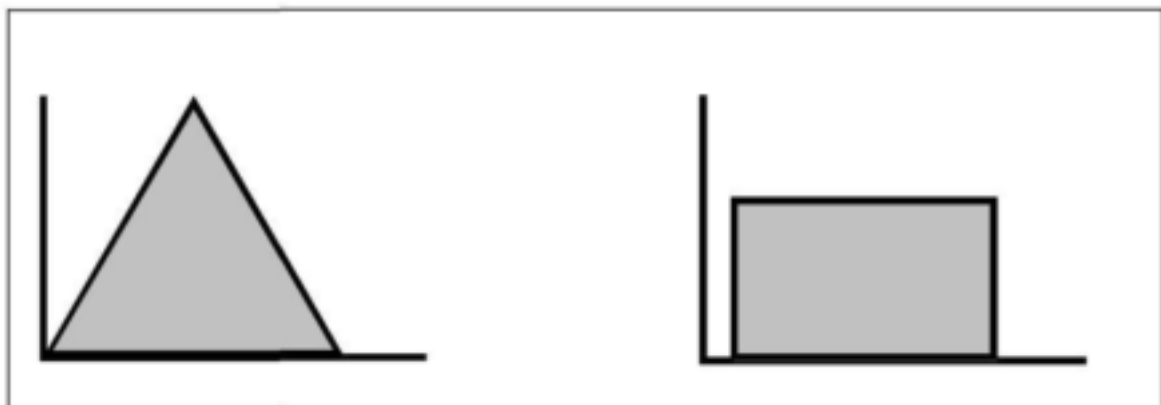


Figure 9.2: Effluent Spill Hydrograph Shapes

A DUFLOW simulation run is then performed and the impacts of the spill can be assessed graphically; either as a longitudinal section in a time step (refer to Figures 9.7 to 9.12), or at a specific cross-section over a time period (refer to Figures 9.5 and 9.6). To demonstrate the short-term scenario analysis, two runs were completed: one without releases from Skuifraam Dam and one run with releases.

Simulation without any releases:

The month of February was chosen as a good indication of a 'worst case' scenario, as the flow in the river was very low. The spill occurred over a 4 day period, from the 15th February to the 19th February. The average discharge in the river was between 3 and 4 m^3/s . A phosphate spill of triangular effluent shape (refer to Figure 9.2) and a peak concentration of 10 mg/l were inserted at Wemmers River; the discharge in Wemmers River at the time of the peak (17th February) was 0.2 m^3/s .

Simulation with upstream releases:

For the second simulation run, the same effluent spill incident as for the abovementioned simulation was used, but a release discharge of 20 m^3/s was included additionally in the model. The discharge was released on the 16th February, a day after the occurrence of the effluent spill, and was of trapezoidal shape. By using the simulation model and inserting different volumes of releases, the user can assess on a trial and error approach the volume of water needed to decrease the concentration to an acceptable water quality limit at given downstream points.

Figure 9.3 shows the phosphate concentration over time at selected points downstream from Wemmers River without the release, while Figure 9.4 shows the phosphate concentrations experienced in the river if the release is included in the simulation run. As one can see from Figure 9.3 the concentration between Wemmers River and G1H020 is about 1 mg/l and attenuates to 0.4 mg/l at G1H013, while for the simulation run with the releases included the river experiences a phosphate concentration of 0.6 mg/l between Wemmers River and G1H020 and 0.2 mg/l at G1H013 (refer to Figure 9.4).

The results can also be viewed in space, therefore the user can assess the impact of the spill for a certain time period over the whole river. Figures 9.7, 9.8 and 9.9 illustrate the phosphate concentration for 16th February (one day after the beginning of the spill), the 18th and the 26th February respectively, for the simulation run without any releases. Figures 9.10, 9.11 and 9.12 show the impact the phosphate has on the river with releases discharging from Skuifraam Dam. One can see that with releases from upstream, the concentration in the river is diluted at a faster rate.

The severity of the impact of an effluent spill can therefore be visualized and understood for different scenarios.

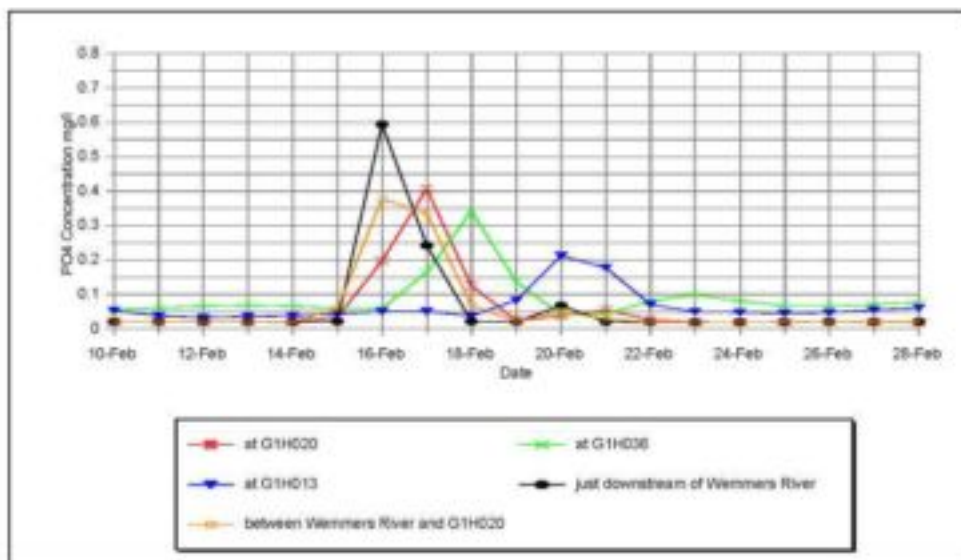


Figure 9.3: Results of Phosphate Spill without release shown in time

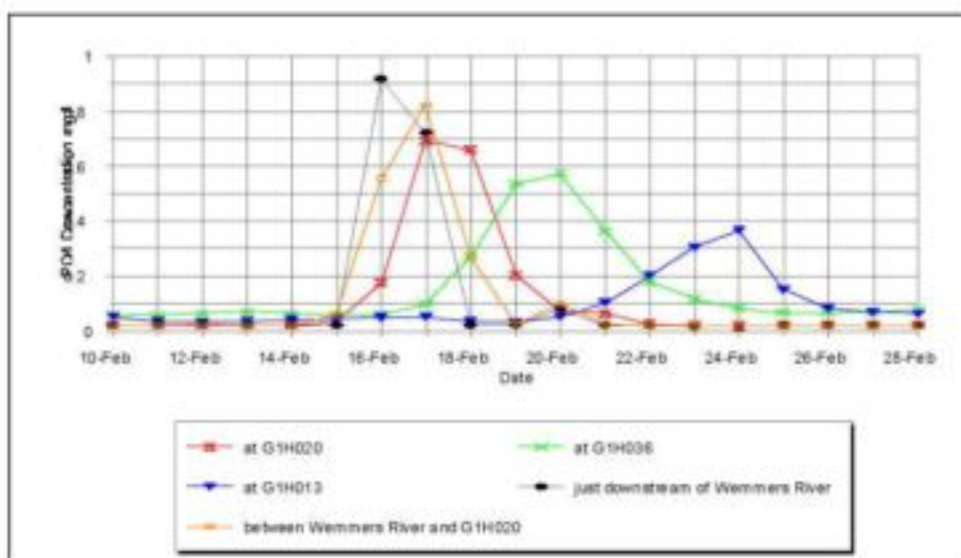


Figure 9.4: Results of Phosphate Spill with release shown in time

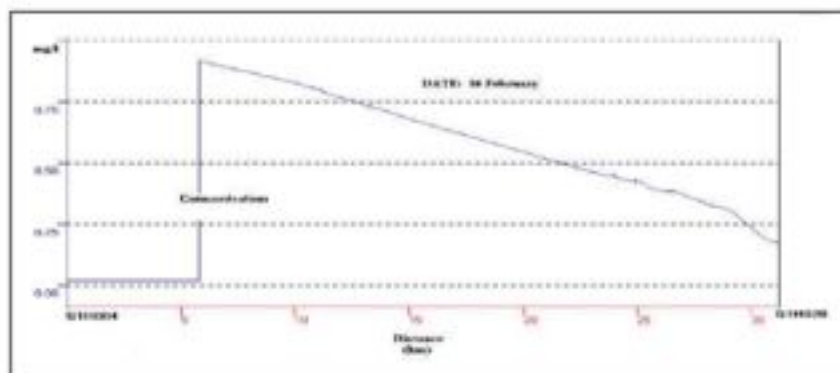


Figure 9.5: Results of Phosphate Spill without release for 16 February

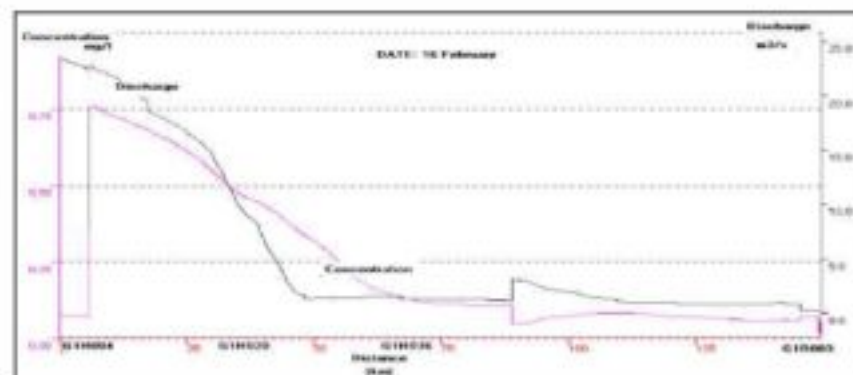


Figure 9.8: Results of Phosphate Spill with release for 16 February

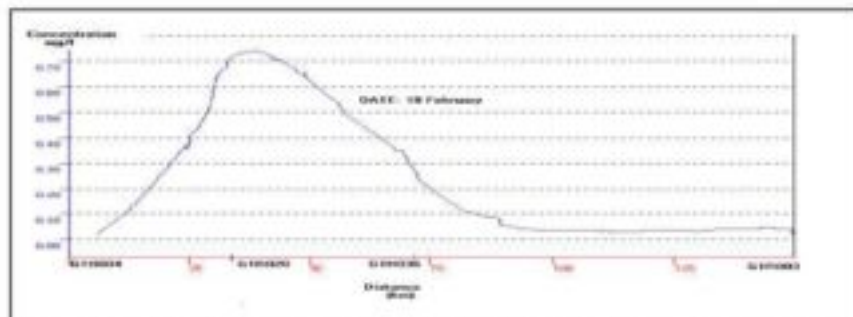


Figure 9.6: Results of Phosphate Spill without release for 18 February

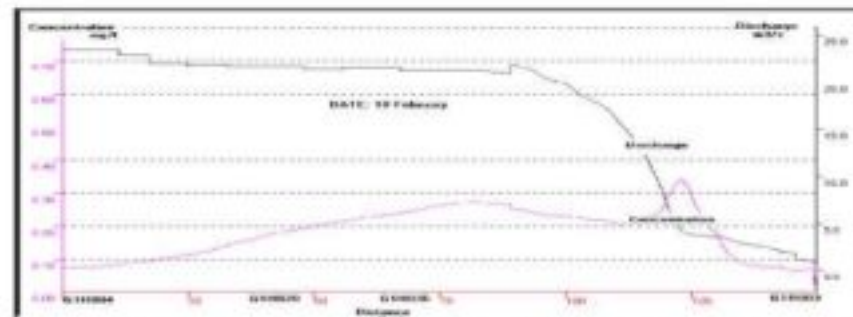


Figure 9.9: Results of Phosphate Spill with release for 18 February

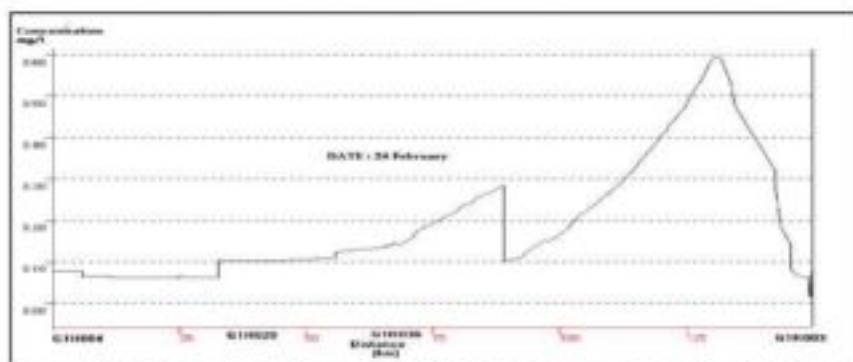


Figure 9.7: Results of Phosphate Spill without release for 24 February

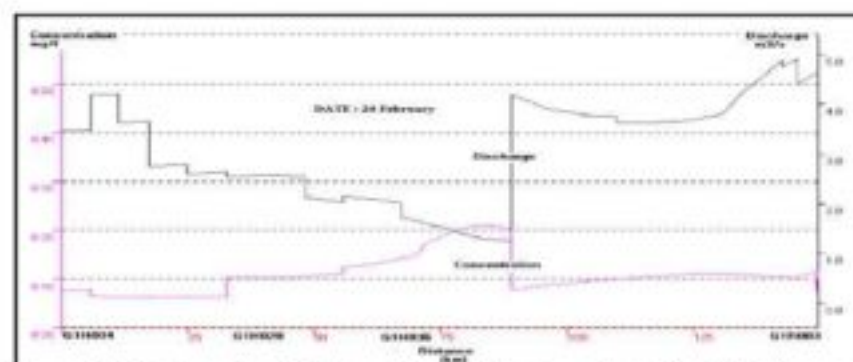


Figure 9.10: Results of Phosphate Spill with release for 24 February

9.3 LINKAGE TO RESERVOIR MODEL

The simulation model can be applied to a scenario where the upstream boundary conditions are varied according to the water quality and the flow releases that would occur if a reservoir were to be constructed in the upstream reaches of the river. The impact of the construction of a dam on the river can therefore be investigated. The reservoir model, CE-QUAL, was configured for Skuifraam Dam, as described in Section 3 of this volume, representing the water quality situation that would occur if Skuifraam Dam were built. The inflows used in the CE-QUAL reservoir model are the corresponding flows (G1H004) that were used originally as inflows into the river model. The water quality readings at G1H004 and the meteorological conditions at the site were used to drive the reservoir model, these are identical to the data that was used for the historical river model. Therefore, all conditions for the reservoir model were the same as in the river model, except that the flow and water quality were first routed through a reservoir before routed down the river. The simulated water quality release and spill time-series of the dam were used as the inflowing boundary water quality in the river model. The variables modelled were: TDS, Phosphate as PO_4 , temperature and oxygen.

9.3.1 Flow

The environmental and agricultural releases calculated for the Berg River for a large-scale water resources planning study (Ninham Shand, 1999) were used as the upper boundary flow pattern. Figure 9.11 shows the comparison between the historical flow hydrograph and the release pattern developed for the reservoir.

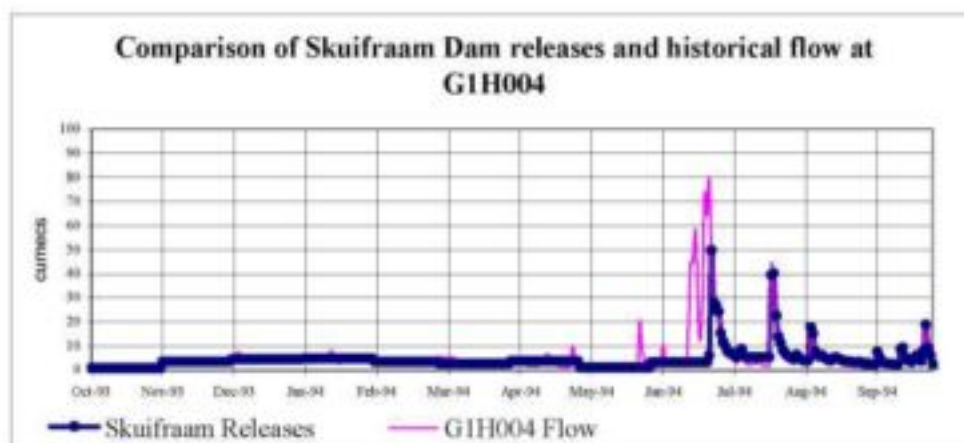


Figure 9.11: Comparison of historical inflow hydrograph and releases of Skuifraam Dam

Table 9.1: Comparison of flows at G1H004 and dam release/spill pattern

| | Skuifraam Dam | Historical Data |
|--------------------------|---------------|-----------------|
| Total (Mm ³) | | |
| Summer | 51.5 | 55.9 |
| Winter | 180.9 | 222.9 |
| Yearly | 232.4 | 278.9 |
| Mean (m ³ /s) | | |
| Summer | 3.3 | 3.6 |
| Winter | 3.8 | 4.7 |
| Yearly | 3.7 | 4.4 |
| Maximum | 49.7 | 79.7 |
| Minimum | 0.8 | 0.4 |

It can be seen that the flood peaks experienced in the winter months would be intercepted in the dam, until spill occurs. The maximum flow that would be experienced downstream in the river is 49 m³/s compared with the 79.9 m³/s of the historical data (refer to Table 9.1). The total water volume does however not change significantly, as the releases are more consistent and additional water is made available in the summer months. The flow in March and April do not deviate in mean, while the summer months experience higher flow than historically, and the winter slightly lower flow.

9.3.2 TDS

It can be noticed from Figure 9.12 that the historical data measured at G1H004 displays more erratic TDS concentrations than the TDS releases of the dam. The consistency is a result of the controlled releases of volumes of water from the dam, smoothed by mixing, while without the dam, the TDS concentration changes with the nature of the historical flow. A slight increase in TDS concentration from 40 mg/l to 48 mg/l is experienced in mid-June. The overall incoming TDS load into the Berg River from upstream does not vary significantly; although the river will experience a slight increase in TDS for all months. The TDS concentration measured in the upper reaches of the Berg River are minimal when compared with the concentrations that are found in the lower reaches.

Table 9.2: Comparison of released TDS from Skuifraam Dam and historical TDS at G1H004

| | Skuifraam Dam | Historical Data |
|---------------------|----------------------|------------------------|
| Total (tons) | | |
| Summer | 752.3 | 666.4 |
| Winter | 777.6 | 619.2 |
| Yearly | 1529.9 | 1285.9 |
| Mean (mg/l) | | |
| Summer | 43.5 | 38.5 |
| Winter | 44.7 | 35.6 |
| Yearly | 44.1 | 37 |
| Maximum | 48.9 | 79.8 |
| Minimum | 26.6 | 23.5 |

Results:

The results of the simulation are shown in Table 9.3 for the concentrations and Table 9.4 for the TDS loads. The mean of the TDS concentration does not show much difference for all the stations. The total load has increased in the summer months and decreased in the winter months (refer to Table 9.4). It can therefore be concluded that the construction of the dam for this particular year would have had ineffectual impact on the TDS in the river, as the higher salinities experienced in the river are due to the high salinity discharged from the lower tributaries. A WCSA study (DWAF(a), 1993) on the salinity experienced in the river after construction of Skuifraam Dam, also calculated that the effect of the dam on TDS concentration would be relatively small if 1990 conditions persisted.

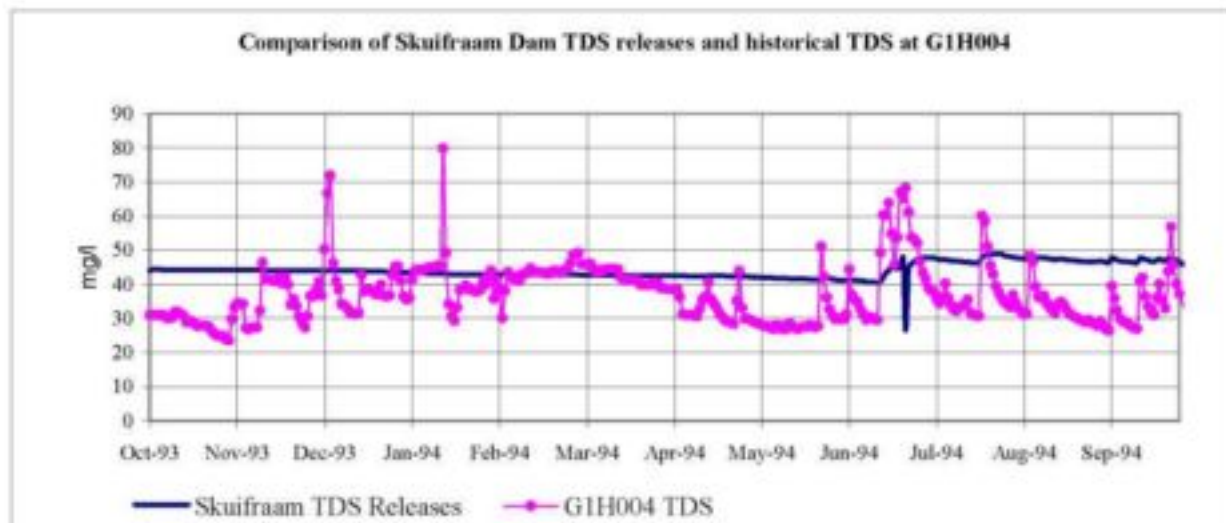


Figure 9.12: Comparison of historical TDS at G1H004 and TDS releases of Skuifraam Dam at G1H004

Table 9.3: TDS Concentration after simulation of dam releases

| | mean (simulation with historical data) mg/l | mean (simulation with dam concentration) mg/l | % diff in mean |
|-------------------------|--|--|----------------|
| Low flow period | | | |
| G1H020 | 43 | 45 | 5 |
| G1H036 | 136 | 141 | 3.4 |
| G1H013 | 123 | 118 | -4 |
| G1R003 | 162 | 148 | -8 |
| High flow period | | | |
| G1H020 | 41 | 45 | 9.7 |
| G1H036 | 177 | 178 | 0.6 |
| G1H013 | 196 | 177 | -9.7 |
| G1R003 | 224 | 217 | -7 |
| Yearly | | | |
| G1H020 | 42 | 44 | 4.7 |
| G1H036 | 156 | 159 | 2 |
| G1H013 | 159 | 147 | -7.5 |
| G1R003 | 193 | 184 | -4.7 |

Table 9.4: TDS Loads after simulation using dam spills and releases as the upstream boundary

| | Total Load Historical Data (tons) | Total Load Dam Releases (tons) | % Difference |
|-------------------------|-----------------------------------|--------------------------------|--------------|
| Low flow period | | | |
| G1H020 | 2077 | 3077 | 48 |
| G1H036 | 5401 | 6333 | 17 |
| G1H013 | 6751 | 7624 | 13 |
| G1R003 | 7595 | 8196 | 7.9 |
| High flow period | | | |
| G1H020 | 12729 | 9896 | -22 |
| G1H036 | 54475 | 47694 | -12 |
| G1H013 | 99558 | 79615 | -20 |
| G1R003 | 133148 | 119376 | -10 |
| Yearly | | | |
| G1H020 | 14806 | 12973 | -12 |
| G1H036 | 58760 | 54027 | -9.7 |
| G1H013 | 106309 | 87240 | -18 |
| G1R003 | 140744 | 127572 | -9 |

9.3.3 Phosphate as PO₄

Comparing the phosphates of the historical data measured at G1H004 and the phosphates that would be released from Skuifraam Dam at G1H004, one can conclude that the phosphate values will increase after construction of the dam. The phosphate values show a 200% increase in the summer months. This could be due to eutrophication. Algae growth is significant at this time, as the temperature and radiation are at a maximum (refer to Section 5.4.5.2 for description of phosphate sinks and sources). In the months July to September the phosphate values are also slightly higher for the dam releases than for the actual grab samples taken in the river without dam (refer to Table 9.5 and Figure 9.13). This could also be due to algae growth in the dam, which will be more significant in a reservoir as in a river.

Table 9.5: Comparison of Phosphate as PO₄ released from Skuifraam Dam and historical data at G1H004

| | Skuifraam Dam | Historical Data at G1H004 |
|--------------|---------------|---------------------------|
| Total (tons) | | |
| Summer | 1.2 | 0.4 |
| Winter | 0.7 | 0.3 |
| Yearly | 1.9 | 0.8 |
| Mean (mg/l) | | |
| Summer | 0.07 | 0.03 |
| Winter | 0.04 | 0.02 |
| Yearly | 0.05 | 0.02 |
| Maximum | 0.09 | 0.05 |
| Minimum | 0.01 | 0.005 |

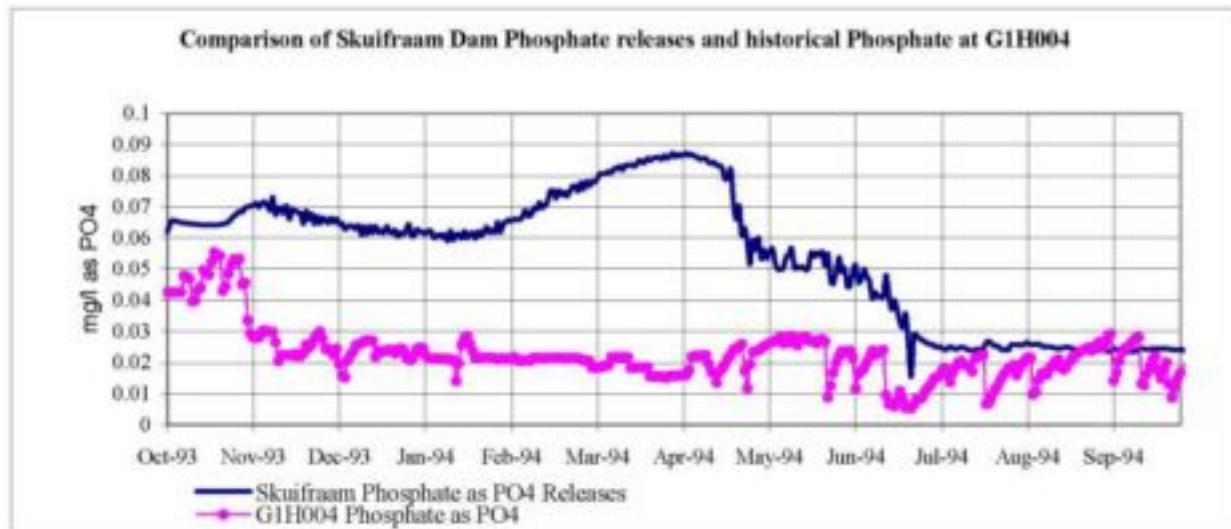


Figure 9.13: Comparison of historical Phosphate as PO₄ and releases from Skuifraam Dam

Results:

Table 9.6 summarizes the simulated concentration, while Table 9.7 shows the loads that will be experienced when the dam is constructed.

Higher phosphate loads are experienced in the dam for the summer months. This increase has an impact on the river, as can be seen from the simulation results. The results are higher for all months and at all stations, with the summer concentration showing an increase of about 76% at G1H020. The loads are also more significant and a 230% increase in the loads is experienced in the river reach from Skuifraam Dam and G1H020 during the summer months. The loads simulated in the winter months show only 12% difference. The increase in phosphate values perceived could have a vital impact on the already high phosphate values measured in the river.

Table 9.6: Phosphate Concentration after simulation using dam spills and releases as the upstream boundary

| | Mean (Simulation with Historical Data) mg/l | Mean (Simulation with Dam Concentration) mg/l | % Diff in mean |
|-------------------------|--|--|----------------|
| Low flow period | | | |
| G1H020 | 0.025 | 0.044 | 76 |
| G1H036 | 0.026 | 0.049 | 88 |
| G1H013 | 0.023 | 0.041 | 78 |
| G1R003 | 0.023 | 0.042 | 83 |
| High flow period | | | |
| G1H020 | 0.023 | 0.027 | 17 |
| G1H036 | 0.040 | 0.042 | 5 |
| G1H013 | 0.034 | 0.040 | 17 |
| G1R003 | 0.034 | 0.040 | 17 |
| Yearly | | | |
| G1H020 | 0.023 | 0.036 | 56 |
| G1H036 | 0.031 | 0.046 | 48 |
| G1H013 | 0.028 | 0.040 | 43 |
| G1R003 | 0.028 | 0.041 | 46 |

Table 9.7: Phosphate Loads after simulation using dam spills and releases as the upstream boundary

| | Total Load historical data (tons) | Total Load dam releases (tons) | % difference |
|-------------------------|-----------------------------------|--------------------------------|--------------|
| Low flow period | | | |
| G1H020 | 1.0 | 3.3 | 230 |
| G1H036 | 1.2 | 3.0 | 150 |
| G1H013 | 1.4 | 3.0 | 114 |
| G1R003 | 1.2 | 2.8 | 133 |
| High flow period | | | |
| G1H020 | 7.9 | 8.1 | 2.5 |
| G1H036 | 15.9 | 17.8 | 12 |
| G1H013 | 21.2 | 23.0 | 8.5 |
| G1R003 | 24.0 | 26.1 | 8.8 |
| Yearly | | | |
| G1H020 | 9.0 | 11.4 | 26 |
| G1H036 | 17.2 | 20.8 | 21 |
| G1H013 | 22.6 | 26 | 15 |
| G1R003 | 25.2 | 28.9 | 14.7 |

9.3.4 Temperature

The temperatures of the dam simulation outflows and G1H004 vary significantly. The maximum temperature is of equal value, but it is experienced in April, while for the historical data the maximum temperature is experienced in December and January (refer to Figure 9.14 and Table 9.8). The temperature of the dam releases do not drop as low as the historical data, as the temperature in the dam will not change as significantly with the meteorological conditions as the river, due to the smoothing effect of the storage in the dam. In December, a difference of -10° Celsius is simulated. The upper layer of the dam will experience these summer increases at nearly the same time as the river, while the lower layers of the dam (where the release takes place) stay cold due to stratification. These differences could have a significant ecological impact in the river. Additional research should be undertaken to investigate the impact these changes would have on the river ecology.

Table 9.8: Comparison of temperature released from Skuifraam Dam and historical temperature at G1H004

| | Skuifraam Dam Outflows | Historical Data at G1H004 |
|---------------------|------------------------|---------------------------|
| Mean (°C) | | |
| Summer | 15.2 | 22 |
| Winter | 19.7 | 13.1 |
| Yearly | 17.5 | 17.5 |
| Maximum (°C) | 24.6 | 25 |
| Minimum (°C) | 13 | 10 |

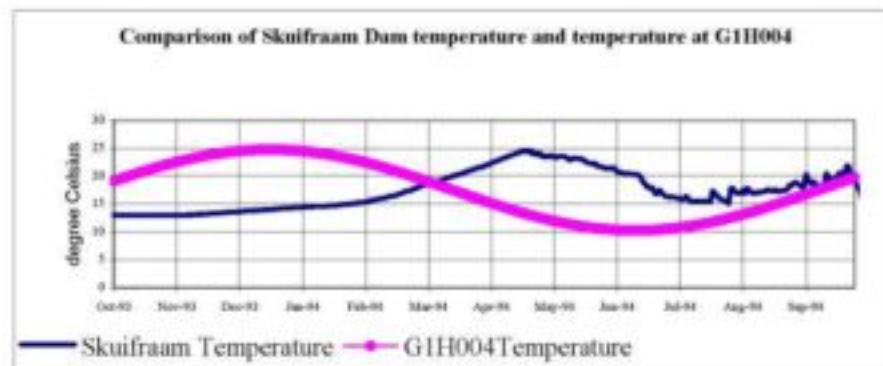


Figure 9.14: Comparison of historical temperature and temperature releases of Skuifraam Dam

Results:

The results of the simulation (refer to Table 9.8) show that the temperature experienced in the river will be lower for the summer months and higher in the winter months. The effect the released temperature of the dam will have on the river will be felt particularly in the reach from the dam (G1H004) to G1H020. The effect the delay of the maximum temperature has on the overall statistics is averaged out when calculating the temperature values over 6 months. The mean temperature is lower in the summer months, while in the winter months the temperatures all show higher values. This can also be seen when comparing the released temperature of Skuifraam Dam to the temperatures in the river prior to a dam (Figure 9.14) The maximum temperature in the river does not vary in value, but in time, as was seen in Figure 9.14, this delay in maximum temperature could have a significant effect on the ecology of the river and further studies should take place on the degree of impact this delay will have.

Table 9.9: Temperature after simulation using dam spills and releases as the upstream boundary

| | Mean Historical Data (°C) | Mean Dam (°C) | % Diff. in Mean | Standard Deviation Historical Data | Standard Deviation Dam | % Diff. in Standard Deviation |
|-------------------------|---------------------------|---------------|-----------------|------------------------------------|------------------------|-------------------------------|
| Low flow period | | | | | | |
| G1H020 | 23 | 20.1 | -13 | 3.0 | 3.1 | 3 |
| G1H036 | 24 | 20.7 | -14 | 2.7 | 2.8 | 4 |
| G1H013 | 24.5 | 22 | -10 | 3.6 | 3.1 | -14 |
| G1R003 | 24.7 | 22.8 | -7 | 3.5 | 3.1 | -11 |
| High flow period | | | | | | |
| G1H020 | 13 | 15.1 | 16 | 2.5 | 3.4 | 36 |
| G1H036 | 12.8 | 14.1 | 10 | 2.7 | 3.3 | 22 |
| G1H013 | 12.5 | 12.7 | 2 | 2.9 | 3.3 | 14 |
| G1R003 | 12.5 | 12.3 | -2 | 2.9 | 3.4 | 14 |
| Yearly | | | | | | |
| G1H020 | 18 | 17.6 | -2 | 5.7 | 4.1 | -28 |
| G1H036 | 18.3 | 17.4 | -5 | 6.5 | 4.5 | -30 |
| G1H013 | 18.5 | 17.3 | -6 | 6.9 | 5.7 | -17 |
| G1R003 | 18.5 | 17.5 | -5 | 6.9 | 6.2 | -10 |

9.3.5 Oxygen

The oxygen discharged from the dam is much lower than the oxygen values estimated at G1H004. This difference is because the oxygen calculated for the river simulation is the actual saturation oxygen, as no real data was available to include into the model. The oxygen of the dam is less than the saturation oxygen, because of the dynamics that influence and depletes the oxygen concentration in the dam (refer to Section 5.4.5.3 for more description on oxygen processes in a water body) and because the releases are made from the lower layers of the dam. A minimum of 1.3 mg/l is calculated for the dam oxygen, while the saturation oxygen only decreases to a minimum of 8.4 mg/l. Higher oxygen is released in the winter months, when the spill occurs and oxygen from the upper layers of the dam is released into the river (refer to Figure 9.15).

Table 9.10: Comparison of oxygen released from Skuifraam Dam and oxygen at G1H004

| | Skuifraam Dam | Historical Calculated Saturation Values |
|----------------|---------------|---|
| Mean (mg/l) | | |
| Summer | 0.3 | 8.8 |
| Winter | 5.3 | 10.5 |
| Yearly | 2.8 | 9.7 |
| Maximum (mg/l) | 8.6 | 11.2 |
| Minimum (mg/l) | 0 | 8.4 |

Results:

Referring to Table 9.11, there is an insignificant difference in oxygen mean for low and high flow period. The yearly values show that there is 0% difference, while the low flow period indicates slightly higher values, with 3% difference the maximum at G1H020, and the high flow period shows slightly lower values, with -5% the maximum difference experienced at G1H020. The minimal differences perceived from the simulations might be due to high saturation oxygen discharging into the river from the tributaries and also that reaeration of the depleted oxygen takes place shortly after the upstream releases. Therefore, the oxygen level in the river increases to saturation oxygen before reaching the gauging stations. The results indicate that although the oxygen concentration is low in the top reaches of the river, the river has the ability to reaerate and depending on the quality of the water from the tributaries, the oxygen in the river could recover at a fast rate. There is however need for additional research on the severity of the impact of low oxygen discharging into the river.

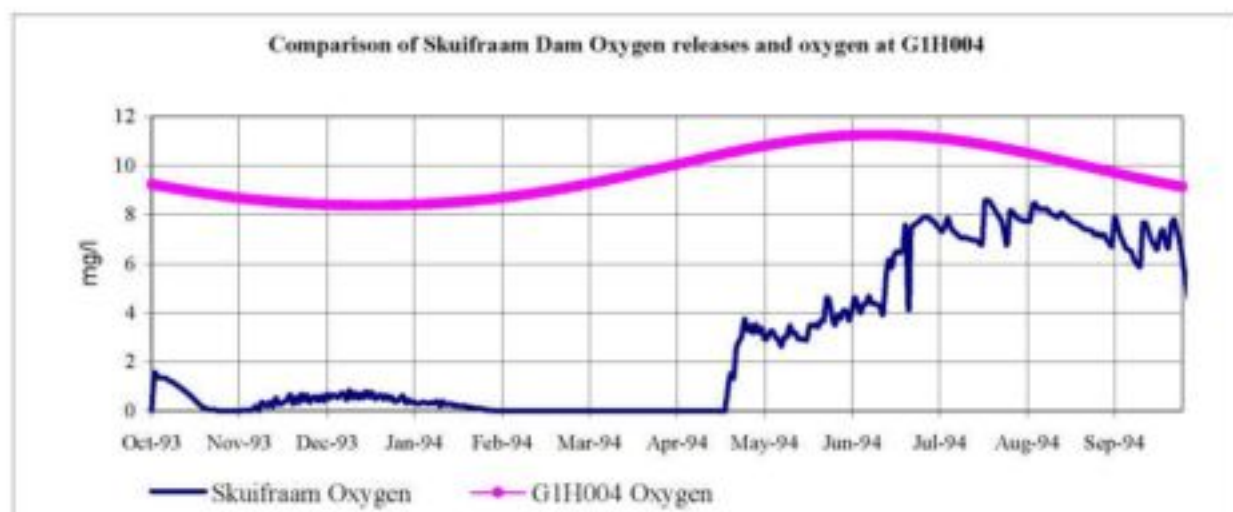


Figure 9.15: Comparison of historical oxygen and releases of Skuifraam Dam

Table 9.11: Oxygen after simulation using dam spills and releases as inflow

| | Mean Historical Data (°C) | Mean Dam Spills and Releases (°C) | % Diff. in Mean | Standard Deviation Historical Data | Standard Deviation Dam Spill and Releases | % Diff. in Standard Deviation |
|-------------------------|---------------------------|-----------------------------------|-----------------|------------------------------------|---|-------------------------------|
| Low flow period | | | | | | |
| G1H020 | 8.7 | 9.0 | 3 | 0.44 | 0.45 | 2 |
| G1H036 | 8.6 | 9.1 | 6 | 0.50 | 0.47 | -6 |
| G1H013 | 8.5 | 8.8 | 3.5 | 0.53 | 0.50 | -6 |
| G1R003 | 8.9 | 9.2 | 3 | 0.42 | 0.41 | -3 |
| High flow period | | | | | | |
| G1H020 | 10.3 | 9.8 | -5 | 0.60 | 0.69 | 15 |
| G1H036 | 10.6 | 10.2 | -4 | 0.86 | 0.76 | -12 |
| G1H013 | 10.7 | 10.5 | -2 | 0.76 | 0.96 | 26 |
| G1R003 | 10.8 | 10.6 | -2 | 0.82 | 0.74 | -10 |
| Yearly | | | | | | |
| G1H020 | 9.6 | 9.4 | -2 | 0.9 | 0.66 | -26 |
| G1H036 | 9.6 | 9.6 | 0 | 1.2 | 0.85 | -29 |
| G1H013 | 9.7 | 9.7 | 0 | 1.3 | 1.12 | -14 |
| G1R003 | 9.8 | 9.9 | -1 | 1.4 | 0.95 | -32 |

9.4 LONG-TERM CONTROL

A central problem of water quality management is the assignment of allowable discharges to a waterbody so that a given water quality standard downstream of a particular effluent point is met. For instance, the deteriorating water quality in the Berg River is a result of the return flow from the agricultural land (i.e. non-point sources) and from the sewage treatment plants (i.e. point sources). Thus, the question can be asked: how should the load allocation between these two be divided ?

DUFLOW cannot model non-point sources. Therefore, to investigate the aforementioned management question, the non-point sources were modelled as distributed "point sources". The user can insert water quality limits upstream at a selected discharge point and downstream at the point of interest to the user. The user is also prompted, as for the short-term scenario, for a concentration and a discharge that will be discharged at the selected location. The user can then by a trial and error approach identify the magnitude of loads that may be discharged at the specific location without violating the specific quality limitations. The point loads may also be altered and compared with the non-point discharges.

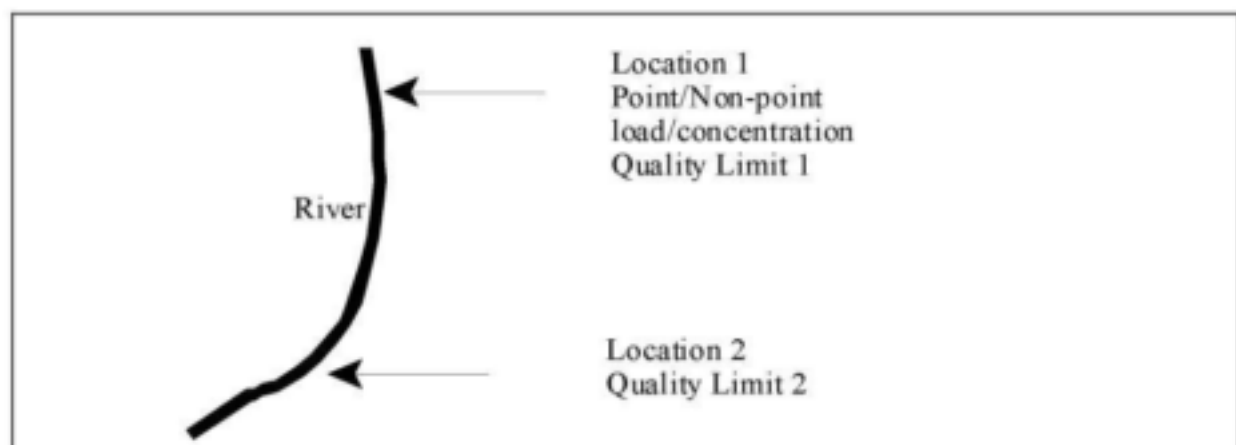


Figure 9.16: Schematisation of long-term control scenario

This scenario is similar to the short-term scenario, except that the user has additional control by assessing which mass a water quality load discharge into the river upstream may have without violating a particular water quality limit at a downstream source.

9.5 DISCUSSION

From the above discussions it is evident that DUFLOW does have the capability to assist in scenario analyses. It seemed reasonably easy to add releases and spills and the model remained computationally stable during the scenario simulation runs.

A limitation of DUFLOW is that no non-point sources can be modelled and this would have allowed for additional load allocation scenario analyses. The incorporation of a catchment model to the WQIS and DUFLOW would therefore be of advantage for the overall understanding and management of the river system. The DUFLOW modelling package does contain an additional precipitation runoff module (RAM) which has been developed by STOWA in order to improve the applicability of surface water models. RAM has however not been applied to many studies yet, and has not been tested for South African conditions. It is therefore recommended to use models that have been used and tested extensively for South African conditions. Examples of modelling systems used in South Africa are:

- *ACRU hydrological and water quality modelling system:*
A sediment-nutrient version of the well-known ACRU modelling system has been configured and used for the Mgeni Catchment (Kienzie *et al*, 1997)
- *IMPAQ*
IMPAQ has been developed by Ninham Shand and has been applied to the Amatole System in the Eastern Cape Catchment (DWAF(a), 1995)
- *HSPF*
(Bricknell *et al*, 1993).

Matji (2000) compares the results of phosphorous runoff from various catchments with different runoff conditions for different catchment models, including some of the abovementioned models. The linkage of one of these runoff models would therefore improve the applicability of operational scenario analyses.

CHAPTER TEN CONCLUSIONS AND RECOMMENDATIONS

10.1 INTRODUCTION

As water quality is becoming an increasingly important issue, the application of a water quality simulation model is useful for integrated management of the existing and future water resource systems. Since the early days of the development of computer models, as described in Chapter 2.2, models have become an essential "tool" to simulate solutions to different types of problems in water resources. The objective of this study was to assess the applicability of an existing European model for a winter-rainfall river in South Africa, under conditions very different to those applicable in its country of origin. Following selection criteria that have been declared important by management-orientated user groups (Chapter 2.6), it was decided to apply the hydrodynamic water-quality model, DUFLOW, and evaluate its adaptability for representing the Berg River with all its complexities.

The Berg River seemed to be a suitable river to model, as it contains a range of challenges for hydraulic modelling (fairly steep slopes, abstractions, diversions of flow, hydraulic structures) and also water quality (non-point and point sources, etc.). Aspects of the water quality in the Berg River are of great concern, especially in the lower reaches of the Berg River catchment, where the salinities are excessive and high nutrients are also becoming an intermittent. In Chapter 4 it was shown that the phosphorous concentrations have increased considerably over the last ten years. In the vicinity of Paarl/Wellington the sandstone formations give way to Malmesbury shale downstream that yield high salt loads into the main stream, via the tributary flows and through irrigation return flows. With the proposed construction of Skuifraam Dam (refer to Chapter 3.4.5), fresh water from the upper Berg River would be captured. Concerns have been raised that the downstream salinity might increase due to reduction of fresh water availability. It is therefore important that the model represents the water quality responses in the river realistically, as it can then be used to assist in developing management strategies.

The limitations and the capabilities of DUFLOW are discussed in the first section of this chapter. Recommendations are made on basis of the conclusions drawn and are presented in the second section of this chapter.

10.2 CONCLUSIONS

10.2.1 Flow Calculations

The finite difference approach that DUFLOW uses to calculate the St Venant equations of continuity and momentum is advanced and therefore allows the user to model complex systems. The finite difference approach allows varied space steps, which proved to be advantageous; especially in the upper Berg, where steep slopes required very small space steps for stable calculations. The lower Berg River could then be modelled in larger space steps in order to save running time and superfluous cross-sections. In total, 108 surveyed cross-sections were included.

Structures that were included are weirs at the specific gauging stations and bridges that are found along the main stem of the Berg River. Information was available for most of the structures, and where difficulties were experienced with computational stability, the roughness coefficient was adjusted. The "trigger function" used in DUFLOW for structure control allows modelling of multiple notches at a weir, such as is often found in South African rivers.

10.2.2 Water Quality Calculations

An advantage of DUFLOW is the open code structure it uses for the water quality module. This allows the user to either change the water quality algorithms according to the degree of complexity required or add additional water quality processes that need to be simulated. In future use of the configured model, water quality processes can be added or deleted. Thus, the model is very flexible. In this study, TDS, COD and Temperature algorithms were added to the EUTROF1 module, as these are variables of concern specifically in the Berg River catchment. The Phosphate algorithm had to be simplified, as most of the processes could not be modelled due to lack of in-stream data. The results of the Temperature algorithms proved to be satisfactory.

Two-weekly water quality samples were available. As the model was configured on a daily time step, the samples had to be 'patched' (infilled) in order to include the variables as time series. DUFLOW has an option of entering the time series at irregular time steps, but DUFLOW linearly interpolates the values for the missing samples, which is not quite correct for the distribution of the water quality variables as they are also dependent on the flow value. A moving regression method was used to infill the TDS and soluble phosphate values, while a simple harmonic function was used for the temperature infilling.

Schematisation points were added at every location where a tributary discharges into the main stem or where a point source had been identified. A considerable number of point sources were not included, due to lack of information. It would be a pre-requisite, if the simulation model will be used as an operational tool, that all primary sources of water quality discharge into the river are identified and included in the model.

A limitation of DUFLOW is that it does not allow incoming loads to be input in a diffuse fashion along the length of the modelling reaches. It is therefore difficult to distinguish between non-point and point sources, if the model is to be used as a scenario tool, because the non-point sources have to be treated as distributed point sources.

10.2.3 Results

The accuracy of the results is mainly determined by the accuracy and availability of the input data. Errors in the water quality simulation are dependent on various factors, such as: accuracy of the 'infilling' method, availability of grab samples in the river, accuracy of the flow simulation, etc. The flow simulation is dependent on various factors such as cross-section data, channel roughness information, etc. The errors that are introduced at the beginning of the flow calculations (i.e. in the first reach) are carried all the way downstream to the end boundary.

The estimation of runoff from ungauged sub-catchments for the calibration of the flow module proved to be problematic. Considerable volumes of water were still missing during peak flows for most of the stations. This could be due to under-estimation of the flood at the various gauging stations, which thus also leads to under-estimation for the ungauged runoff. The accuracy of the simulation of the water quality loads is dependent on minimising errors resulting from the flow simulation.

10.2.4 Learning Curve

The learning curve time to use the model efficiently is greatly reduced by the user friendly interfaces that DUFLOW offers. This is a major advantage, as it can be operated easily for configuration and scenario analyses by the user. An understanding of the underlying hydraulics and water quality processes is however needed to fully understand the system.

10.2.5 Limitations

- i. Although the finite difference approach to calculate the St Venants equations proved to be advantageous due to the stability and the choice of unequal time and space steps, a limitation of this approach is, however, that it is very data intensive compared to other simpler flow calculation methods.
- ii. The different network objects (i.e. weirs, abstraction points, etc.) can only be altered in the network window itself. For adjustments to the objects it would have been easier to change the specific descriptions in an additional textfile or database, especially if numerous objects are configured.
- iii. The results are written in a textfile, which take up considerable space (about 50 Mb for the quality files). For use in other systems, such as the WQIS (Volume 2), a database format would have been more suitable for updating and presenting.
- iv. Like many European or American models, DUFLOW is not able to simulate evaporation losses from the water body. Such losses can be quite significant in South Africa, and are therefore of importance. These losses had to be treated as abstraction flows at schematisation points.
- v. Non-point sources are not modelled as diffuse inflows by DUFLOW. These are however extremely important when considering the nutrient mass balance. From the water quality results it was evident that the agricultural runoff is significant in floods (all loads are under-simulated).
- vi. Water Quality calculations became unstable when "negative" water depths were experienced for the different runs. Negative water depths are a physical impossibility, but are sometimes simulated in the low flow period, due to inaccuracies between the calculated water level and the configured cross-section's reference level. Although the process calculations were able to be coded to overcome this problem, the transport mathematical formulations were fixed, and the negative water

depths affected the calculations. Much effort went into altering the time and space steps until a stable flow calculation was achieved.

10.2.6 Scenario Analysis

The text files produced by DUFLOW are easily altered for different scenario runs. DUFLOW is capable of simulating different scenarios that are of interest to the user. Three scenarios were looked at: a short term effluent spill scenario, a linkage to the hydrodynamic reservoir model, which is described in Section 3 of this volume, and thirdly an operational long-term management scenario. Although simulation time was long due to small calculation time steps (a calculation time step of 10 minutes proved to be stable) and the result file is large in terms of computer space, DUFLOW is capable of simulating various water quality related changes and predicting the outcomes of different water management scenarios.

10.3 RECOMMENDATIONS

Although the information for the Berg River Catchment is probably more extensive than for many other catchments in South Africa, there is still considerable need for additional research and data if a realistic representation of the river is desired. This is especially important when the model is not only used as an analysing "tool" for historical data, but also used to examine management scenarios. Research into the following areas may produce results that would strengthen the model's capability to represent the Berg River Catchment:

10.3.1 Non-point and Point Sources

There is considerable need to improve the monitoring system for point and non-point sources along the Berg River catchment. This would make a database available of different sources that contribute to nutrient and salt loads in the river. Although DWAF already monitors point sources that have been issued with a water quality permit, there are numerous sources that contribute to the deteriorating water quality in the Berg River. As most of the phosphorous in the river is due to runoff from agricultural land (Bath, 1989), it would be of benefit to link the hydrodynamic river model to a catchment model to estimate water quality loads from ungauged areas, rather than the ungauged runoff estimation methods used in this study.

10.3.2 Expansion of Data Information on Variables of Interest in the Berg River

Oxygen is of interest in the river for ecological reasons, therefore it would be important to explore the oxygen mass balance in the Berg River, by taking grab samples over a longer period and incorporating COD discharges of the point sources into the river. Different algorithms relating to oxygen should be studied and adopted according to the specific river.

The scenario analysis showed that the summer temperature in the river would change considerably (-10 degree Celsius change) if Skuifraam Dam were to be built in the upper reaches. This is obviously of concern and there is need to investigate the ecological impact of these temperature changes in the river.

Although earlier studies have been conducted on the phosphorous transport in the Berg River (Bath, 1989), the DUFLOW model has been activated in only the advection equation to analyse the phosphate concentration, as insufficient data is available on other dependent variables. By including data on the suspended solids and therefore the mobilisation of particulates into the river, as well as production of algae, improved results on the simulation and a better understanding on the phosphorous concentration in the river can be expected.

10.3.3 Linkage to Other Models

As mentioned above, it would be beneficial for management support, if DUFLOW were to be linked to other models as this would also ensure that DUFLOW could be used in catchment-wide applications. In this research, a user-friendly interface environment was developed and implemented as a Water-Quality Information System (WQIS) that provides analytical, spatial and graphical information based on the requirements of a wide spectrum of users and which integrates simulation models (river and reservoir) into the WQIS, as described in Volume 2. It would be important to broaden this study and integrate a catchment model into the WQIS so that it can provide tributary inputs to DUFLOW, as well as further develop the DUFLOW model to support scenario analysis to support decision making for integrated water management.

SECTION 2

**APPLICATION OF A TWO DIMENSIONAL HYDRODYNAMIC RESERVOIR
WATER QUALITY MODEL : CE-QUAL-W2:**

**APPLICATION TO THE PROPOSED SKUIFRAAM DAM
ON THE BERG RIVER**

CHAPTER ONE INTRODUCTION

1.1 BACKGROUND

Impoundments and associated bulk water supply infrastructure are present in most South African river systems. Because of the disparate natural occurrence of rainfall and runoff, and its mismatch with water demand concentrations, many of these schemes have to incorporate inter-catchment transfers to meet demands in the face of inadequate local availability. Furthermore, water quality deterioration, because of human impacts through a wide range of land-uses and waste discharges, has for some time been recognised as a threat in South Africa, as it diminishes the utilisable part of the runoff in many catchments. These complexities increasingly offer challenges to water resource managers that require a response with integrative management philosophies and innovative management tools.

During 1997, in recognition of the aforementioned needs, the Department of Civil Engineering of the University of Stellenbosch, formulated a research proposal to the Water Research Commission (WRC) whose aim would be to serve the philosophy of Integrated Water Resource Management (IWRM), through the development of an integrated information system specifically for water quality – here abbreviated to “WQIS”. To be useful to IWRM, this WQIS was to provide diagnostic and predictive utilities to serve technical planning and operational decision-making in a river system, but, simultaneously, provide appropriate information to support water managers in communication with technical stakeholders. It was also recognised that the project would need identification of a “prototype” catchment for development of appropriate WQIS approaches and to provide a relevant database.

One of the aims of this project was to develop Water Quality Information Systems (WQIS) to support both integrated management of a water resources system, and to support communication about water quality management with stakeholders and communities in the catchments of that system - In this study the Riviersonderend-Berg River (RSE-BR) System was used as the prototype catchment. To develop this WQIS, however, it was necessary to combine a suite of water quality models with a user interface so that the results of the modelling could be visually interpreted. **DUFLOW** (refer to Section 2 of this report) was the model selected for simulating the river flow and quality within the system while **CE-QUAL-W2**, a two-dimensional hydrodynamic and water quality model, was used to simulate the flow pattern and constituent profiles in the proposed impoundment in the system. The application of the reservoir model, **CE-QUAL-W2**, is discussed in the ensuing chapters.

1.2 OVERVIEW OF CE-QUAL-W2 MODEL

As mentioned previously **CE-QUAL-W2** is a two-dimensional hydrodynamic and water quality model capable of simulating the flow patterns and constituent profiles within rivers, lakes, reservoirs and estuaries.

The model has been under development since 1975 and was originally known as **LARM** - Laterally Averaged Reservoir Model (Edinger and Buchak, 1975). Subsequent additions of water quality algorithms by the United States Army Corps of Engineers have resulted in the version known as **CE-QUAL-W2**. Several South African reservoirs have been modelled using **CE-QUAL-W2** and the results obtained provided insight into the biochemical processes, temperature changes, stratification and flow patterns which occur in these reservoirs (Bath *et al*, 1998 and Görgens *et al*, 1993).

Inputs to the model include the following:

- **Bathymetric data** - Data representing the lay-out and volumetric dimensions of the water body.
- **Initial Conditions** - Data representing the starting conditions within the reservoir in terms of temperature and constituent distribution.
- **Meteorological Data** - This data includes the site-specific values for air temperature, wind speed, wind direction, dew point temperature and cloud-cover.
- **Upstream Boundary Conditions** - This data includes the flow rates of the incoming streams as well as the time-varying concentrations of the constituents being modelled.
- **Flow Rates of Releases** - This includes the data describing the predicted (or measured) release pattern from the reservoir and is essential for volume balance calculations.

Output from the model can be specified in various forms depending on the type of information required and the post-processor available to the modeller. The standard output parameters are the time-varying water surface elevations, water velocities within a cell, constituent concentrations and temperature profiles.

Special features of the model are the abilities to simulate the chemical interactions of up to 21 constituents and to model dendritic-type reservoirs by using a branch algorithm.

An obvious limitation of any 2-dimensional model is the intensive data requirements. This is particularly true for the variables regarded as the driving forces (meteorological data, flow data and constituent concentration data).

1.3 LINKAGE TO RIVER MODEL

Growing demands from Theewaterskloof, Vöelvllei, Steenbras and Wemmershoek Dams threatened to exceed supply and it has been envisaged that the construction of a new dam would go some way towards solving this problem. The proposed Skuifraam Dam will be situated on the Berg River in the Western Cape Province, some 6.5 km south-west of Franchhoek. Water to be released from this dam is intended for irrigation as well as urban usage.

River modelling of the Berg River has been undertaken, using the hydrodynamic river flow model, DUFLOW (Section 2 of this Volume). In order to link the reservoir model to the river model, it was required that the water quality and quantity outputs from CE-QUAL-W2 have to be fed into DUFLOW as upstream boundary conditions. The water quality constituents of concern are phosphates, temperature, TDS and dissolved oxygen. Reservoir spills as well as the environmental flow releases are important flow inputs to DUFLOW.

CHAPTER TWO PREPARATION OF INPUT PARAMETERS FOR SKUIFRAAM DAM

2.1 GEOMETRIC DATA

The geometric description of the water body defines the finite difference matrix which allows the momentum and heat transfer equations to be solved numerically. The information required to perform this task was obtained from a 1:50 000 topographical map of the area and an area-capacity table obtained from the Department of Water Affairs (DWAF). The following procedure was followed:

- The full supply area of the proposed reservoir was digitised from a 1:50 000 topographical map.
- The reservoir was then divided into a number of longitudinal segments along the flow path. The user's manual suggest that the segment length should be between 500 m and 5000 m. As a first attempt, 17 segments were selected, with the segment length varying between 250 m and 500 m. These segment lengths proved to be too small and resulted in very long computer run-times. Eight active segments of lengths between 500 m and 1000 m were eventually selected (see Figure 2.1).

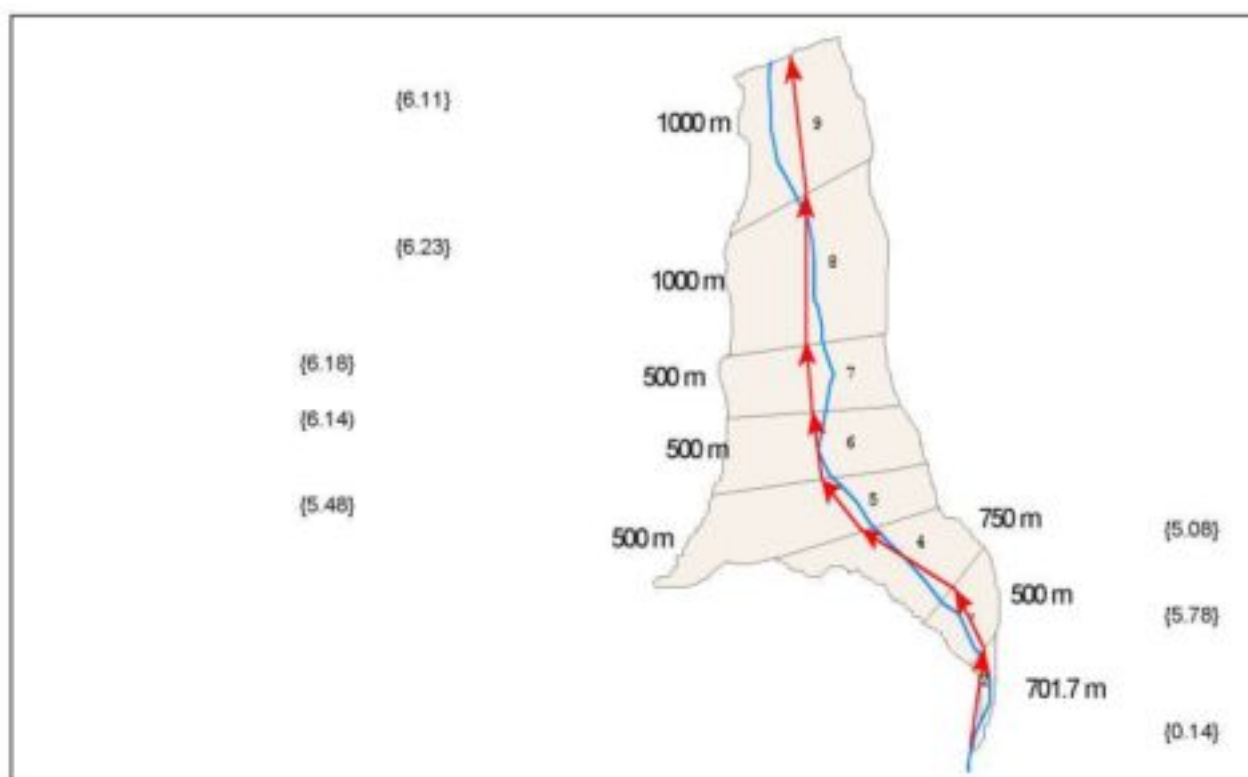


Figure 2.1 : Segments of proposed Skuifraam Dam
{ } = orientation in radians

- The reservoir was then divided into vertical layers extending from the top water level to the bottom of the reservoir. The user's manual suggests a layer height of between 2 m and 5 m. A uniform layer height of 2 m was selected for this application.

The "width" of each cell within the matrix was obtained by dividing the area for each segment at a specific contour value by the length of the segment.

- The widths of the cells for which there was no direct information was obtained by interpolating between the known contours.

- The orientation of each segment was obtained by measuring the direction of a line drawn from the centre of a segment to the centre of the following segment.

It should be kept in mind that the bathymetric data is only a mathematical representation of reality and should be tested to confirm its description of the reservoir. Figure 2.2 shows the agreement between the area-capacity table and the simulated values. The graph shows that the correspondence between the mathematical description and the measured reservoir volumes is favourable.

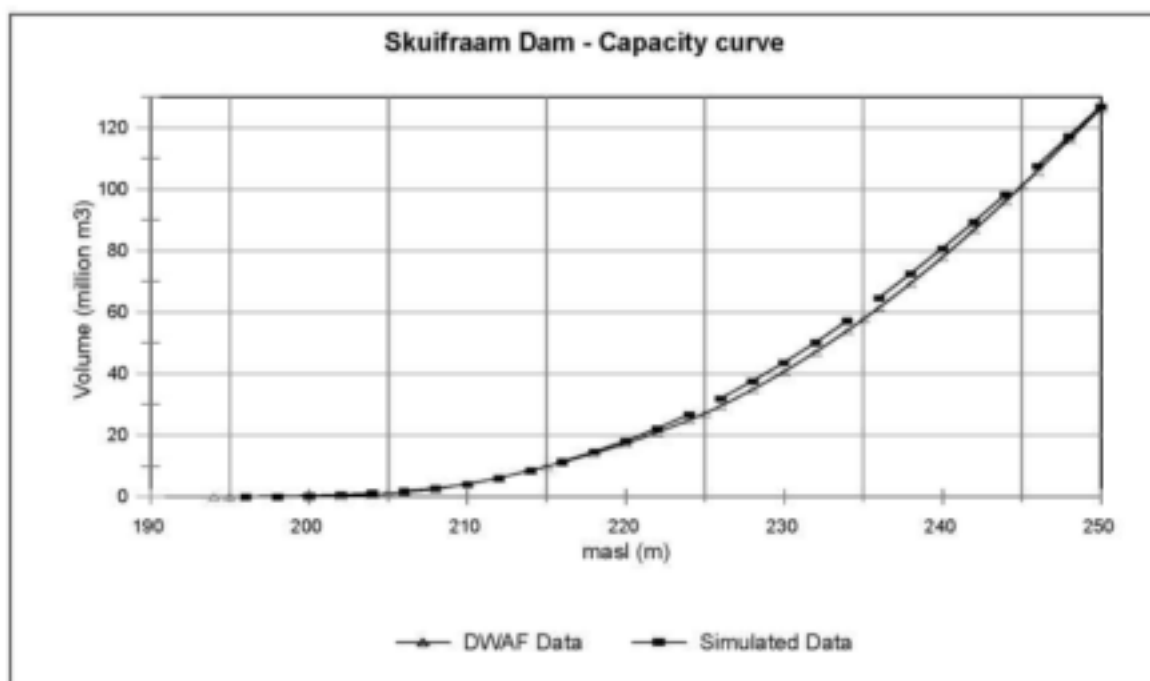


Figure 2.2 : Comparison between measured and simulated data for the proposed Skuifraam Dam

The information matrices from which Figure 2.2 was generated are shown in Tables 2.1 and 2.2. It should be mentioned that the grid developed from the method described above over estimated the measured data and had to be scaled down by some 12% to render the agreement depicted in Figure 2.2.

Table 2.1 : Lateral cell widths used to describe the bathymetry of the proposed Skuifraam Dam

| m.a.s.l | SEGMENT NUMBERS | | | | | | | | | | Layer number |
|---------|-----------------------|-----|-----|-----|------|------|------|------|-----|----|--------------|
| | 1 | 2 | 3 | 4 | 5 | 6 | 7 | 8 | 9 | 10 | |
| | CELL WIDTHS IN METRES | | | | | | | | | | |
| 252 | 0 | 0 | 0 | 0 | 0 | 0 | 0 | 0 | 0 | 0 | 1 |
| 250 | 0 | 108 | 490 | 690 | 1632 | 1327 | 1156 | 1146 | 843 | 0 | 2 |
| 248 | 0 | 77 | 468 | 664 | 1582 | 1314 | 1140 | 1133 | 824 | 0 | 3 |
| 246 | 0 | 45 | 447 | 638 | 1533 | 1302 | 1124 | 1120 | 806 | 0 | 4 |
| 244 | 0 | 24 | 396 | 610 | 1463 | 1282 | 1106 | 1104 | 786 | 0 | 5 |
| 242 | 0 | 12 | 313 | 578 | 1374 | 1254 | 1083 | 1085 | 764 | 0 | 6 |
| 240 | 0 | 0 | 231 | 547 | 1285 | 1227 | 1061 | 1066 | 742 | 0 | 7 |
| 238 | 0 | 0 | 139 | 488 | 1206 | 1202 | 1039 | 1046 | 722 | 0 | 8 |
| 236 | 0 | 0 | 47 | 430 | 1127 | 1178 | 1017 | 1026 | 701 | 0 | 9 |
| 234 | 0 | 0 | 0 | 344 | 1016 | 1147 | 987 | 1005 | 680 | 0 | 10 |
| 232 | 0 | 0 | 0 | 229 | 873 | 1111 | 948 | 982 | 659 | 0 | 11 |
| 230 | 0 | 0 | 0 | 114 | 729 | 1075 | 908 | 959 | 637 | 0 | 12 |
| 228 | 0 | 0 | 0 | 68 | 562 | 1008 | 853 | 926 | 618 | 0 | 13 |
| 226 | 0 | 0 | 0 | 23 | 395 | 942 | 797 | 893 | 598 | 0 | 14 |
| 224 | 0 | 0 | 0 | 0 | 250 | 786 | 715 | 858 | 579 | 0 | 15 |
| 222 | 0 | 0 | 0 | 0 | 127 | 539 | 607 | 820 | 561 | 0 | 16 |
| 220 | 0 | 0 | 0 | 0 | 3 | 293 | 498 | 781 | 542 | 0 | 17 |
| 218 | 0 | 0 | 0 | 0 | 2 | 195 | 440 | 745 | 523 | 0 | 18 |
| 216 | 0 | 0 | 0 | 0 | 1 | 96 | 381 | 708 | 503 | 0 | 19 |
| 214 | 0 | 0 | 0 | 0 | 0 | 38 | 282 | 624 | 478 | 0 | 20 |
| 212 | 0 | 0 | 0 | 0 | 0 | 19 | 141 | 492 | 447 | 0 | 21 |
| 210 | 0 | 0 | 0 | 0 | 0 | 0 | 0 | 219 | 416 | 0 | 22 |
| 208 | 0 | 0 | 0 | 0 | 0 | 0 | 0 | 77 | 370 | 0 | 23 |
| 206 | 0 | 0 | 0 | 0 | 0 | 0 | 0 | 5 | 325 | 0 | 24 |
| 204 | 0 | 0 | 0 | 0 | 0 | 0 | 0 | 2 | 261 | 0 | 25 |
| 202 | 0 | 0 | 0 | 0 | 0 | 0 | 0 | 0 | 181 | 0 | 26 |
| 200 | 0 | 0 | 0 | 0 | 0 | 0 | 0 | 0 | 100 | 0 | 27 |
| 198 | 0 | 0 | 0 | 0 | 0 | 0 | 0 | 0 | 67 | 0 | 28 |
| 196 | 0 | 0 | 0 | 0 | 0 | 0 | 0 | 0 | 33 | 0 | 29 |
| 194 | 0 | 0 | 0 | 0 | 0 | 0 | 0 | 0 | 0 | 0 | 30 |

The boundary cells are non-active and have zero lateral width and volume. The model, however, requires that these cells be specified in the bathymetry input file.

Table 2.2 : Cell volumes obtained from the bathymetry of the proposed Skuifraam Dam

| masl | SEGMENT NUMBERS | | | | | | | | Layer volume (m ³) | Total volume (m ³) |
|------|--------------------------------|--------|---------|---------|---------|---------|---------|---------|--------------------------------|--------------------------------|
| | 2 | 3 | 4 | 5 | 6 | 7 | 8 | 9 | | |
| | CELL VOLUMES IN m ³ | | | | | | | | | |
| 250 | 151896 | 489610 | 1034438 | 1632141 | 1326860 | 1155620 | 2291171 | 1685165 | 9766900 | 9766900 |
| 248 | 107713 | 468382 | 995821 | 1582432 | 1314421 | 1140044 | 2265683 | 1648557 | 9523052 | 19289953 |
| 246 | 63532 | 447149 | 957198 | 1532719 | 1301978 | 1124471 | 2240198 | 1611949 | 9279194 | 28569147 |
| 244 | 33153 | 395518 | 914298 | 1463345 | 1281910 | 1105588 | 2208423 | 1571838 | 8974074 | 37543220 |
| 242 | 16577 | 313488 | 867121 | 1374310 | 1254218 | 1083394 | 2170358 | 1528226 | 8607692 | 46150912 |
| 240 | 0 | 231454 | 819943 | 1285275 | 1226530 | 1061199 | 2132288 | 1484619 | 8241309 | 54392221 |
| 238 | 0 | 139124 | 732560 | 1206202 | 1202094 | 1039250 | 2092341 | 1443471 | 7855043 | 62247264 |
| 236 | 0 | 46791 | 645176 | 1127129 | 1177662 | 1017299 | 2052389 | 1402329 | 7468776 | 69716040 |
| 234 | 0 | 0 | 515294 | 1015925 | 1147293 | 986726 | 2009388 | 1360385 | 7035011 | 76751051 |
| 232 | 0 | 0 | 342912 | 872590 | 1110988 | 947531 | 1963340 | 1317638 | 6554999 | 83306051 |
| 230 | 0 | 0 | 170535 | 729258 | 1074679 | 908332 | 1917297 | 1274897 | 6074999 | 89381049 |
| 228 | 0 | 0 | 102318 | 562179 | 1008330 | 852812 | 1851960 | 1235531 | 5613130 | 94994179 |
| 226 | 0 | 0 | 34106 | 395102 | 941978 | 797287 | 1786629 | 1196170 | 5151273 | 100145452 |
| 224 | 0 | 0 | 0 | 249892 | 785590 | 715276 | 1715659 | 1158119 | 4624536 | 104769988 |
| 222 | 0 | 0 | 0 | 126548 | 539165 | 606779 | 1639049 | 1121377 | 4032919 | 108802906 |
| 220 | 0 | 0 | 0 | 3211 | 292745 | 498286 | 1562432 | 1084631 | 3441305 | 112244211 |
| 218 | 0 | 0 | 0 | 1922 | 194561 | 439769 | 1489180 | 1045352 | 3170784 | 115414995 |
| 216 | 0 | 0 | 0 | 641 | 96381 | 381256 | 1415919 | 1006069 | 2900266 | 118315262 |
| 214 | 0 | 0 | 0 | 0 | 37833 | 281600 | 1247762 | 955469 | 2522664 | 120837925 |
| 212 | 0 | 0 | 0 | 0 | 18916 | 140800 | 984707 | 893552 | 2037976 | 122875901 |
| 210 | 0 | 0 | 0 | 0 | 0 | 0 | 437617 | 831639 | 1269256 | 124145157 |
| 208 | 0 | 0 | 0 | 0 | 0 | 0 | 153581 | 740340 | 893922 | 125039078 |
| 206 | 0 | 0 | 0 | 0 | 0 | 0 | 9251 | 649046 | 658296 | 125697375 |
| 204 | 0 | 0 | 0 | 0 | 0 | 0 | 4625 | 522878 | 527504 | 126224878 |
| 202 | 0 | 0 | 0 | 0 | 0 | 0 | 0 | 361838 | 361838 | 126586717 |
| 200 | 0 | 0 | 0 | 0 | 0 | 0 | 0 | 200791 | 200791 | 126787508 |
| 198 | 0 | 0 | 0 | 0 | 0 | 0 | 0 | 133866 | 133866 | 126921373 |
| 196 | 0 | 0 | 0 | 0 | 0 | 0 | 0 | 66933 | 66933 | 126988306 |

Although only the active layers and segments are reflected in Table 2.2, the matrix structure is the same as reflected in Table 2.1. The 'layer volume' is the volume of a particular layer while the 'total volume' is the cumulative volume at that particular height measured from the uppermost layer.

2.2 INITIAL CONDITIONS

These conditions describe the constituent and temperature profile which exist within the reservoir at the start of the simulation period and can be specified either as a single value or a vertical profile or a longitudinal profile. Since Skuifraam Dam has not been built, these profiles cannot be measured. To obtain a reasonable estimate of the profile the model was run from 1 October 1993 to 1 November 1994 (with a single value as the starting condition) and the profile that existed on 1 October 1994 was then substituted to represent typical conditions at the start of the simulation period. The parameters modelled include temperature, total dissolved solids (TDS), phosphate and dissolved oxygen (DO) content. The starting condition for these parameters had been assumed as a vertical profile, implying that there were no longitudinal differences in water quality at the start of a simulation.

In addition, it was also required that an initial water level be specified. System analysis performed on other reservoirs in the Western Cape suggest that it is reasonable to assume that the dam could be between 90% and 100% full at the beginning of October (end of rainfall season).

The position of the inflows to the reservoir were also considered as starting conditions and for this application the flow from the Wolwekloof River (shown on Figure 2.1) had been combined with the flow from the Berg River to effectively create a single mainstem inflow. The feasibility study for the proposed Skuifraam Dam indicated the need to pump water into the reservoir from the Skuifraam supplement scheme (located downstream of the proposed Skuifraam Dam), while water from Theewaterskloof Dam entered Skuifraam Dam from the tunnel (DWAF, 2000). The Skuifraam supplement inflow was treated as a point source inflow and tentative positioning of this inflow was undertaken. The transfer from Theewaterskloof to Skuifraam Dam would only be done when there is insufficient volume of water in Skuifraam to meet the agricultural demand and is then made directly into the Berg River upstream of the inflow to Skuifraam Dam. The grid positions of these inflows and the outflows are reflected in Table 2.3 below. Releases from Skuifraam Dam include the base flow irrigation and environmental releases, transfers to Theewaterskloof Dam and spill from the dam. In this application the transfer was modelled as a lateral withdrawal at the dam wall. All other releases were modelled as flow through outlets.

Table 2.3 : Positions of major inflows and outflows on the Proposed Skuifraam Dam

| DESCRIPTION | SEGMENT | LAYER |
|--|---------|-------------------------------|
| Berg River Inflow | 2 | Top Water Layer |
| Skuifraam supplement | 9 | 23 |
| Theewaterskloof Inflow | - | Combined with mainstem inflow |
| IFR flood releases (only in the example application) | 9 | 6, 11, 16 or 23 |
| Base Environmental and Agricultural Releases | 9 | 23 |

2.2.1 Meteorological Data

This data includes the daily varying values for air temperature, dew point temperature, cloud cover, wind speed and wind direction. Each variable is discussed below.

Air temperature

This is defined as the site specific dry bulb air temperature. No weather station is situated at the site for the proposed Skuifraam Dam and the air temperatures had to be obtained from weather stations located in nearby towns. The closest weather stations recording temperature are situated at Jonkershoek and Villiersdorp. The information for these stations was obtained from the South African Weather Bureau (SAWB) and extends from 1 August 1993 to 31 December 1999. No infilling of temperature data was performed, but gaps in the Jonkershoek data set was replaced with values from the Villiersdorp data set and vice versa. This method was justified because the weather stations are relatively close to one another.

Figure 2.3 shows the relationship between the temperatures measured at the different locations.

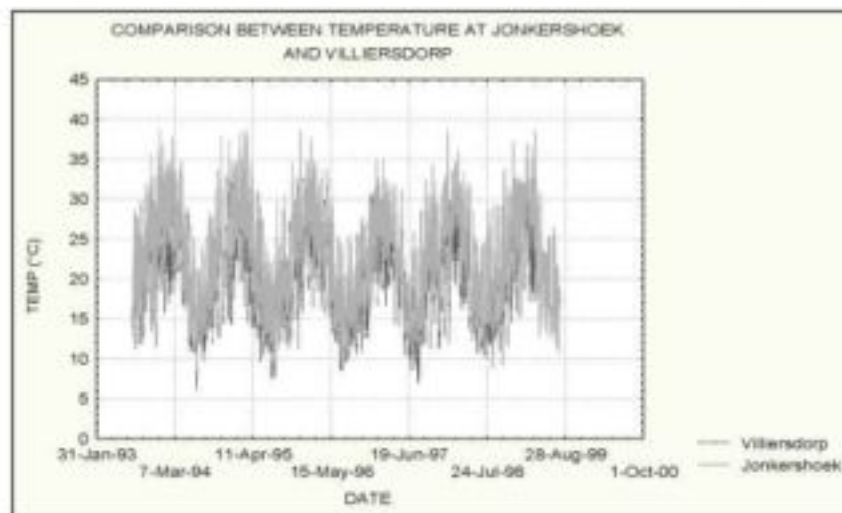


Figure 2.3 : Comparison of temperatures at Jonkershoek and Villiersdorp

The Jonkershoek and Villiersdorp stations are located at 244m and 312m above sea level, respectively.

Dew Point Temperature

This is temperature at which the first drop of dew is formed and the data was obtained from the SAWB. The closest station to the reservoir site is located at Cape Town International Airport.

Cloud Cover

The data for cloud cover was also measured at Cape Town International Airport and the data was obtained from the SAWB.

Wind Speed and Wind Direction

The site for the proposed Skuifraam Dam is very sheltered and it is assumed that calm conditions would exist for most of the time. Wind speed data was obtained for the Paarl and Villiersdorp area. Figure 2.4 shows the comparison between the two sites. It is clearly visible that the wind speed at Villiersdorp is much higher than the values at Paarl and because the wind has a big effect on the mixing properties it is essential that the appropriate data set be chosen. The Paarl station is located at 104 masl (metres above sea level) while the Villiersdorp station is located at 312 masl. The wind data at Paarl is measured at much lower height than the water level of the proposed reservoir while at Jonkershoek it is measured at much higher elevation. In the model, however, the effect of the wind is applied at the water surface where as wind speed is measured at 3m above the ground. Adjusting the Wind Sheltering Coefficient (WSC) allows for this effect to be decreased appropriately.

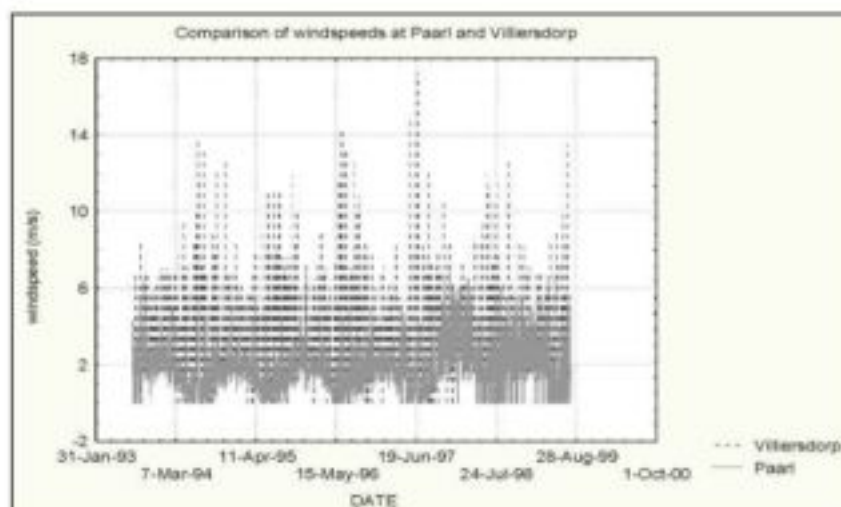


Figure 2.4 : Comparison of wind speed at Villiersdorp and Paarl

2.2.2 Upstream Boundary Conditions

This data include the flow rates and temperatures of the incoming streams, as well as the time varying concentrations of the constituents. Data for the inflow was readily available on a daily basis, but constituent data was only available on a two-weekly basis and a substantial amount of infilling was required to produce a daily time series. The flow rates of the inflows from the Skuifraam supplement (SS) and from Theewaterskloof Dam (TWD) were obtained from the Skuifraam System Analysis report (DWAF, 2000) and are reflected in Table 2.4.

Table 2.4 : Flow rates of other inflows into the proposed Skuifraam Dam

| Month | Oct | Nov | Dec | Jan | Feb | Mar | Apr | May | Jun | Jul | Aug | Sep |
|-------|------|-------|-----|-------|-------|-------|-------|------|-------|-------|-------|-------|
| SS | 0.91 | 0 | 0 | 0 | 0 | 0 | 0 | 1.39 | 1.98 | 2.15 | 1.93 | 1.42 |
| TWD | 0 | 0.013 | 0 | 0.035 | 0.112 | 0.112 | 0.121 | 0 | 0.059 | 0.254 | 0.091 | 0.139 |

Flow rates in m³/s

The gaps which existed in the daily flow data for the simulation period was infilled by using a very simple approach. The periods with missing data were as follows:

- 27 July 1995 to 31 July 1995
- 1 August 1995 to 17 August 1995
- 16 May 1996 to 30 May 1996

In the infilling procedure, use was made of the flow record which exists at the downstream flow gauging station G1H020Q01. It was assumed that some relationship existed between flow measured at the upstream and downstream gauging stations and that particular relationships existed between the **low flows** (below 10 m³/sec) and the **high flows** (above 10 m³/sec). Linear regressions revealed that the following approximate relationships existed.

- **For low flows :** Flow (G1H004) = 0.101 x Flow (G1H020) + 2.355
- **For high flows:** Flow (G1H004) = 0.312 x Flow (G1H020) + 1.065

Gaps in the data set at G1H004Q01 were then filled by using the relationships displayed above.

As previously mentioned, the constituent data required substantial infilling. Figures 2.5 and 2.6 below show the agreement between the measured and infilled TDS and phosphate concentrations.

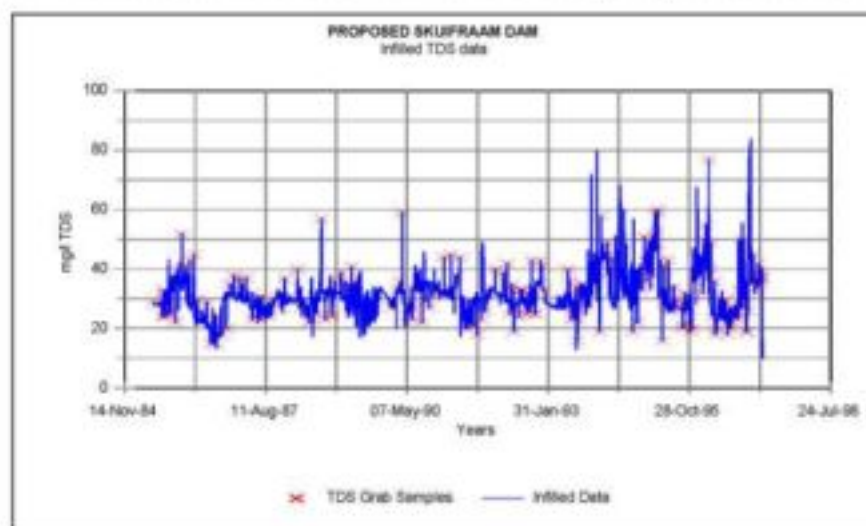


Figure 2.5 : Simulated and measured TDS data for the Berg River flowing into the proposed Skuifraam Dam

Figure 2.5 shows relatively large fluctuations in the TDS values. The fact that the simulated data roughly follows the measured data indicates that there is a relationship between the river discharge and the TDS concentration. The method used to infill the upstream constituent data was described in the Amatole Water Resources System Analysis study report (DWAF, 1998) and will not be discussed in this report.

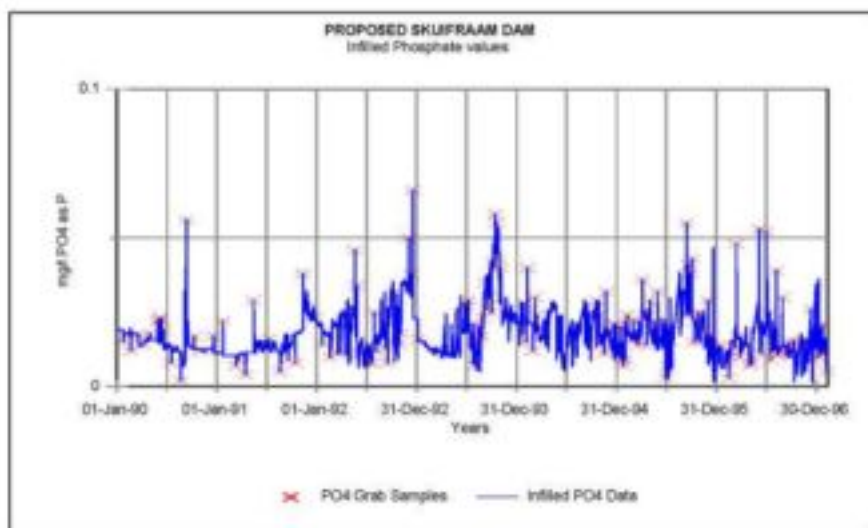


Figure 2.6 : Simulated and measured phosphate data for the Berg River flowing into the proposed Skuifraam Dam

The temperature for the inflowing Berg River (at G1H004Q01) was measured every 7 to 14 days and the data was infilled by using the following relationship :

$$y_t = A * (\cos \omega t + B)$$

where

- y_t = Temperature (°C) value of function at time (t)
- ω = $360^\circ / \text{number of samples per year}$
- A, B = Constants

At gauging station G1H004Q01 the relationship is : $y_t = 6.2 * (\cos (t) - +31450) + 16.5$

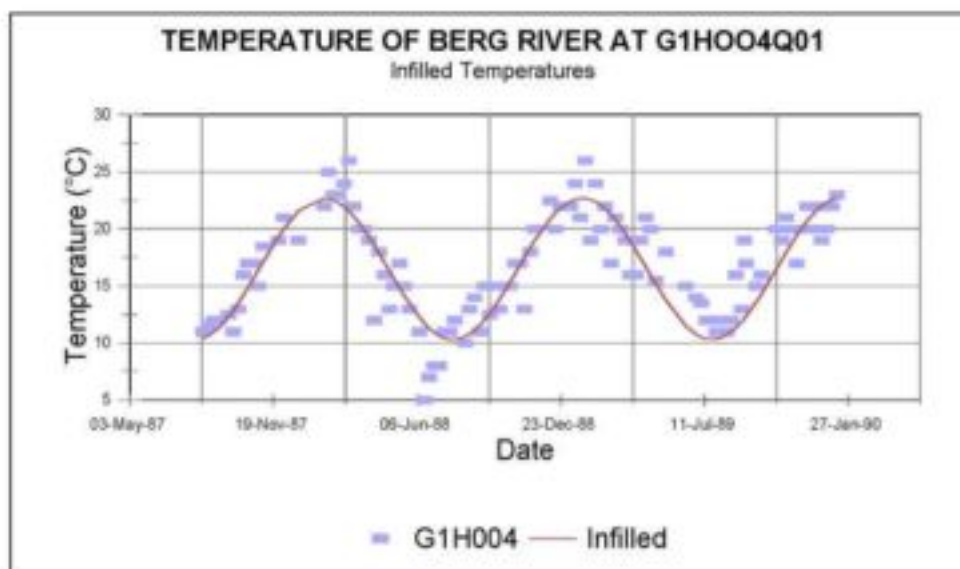


Figure 2.7 : Measured and infilled data for the Berg River at gauging station G1H004Q01

2.2.3 Flow Rates and Patterns of Releases

Since Skuifraam Dam has not been built yet, no measured data is available for the withdrawal and release flow rates. These rates were, however, estimated in a study focussing on the sustainable yield obtainable from the Dam (DWAF, 2000). It should be noted that the simulation in this yield exercise only extended up to the year 1988 and did not overlap with the meteorological data set (1 October 1993 - 31 March 1997) used in this study. In this application the values for 1988 have been assumed to apply for the subsequent years.

Table 2.5 : Flow rates of releases and withdrawals from the proposed Skuifraam Dam

| MONTH | ENVIRONMENTAL + IRRIGATION RELEASES (m ³ /sec) | VOLUME PUMPED FROM SKUIFRAAM TO THEEWATERSKLOOF |
|-----------|---|---|
| October | 0.78 | 2.00 |
| November | 3.53 | 2.00 |
| December | 4.46 | 1.11 |
| January | 4.73 | 2.00 |
| February | 3.48 | 2.02 |
| March | 2.70 | 2.00 |
| April | 3.76 | 2.00 |
| May | 1.01 | 1.70 |
| June | 3.32 | 0 |
| July | 5.26 | 0 |
| August | 1.61 | 0 |
| September | 1.20 | 0 |

To determine the spill flow rate from the dam, the daily reservoir volume balance model, **DAYRESIM** (Ninham Shand in-house software), was implemented with the inputs and demands as specified in Table 2.5 above. The same flow data implemented in **CE-QUAL-W2** was used in the volume balance reservoir model and the results are depicted in Figure 2.8 below.

The inflow rates of the Theewaterskloof transfer as well as the Skuifraam Supplement Scheme were considered in the water balance, even though they were small in comparison to the Berg River inflow. With time, however, the volume contribution of these minor inflows could become more significant.

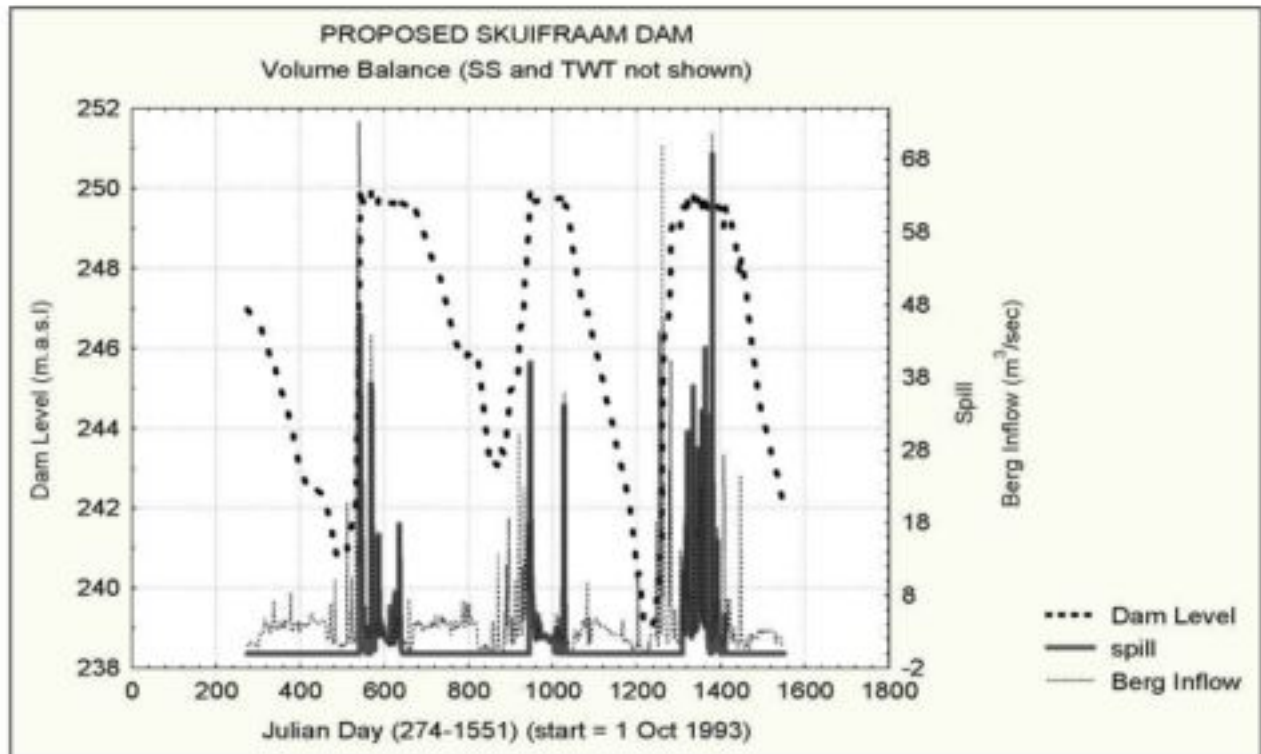


Figure 2.8 : Volume balance for the proposed Skuifraam Dam

It is vitally important to assess the validity of the water balance before the inflow and outflow files are used as inputs to **CE-QUAL-W2**, because the model does not account for any spill unless it is explicitly specified¹. Failure to do this would result in artificial build-up of water above the full supply height with the subsequent misrepresentation of water quality, temperature and flow patterns within the reservoir.

CHAPTER THREE SIMULATION RESULTS

3.1 SELECTION OF METEOROLOGICAL DATA SET

Both meteorological data sets were tested before applying the model to evaluate scenarios. The model simulations were first performed with the temperatures measured at Jonkershoek and the wind speed measured at Paarl and then with temperatures measured at Villiersdorp and wind at Villiersdorp. The site for the proposed Dam is relatively sheltered and it is reasonable to assume that the full wind effect of Villiersdorp and Paarl will not be experienced at the Dam. With this in mind it should be noted that the wind effect at Jonkershoek and Villiersdorp have been multiplied by factors 0.8 and 0.5 respectively to reduce the mixing effect of wind on the Dam to a realistic level.

A comparison of the time-depth plots and profile plots for winter and summer suggested that both temperature data sets give rise to almost similar profiles and that meteorological data obtained from Jonkershoek and Paarl is the more conservative data set. It was thus decided to use this data set in all subsequent model runs.

3.2 INTERPRETATION OF SIMULATION RESULTS

The following coefficients in **Table 3.1** were used in modelling the hydrodynamics and the temperature of the system.

Table 3.1 : Calibration coefficients for hydrodynamics and temperature

| COEFFICIENT | UNIT | VALUE USED IN SIMULATION |
|---|--|--------------------------|
| Horizontal Eddy Viscosity | m ² /sec | 1.0 |
| Horizontal Eddy Diffusivity | m ² /sec | 1.0 |
| Chezy friction coefficient | m ^{0.5} /sec | 70.0 |
| Wind Sheltering coefficient | dimensionless | 0.8 |
| Fraction of solar radiation absorbed in surface layer | dimensionless | 0.7 |
| Extinction coefficient for pure water | m ⁻¹ | 0.45 |
| Extinction coefficient for inorganic solids | m ³ m ⁻¹ g ⁻¹ | 0.05 |
| Extinction coefficient for organic solids | m ³ m ⁻¹ g ⁻¹ | 0.2 |

The Horizontal Eddy viscosity, Chezy friction coefficient and wind sheltering coefficient affect the hydrodynamics and heat transport of the system, while the other coefficients have a direct influence on the water temperature. It should be noted that the heat transport and hydrodynamics are not mutually exclusive and that the flow characteristics within the dam can influence the heat transfer process.

If measured in-lake data were available for Skuifraam Dam then the simulated temperatures would have been calibrated by adjusting the coefficients above.

The water quality variables that were modelled include Phosphate, Oxygen and Total Dissolved Solids (TDS).

The **TDS** in the system was modelled as a **conservative substance**, which implies that the constituent is not affected by chemical reactions.

Phosphorus was treated as a non-conservative substance and can be accumulated or consumed/assimilated by several pathways. Phosphorus can be added to the system via the following pathways:

- Decay of dissolved organic matter (DOM) and detritus
- Algal dark respiration
- Desorption from settled sediments (only under anaerobic conditions)

and can be removed via the following:

- Algal photosynthesis
- Adsorption onto sediment particles

With this in mind it can be seen that phosphorus can only be added to the system by desorption from settled material, because no organic matter, detritus, algae or suspended sediment is included in the modelling. This effectively means that the respective concentrations of these constituents are zero and therefore their contribution to the overall rate is zero.

Dissolved oxygen was also not treated as a conservative substance and can be removed from the system via the following mechanisms:

- Transfer to atmosphere
- Algal respiration
- Nitrification
- Decay of material

It can be added to the system via the following mechanisms:

- Transfer from atmosphere
- Algal photosynthesis

From the description of the above processes it can be seen that a change in oxygen concentration can only be effected by mass transport between the atmosphere and the water interface and by the oxygen consumed during the decay of organic material on the sediment.

It should be noted that the omission of components such as algae, detritus and dissolved organic matter (DOM) may not be entirely correct, because these constituents may be present in the real situation.

CHAPTER FOUR SCENARIO CASE STUDIES

4.1 SCENARIO CASE STUDIES

The simulation period extends from 1 October 1993 to 31 March 1997 and the configuration of the reservoir system is as follows:

Two major inflows, viz. main Berg River inflow and the Skuifraam Supplement Scheme inflow.

Meteorological Data : Temperature at Jonkershoek and wind at Paarl (wind * 0.8).

Two outlets, viz. irrigation/environmental base releases and spills.

Sediment oxygen demand (SOD) = 0.2 g/m²/day (Bath *et. al.*, 1997).

Temperature and hydrodynamic coefficients as mentioned in Table 3.1.

The scenarios which were evaluated relative to the control case are listed below:

Scenario 1 - SOD = 0.5 g/m²/day - To introduce an upper limit for the SOD value.

Scenario 2 - SOD = 0.5 g/m²/day and Skuifraam Supplement transfers entering at layer 25 (near the bottom of the dam)

4.2 PRESENTATION OF RESULTS

The variables which are changed in the scenarios above have a direct impact on the dissolved oxygen distribution in the Dam. Figures 4.1 to 4.3 (the colour version of these figures are more informative and appear on the enclosed CD) depict the time-depth plots for oxygen at the dam wall in the three scenarios at segment 9, adjacent to the dam wall.

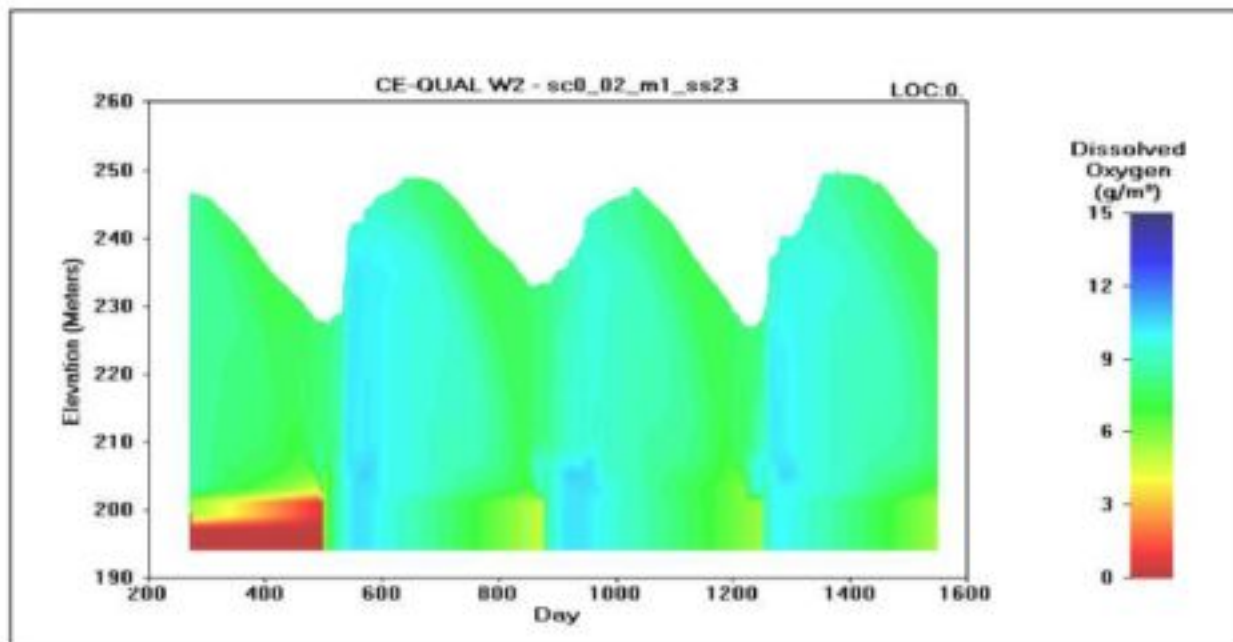


Figure 4.1 : Dissolved oxygen profile for Segment 9 in the control scenario (SOD = 0.2 g/m²/day)

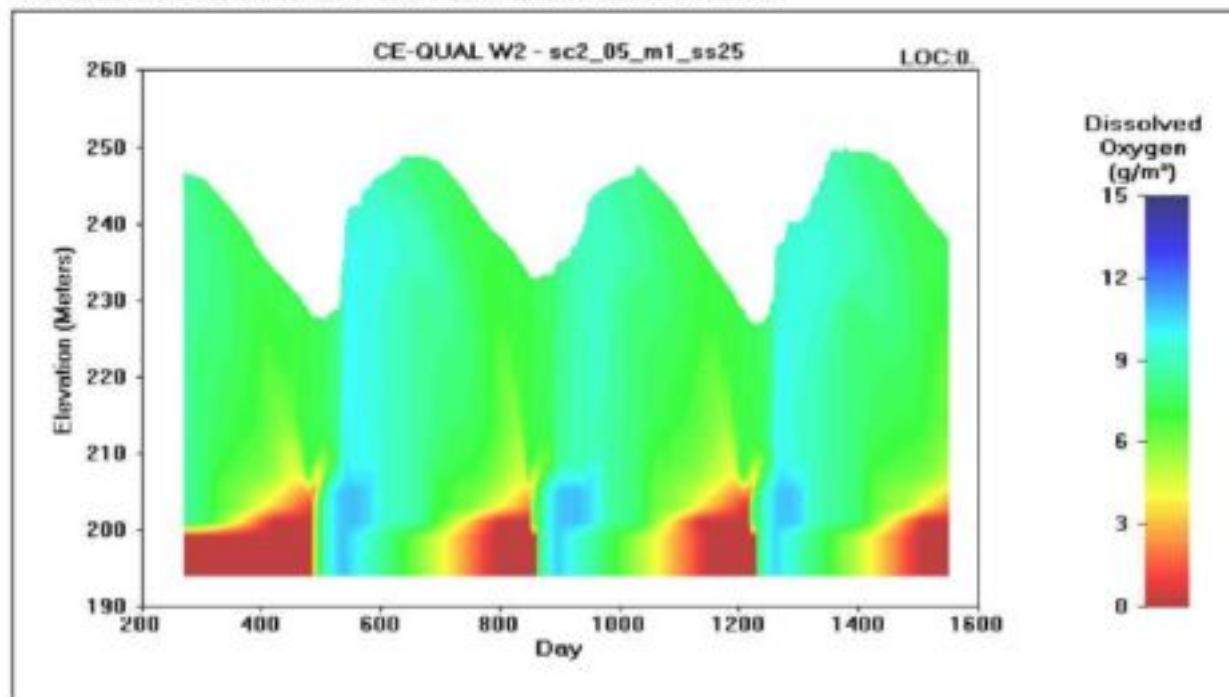


Figure 4.2 : Dissolved oxygen profile for Segment 9 in Scenario 1 (SOD = 0.5 g/m²/day)

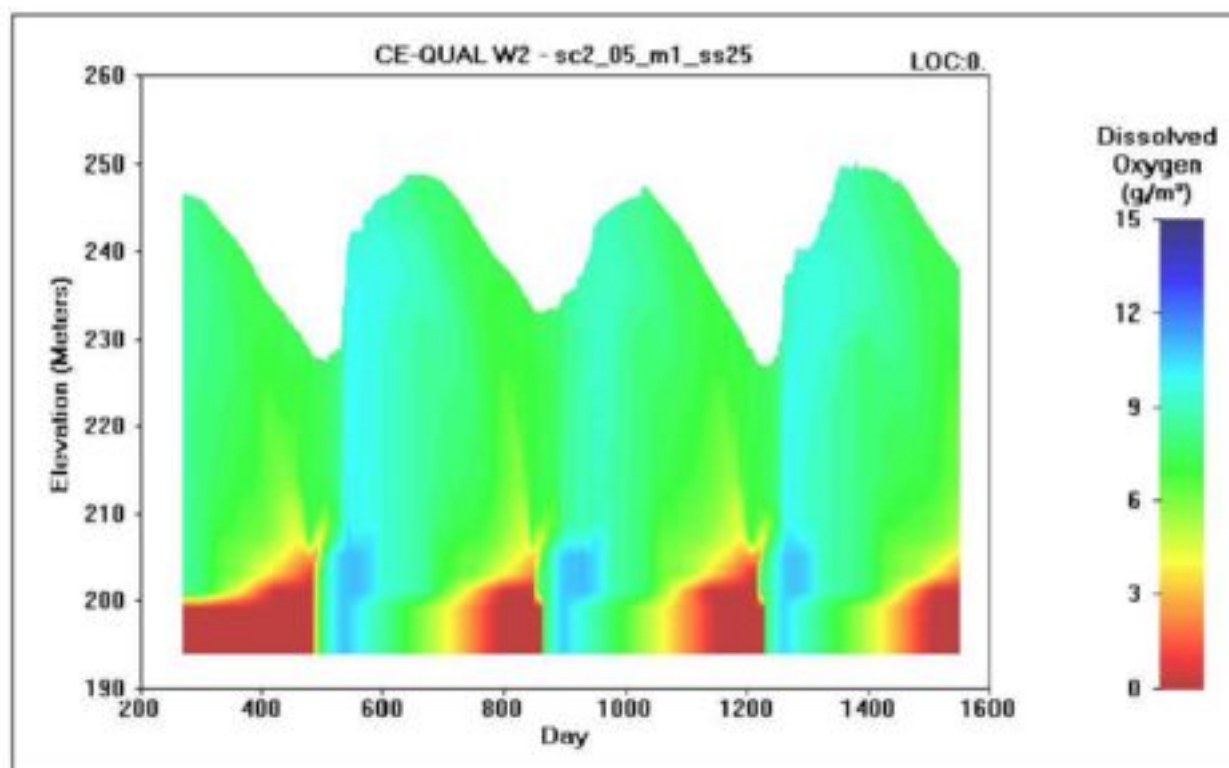


Figure 4.3 : Dissolved oxygen profile for Segment 9 in Scenario 1 (SOD = 0.5 g/m²/day; Skuifraam Supplement entering at layer 25)

The results depicted above suggested that the model is relatively sensitive to the SOD value. With the change in SOD value from 0.2 to 0.5 g/m²/day, the de-oxygenated layer appeared during each of the years being modelled. In addition, it can also be seen that the de-oxygenated layer protruded higher into the dam and thus closer to the outlet level (at 206 masl) of the base agricultural and environmental releases. In both the control scenario and Scenario 1 the reservoir was completely mixed in winter, but in the control, the natural mixing which occurs after winter, was sufficient to prevent the lower portion of the reservoir from becoming completely de-oxygenated. In Scenario 1, however, the SOD rate was greater than the rate of oxygen transfer to the lower portion of the reservoir and this section subsequently became de-oxygenated. The introduction of the Skuifraam Supplement inflows at layer 25 (refer Figure 4.3) did not prevent the formation of the de-oxygenated layer. Introducing the Supplement inflows at an even lower level, however, may reduce the possibility of the formation of a de-oxygenated layer.

CHAPTER FIVE CE-QUAL-W2 : APPLICATION

5.1 APPLICATION OF CE-QUAL-W2 : THE OPERATING LEVELS OF SKUIFRAAM DAM AND THE POTENTIAL USE OF A HIGH LEVEL SLUICE GATE FOR THE ENVIRONMENTAL FLOOD RELEASE

The 'flood' IFR releases from the proposed Skuifraam Dam can either be made through large sleeve valves situated near the base of the dam or through sluice gates located higher up the wall. Table 5.1 summarizes the proposed 'flood' (or high) flow and 'base' (or low) flow IFR releases for Skuifraam Dam. This brief study investigates how often the water level in the dam will be high enough to make releases from gates situated 10, 20 and 30 metres below the dam's Full Supply Level (FSL). The report also compares the water quality of the base release from RL206 (44 m below the FSL) (DWAf, 2000) with the water quality of releases from the gates (higher up the wall).

Table 5.1 : In-Stream Flow Requirements Release Pattern (Skuifraam Dam) (DWAf, 2000)

| MONTH | AVERAGE YEAR | | | | | DROUGHT YEAR | | | | |
|-----------|-------------------|---------------------------------------|------------------------|----------------------------------|------|-------------------|---------------------------------------|-------------------|----------------------------------|------|
| | LOW FLOW | | HIGH FLOW ¹ | | | LOW FLOW | | HIGH FLOW | | |
| | m ³ /s | m ³ x 10 ⁶ | m ³ /s | m ³ x 10 ⁶ | Days | m ³ /s | m ³ x 10 ⁶ | m ³ /s | m ³ x 10 ⁶ | Days |
| October | 0,8 | 2,14 | | | | 0,5 | 1,34 | 0,8 | 0,07 | 1 |
| November | 0,5 | 1,30 | 4,5 | 0,5 | 1 | 0,3 | 0,78 | | | |
| December | 0,4 | 1,07 | 4,5 | 0,5 | 1 | 0,16 | 0,43 | | | |
| January | 0,3 | 0,80 | | | | 0,16 | 0,43 | 0,3 | 0,03 | 1 |
| February | 0,3 | 0,73 | | | | 0,16 | 0,39 | | | |
| March | 0,3 | 0,80 | | | | 0,16 | 0,43 | | | |
| April | 0,5 | 1,30 | 5,0 | 0,8 | 5 | 0,30 | 0,78 | | | |
| May | 1,0 | 2,68 | | | | 0,50 | 1,34 | | | |
| June | 1,6 | 4,15 | 30,0 | 4,5 | 7 | 0,80 | 2,07 | 15 | 3,0 | 7 |
| July | 1,6 | 4,29 | 65,0 | 9,8 | 7 | 0,80 | 2,14 | | | |
| August | 1,6 | 4,29 | | | | 1,0 | 2,68 | | | |
| September | 1,2 | 3,11 | | | | 1,0 | 2,59 | | | |
| TOTAL | | 26,66 | | 16,1 | | | 15,40 | | 3,10 | |
| | | 42,8 m ³ x 10 ⁶ | | | | | 18,5 m ³ x 10 ⁶ | | | |

Note 1. The flow rate for high flow releases is given as the maximum

5.2 RE-ASSESS PREVIOUS WORK ON FUTURE OPERATING RULES

An operating rule defines the best way to manage a system to achieve a given objective. The operating rule described in an earlier document titled 'Operating Rules for the Proposed Skuifraam Schemes' (see Appendix 2.3) was felt to be adequate for this analysis. Briefly, this operating rule maximizes the yield from the system by equalizing the ratio of available storage to likely inflow in the Skuifraam and Theewaterskloof Dams.

5.3 RE-RUN THE YIELD MODEL WITH REALISTIC MAXIMUM DEMANDS PLACED ON THE SKUIFRAAM / THEEWATERSKLOOF SYSTEM

For this analysis the system was operated at its historical firm yield - which means that there is almost one failure in the 61 year long inflow record. The operating rule is affected by the magnitude of the agricultural releases from Skuifraam Dam and a scenario with present day (summer 1999) demands of 59 million m³/a was compared with a scenario in which the demands had grown by a further 23 million m³/a. Theoretically, the future releases from Skuifraam Dam could be 47 million m³/a more than the 1999 demands.

5.4 CONTINUOUS PLOTS AND BOX PLOTS OF MONTHLY WATER LEVELS

Figure 5.1 shows the storage in the Theewaterskloof and Skuifraam Dams if they supply their Historical Firm Yield and the dams are almost drawn down to their dead storage levels in 1939 and 1973. Figure 5.2 is a box plot of the storage level of Skuifraam Dam for the present (1999) and future (2008) agricultural demand scenarios. Table 5.1 shows that the major IFR flood releases are planned in June and July with a smaller release in April. Table 5.2 indicates how often the desired IFR release could be made from each of the outlet levels being considered for the IFR flood releases for the present agricultural demand scenario.

Table 5.2 : Frequency of IFR flood releases being made from different levels

| Reduced Level of Outlet Level | % Frequency of Dam Storage Level Exceeding Outlet Level | | | | | | | |
|-------------------------------|---|-----|-----|-----|-----|-----|-----|-----|
| | masl | Apr | May | Jun | Jul | Aug | Sep | Oct |
| 240 | 5 | 25 | 44 | 54 | 69 | 80 | 80 | 80 |
| 230 | 62 | 70 | 79 | 84 | 92 | 93 | 95 | 95 |
| 220 | 82 | 89 | 95 | 97 | 100 | 100 | 100 | 100 |
| 210 | 90 | 95 | 98 | 100 | 100 | 100 | 100 | 100 |

The preparation and configuration of CE-QUAL-W2 has been discussed in Chapter 2 of this report and will not be discussed in this chapter. Using the observed inflow from 1993 to 1997, two scenarios were developed:

- **Stratified¹ Scenario** - Demands are kept low and mixing is not promoted (dam levels remain high)
- **Mixed Scenario** - Demands are kept high and mixing is promoted (dam levels are drawn down)

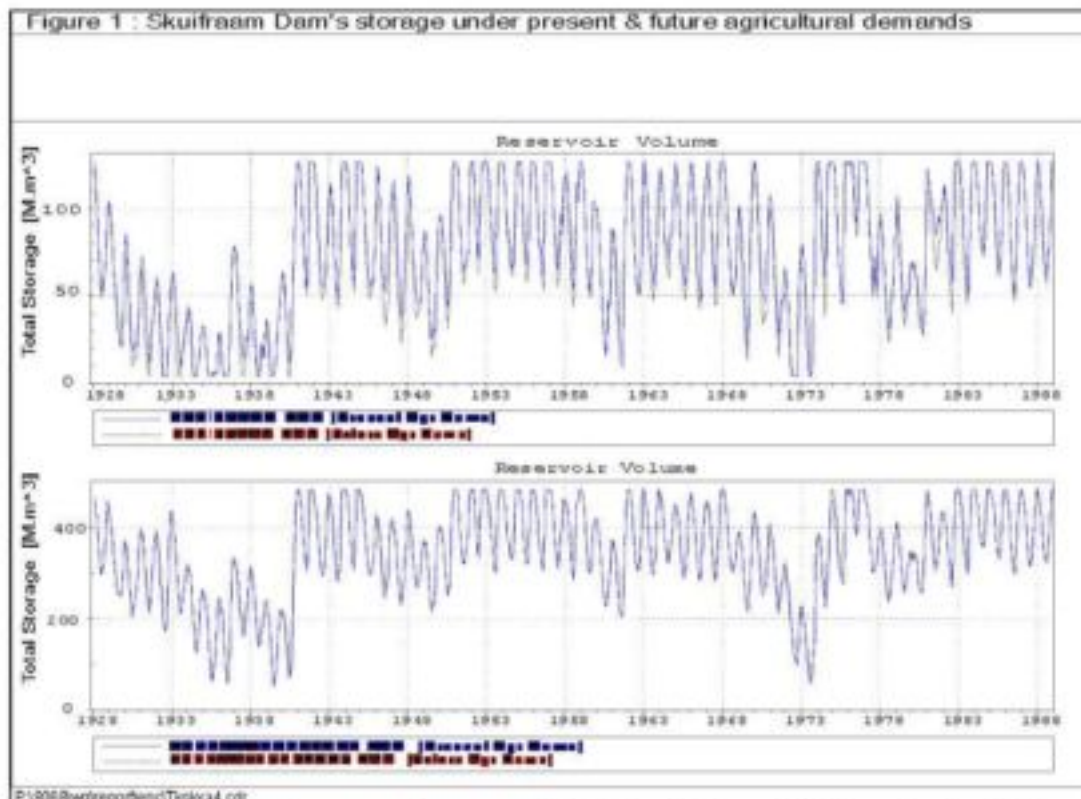


Figure 5.1 : Skuifraam Dam's storage under present (1999) and future (2008) agricultural demands

¹ Stratified refers to the reservoir not being well-mixed. Definite layers (strata) with distinctive water quality and temperature characteristics are normally evident under these conditions.

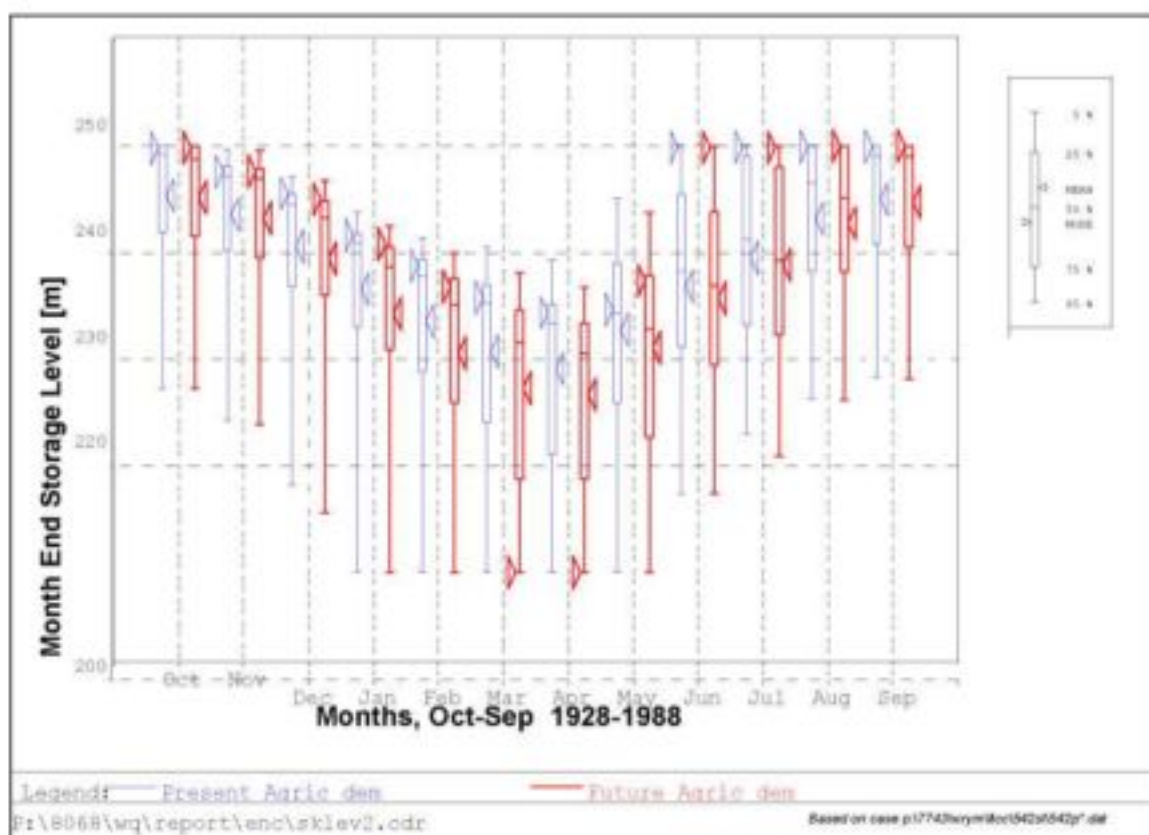


Figure 5.2 : Skuifraam Dam - storage under present and future agricultural demands

The flow in the above-mentioned scenarios were based on the 'present day' scenario. The agricultural release in the 'stratified scenario' assumed that the agricultural release would be curtailed to half the present day consumption, as would occur during a drought. Similarly the IFR release in the stratified scenario was reduced from the damage control ($42 \text{ m}^3 \cdot 10^6/\text{a}$) to the drought ($18.5 \text{ m}^3 \cdot 10^6/\text{a}$). The annual transfer from the Supplement to Skuifraam Dam in the stratified scenario was the third lowest annual transfer modelled for the 'present day' scenario in the yield analysis which was performed as part of this study. The smaller transfers during 1975 and 1976 occurred during wet years when transfers were reduced to avoid spillage over the Skuifraam and Theewaterskloof Dams. Conversely, the transfers in the 'mixed scenario' were similar to the high transfers modelled in 1947-49. The flows transferred from Skuifraam Dam to Theewaterskloof Dam in the stratified scenario ($6.3 \text{ m}^3 \cdot 10^6/\text{a}$) and the mixed scenario ($63 \text{ m}^3 \cdot 10^6/\text{a}$) are similar to the minimum and maximum transfers in the present day scenario.

Table 5.3 below summarizes the differences between the two scenarios.

Table 5.3 : Comparison of the Scenarios promoting stratification and mixing

| Parameter | Stratified Scenario | Mixed Scenario |
|---|----------------------|----------------------------|
| Volume transferred from the Supplement (million m^3/a) | 9.4 | 40 |
| Reduced Level at which Supplement water introduced to Skuifraam Dam (m) | 240 - 50 | 206 - 8 |
| Magnitude of agricultural releases (million m^3/a) | 25.3 | 51.5 |
| Reduced Level of IFR Flood Release (m) | 206/220/230/240 | 220 |
| Magnitude of IFR Release (million m^3/a) | 18.5 | 42 |
| Volume transferred to Theewaterskloof (million m^3/a) | 6.3 | 63 |
| Wind | Paarl*0.8 | Villiersdorp*0.8 (windier) |
| Air Temperature | Jonkershoek (warmer) | Villiersdorp |

Refer to Figures F_s and F_m in Appendix 2.2 for the timing and magnitude of the IFR flood releases and the magnitude of the combined baseflow releases for agriculture and the IFR.

The following additional assumptions, necessary to configure the model, could affect the results significantly. The ground temperature at the bottom of the dam was assumed to be 13.5° C and the sediment oxygen demand was assumed to be 0.2g/m²/day, a value used for a number of other dams analysed in South Africa (Bath, 1998).

An analysis of the simulation results for the two scenarios indicated the following:

5.4.1 Dissolved Oxygen

- *Flood Releases* : In both the stratified and mixed scenarios the dissolved oxygen in the IFR flood releases made from RL220 did not drop below 7mg/l.
- *Base Flow* : In the stratified scenario the dissolved oxygen level might drop below 7mg/l (Appendix 2.2:C_s) to less than 50% of the saturated level. The time – depth plot (Appendix 2.1:B_s) shows that an anoxic zone develops just below the base release outlet level. In reality this zone may be higher and measures should be implemented to break down this zone and to avoid releasing this anoxic water. However, it is unlikely that the low oxygen in the outflow would affect the downstream river. The outflow valve is designed to spray the water and this should result in good re-oxygenation and acceptable dissolved oxygen levels in the downstream river reach.

5.4.2 Temperature

The average temperatures for the summer (November-April) and winter (May – October) seasons in the two scenarios are summarized in Table 5.4.

Table 5.4 : Comparing the seasonal temperature of the inflow with the temperatures of the releases at different levels.

| Scenario | Season | Temperatures at Different Positions | | | | |
|------------|--------|-------------------------------------|----------------------------|----------------------------|----------------------------|-------------------------|
| | | Inflow | RL240: 10m below FSL | RL230: 20m below FSL | RL220: 30m below FSL | RL206: Base releases |
| Stratified | Summer | 20.6 | 22.8 | 15.7 | 14.6 | 14.2 |
| | Winter | 13.1 | 17.8 | 16.8 | 14.8 | 14.0 |
| Mixed | Summer | 20.6 | | | 19.2 | 17.5 |
| | Winter | 13.1 | | | 15.9 | 14.1 |

- *Flood Releases* : In the 'stratified scenario' the average temperatures 10 metres below the full supply level are up to 5 degrees warmer than the incoming streamflow. Releases from lower down – say 30 meters below the full supply level, are about 2 degrees warmer than the inflow. In the mixed scenario the releases from lower down are about 3 degrees warmer than the inflow. However, in late winter the temperature increase in the dam lags behind that of the inflow so that the release temperatures are colder than the inflow temperatures (see Appendix 2.2 : D_s & D_m)
- *Base Flow* : In summer the baseflow releases of the 'stratified scenario' are about 6 degrees colder than the incoming streamflow while in the 'mixed scenario' the baseflow releases are about 3 degrees colder than the incoming streamflow. However, releases from higher up can be at the same temperature or even warmer than the inflow during summer. In winter the average temperature of the baseflow releases is within a degree of the incoming streamflow, though at times the temperature of the baseflow can exceed the incoming stream temperature by 4 degrees (see Appendix 2.2 : D_s & D_m).

5.4.3 Bottom Inflow from Supplement

In the mixed scenario the water from the Supplement diversion was pumped in near the bottom of the Skuifraam Dam (RL206) introducing oxygenated water and promoting mixing at that level. This strategy did not appear to work during October (Julien days 273 to 303) because the water was transferred immediately to Theewaterskloof Dam (short-circuit) by pumps acting at RL 213 before it had an opportunity to mix (Appendix 2.1 : B_m). In this case the inflow from the Supplement should be introduced as low and as far from the inlet of the pumps transferring water to Theewaterskloof Dam as possible, to encourage mixing.

5.5 CONCLUSIONS

Table 5.5 summarizes the frequency of making releases from various off-take levels and gives some indication of the dissolved oxygen and temperature of the released water. One can draw the following conclusions from Tables 5.4 and 5.5:

- **** **If sluice gates are used for IFR 'flood' releases then the gates should be located below RL230 to be able to make the releases frequently enough.** At RL240 and above the flood releases in July and June can only be made for about half of the time. During drier periods a few years may elapse before a flood release can be made. A gate at RL230 will be able to make releases at a more acceptable frequency.
- **** **During summer and until some time in June, releases from the upper zones of the dam will be considerably warmer than the streamflow, which may impact on the riverine ecology.** Later in winter, possibly in July, the temperatures of the releases from all levels of the dam are similar to the inflow. Thereafter, the streamflow warms up faster than the stored water so that the releases are colder than the streamflow.
- **** **A multilevel intake tower with intakes at RL206, RL210 and higher should be used for base releases.** There is a danger of anoxic base releases and an intake tower to take water from a higher level should be considered. Should the sediment oxygen demand be greater than the 0.2mg/l assumed, then the depth of the lower anoxic layer will increase. During summer the baseflow releases from Skuifraam Dam can average about 6 degrees C lower than the inflow, which may also impact on the riverine ecology. Figures D₀ and D_m in Appendix 2.2, as well as Table 5.4, show how summer temperature at the dam wall varies with time and depth. A multilevel intake tower will enable water from the appropriate level to be released to keep summer baseflow releases at the same temperature as the inflow.
- **** **Introduce the transfer from the Supplement Scheme at as low a level as possible into Skuifraam Dam to help break up the anoxic zone.** It would also be useful to be able to introduce water from the Supplement as low as possible into Skuifraam Dam (even below the bottom release level) when required to prevent an anoxic bottom zone from developing. The inlet for the pumps transferring water to Theewaterskloof should be positioned so that the Supplement inflows mix with the water in Skuifraam Dam and are not transferred directly to Theewaterskloof Dam.

Table 5.5 : The frequency, Dissolved Oxygen Range, and Temperature Range of IFR releases made from different levels

| Reduced Level of Release | Apr | | | | Jun | | | | Jul | | | |
|--------------------------|----------|---------|----------|-----------------------------|----------|-----------------|----------|-----------------------------|----------|-------------------|----------|-----------------------------|
| | Freq (%) | DO mg/l | Temp (C) | Temp relative to Inflow (C) | Freq (%) | DO mg/l | Temp (C) | Temp relative to Inflow (C) | Freq (%) | DO mg/l | Temp (C) | Temp relative to Inflow (C) |
| 240 | 5 | >7.5 | 8 to 25 | +9 to 13 | 44 | >8 | 12 to 20 | +2 to 10 | 54 | >8.5 | 12 to 15 | 0 to 3 |
| 230 | 62 | >7.5 | 16 to 28 | +0 to 12 | 79 | >7.5 | 12 to 18 | +2 to 8 | 84 | >8.5 | 12 to 15 | 0 to 3 |
| 220 | 82 | >7.5 | 15 to 24 | -1 to +8 | 95 | >7 | 12 to 16 | +2 to 6 | 97 | >7.5 | 12 to 15 | 0 to 3 |
| 206 | 90 | >6.5 | 14 to 22 | -2 to +6 | 98 | >6 [†] | 12 to 15 | +2 to 5 | 100 | >6.5 [†] | 12 to 15 | 0 to 3 |

CHAPTER SIX CONCLUSIONS AND RECOMMENDATIONS

6.1 CONCLUSIONS

From the above discussion the following conclusions can be drawn:

- • • Two-dimensional hydrodynamic and water quality models can provide useful insight into the mixing of water and water quality variables as well as bio-chemical processes which occur within reservoirs.
- • • Outputs from two-dimensional models are useful in assisting decision-makers in the task of determining the water quality component of the ecological reserve.
- • • Regional meteorological data has proven extremely valuable as input (driving force) for CE-QUAL-W2 in the absence of site-specific meteorological data.
- • • Two-dimensional hydrodynamic and water quality models such as CE-QUAL-W2 require various rate constants to accurately model bio-chemical reactions. In this study it was found that the oxygen profile within dams are particularly sensitive to the Sediment Oxygen Demand (SOD) and that this data is not readily available for this type of modelling. Availability of this type of data will greatly improve the reliability of the model outputs.
- • • Water quality monitoring of inflowing streams is of utmost importance for water quality modelling. This study revealed the lack of stream temperature data which is an important driving force for heat transfer within the reservoir.
- • • The Berg River Water Quality Information System (WQIS) is a useful tool for managers and decision-makers, bringing together various modelling tools (DUFLOW and CE-QUAL-W2) and providing post-processing which allows visualization of model outputs.

6.2 RECOMMENDATION

From the above conclusions the following recommendations can be made:

- • • The systematic monitoring of meteorological data throughout the country should be continued and new initiatives should attempt to gather site-specific meteorological data specifically for important water storage facilities and along important river courses.
- • • The systematic monitoring of water quality constituents should be continued throughout the country and special attention should be given to **temperature and nutrient** data sampling.
- • • In September 2001 Nico Rossouw and Wageed Kamish of Ninham Shand Consulting Services attended a course on CE-QUAL-W2 (v3.1), in Portland (U.S.A) and personal contact was made with the developers of the model. It is therefore recommended that close relationship and contact with these developers be maintained so that modelling of this type remains active in South Africa.

CHAPTER SEVEN REFERENCES

Bath, A.J., De Smidt, K O, Görgens, A H M, and Larsen, E J. 1998. *Applicability of hydrodynamic reservoir models for water quality management in stratified water bodies in South Africa: Application of DYRESM and CE-QUAL-W2*, Report by Ninham Shand Inc. to the Water Research Commission, Pretoria.

Cole, T M and Buchak, E M. 1995. *CE-QUAL-W2: A two-dimensional, laterally averaged, Hydrodynamic and Water Quality Model, Version 2.0*, Instruction Report EL- 95-, US Army Engineer Waterways Experiment Station, Vicksburg, MS.

Department of Water Affairs and Forestry, South Africa. 1998. *Amatole Water Resource System Analysis. Water Quality Modelling*. Prepared in association with Gibb Africa. DWAF Report No. Pr 000/00/0295.

Department of Water Affairs and Forestry, South Africa. 2000. *Skuifraam Water Supply Scheme Comprising Skuifraam Dam and the Skuifraam Supplement Scheme - Guidelines for Implementation*. Prepared by P R Little and C A Carter of Ninham Shand as part of the Skuifraam Dam and Skuifraam Supplement Scheme Feasibility Studies. DWAF Report No. PG100/00/0698.

Dunn, P and Larsen, J. 1994. *In-stream flow requirements. Volume II: Methodology and first estimates*. Western Cape Systems Analysis. DWAF Report No. PG000/00/4793.

Edinger, J E and Buchak, E M. 1975. *A Hydrodynamic, Two-Dimensional Reservoir Model: The computational Basis*. Prepared for US Army Engineer Division, Ohio River, Cincinnati, Ohio.

Görgens, A H M, Bath, A J, Venter, A, De Smidt, K and Marais, G V R. 1993. *Applicability of Hydrodynamic reservoir models for water quality management in stratified water bodies in South Africa*. Report by Ninham Shand Inc. and the University of Cape Town to the Water Research Commission, Pretoria. Report No. 304/1/93.

APPENDIX 1.1

**REVIEW OF WATER QUALITY STATUS OF BERG RIVER MAIN STEM
TABLES AND GRAPHS**

Table 1.1.1 Intervals of pH values used in the Situation Analysis (DWAF(a), 1993) to assess the quality of the water for irrigation usage

| pH | Impact |
|--------------|--|
| <7 | Possible problems when used on acidic soils, the water is corrosive, and may cause eye irritation in swimmers. |
| >= 6.5 < 8.5 | No significant problems identified. |
| >= 8.5 | Possible problems when irrigated on alkaline soils, restrictions on drip irrigation. |

Table 1.1.2 Percentage of pH values falling below pH 7 for raw water users

| Station | | Prior 1991 DWAF Situation Analysis (data from 1980 where available) | Jan 1991 to May 1998 |
|------------------------------|--------|---|----------------------|
| River Reach 1 | | | |
| G1H004 (Upper Berg River) | pH < 7 | 90% | 58% |
| | pH > 7 | 10% | 42% |
| G1H020 (Paarl) | pH < 7 | 82% | 17% |
| | pH > 7 | 18% | 83% |
| River Reach 2 | | | |
| G1H036 | pH < 7 | 63% | 4% |
| | pH > 7 | 37% | 96% |
| G1H037 (Krom River) | pH < 7 | 74% | 3% |
| | pH > 7 | 26% | 97% |
| G1H041 (Kompanjies River) | pH < 7 | 65% | 3% |
| | pH > 7 | 35% | 97% |
| River Reach 3 | | | |
| G1H008 (Little Berg River) | pH < 7 | 83% | 4% |
| | pH > 7 | 17% | 96% |
| G1H013 (Drie Heuwels) | pH < 7 | 65% | 3% |
| | pH > 7 | 35% | 97% |
| River Reach 4 | | | |
| G1H023 (Old Pumping Station) | pH < 7 | 12% | 1% |
| | pH > 7 | 88% | 99% |

Table 1.1.3 Intervals of pH values used in the Situation Analysis (DWAF(a), 1993) to assess the quality of the water with respect to raw water supplied to water treatment works

| pH | Impact |
|--------------|--|
| <6.5 | The water is aggressive to cement, and requires increased lime dosage. |
| >= 6.5 < 8.5 | The water can be treated without significant problems. |
| >= 8.5 | The water cannot be effectively disinfected. |

Table 1.1.4 Percentage of pH values falling below pH 7 for municipal supply

| Station | | Prior 1991 DWAF Situation Analysis (data from 1980 where available) | Jan 1991 to May 1998 |
|---|-------------------------------------|---|----------------------|
| <u>G1R002</u> Wemmershoek Water Treatment Works | pH < 6.5 pH >6.5 <8.5 pH >8.5 | 70% 30% | 63% 37% |
| <u>G1R001</u> Swartland Water Treatment Works | pH < 6.5 pH >6.5 <8.5 pH >8.5 | 35% 62% 3% | 1% 98% 1% |
| <u>G1R003</u> Withoogte Water Treatment Works | pH < 6.5 pH >6.5 <8.5 pH >8.5 | 19% 80% 1% | 2% 98% |

Table 1.1.5 Intervals of EC values used in the Situation Analysis (DWAF(a), 1993) to assess the quality of the water for irrigation usage

| EC (mS/m) | Impact |
|--------------|--|
| <40 | SA target guideline range. 100% yield on all crops. |
| >= 40 < 90 | 95% yield for moderately sensitive crops for surface irrigation. |
| >= 90 < 270 | 90% yield for all moderately tolerant crops. |
| >= 270 < 430 | 80% yield for all moderately tolerant crops. |
| >= 430 | Not recommended for irrigation on any crops. |

Table 1.1.6 Percentage of EC values for irrigation

| Station | | Prior 1991 DWAF Situation Analysis (data from 1980 where available) | Jan 1991 to May 1998 |
|------------------------------|--|--|--------------------------------------|
| River Reach 1 | | | |
| G1H004 (Upper Berg River) | EC < 40 | 100% | 100% |
| G1H020 (Paarl) | EC < 40 | 100% | 100% |
| River Reach 2 | | | |
| G1H036 | EC < 40 EC >= 40 < 90 | 97.5% 2.5% | 99.2% 0.8% |
| G1H037 (Krom River) | EC < 40 EC >= 40 < 90 | 99.8% 0.2% | 100% 0% |
| G1H041 (Kompanjies River) | EC < 40 EC >= 40 < 90 EC >= 90 < 270 | 84% 15% 1% | 82.3% 17% 0.7% |
| River Reach 3 | | | |
| G1H008 (Little Berg River) | EC < 40 EC >= 40 < 90 | 100% 0% | 98% 2% |
| G1H013 (Drie Heuwels) | EC < 40 EC >= 40 < 90 | 99% 1% | 98% 2% |
| River Reach 4 | | | |
| G1H023 (Old Pumping Station) | EC < 40 EC >= 40 < 90 EC >= 90 < 270 EC >= 270 < 430 EC >= 430 | 9% 30% 53% 7% 1% | 6.5% 48% 40.3% 2.6% 2.6% |

Table 1.1.7 Intervals of EC values used in the Situation Analysis (DWAF(a), 1993) to assess the quality of the water with respect to raw water supplied to water treatment works

| EC (mS/m) | Impact |
|-------------|--|
| <70 | Below the drinking water criteria, but some sensitive industries may experience problems. The SA target guideline range for the leather industry. |
| >= 70 < 150 | Exceeds the recommended limit for SA drinking water, and the US EPA limit (above 77 mS/m). Moderate increases in water costs for the leather industry. |
| >= 150 <300 | Possible palatability problems. Problematic for most industries. Corrosion for scale forming properties evident. Substantial increase in water costs for the leather industry. |
| >=300 | Laxative effects in humans. Exceeds the maximum permissible limit for EC in SA drinking water. Unsuitable for most industries. |

Table 1.1.8 Percentage of EC values falling in the indicated intervals for municipal users

| Station | | Prior 1991 DWAF Situation Analysis (data from 1980 where available) | Jan 1991 to May 1998 |
|---|---------------------|--|----------------------|
| <u>G1R002</u> Wemmershoek Water Treatment Works | EC <70 | 100% | 100% |
| <u>G1R001</u> Swartland Water Treatment Works | EC <70 | 100% | 100% |
| <u>G1R003</u> Withoogte Water Treatment Works | EC <70 EC 70-150 | 97% 3% | 98% 2% |

APPENDIX 1.1

Table 1.1.9 Statistics of pH at River Gauging Stations

| Station | | Prior 1991 DWAF Situation Analysis (data from 1980 where available) | Jan 1991 to May 1998 |
|---------------------------------|--------------------|--|-------------------------|
| River Reach 1 | | | |
| G1H004 (Upper Berg River) | Mean | 5.62 | 6.61 |
| | Standard Deviation | 0.977 | 0.65 |
| | Minimum Value | 3.76 | 4.83 |
| | Maximum Value | 7.89 | 8.49 |
| | Number of samples | 95 | 226 |
| G1H020 (Paarl) | Mean | 6.205 | 7.29 |
| | Standard Deviation | 0.765 | 0.316 |
| | Minimum Value | 3.26 | 6.4 |
| | Maximum Value | 8.45 | 8.91 |
| | Number of samples | 601 | 308 |
| River Reach 2 | | | |
| G1H036 | Mean | 6.96 | 7.55 |
| | Standard Deviation | 0.65 | 0.504 |
| | Minimum Value | 4.1 | 0.01 |
| | Maximum Value | 8.63 | 8.49 |
| | Number of samples | 341 | 311 |
| G1H041 (Kompanjies River) | Mean | 6.74 | 7.59 |
| | Standard Deviation | 0.876 | 0.3 |
| | Minimum Value | 2.07 | 6.57 |
| | Maximum Value | 9.9 | 8.45 |
| | Number of samples | 502 | 226 |
| River Reach 3 | | | |
| G1H008 (Little Berg River) | Mean | 6.71 | 7.53 |
| | Standard Deviation | 0.676 | 0.261 |
| | Minimum Value | 4.6 | 6.77 |
| | Maximum Value | 8.58 | 8.45 |
| | Number of samples | 444 | 297 |
| G1H013 (Drie Heuwels) | Mean | 6.73 | 7.589 |
| | Standard Deviation | 0.67 | 0.379 |
| | Minimum Value | 3.48 | 4.25 |
| | Maximum Value | 9.4 | 8.48 |
| | Number of samples | 598 | 313 |
| River Reach 4 | | | |
| G1H023 (Old Pumping Station) | Mean | 7.08 | 7.67 |
| | Standard Deviation | 0.478 | 0.245 |
| | Minimum Value | 5.9 | 7 |
| | Maximum Value | 8.14 | 8.2 |
| | Number of samples | 95 | 68 |

Table 1.1.10 Statistics of Electrical Conductivity at River Gauging Stations

| Station | | Prior 1991 DWAF Situation Analysis (data from 1980 where available) | Jan 1991 to May 1998 |
|------------------------------|--------------------|---|----------------------|
| River Reach 1 | | | |
| G1H004 (Upper Berg River) | Mean | 5.67 | 5.59 |
| | Standard Deviation | 2.9 | 1.17 |
| | Minimum Value | 2.4 | 2.9 |
| | Maximum Value | 19.5 | 11.2 |
| | Number of samples | 344 | 238 |
| G1H020 (Paarl) | Mean | 11 | 10.56 |
| | Standard Deviation | 3.15 | 3 |
| | Minimum Value | 3.3 | 5.8 |
| | Maximum Value | 42.6 | 41.9 |
| | Number of samples | 603 | 308 |
| River Reach 2 | | | |
| G1H036 | Mean | 22.35 | 21.67 |
| | Standard Deviation | 8.38 | 6.34 |
| | Minimum Value | 6.5 | 7.8 |
| | Maximum Value | 111.8 | 69.5 |
| | Number of samples | 413 | 311 |
| G1H041 (Kompanjies River) | Mean | 29.68 | 31 |
| | Standard Deviation | 40.74 | 15 |
| | Minimum Value | 7.3 | 10.6 |
| | Maximum Value | 865 | 95 |
| | Number of samples | 502 | 226 |
| River Reach 3 | | | |
| G1H008 (Little Berg River) | Mean | 17.58 | 20.73 |
| | Standard Deviation | 5.62 | 6 |
| | Minimum Value | 3.1 | 5.2 |
| | Maximum Value | 51.2 | 50.9 |
| | Number of samples | 444 | 297 |
| G1H013 (Drie Heuwels) | Mean | 26.11 | 26.26 |
| | Standard Deviation | 9.88 | 8.79 |
| | Minimum Value | 3.5 | 7.4 |
| | Maximum Value | 69.5 | 63 |
| | Number of samples | 548 | 364 |
| River Reach 4 | | | |
| G1H023 (Old Pumping Station) | Mean | 119.24 | 111.1 |
| | Standard Deviation | 73.96 | 109.65 |
| | Minimum Value | 21.8 | 23.9 |
| | Maximum Value | 437.7 | 737 |
| | Number of samples | 95 | 68 |

APPENDIX 1.1

Table 1.1.11 Statistics of Phosphate Values at River Gauging Stations

| Station | | Prior 1991 DWAF Situation Analysis (data from 1980 where available) | Jan 1991 to May 1998 |
|------------------------------|--------------------|---|----------------------|
| River Reach 1 | | | |
| G1H004 (Upper Berg River) | Mean | 0.0155 | 0.022 |
| | Standard Deviation | 0.014 | 0.0295 |
| | Minimum Value | 0 | 0 |
| | Maximum Value | 0.073 | 0.416 |
| | Number of samples | 95 | |
| G1H020 (Paarl) | Mean | 0.0371 | 0.0309 |
| | Standard Deviation | 0.2188 | 0.048 |
| | Minimum Value | 0 | 0 |
| | Maximum Value | 3.344 | 0.78 |
| | Number of samples | 553 | 294 |
| River Reach 2 | | | |
| G1H036 | Mean | 0.0577 | 0.0759 |
| | Standard Deviation | 0.074 | 0.0557 |
| | Minimum Value | 0 | 0.001 |
| | Maximum Value | 0.989 | 0.384 |
| | Number of samples | 319 | 300 |
| G1H041 (Kompanjies River) | Mean | 0.0309 | 0.0255 |
| | Standard Deviation | 0.065 | 0.024 |
| | Minimum Value | 0 | 0 |
| | Maximum Value | 0.853 | 0.223 |
| | Number of samples | 464 | 213 |
| River Reach 3 | | | |
| G1H008 (Little Berg River) | Mean | 0.0132 | 0.0203 |
| | Standard Deviation | 0.0593 | 0.0132 |
| | Minimum Value | 0 | 0 |
| | Maximum Value | 1.09 | 0.121 |
| | Number of samples | 411 | 289 |
| G1H013 (Drie Heuwels) | Mean | 0.0209 | 0.0318 |
| | Standard Deviation | 0.025 | 0.0335 |
| | Minimum Value | 0 | 0 |
| | Maximum Value | 0.214 | 0.63 |
| | Number of samples | 587 | 313 |
| River Reach 4 | | | |
| G1H023 (Old Pumping Station) | Mean | 0.0142 | 0.0316 |
| | Standard Deviation | 0.0124 | 0.0239 |
| | Minimum Value | 0 | 0.002 |
| | Maximum Value | 0.067 | 0.12 |
| | Number of samples | 95 | 68 |

Table 1.1.12 Statistics of pH for Water Treatment Works

| Station | | Prior 1991 DWF Situation Analysis (data from 1980 where available) | Jan 1991 to May 1998 |
|---|--------------------|---|----------------------|
| <u>G1R002</u> Wemmershoek Water Treatment Works | Mean | 5.25 | 6.453 |
| | Standard Deviation | 0.816 | 0.528 |
| | Minimum Value | 4 | 5.11 |
| | Maximum Value | 7.42 | 8.04 |
| | Number of Samples | 132 | 33 |
| <u>G1R001</u> Swartland Water Treatment Works | Mean | 6.89 | 7.465 |
| | Standard Deviation | 0.704 | 0.358 |
| | Minimum Value | 4.24 | 4.46 |
| | Maximum Value | 9.26 | 8.82 |
| | Number of Samples | 494 | 431 |
| <u>G1R003</u> Withoogte Water Treatment Works | Mean | 7.02 | 7.597 |
| | Standard Deviation | 0.535 | 0.528 |
| | Minimum Value | 5.34 | 4.35 |
| | Maximum Value | 8.81 | 8.39 |
| | Number of Samples | 486 | 308 |

Table 1.1.13 Statistics of Electrical Conductivity for Water Treatment Works

| Station | | Prior 1991 DWF Situation Analysis (data from 1980 where available) | Jan 1991 to May 1998 |
|---|--------------------|---|----------------------|
| <u>G1R002</u> Wemmershoek Water Treatment Works | Mean | 5.135 | 4.436 |
| | Standard Deviation | 7.341 | 2.977 |
| | Minimum Value | 3.1 | 3.2 |
| | Maximum Value | 88 | 20.7 |
| | Number of Samples | 132 | 33 |
| <u>G1R001</u> Swartland Water Treatment Works | Mean | 12.05 | 11.95 |
| | Standard Deviation | 1.4 | 1.82 |
| | Minimum Value | 2.8 | 8.8 |
| | Maximum Value | 17.5 | 27.5 |
| | Number of Samples | 494 | 431 |
| <u>G1R003</u> Withoogte Water Treatment Works | Mean | 39.3 | 36.12 |
| | Standard Deviation | 13.54 | 13.82 |
| | Minimum Value | 8.6 | 3.5 |
| | Maximum Value | 108.2 | 110.1 |
| | Number of Samples | 486 | 308 |

Table 1.1.14 Statistics of Phosphate Values for Water Treatment Works

| Station | | Prior 1991 DWAF Situation Analysis (data from 1980 where available) | Jan 1991 to May 1998 |
|---|---|--|---|
| <u>G1R002</u> Wemmershoek Water Treatment Works | Mean Standard Deviation Minimum Value Maximum Value Number of Samples | 0.005 0.006 0 0.037 132 | 0.01 0.006 0 0.03 33 |
| <u>G1R001</u> Swartland Water Treatment Works | Mean Standard Deviation Minimum Value Maximum Value Number of Samples | 0.0057 0.0064 0 0.046 483 | 0.016 0.0078 0 0.067 431 |
| <u>G1R003</u> Withoogte Water Treatment Works | Mean Standard Deviation Minimum Value Maximum Value Number of Samples | 0.0199 0.0208 0 0.293 485 | 0.0306 0.0251 0.004 0.299 308 |

Fig 1.1.1 pH at G1H004

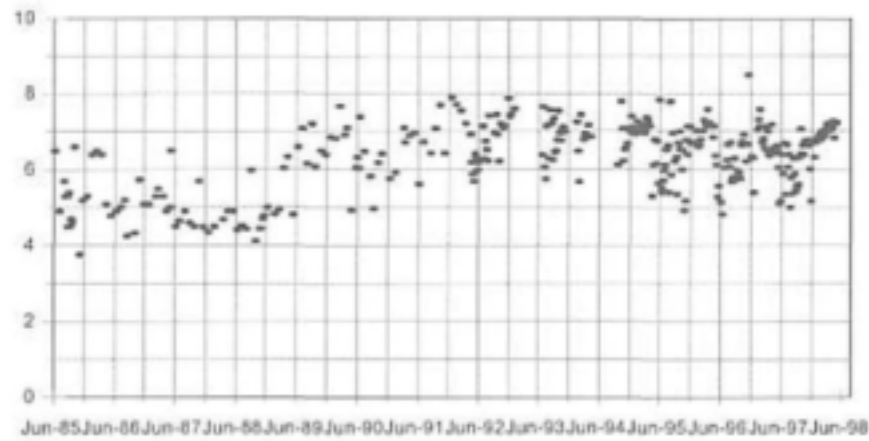


Fig 1.1.3 pH at G1H036

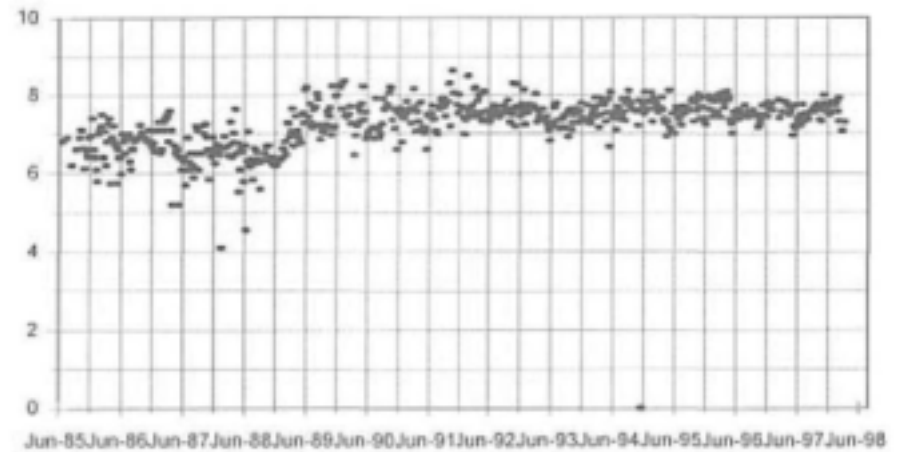


Fig 1.1.2 pH at G1H020

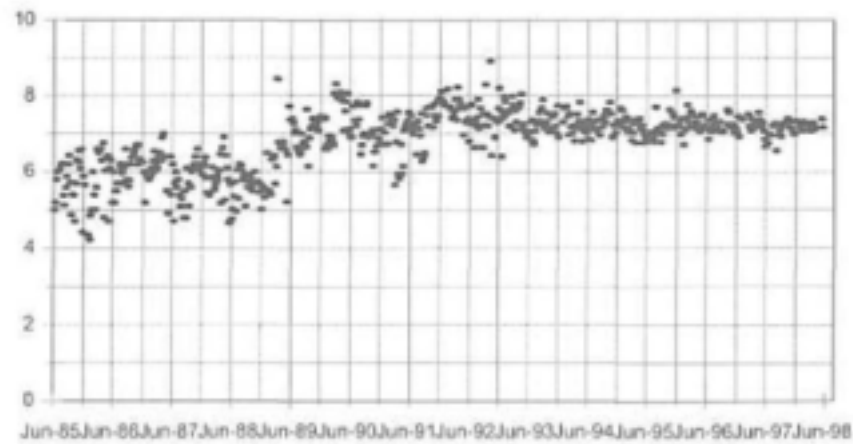


Fig 1.1.4 pH at G1H041

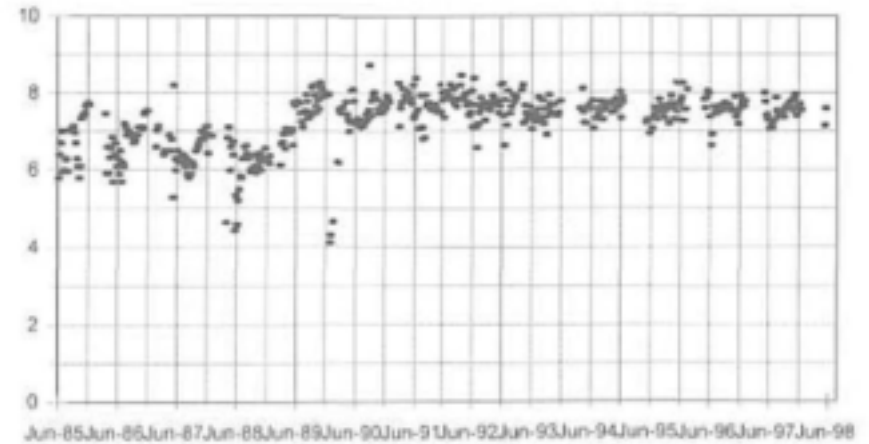


Fig 1.1.5 pH at G1H008

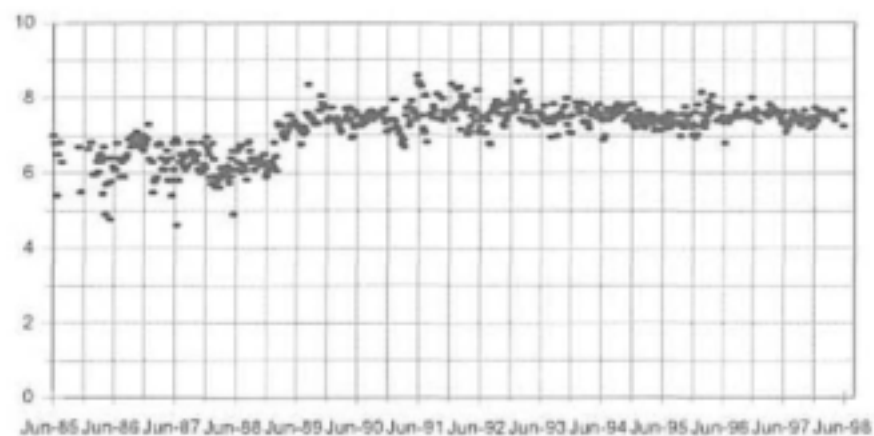


Fig 1.1.6 pH at G1H013

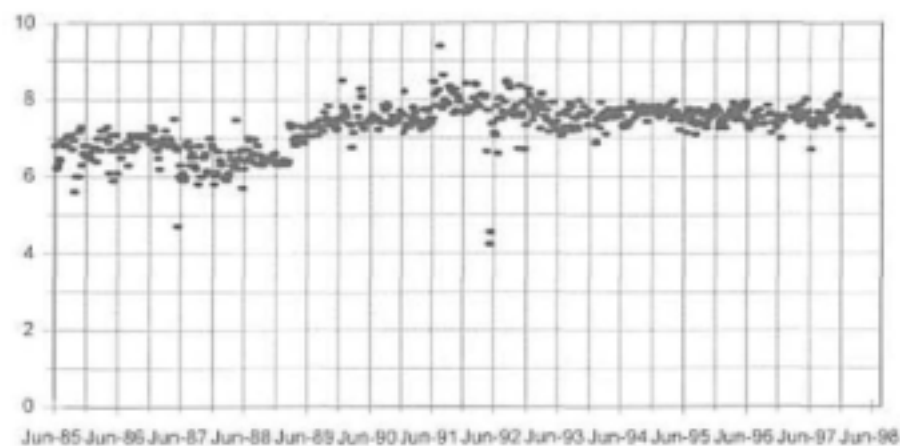


Fig 1.1.7 pH at G1H023

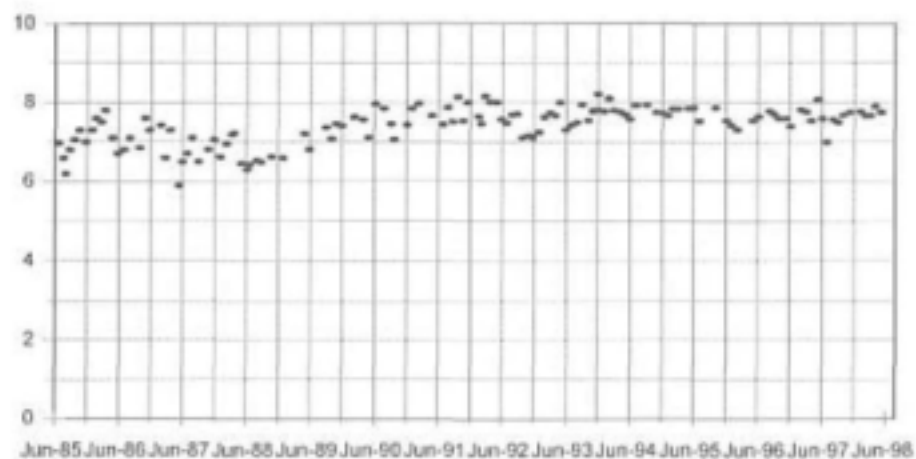


Fig 1.1.8 pH at G1R001

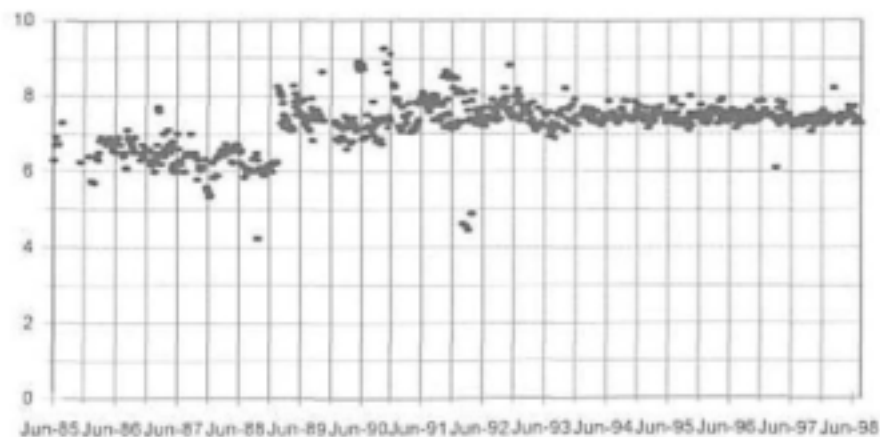


Fig. 1.1.9 pH at G1R002

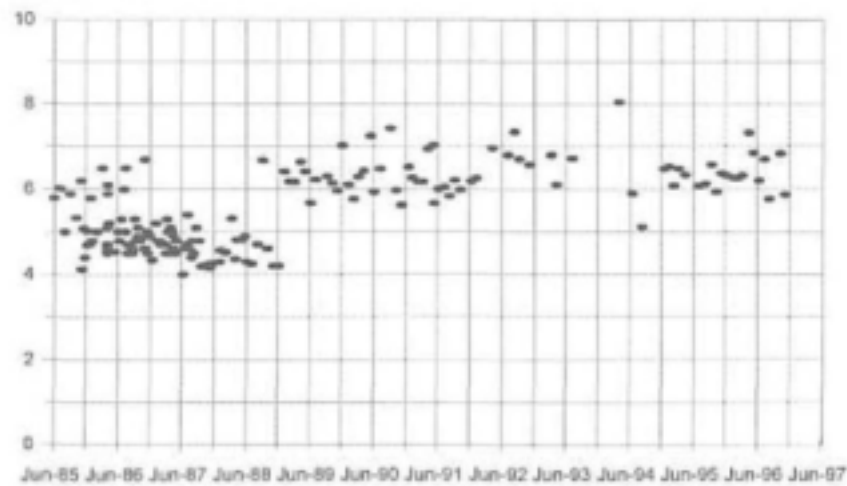


Fig 1.1.10 pH at G1R003

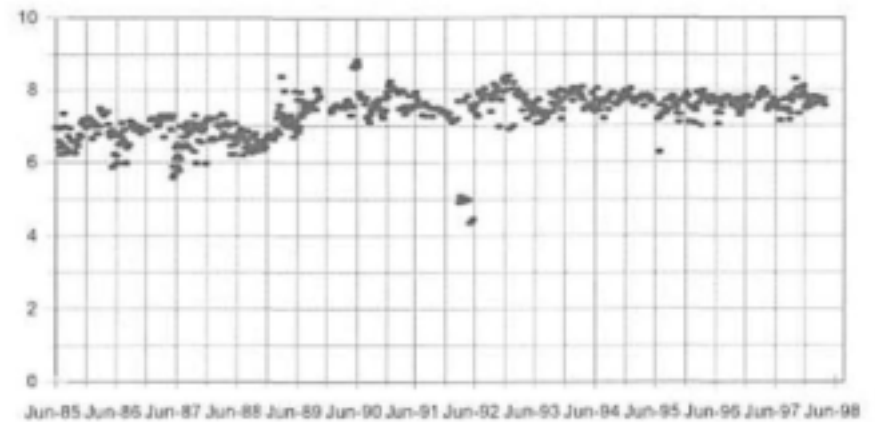


Fig 1.1.11 EC (mS/m) at G1H004

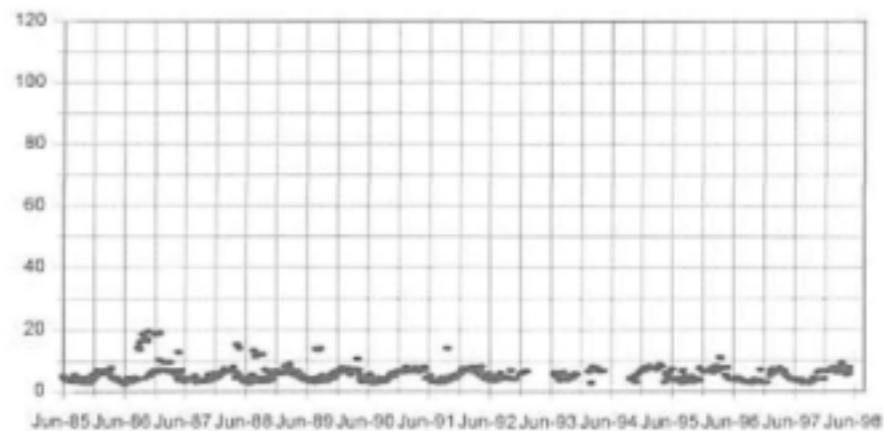


Fig 1.1.12 EC (mS/m) at G1H020

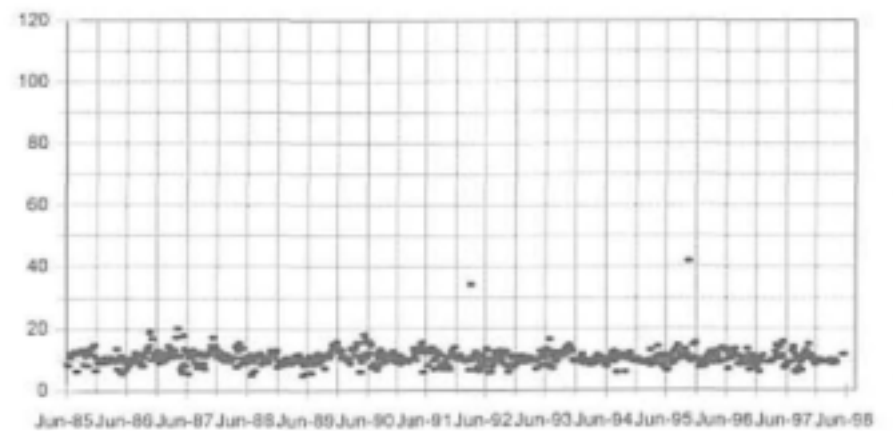


Fig 1.1.13 EC (mS/m) at G1H036

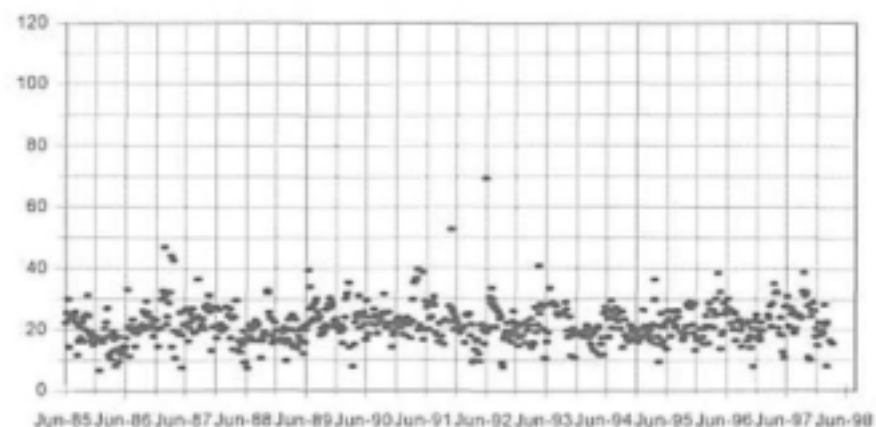


Fig 1.1.14 EC (mS/m) at G1H041

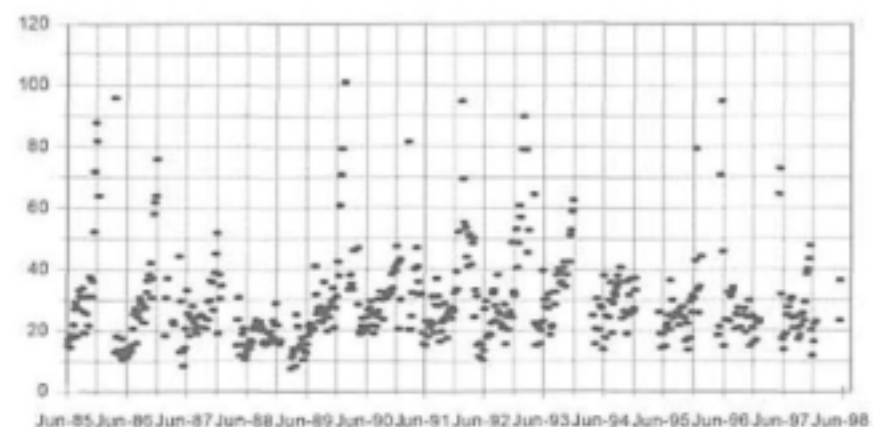


Fig 1.1.15 EC (mS/m) at G1H008

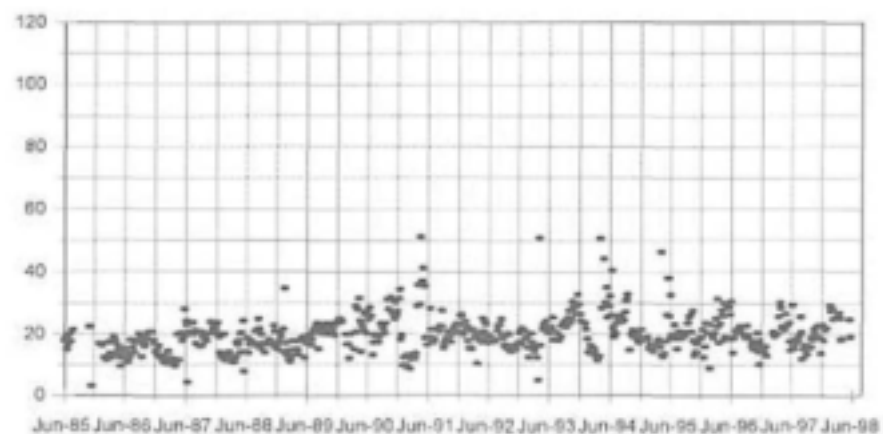


Fig 1.1.16 EC (mS/m) at G1H013

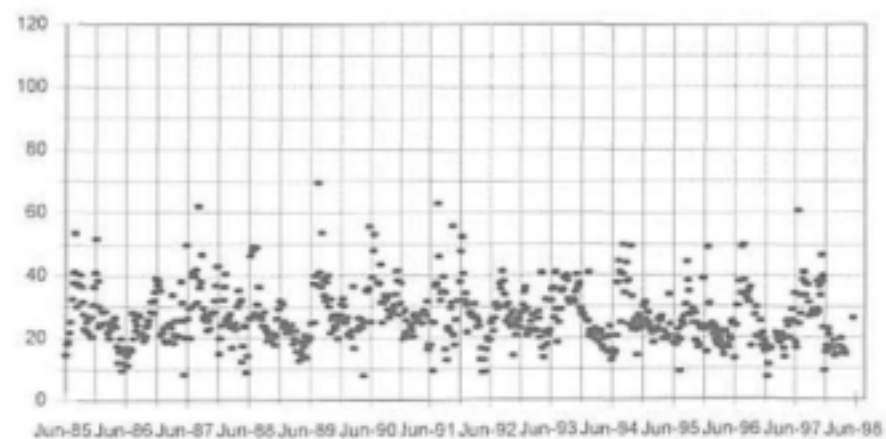


Fig 1.1.17 EC (mS/m) at G1H023

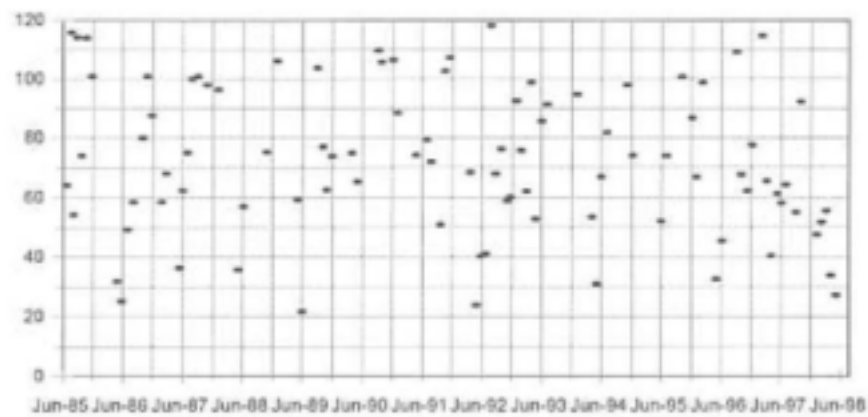


Fig 1.1.18 EC (mS/m) at G1R001

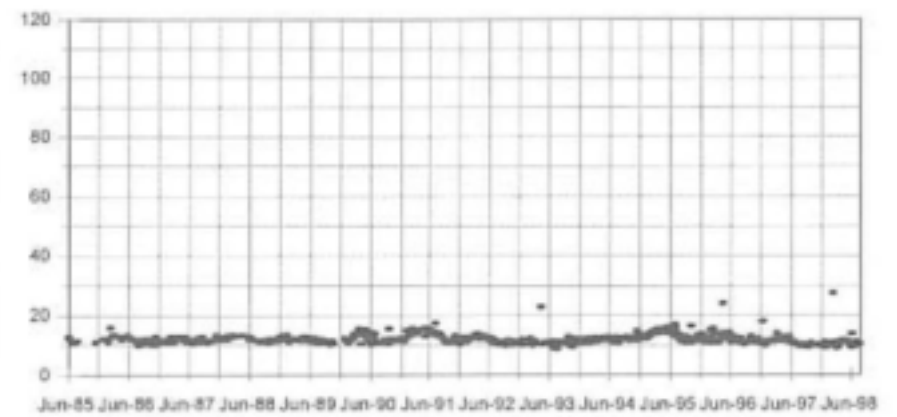


Fig. 1.1.19 EC (mS/m) at G1R002

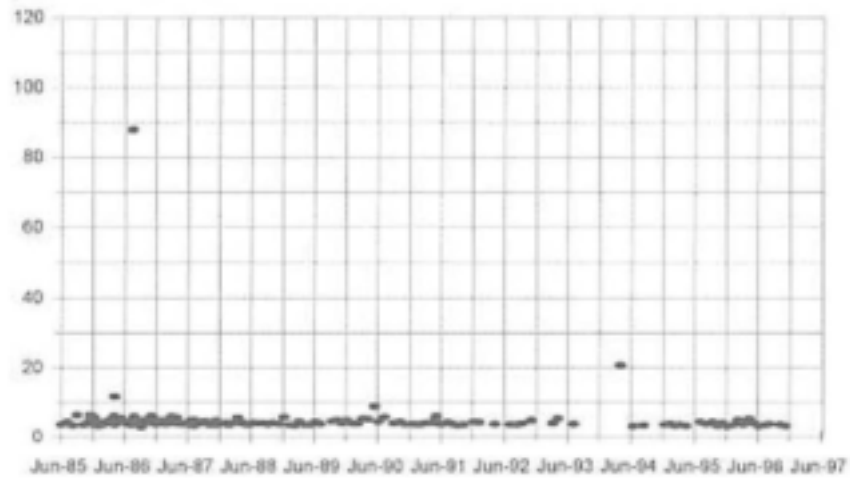


Fig 1.1.20 EC (mS/m) at G1R003

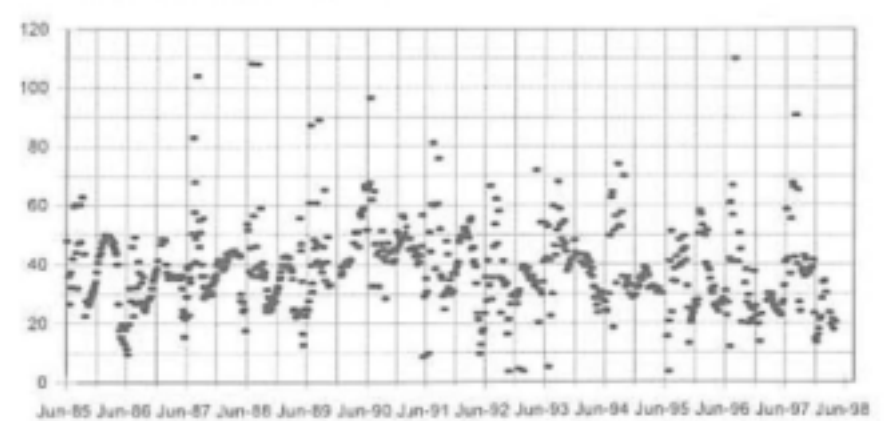


Fig 1.1.21 TDS (mg/l) at G1H004

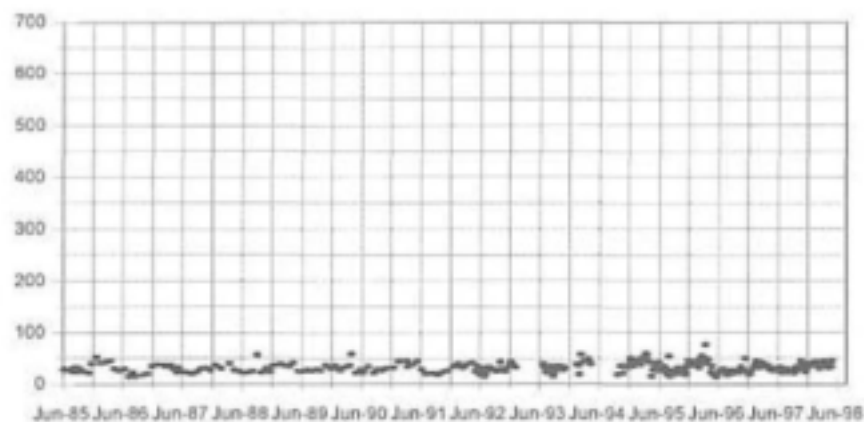


Fig 1.1.22 TDS (mg/l) at G1H020

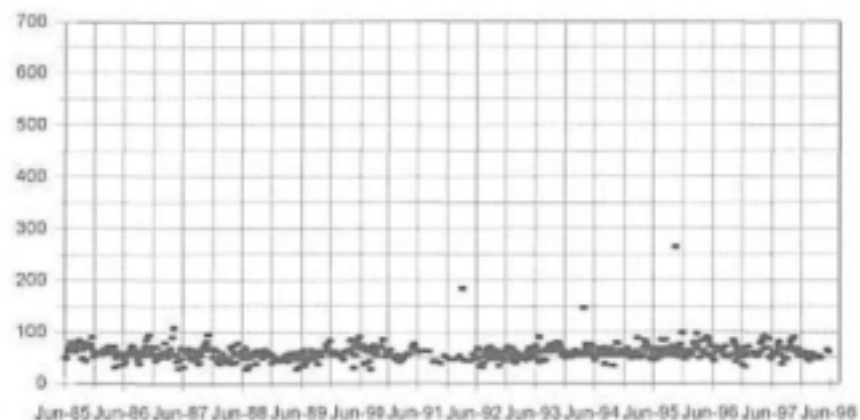


Fig 1.1.23 TDS (mg/l) at G1H036

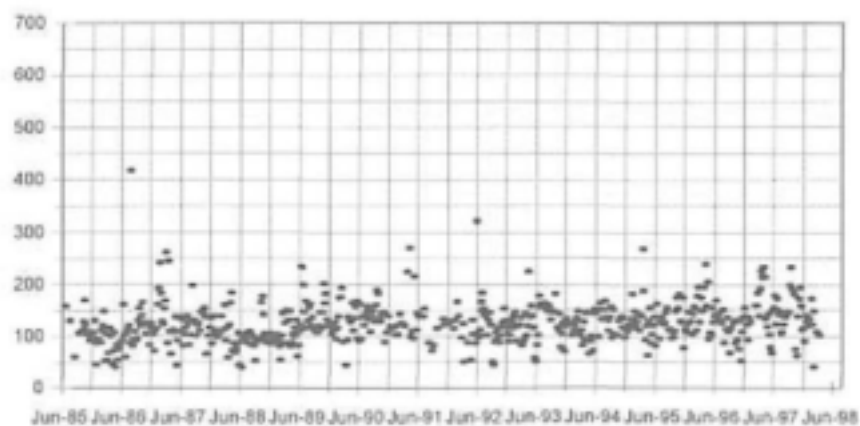


Fig 1.1.24 TDS (mg/l) at G1H041

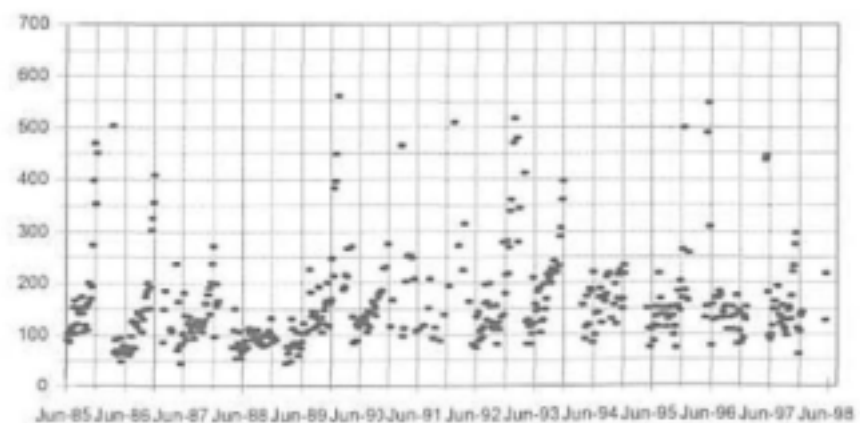


Fig 1.1.25 TDS (mg/l) at G1H008

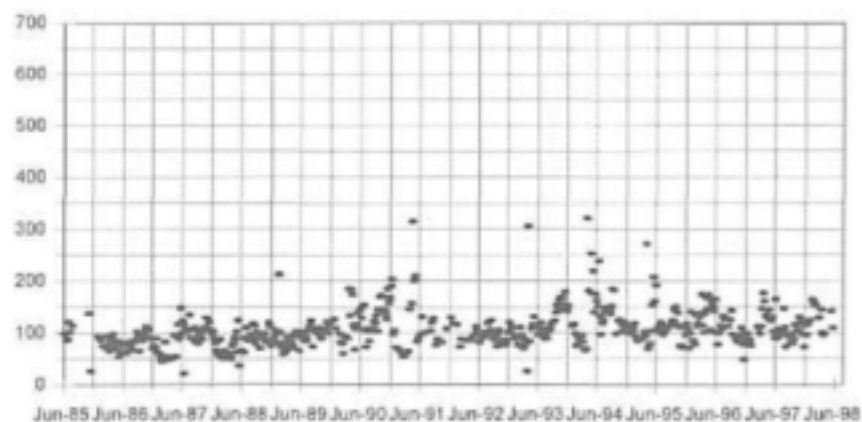


Fig 1.1.26 TDS (mg/l) at G1H013

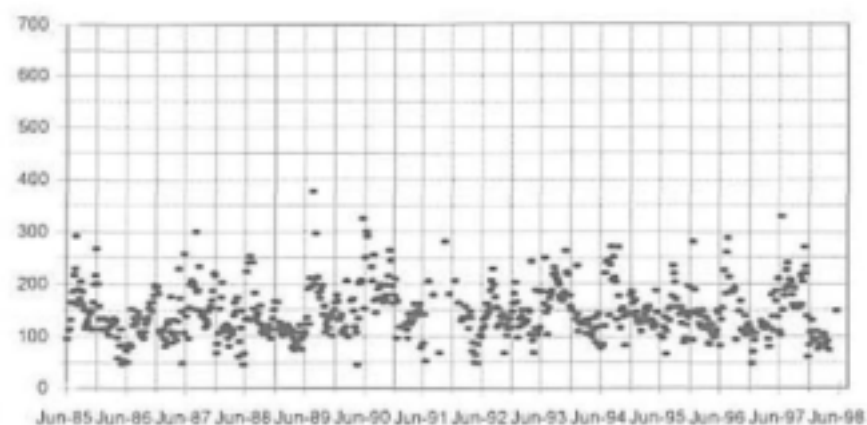


Fig 1.1.27 TDS (mg/l) at G1H023

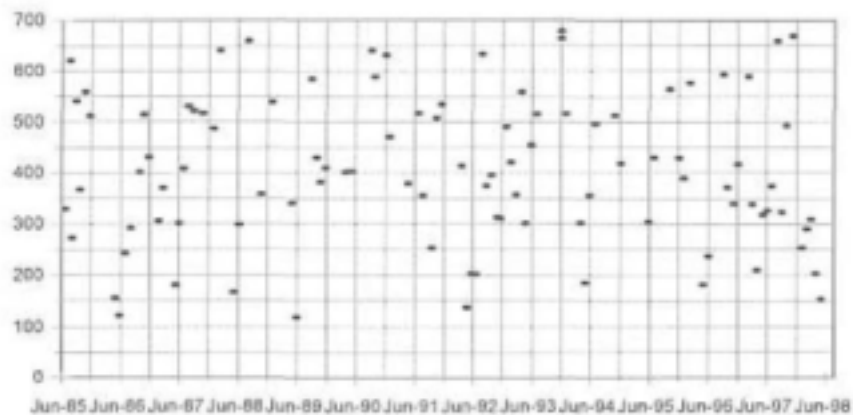


Fig 1.1.28 TDS (mg/l) at G1R001

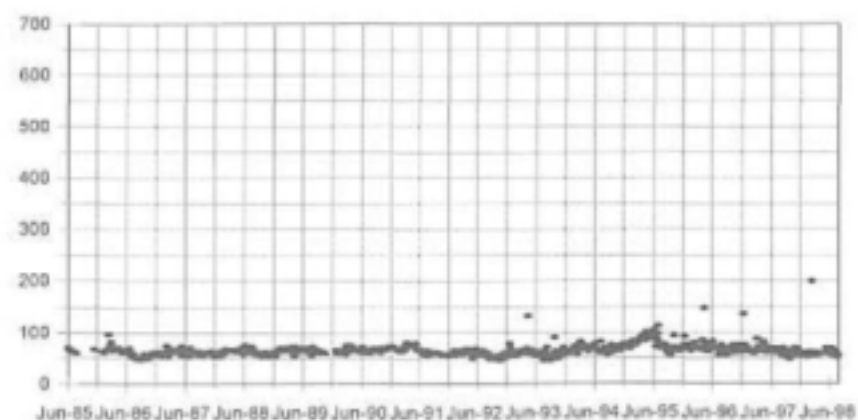


Fig. 1.1.29 TDS (mg/l) at G1R002

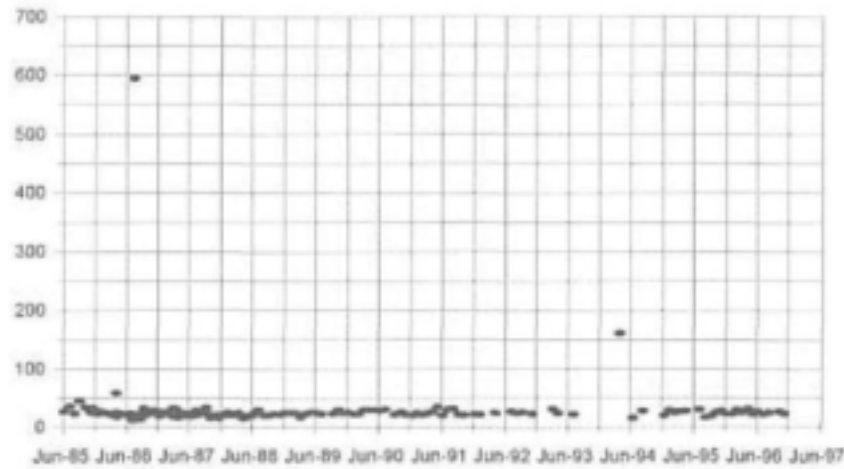


Fig 1.1.30 TDS (mg/l) at G1R003

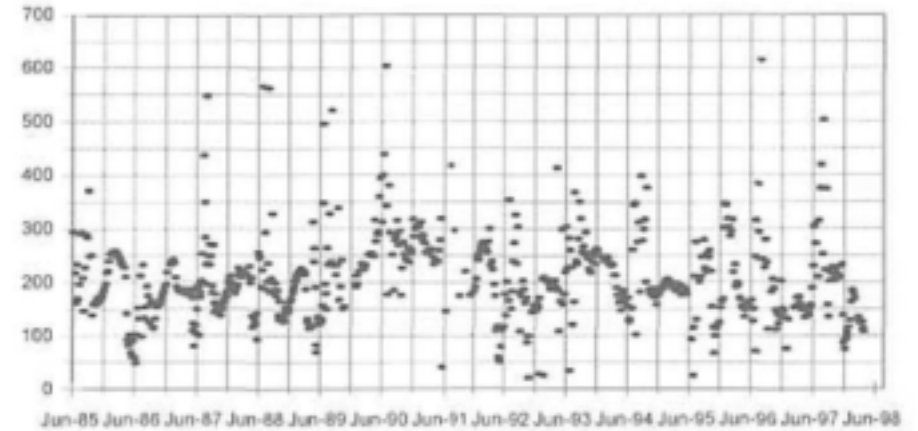


Fig 1.1.31 Phosphates (mg/l PO4 as P) at G1H004

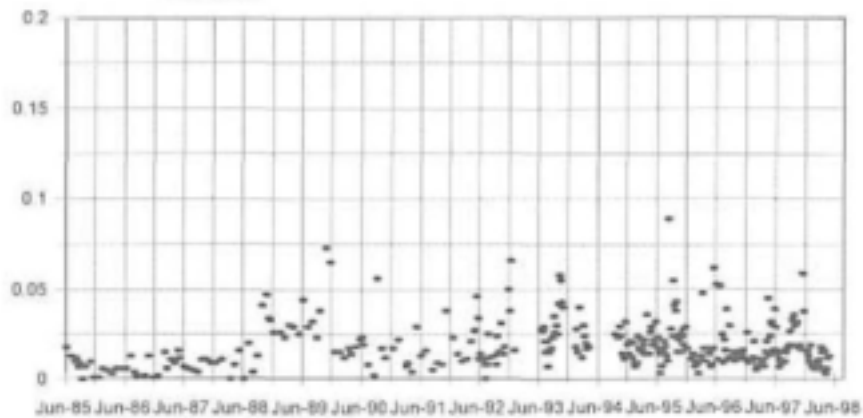
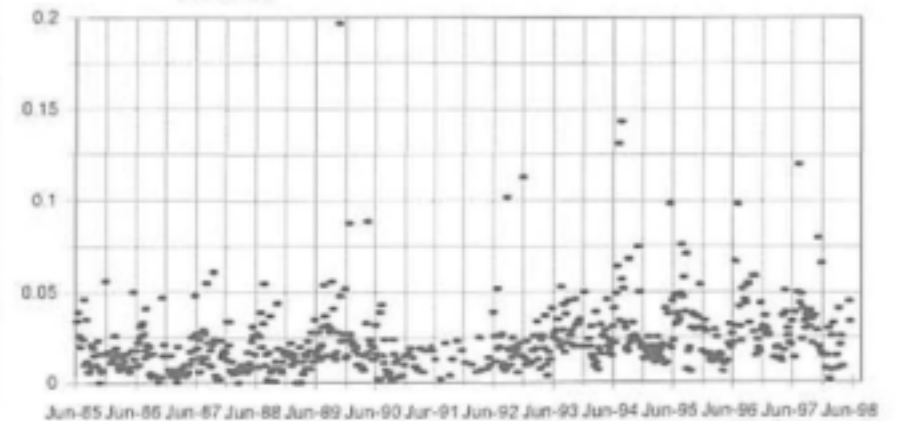
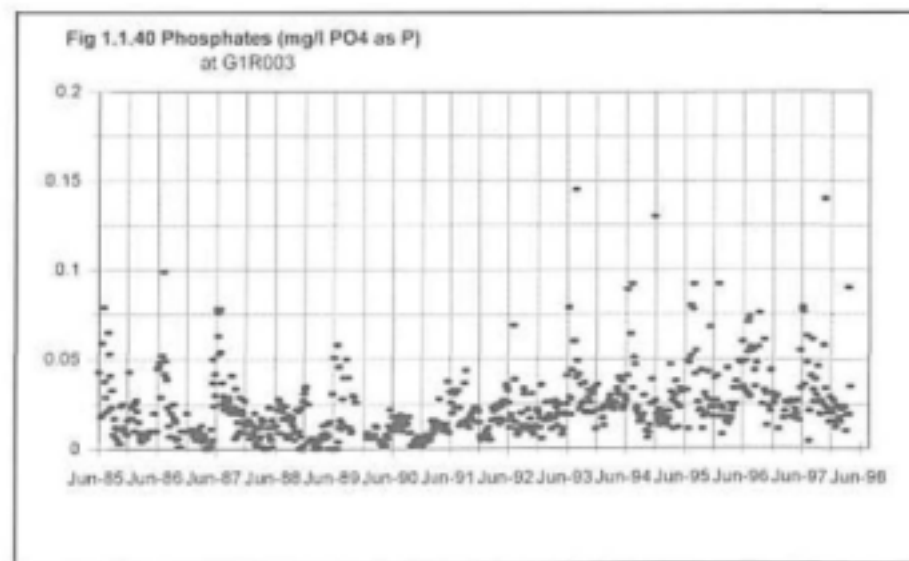
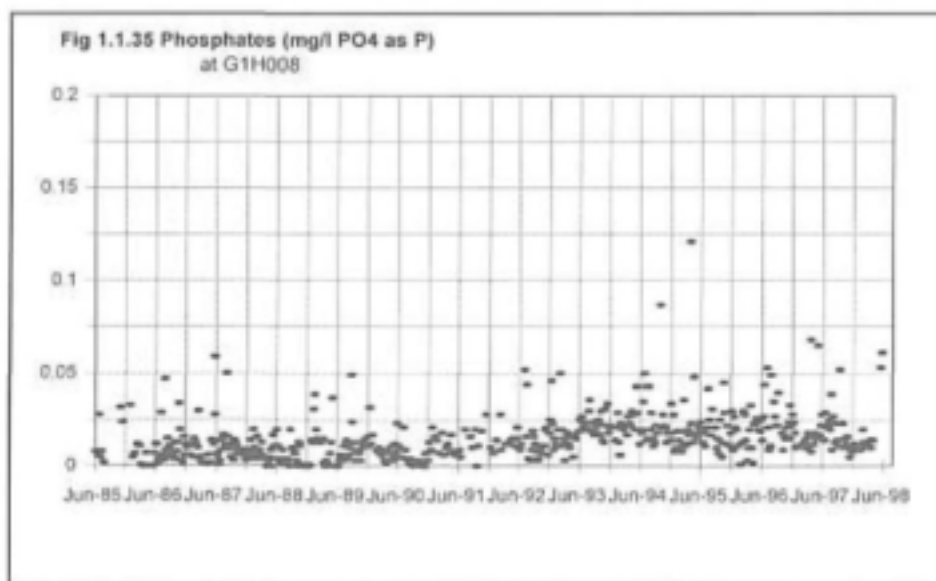
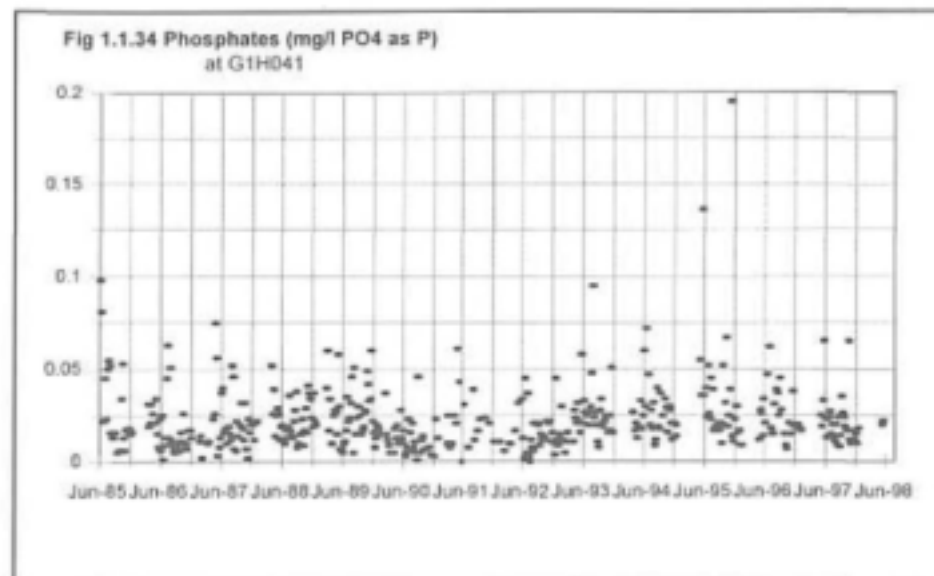
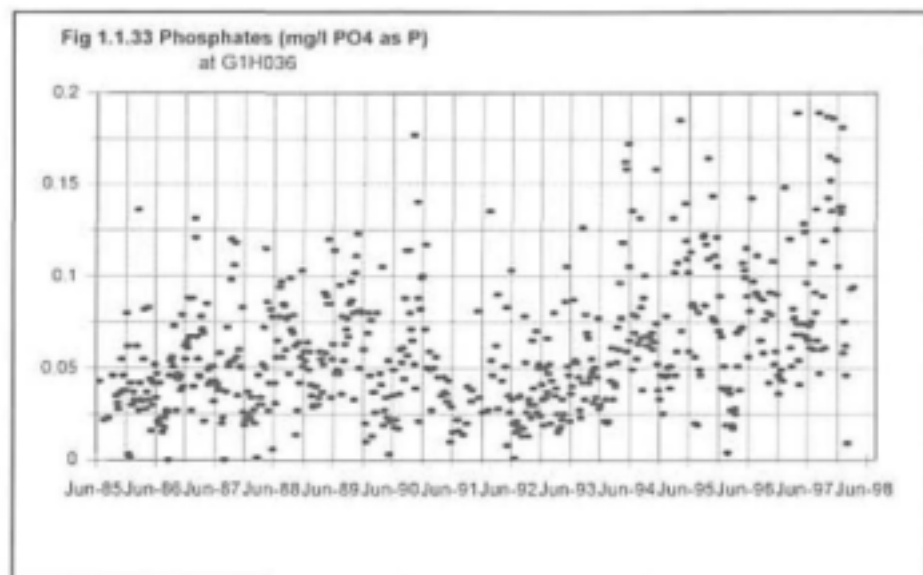
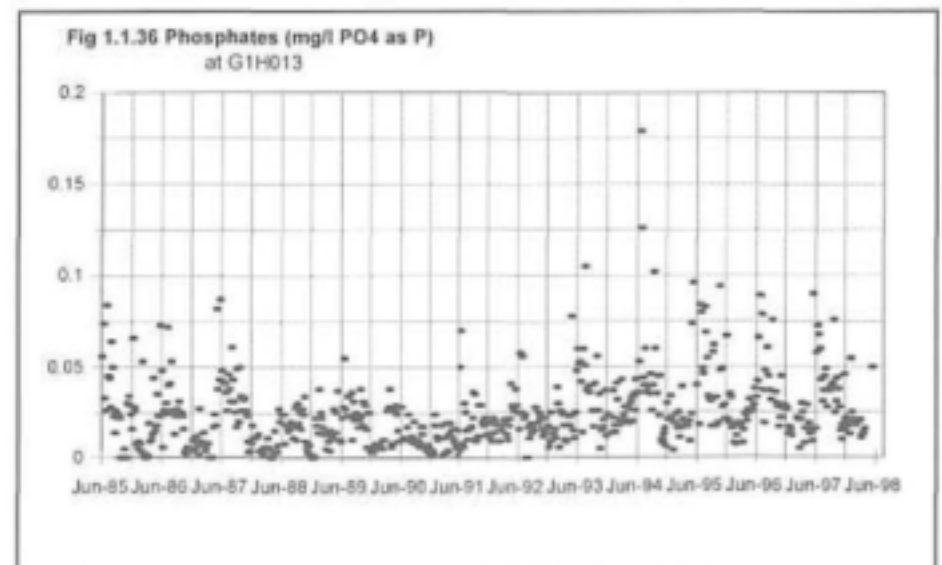
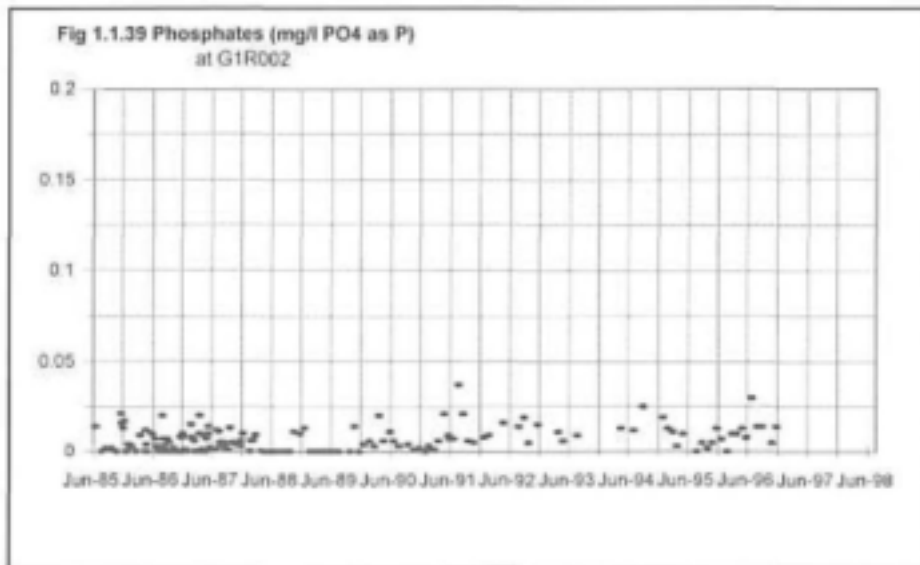
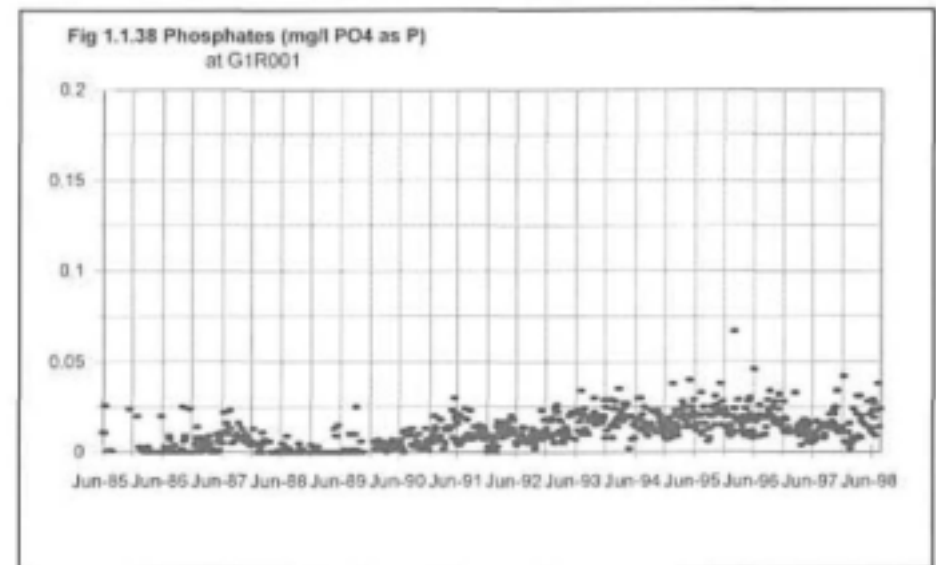
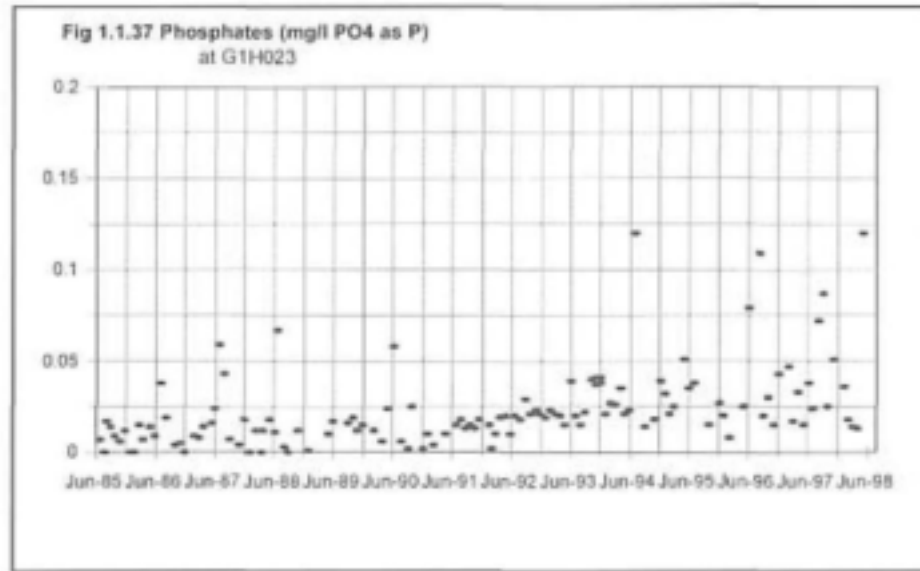


Fig 1.1.32 Phosphates (mg/l PO4 as P) at G1H020







APPENDIX 1.2

**DATA PREPARATION AND CONFIGURATION OF THE DUFLOW MODEL
TABLES AND GRAPHS**

FIGURE 1.2.1 TDS values for G1H004

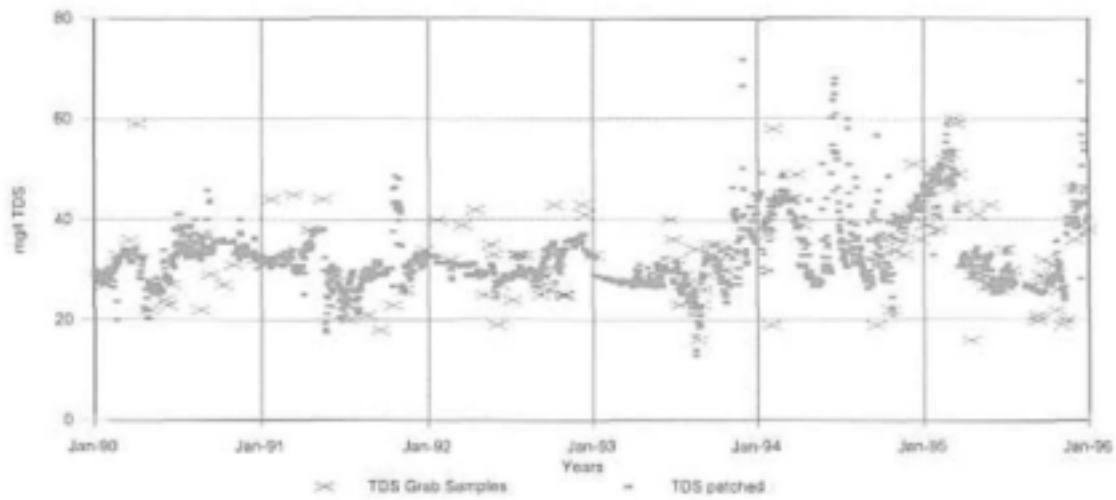


FIGURE 1.2.2 : TDS values for G1H019

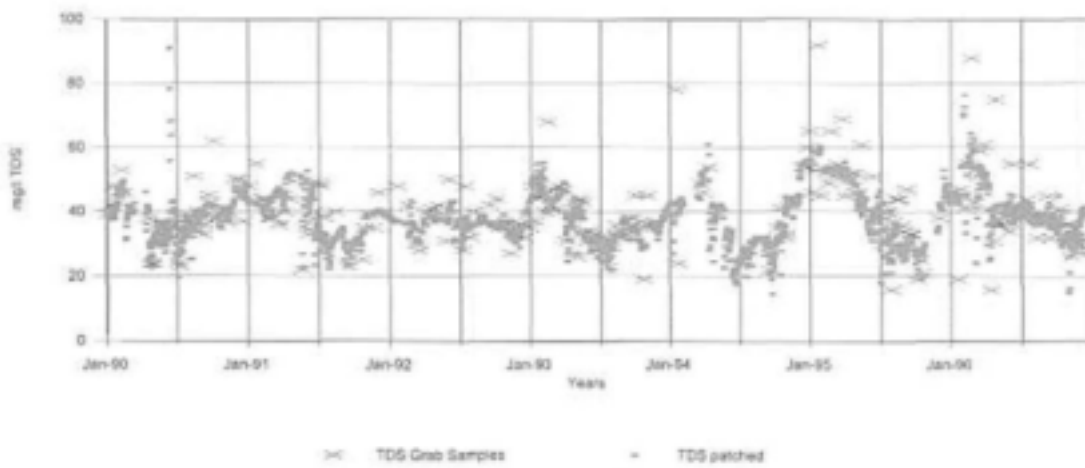
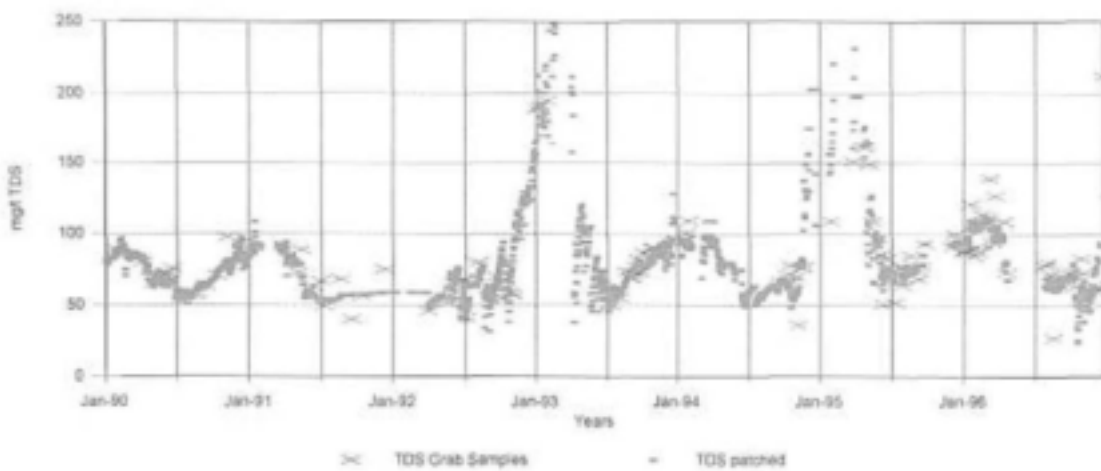
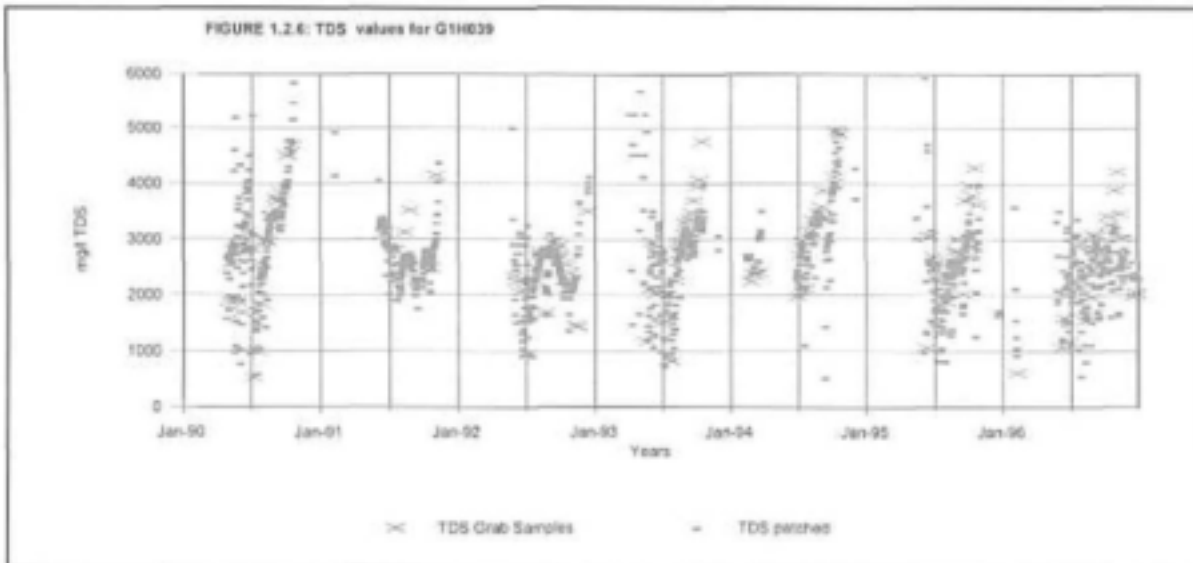
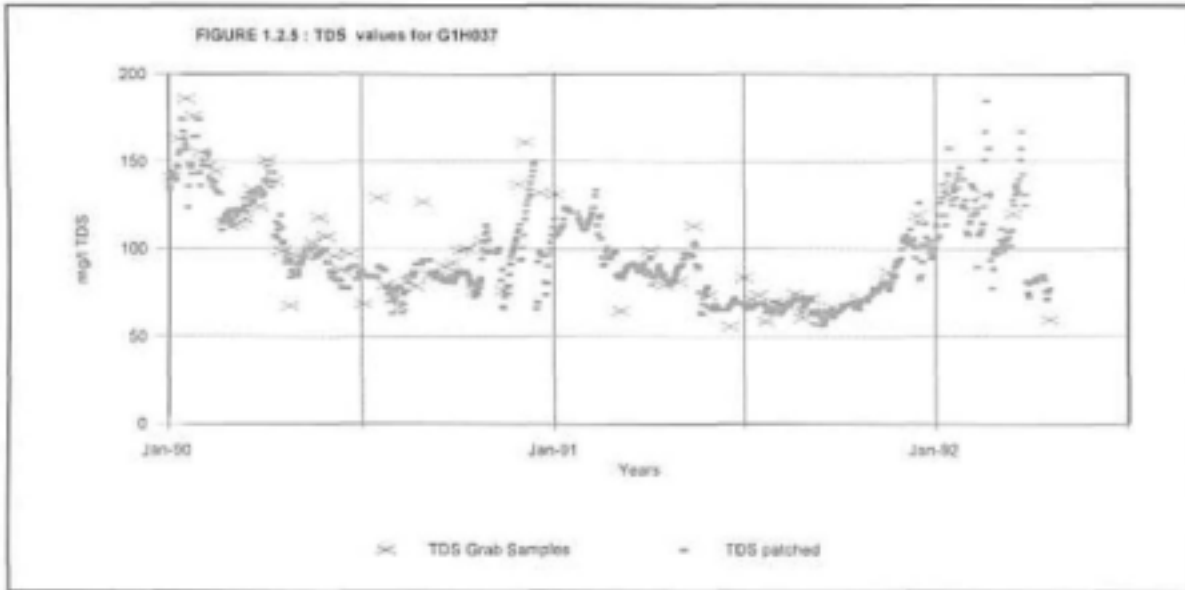
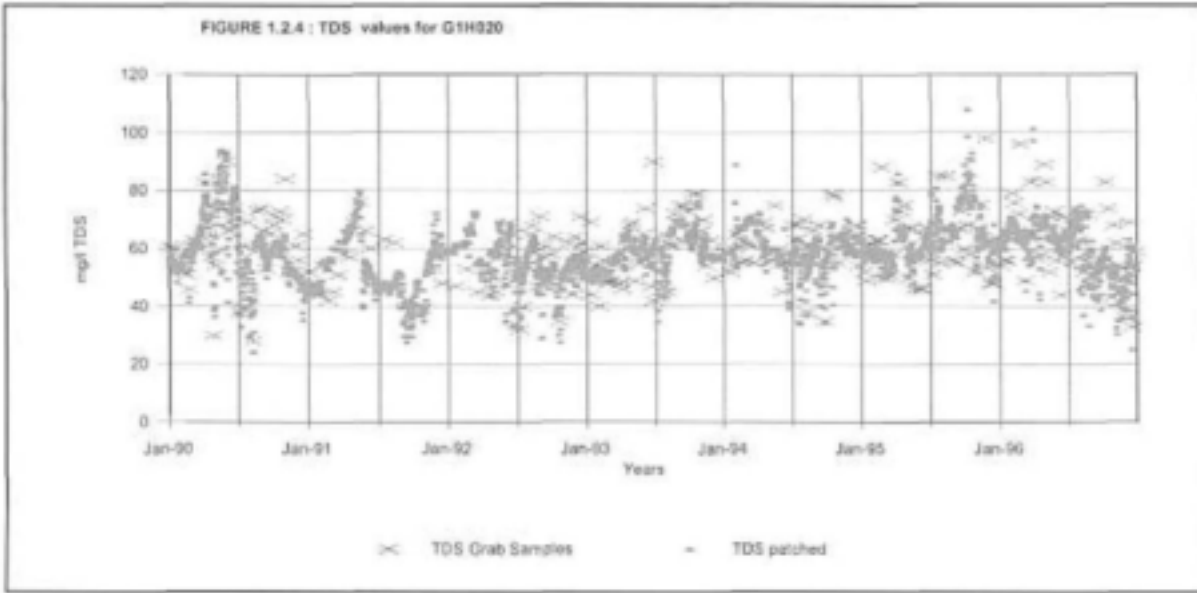
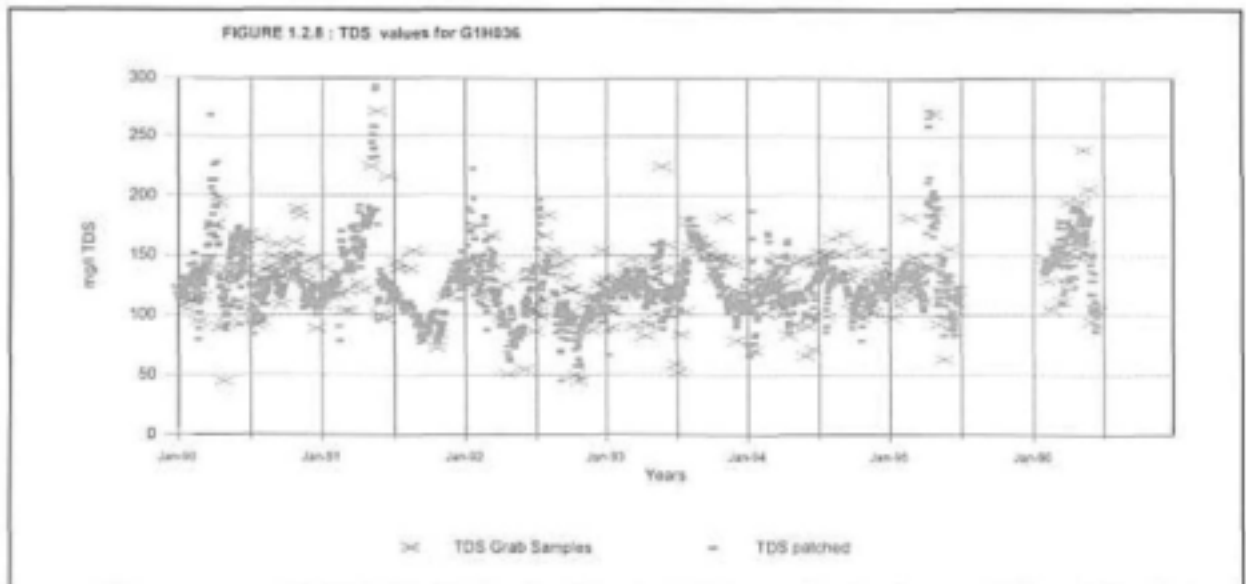
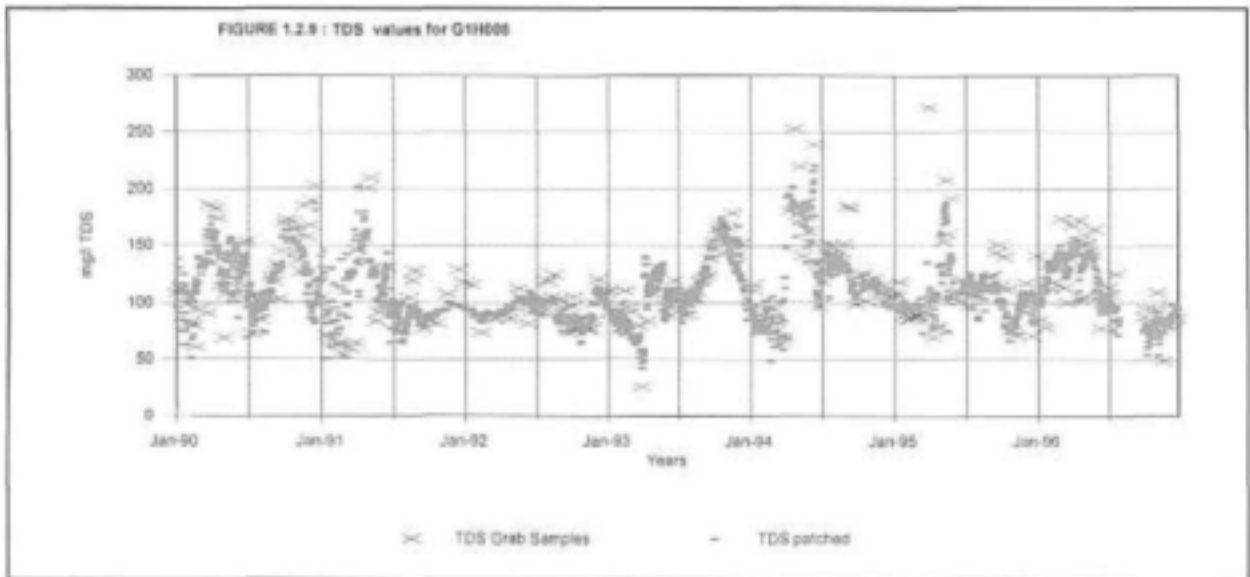
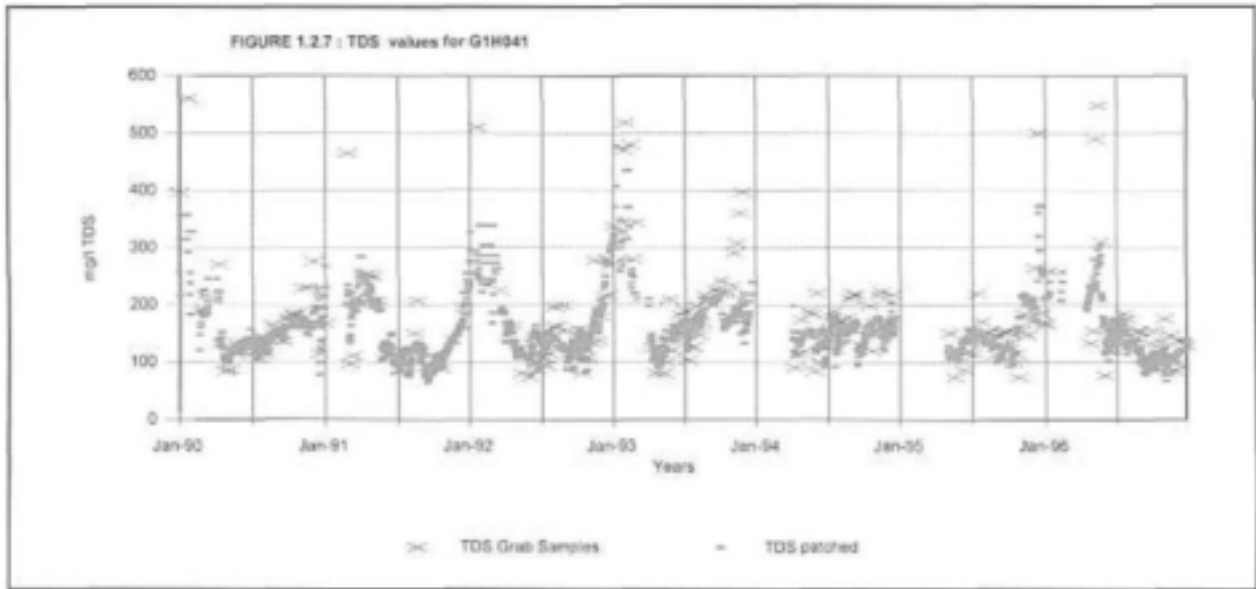
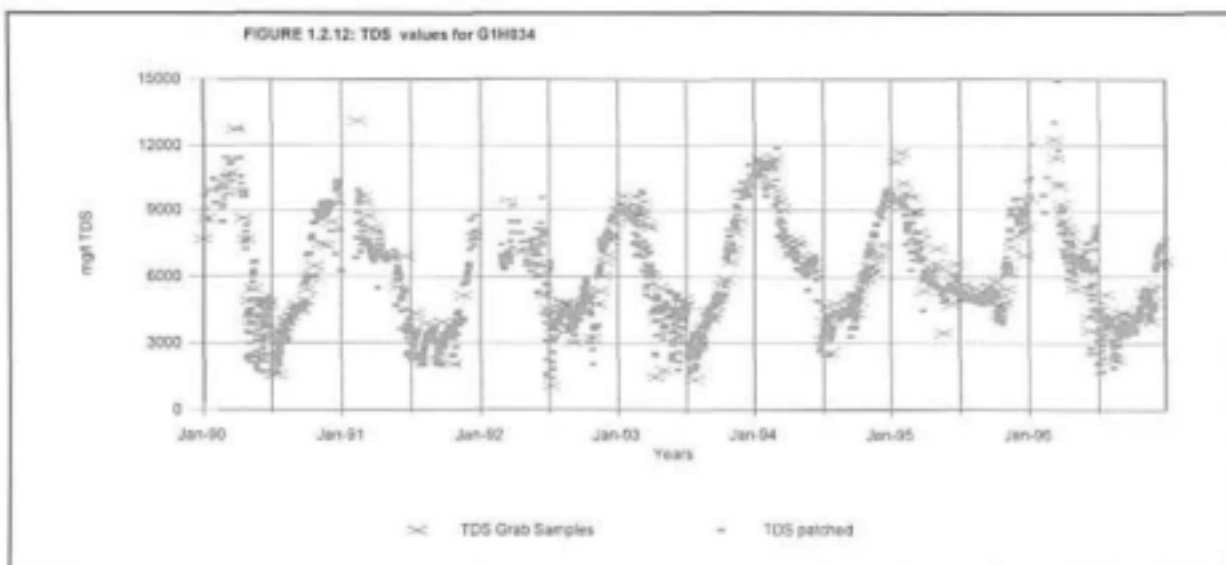
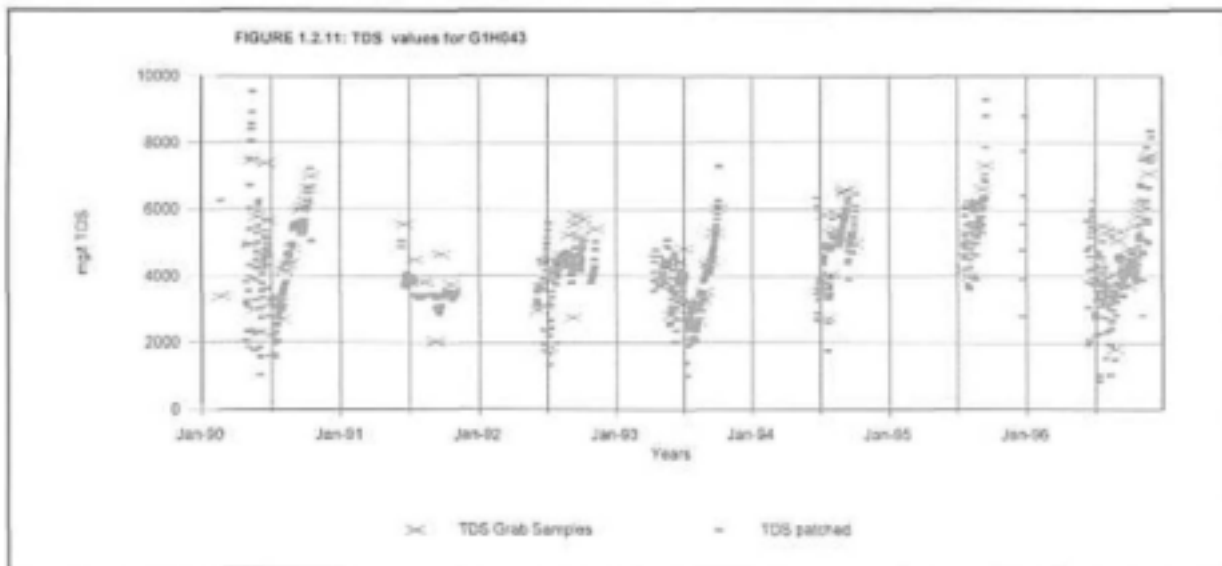
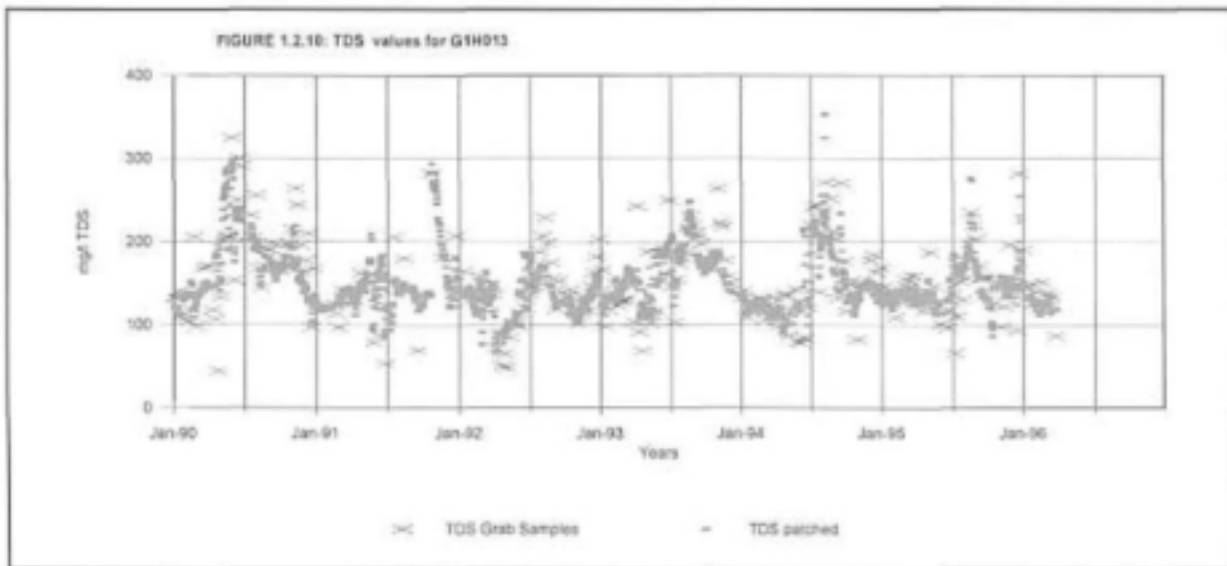


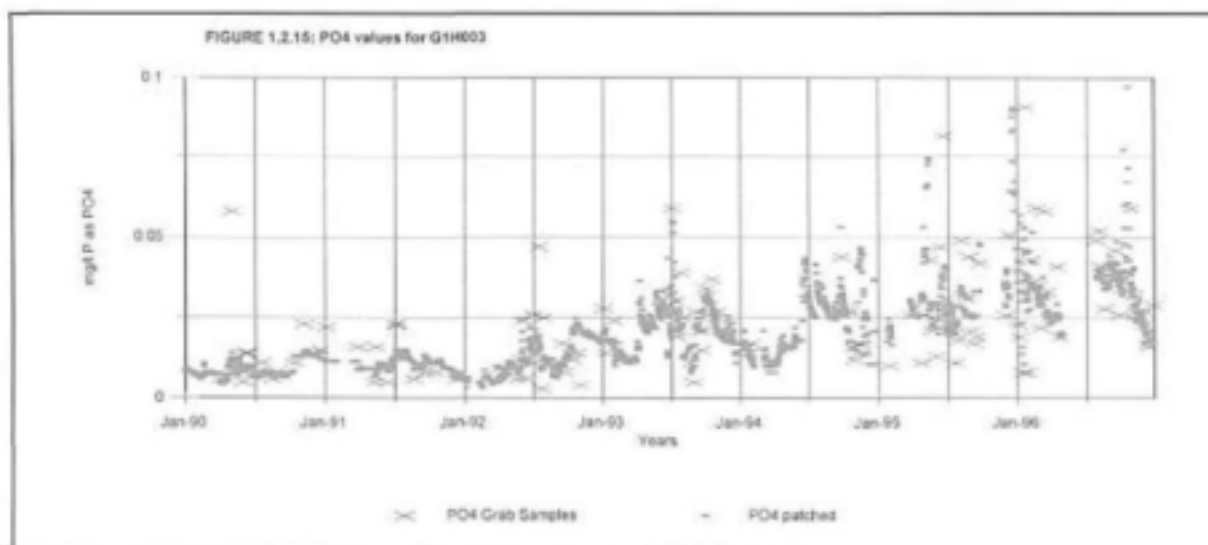
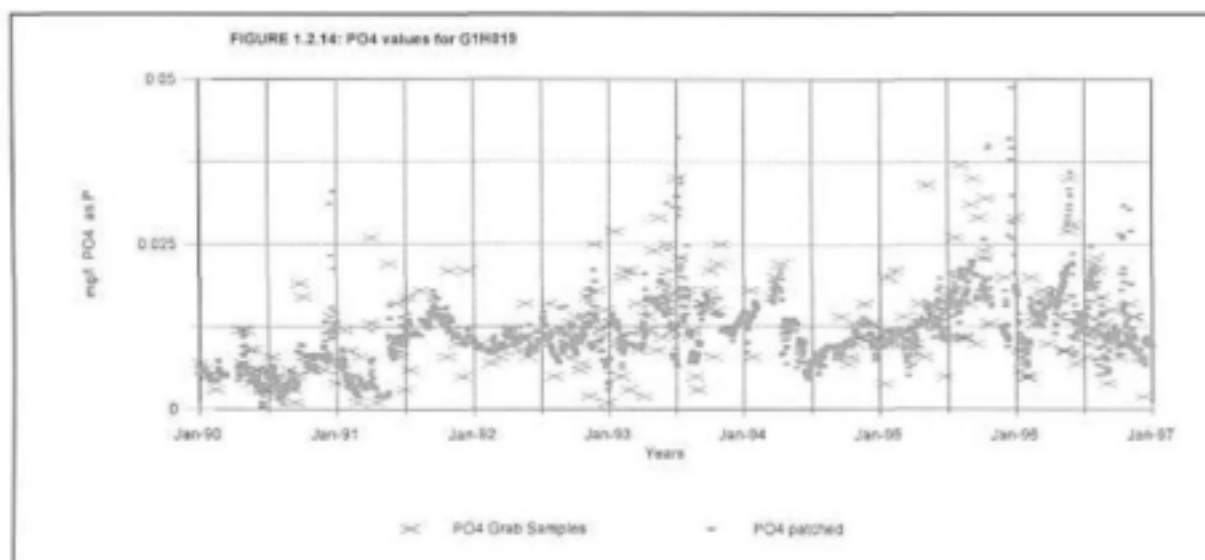
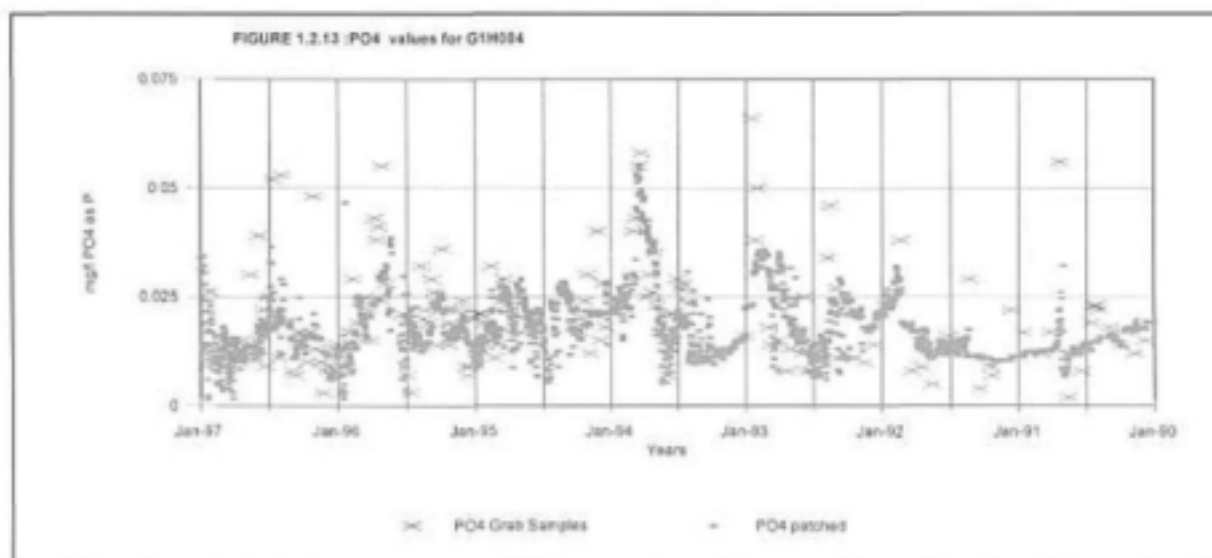
FIGURE 1.2.3: TDS values for G1H003

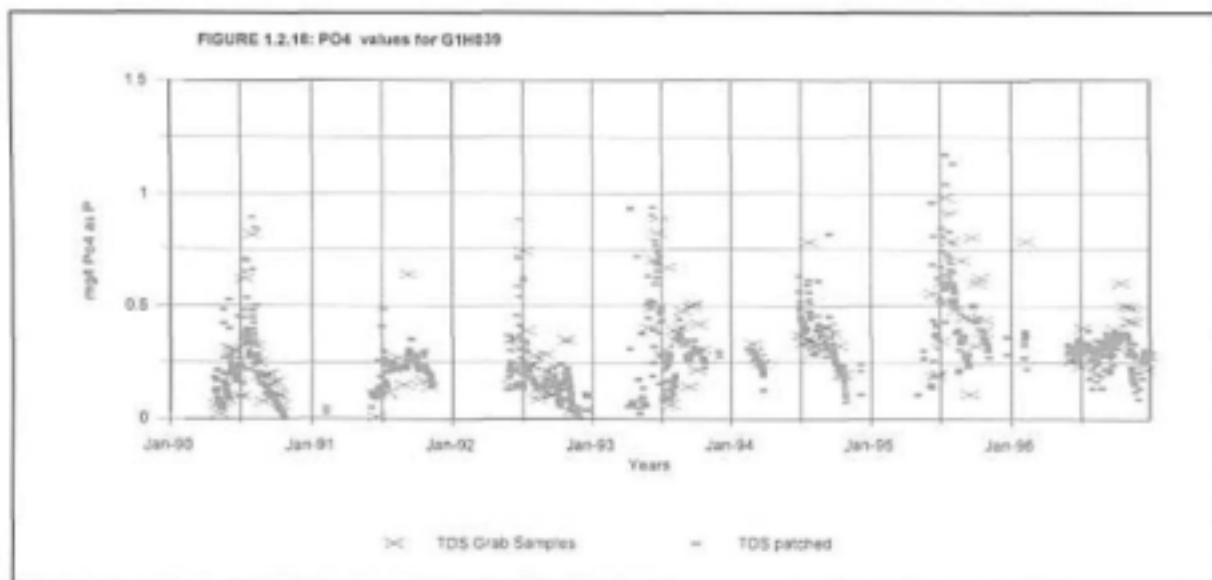
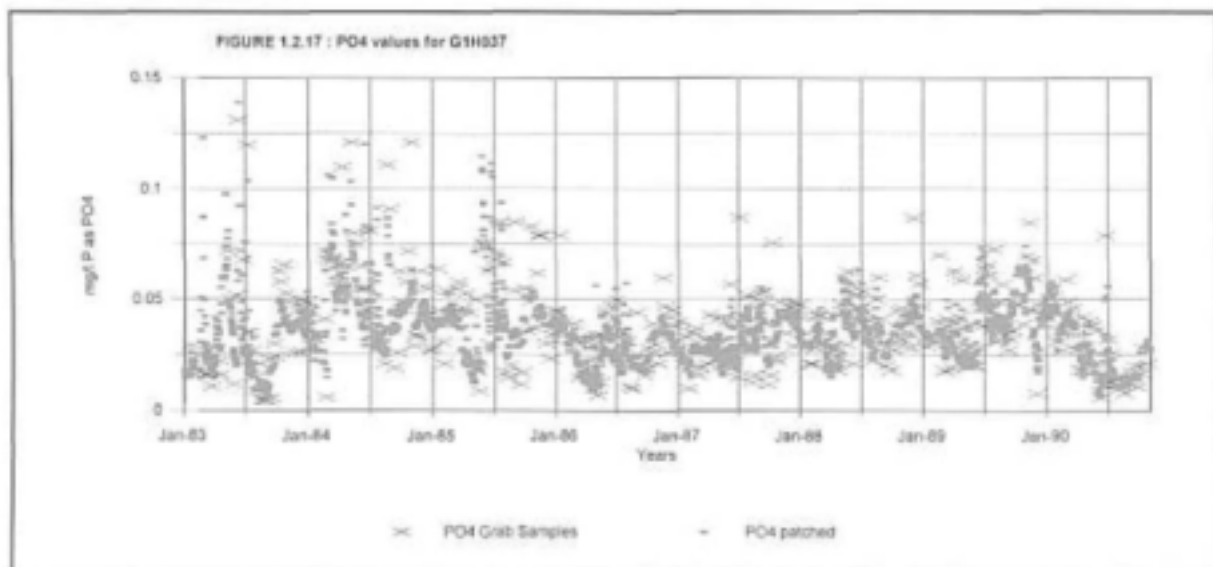
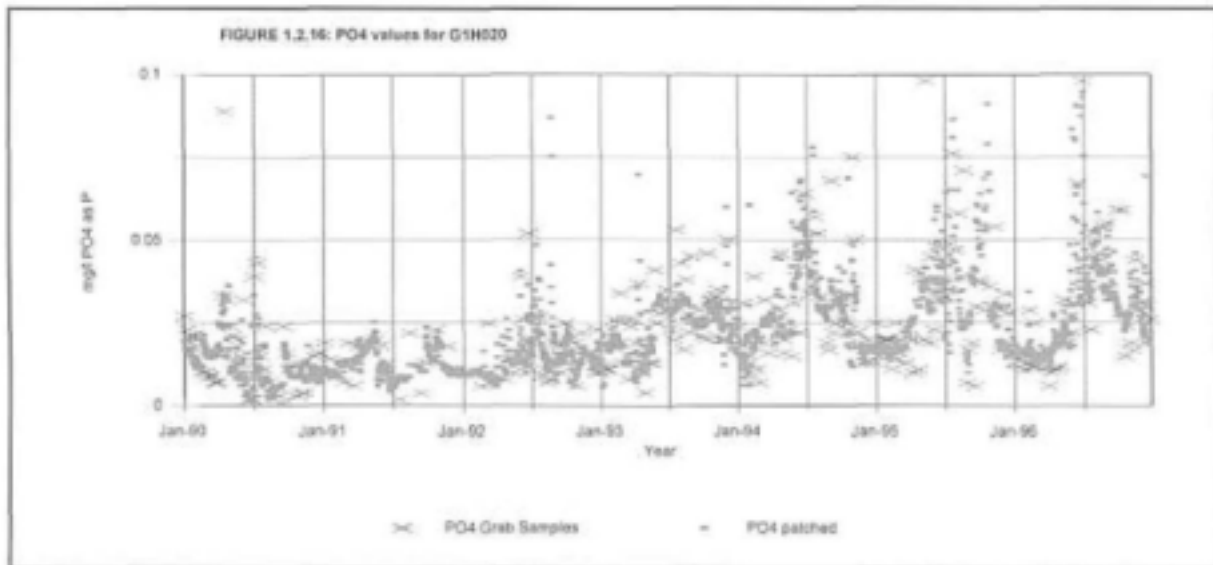


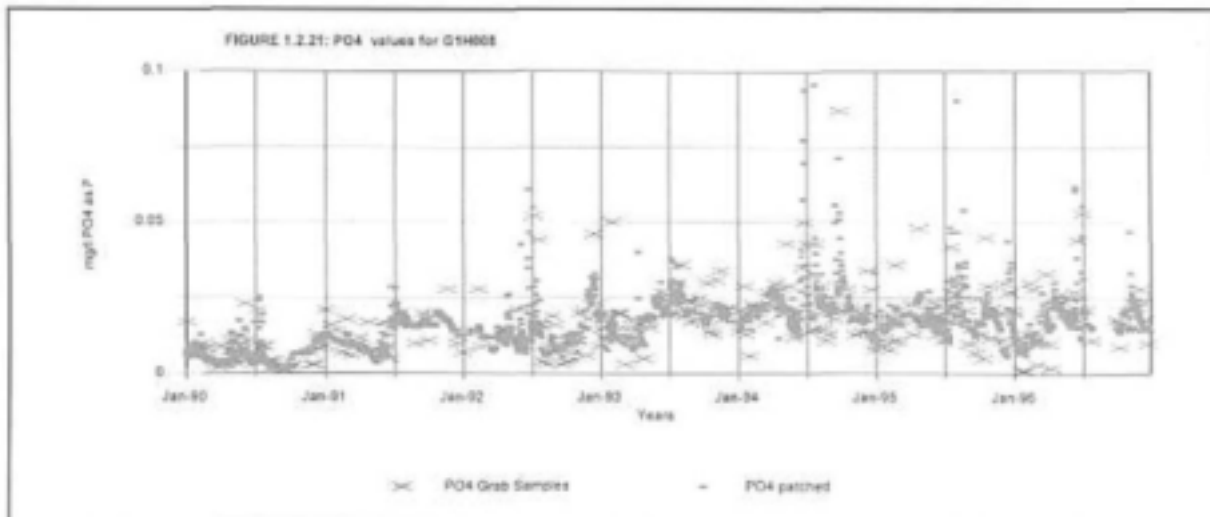
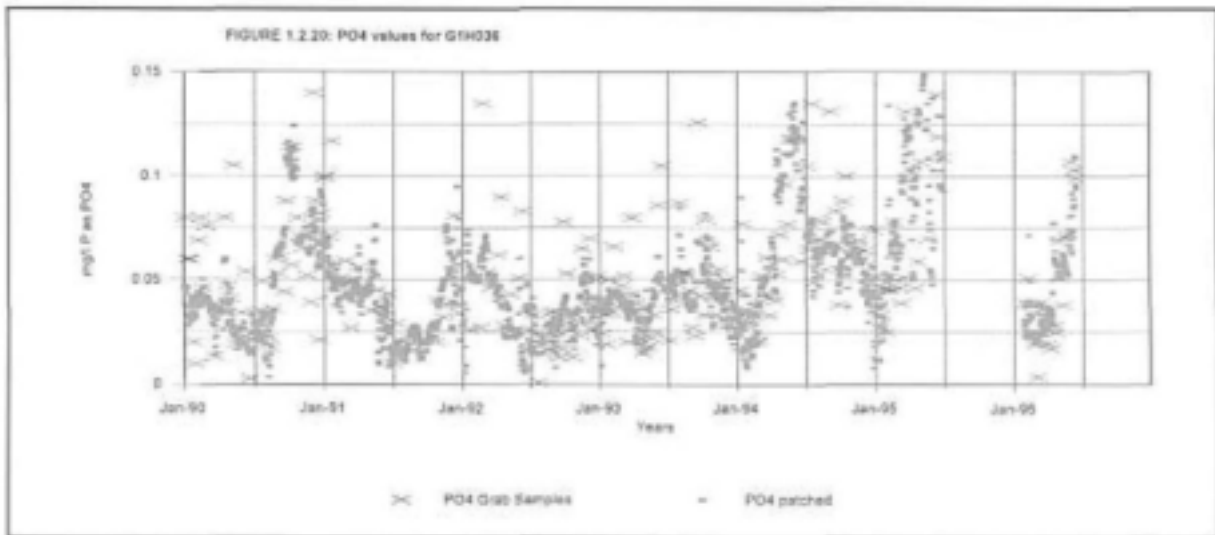
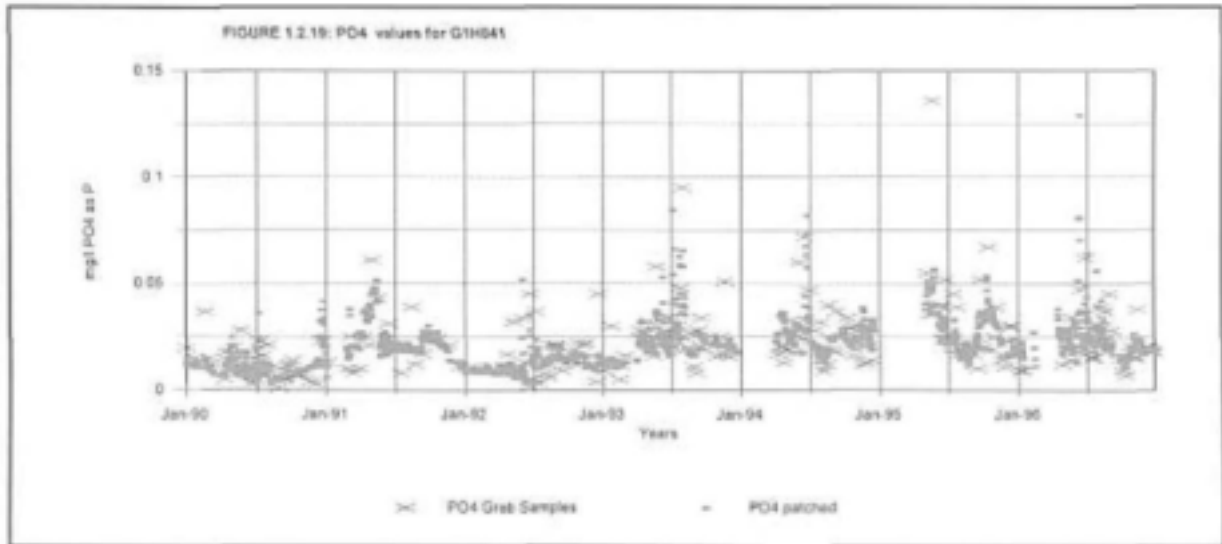


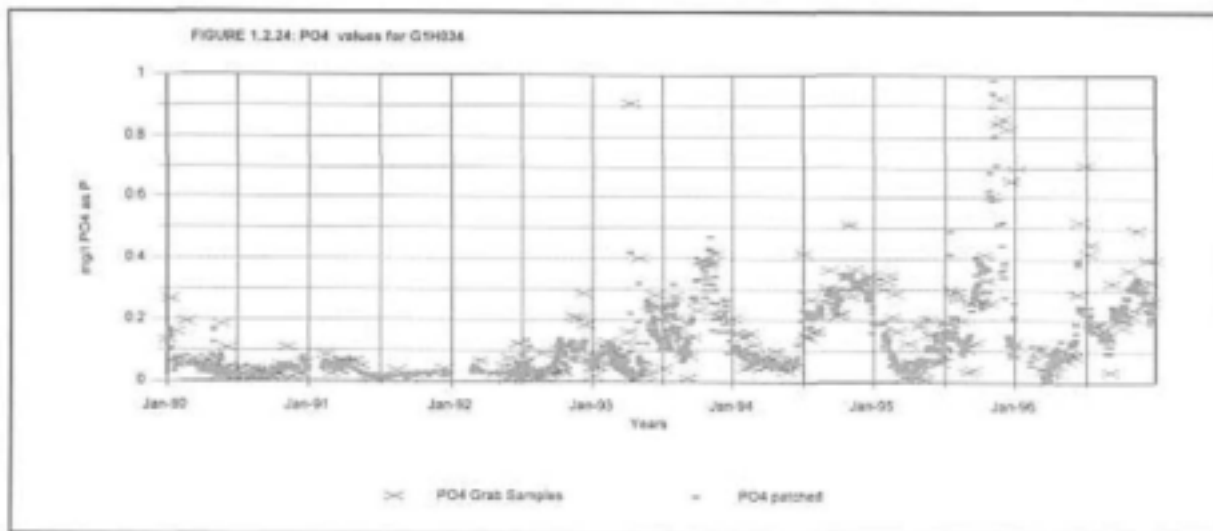
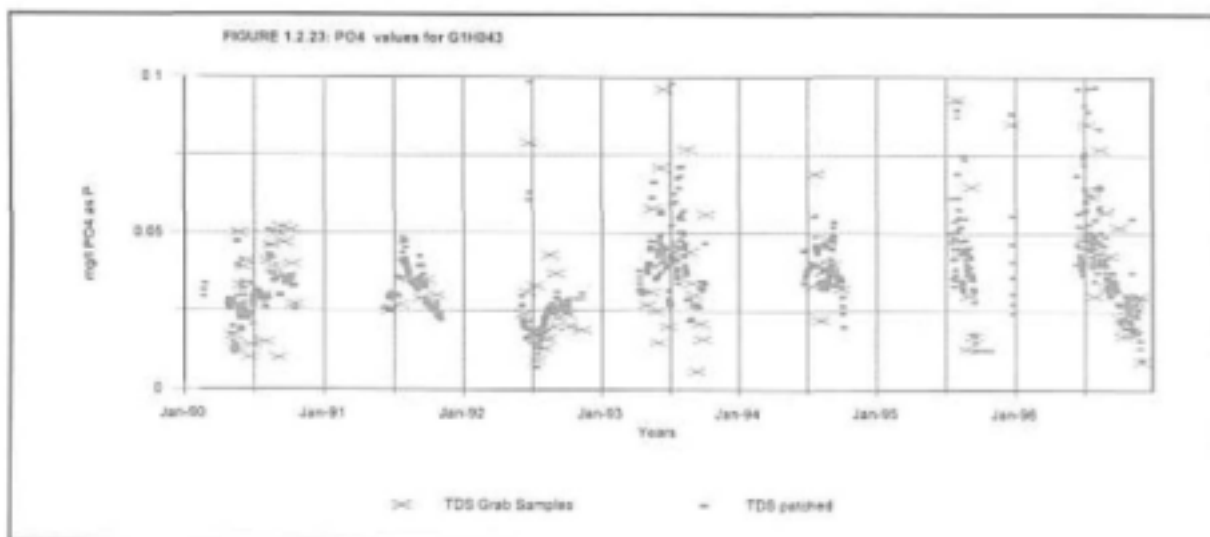
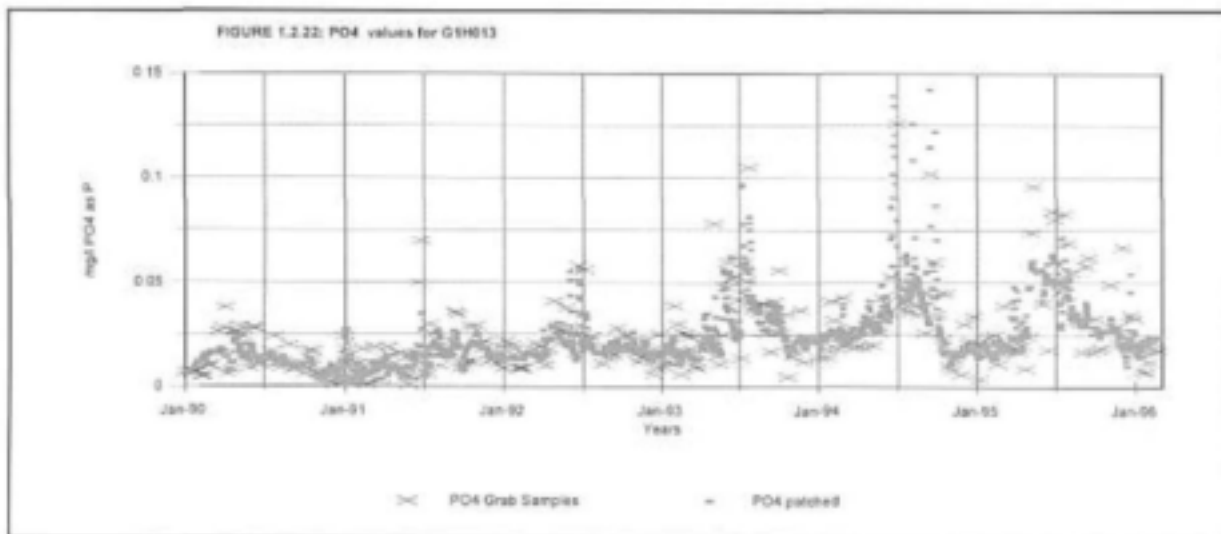












APPENDIX 1.3

**FLOW MODEL SENSITIVITY
DATA PREPARATION AND CONFIGURATION OF THE DUFLOW MODEL
TABLES AND GRAPHS**

Figure 1.3.1 : Discharge at G1H020 for high flows (calibration simulation)

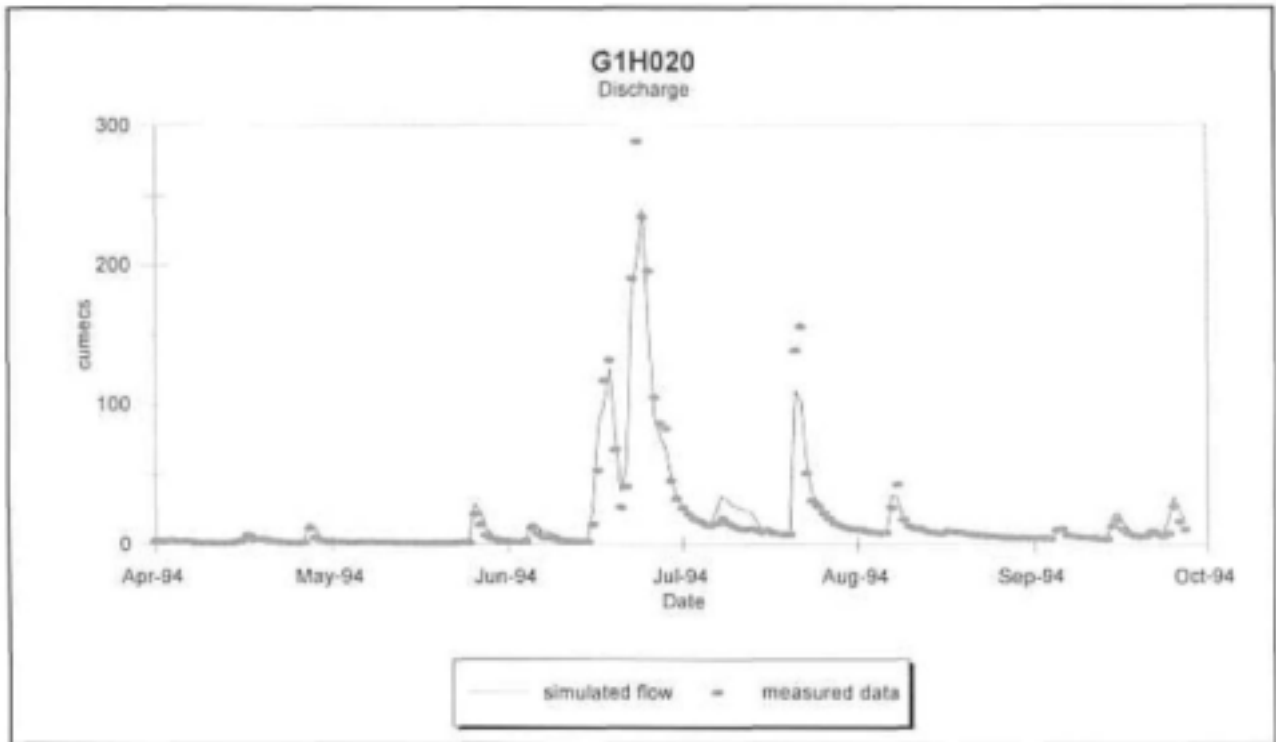


Figure 1.3.2 : Discharge at G1H020 for low flows (calibration simulation)

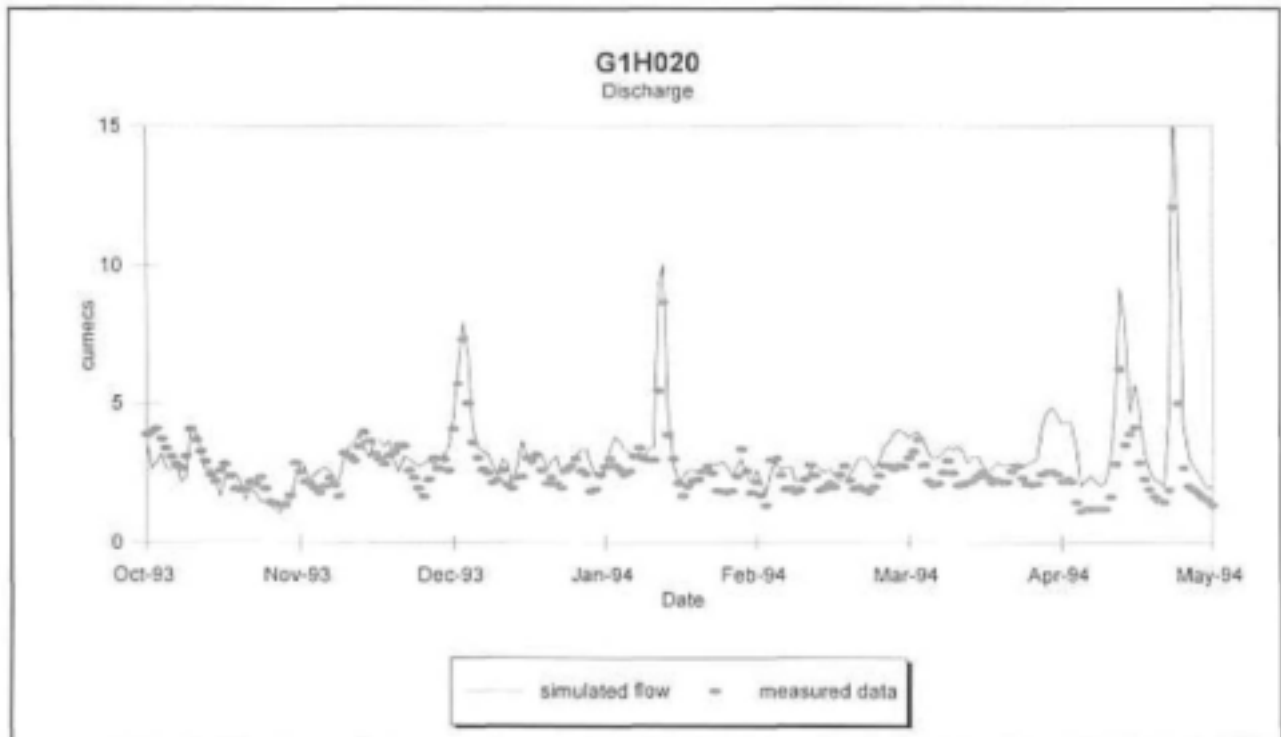


Figure 1.3.3 : Discharge at G1H036 for high flows (calibration simulation)

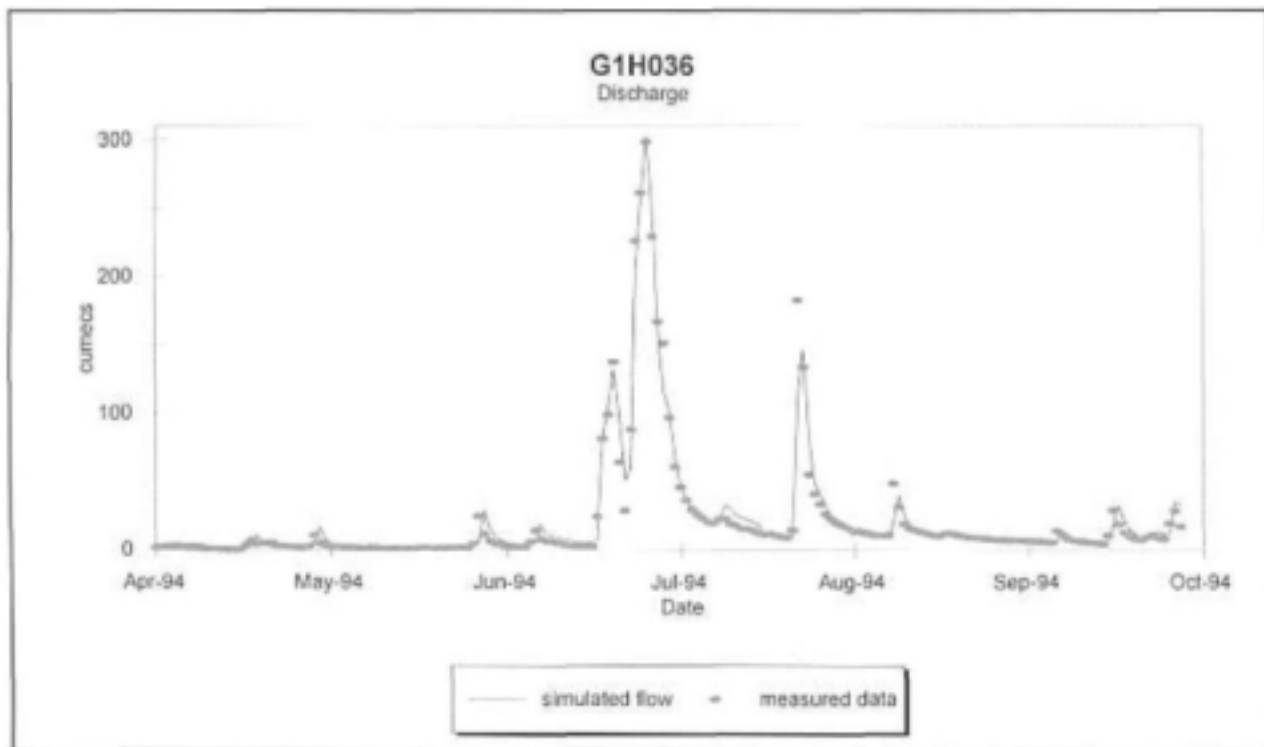


Figure 1.3.4 : Discharge at G1H036 for low flows (calibration simulation)

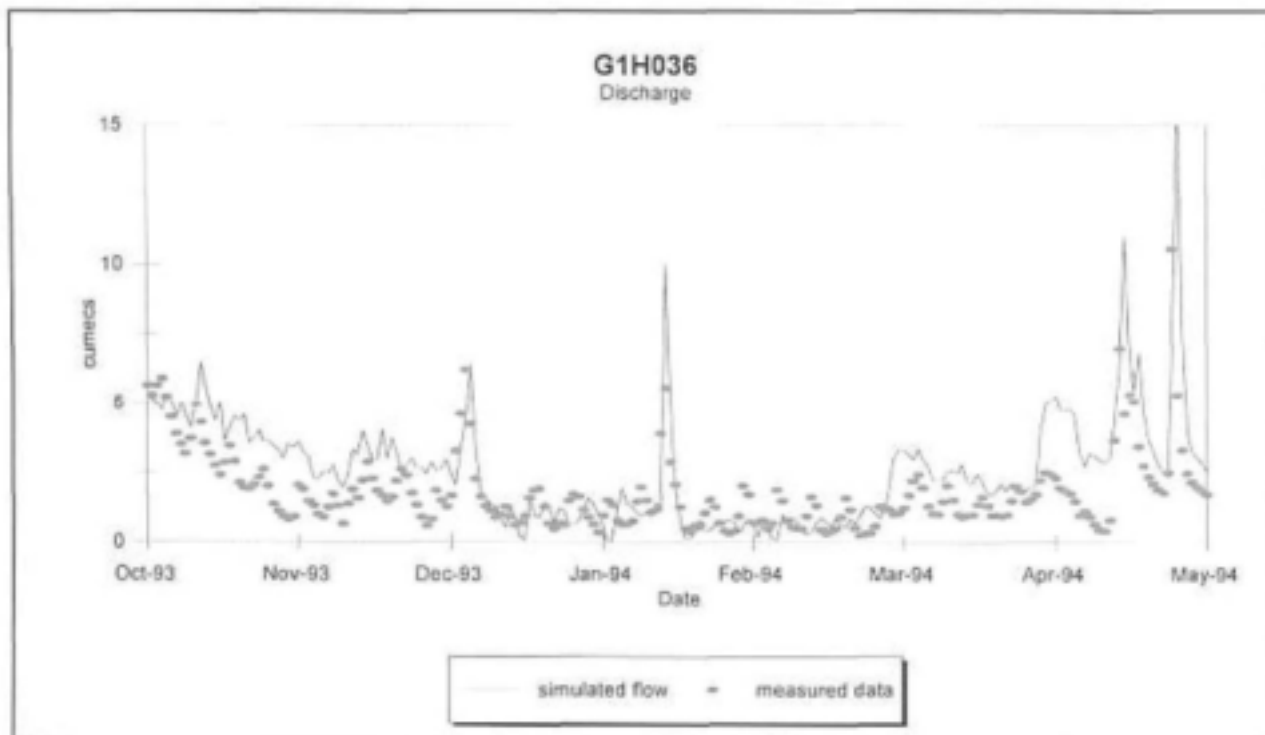


Figure 1.3.5 : Discharge at G1H013 for high flows (calibration simulation)

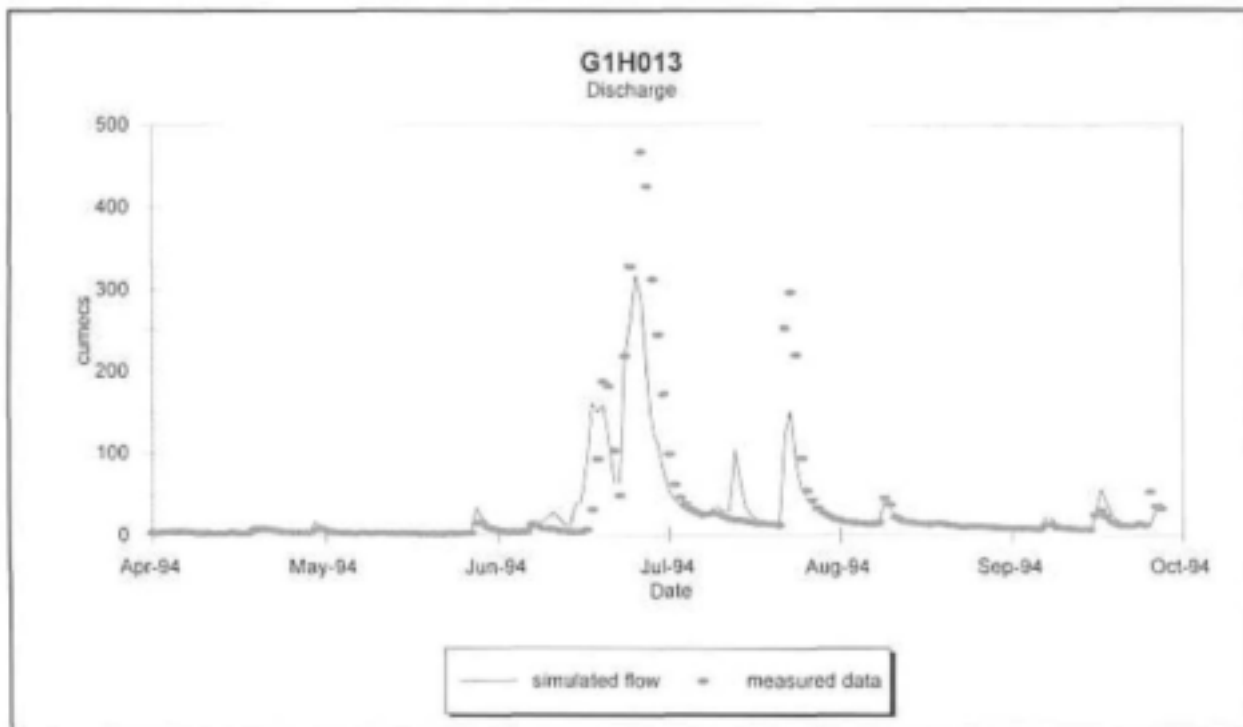


Figure 1.3.6 : Discharge at G1H013 for low flows (calibration simulation)

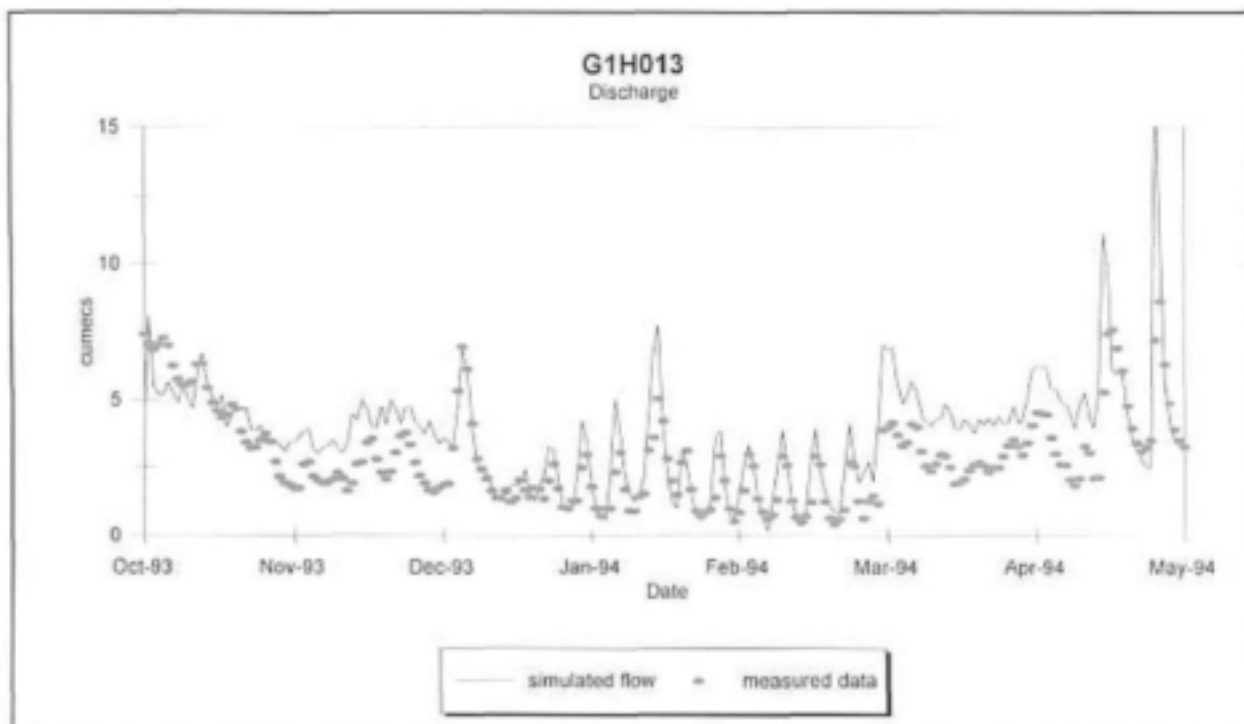


Figure 1.3.7 : Discharge at G1R003 for high flows (calibration simulation)

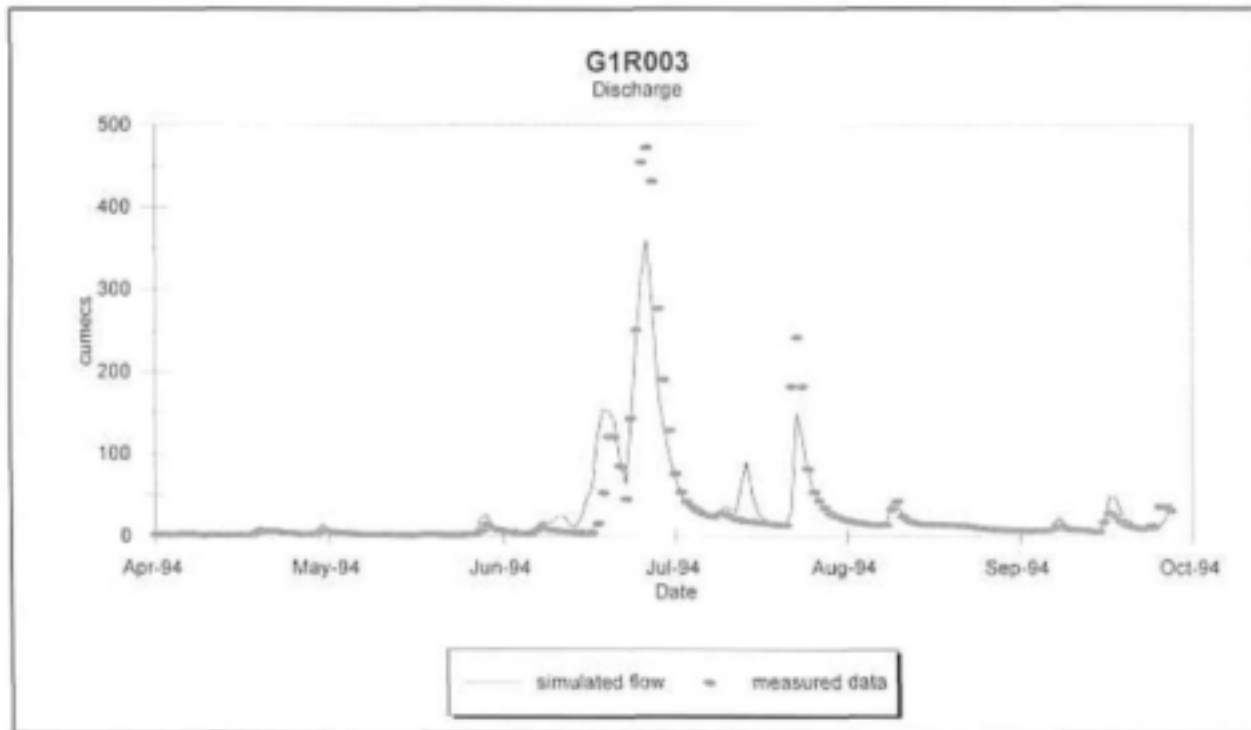


Figure 1.3.8 : Discharge at G1R003 for low flows (calibration simulation)

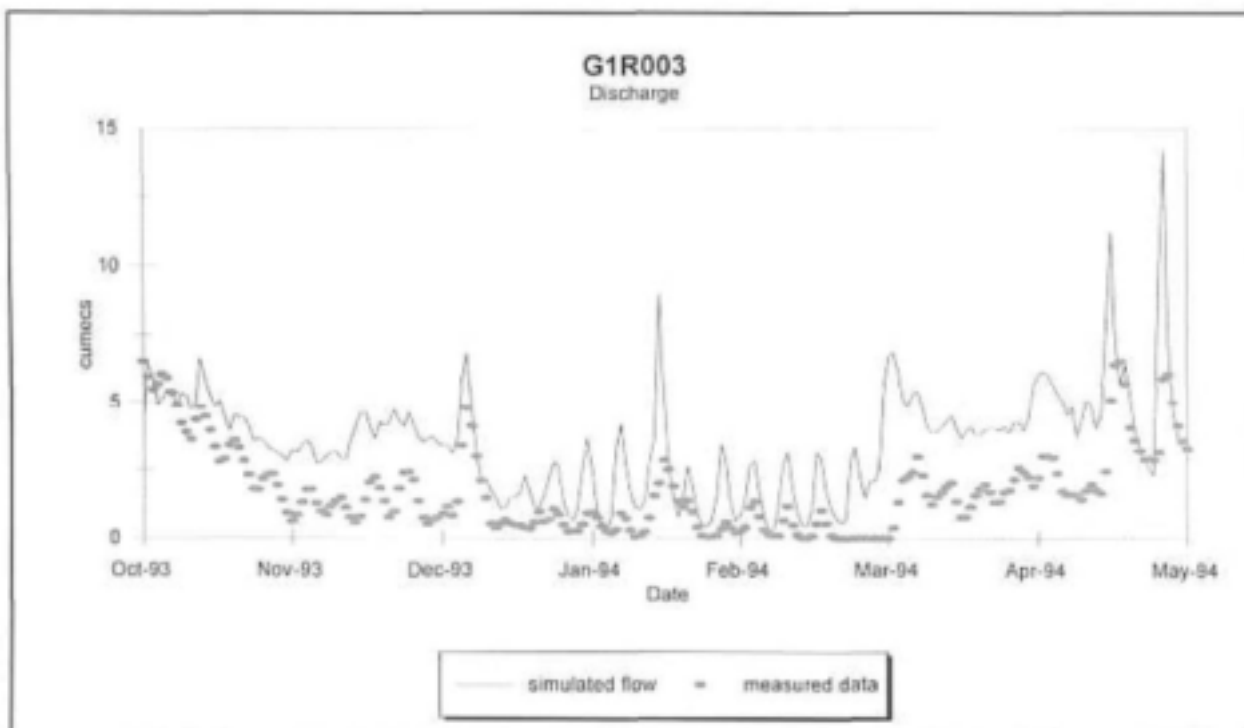
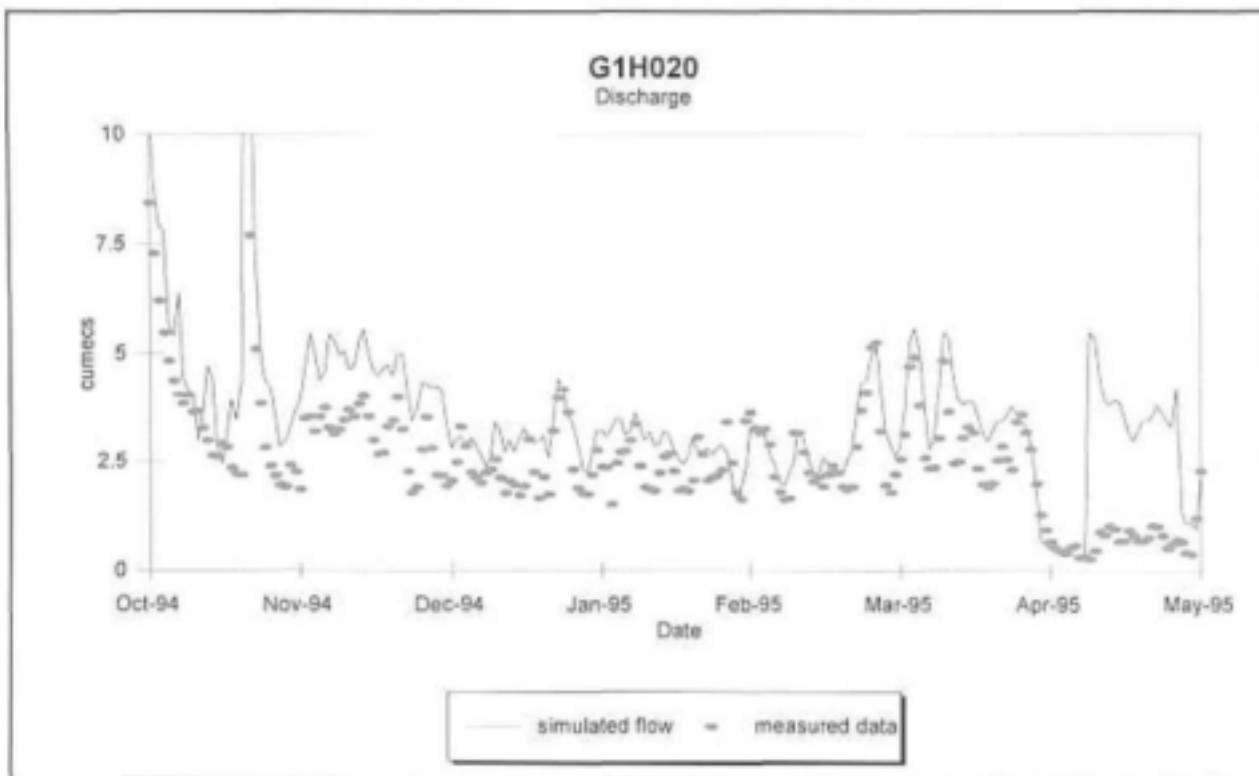


Figure 1.3.9 : Discharge at G1H020 for high flows (verification simulation)

Figure 1.3.10 : Discharge at G1H020 for low flows (verification simulation)



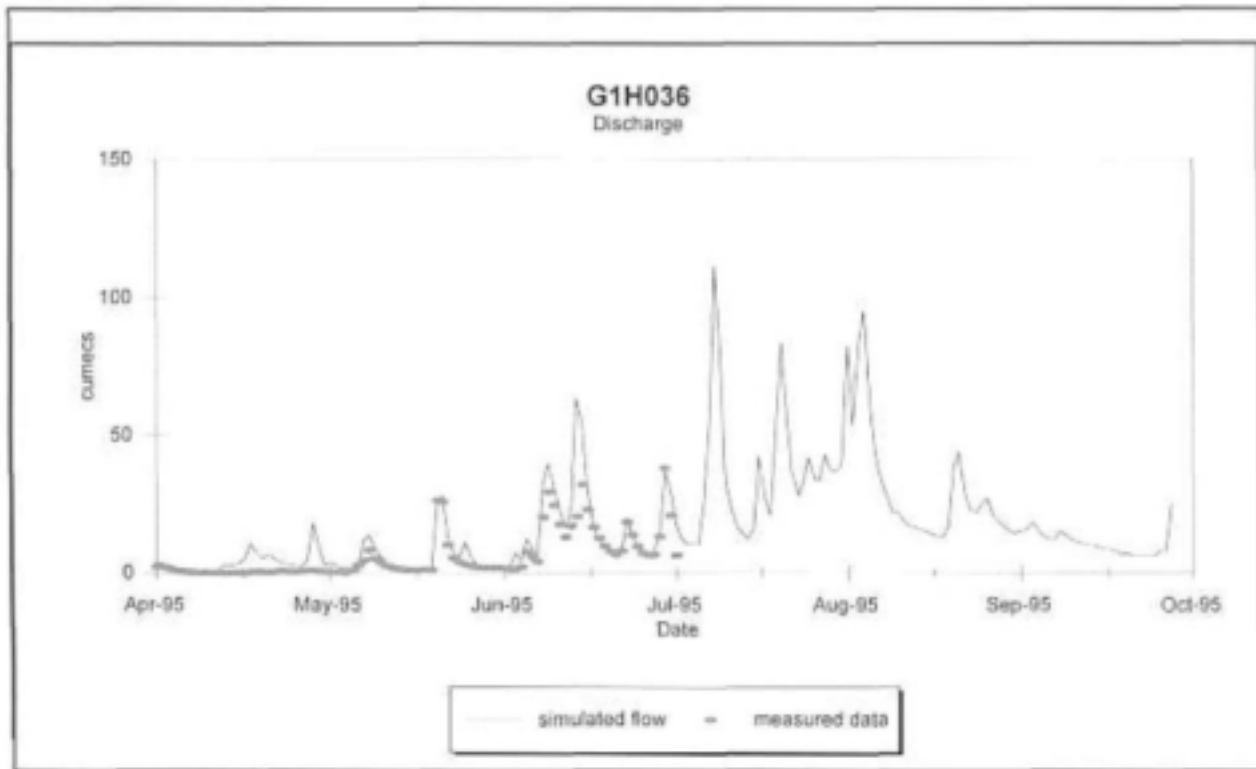


Figure 1.3.11 : Discharge at G1H036 for high flows

(verification simulation)

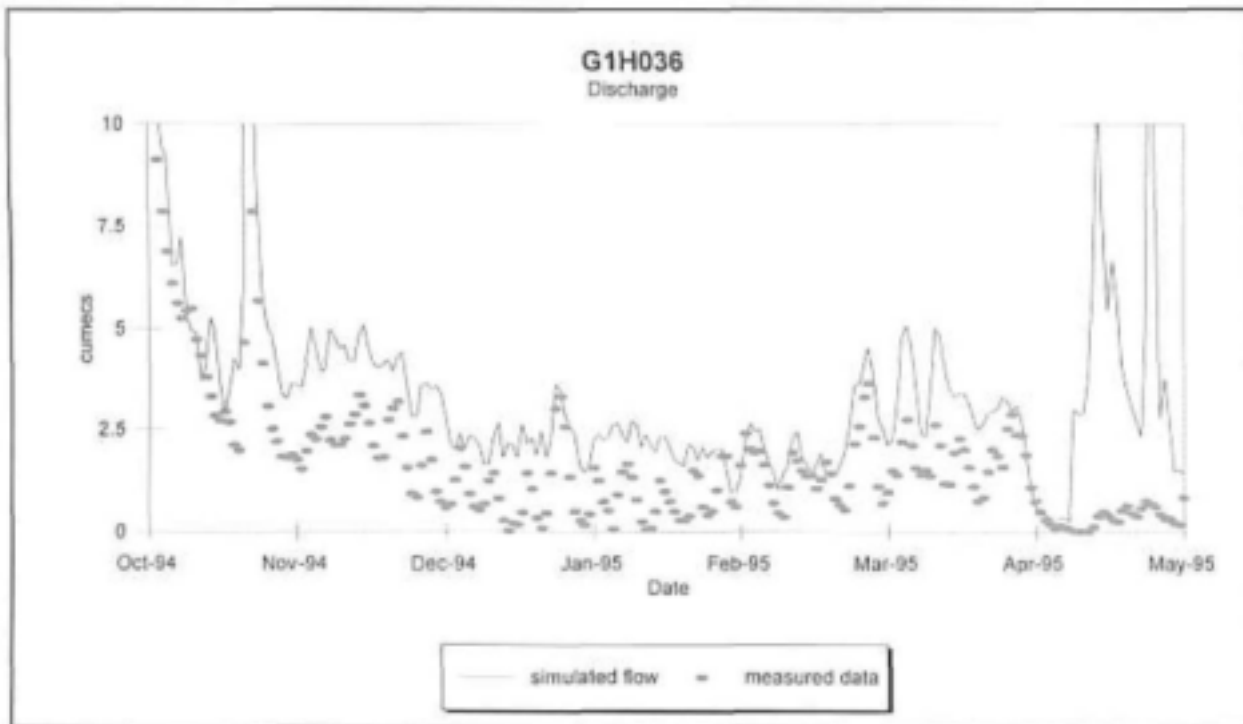


Figure 1.3.12

Discharge at G1H036 for low flows (verification simulation)

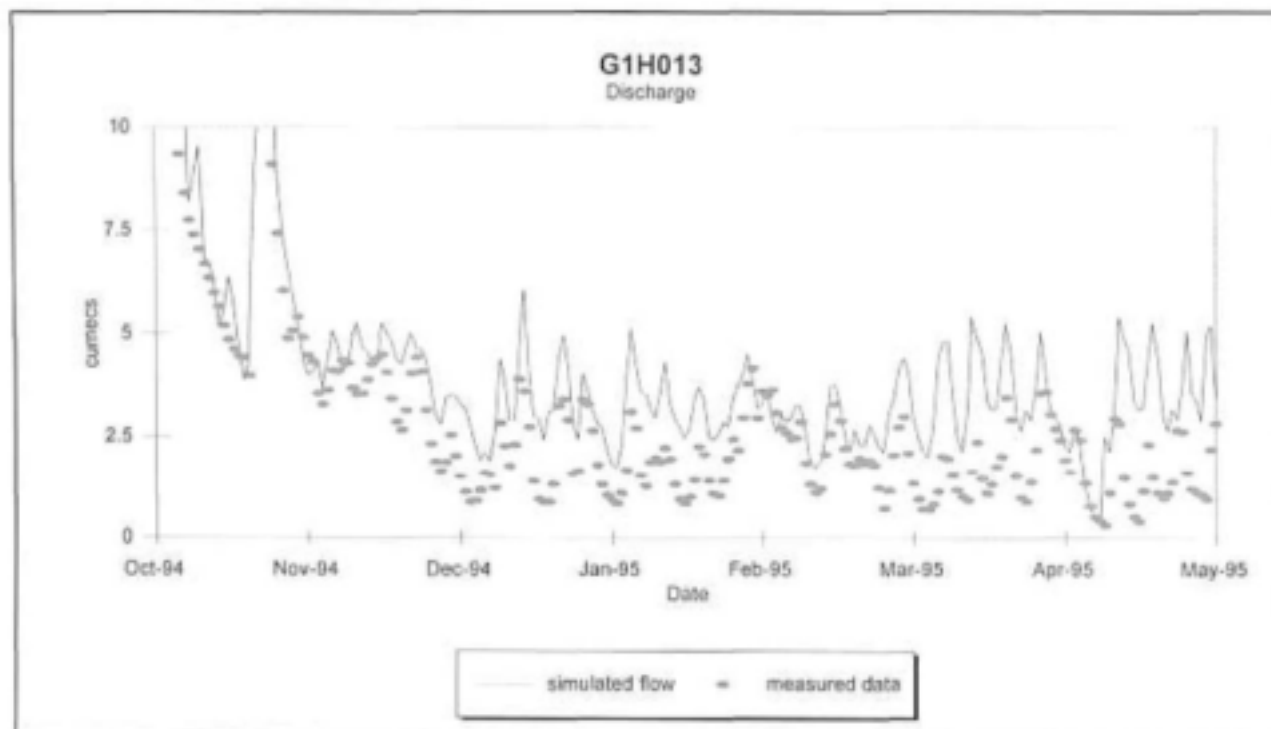
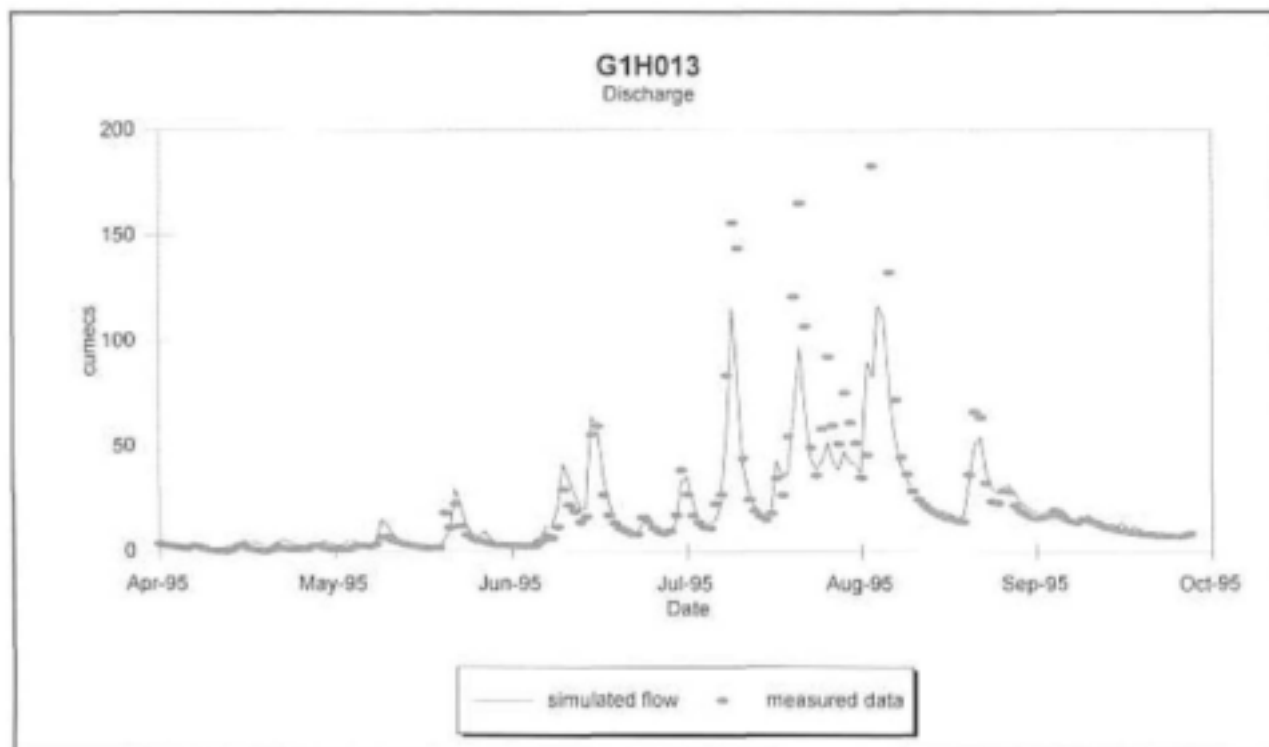


Figure 1.3.13 : Discharge at G1H013 for high flows (verification simulation)

verification simulation)

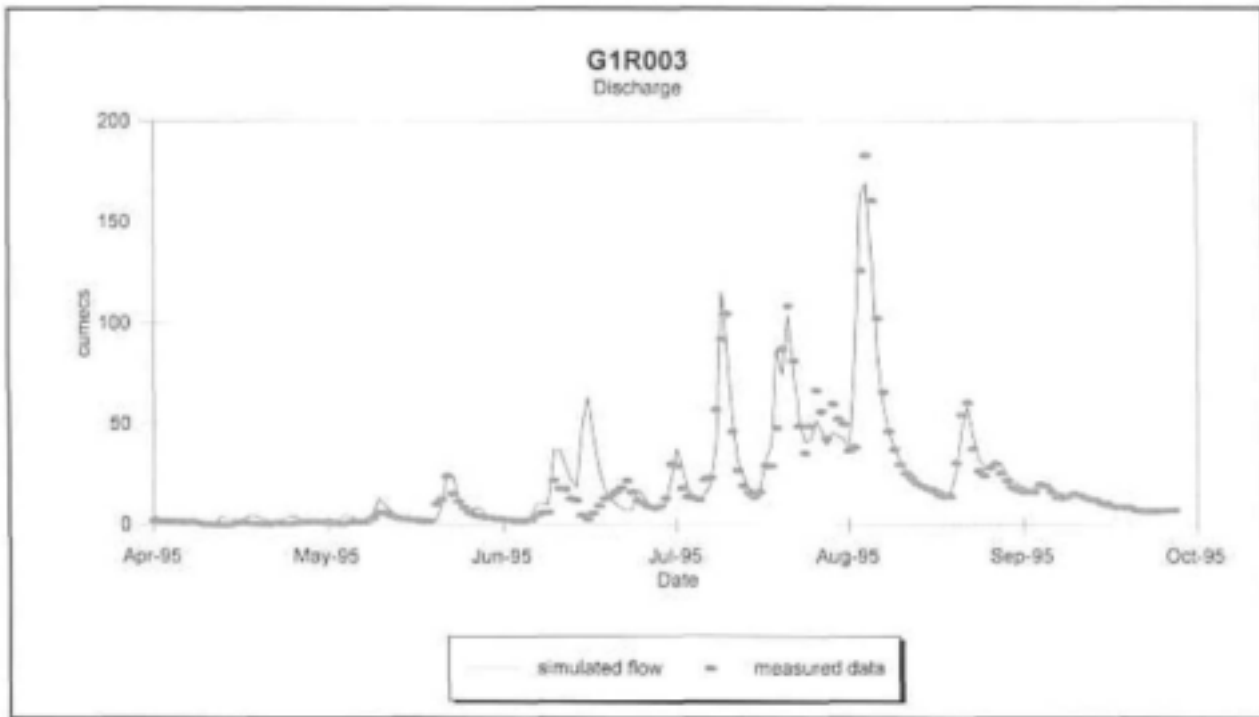
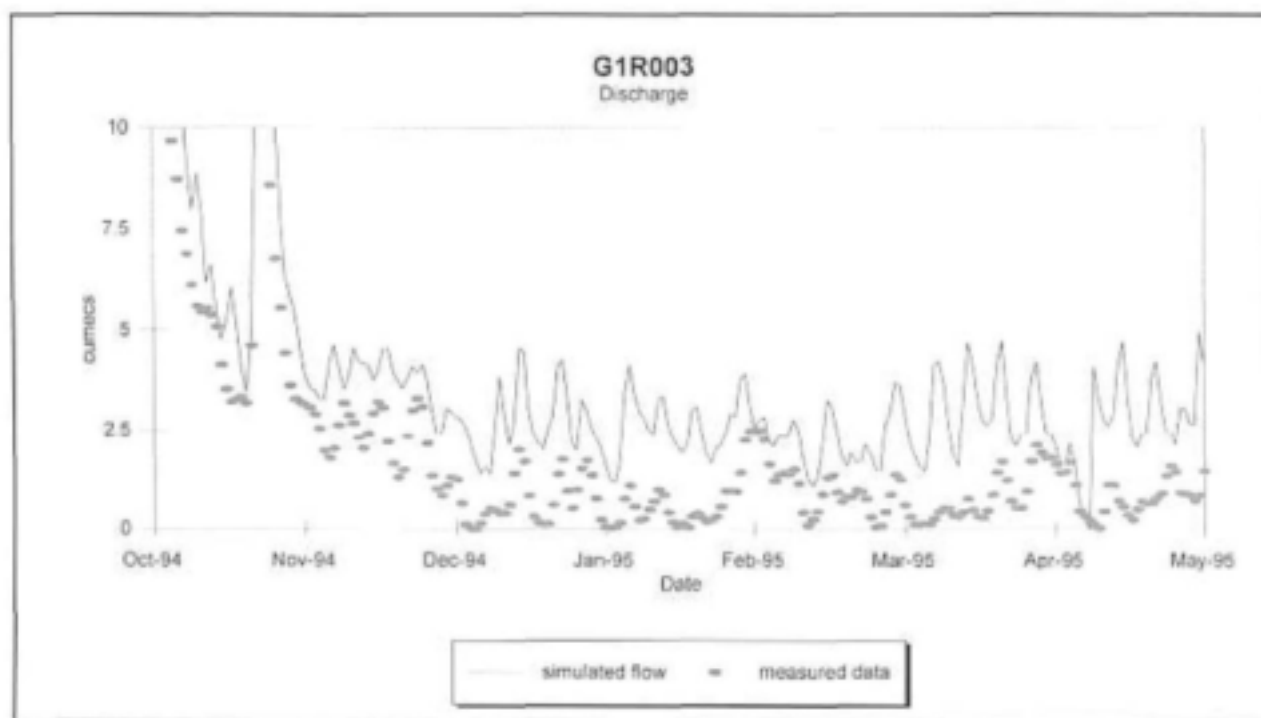


Figure 1.3.14 : Discharge at G1H013 for low flows (verification simulation)

Figure 1.3.15 : Discharge at G1R003 for high flows (verification simulation)

Figure 1.3.16 : Discharge at G1R003 for low flows (verification simulation)



APPENDIX 1.4

WATER QUALITY MODEL SENSITIVITY, CALIBRATION AND VERIFICATION
TABLES AND GRAPHS

Table 1.4.1: Results of TDS Loads after calibration

| | Total Load measured (tons) | Total Load simulated (tons) | % diff in total load | mean measured (g/s) | mean simulated (g/s) | Coeff of determination (R ²) | Coeff of efficiency |
|-------------------------|----------------------------|-----------------------------|----------------------|---------------------|----------------------|--|---------------------|
| Low flow period | | | | | | | |
| G1H020 | 2577 | 2077 | -19.4 | 164 | 132 | 0.84 | 0.13 |
| G1H036 | 3204 | 5401 | 68 | 204 | 343 | 0.38 | -2 |
| G1H013 | 6078 | 6751 | 11 | 386 | 429 | 0.51 | -0.16 |
| G1R003 | 5598 | 7595 | 35 | 356 | 483 | 0.75 | 0.2 |
| High flow period | | | | | | | |
| G1H020 | 13220 | 12729 | -3.7 | 836 | 805 | 0.99 | 0.97 |
| G1H036 | 39214 | 54475 | 39 | 2480 | 3445 | 0.89 | 0.74 |
| G1H013 | 82042 | 99558 | 21.3 | 5189 | 6296 | 0.93 | 0.82 |
| G1R003 | 81497 | 133148 | 63 | 5154 | 8421 | 0.94 | -0.06 |
| Yearly | | | | | | | |
| G1H020 | 15798 | 14806 | -6.3 | 501 | 469 | 0.98 | 0.97 |
| G1H036 | 42419 | 58760 | 41 | 1345 | 1898 | 0.9 | 0.78 |
| G1H013 | 88120 | 106309 | 20.6 | 2794 | 3371 | 0.94 | 0.85 |
| G1R003 | 87097 | 140744 | 61 | 2761 | 4462 | 0.95 | 0.15 |

Table 1.4.2: Results of TDS Concentration after calibration

| | mean measured (mg/l) | mean simulated (mg/l) | % error in mean | Coeff of determination (R ²) |
|-------------------------|----------------------|-----------------------|-----------------|--|
| Low flow period | | | | |
| G1H020 | 62.6 | 43 | -31 | 0.24 |
| G1H036 | 120 | 136 | 13.8 | 0.47 |
| G1H013 | 141 | 123 | -12.3 | 0.03 |
| G1R003 | 219 | 162 | -26 | 0.1 |
| High flow period | | | | |
| G1H020 | 56.5 | 41 | -27 | 0.3 |
| G1H036 | 123 | 176.6 | 44 | 0.5 |
| G1H013 | 158 | 196 | 23 | 0.67 |
| G1R003 | 210 | 224 | 6.7 | 0.57 |
| Yearly | | | | |
| G1H020 | 59.5 | 42 | -29 | 0.08 |
| G1H036 | 121 | 156 | 29 | 0.48 |
| G1H013 | 149 | 159 | 6.8 | 0.56 |
| G1R003 | 215 | 193 | -10 | 0.3 |

Table 1.4.3: Results of PO₄ Loads after calibration

| | Total Load measured (tons) | Total Load simulated (tons) | % diff in total load | mean measured (g/s) | mean simulated (g/s) | Coeff of determination (R ²) | Coeff of efficiency |
|------------------|----------------------------|-----------------------------|----------------------|---------------------|----------------------|--|---------------------|
| Low flow period | | | | | | | |
| G1H020 | 1.02 | 1.07 | 4.7 | 0.065 | 0.068 | 0.39 | 0.15 |
| G1H036 | 1.2 | 1.2 | 0.6 | 0.076 | 0.077 | 0.75 | 0.48 |
| G1H013 | 1 | 1.4 | 38 | 0.06 | 0.09 | 0.76 | 0.3 |
| G1R003 | 0.6 | 1.2 | 103 | 0.04 | 0.08 | 0.98 | 0.92 |
| High flow period | | | | | | | |
| G1H020 | 13.9 | 7.9 | -42 | 0.9 | 0.5 | 0.95 | 0.63 |
| G1H036 | 28.6 | 15.9 | -44 | 1.8 | 1 | 0.96 | 0.66 |
| G1H013 | 48.2 | 21.2 | -56 | 3 | 1.3 | 0.96 | 0.51 |
| G1R003 | 25.6 | 24 | -6.5 | 1.6 | 1.5 | 0.98 | 0.91 |
| Yearly | | | | | | | |
| G1H020 | 14.9 | 9 | -39 | 0.47 | 0.28 | 0.95 | 0.67 |
| G1H036 | 29.8 | 17.2 | -42 | 0.95 | 0.54 | 0.96 | 0.69 |
| G1H013 | 49.3 | 22.6 | -54 | 1.56 | 0.71 | 0.96 | 0.57 |
| G1R003 | 26.2 | 25.2 | -4 | 0.83 | 0.8 | 0.98 | 0.92 |

Table 1.4.4: Results of PO₄ Concentration after calibration

| | mean measured | mean simulated | % error in mean | Coeff of determination (R ²) |
|------------------|---------------|----------------|-----------------|--|
| Low flow period | | | | |
| G1H020 | 0.02 | 0.025 | -0.8 | 0.3 |
| G1H036 | 0.04 | 0.026 | -32 | 0.15 |
| G1H013 | 0.024 | 0.023 | -3.4 | 0.2 |
| G1R003 | 0.024 | 0.023 | -5.9 | 0.57 |
| High flow period | | | | |
| G1H020 | 0.023 | 0.023 | -32 | 0.68 |
| G1H036 | 0.08 | 0.04 | -55 | 0 |
| G1H013 | 0.05 | 0.034 | -33 | 0.32 |
| G1R003 | 0.03 | 0.034 | -9.8 | 0.25 |
| Yearly | | | | |
| G1H020 | 0.03 | 0.023 | -20 | 0.49 |
| G1H036 | 0.06 | 0.031 | -48 | 0.25 |
| G1H013 | 0.04 | 0.028 | -24 | 0.42 |
| G1R003 | 0.027 | 0.028 | 2.9 | 0.36 |

Table 1.4.5: Results of Temperature after calibration

| | mean measured | mean simulated | % error in mean | Std Dev measured | Std Dev simulated | Coeff of determination (R ²) |
|-------------------------|---------------|----------------|-----------------|------------------|-------------------|--|
| Low flow period | | | | | | |
| G1H020 | 24 | 23 | -4.4 | 2.5 | 3 | 0.92 |
| G1H036 | 24.6 | 24 | -2.9 | 2.75 | 2.73 | 0.81 |
| G1H013 | 24.2 | 24.5 | 1.5 | 2.52 | 3.57 | 0.85 |
| G1R003 | 25 | 24.7 | -1.6 | 2.5 | 3.5 | 0.85 |
| High flow period | | | | | | |
| G1H020 | 14 | 13 | -7 | 2.56 | 2.54 | 0.92 |
| G1H036 | 13.6 | 12.8 | -5.9 | 2.9 | 2.75 | 0.81 |
| G1H013 | 14.1 | 12.5 | -11 | 2.8 | 2.9 | 0.8 |
| G1R003 | 15.3 | 12.5 | -18 | 2.77 | 2.87 | 0.83 |
| Yearly | | | | | | |
| G1H020 | 19 | 17.98 | -5.4 | 5.62 | 5.7 | 0.98 |
| G1H036 | 19.1 | 18.3 | -3.9 | 6.2 | 6.5 | 0.95 |
| G1H013 | 19.1 | 18.5 | -3.1 | 5.73 | 6.9 | 0.96 |
| G1R003 | 20.15 | 18.5 | -8 | 5.56 | 6.9 | 0.96 |

Table 1.4.6: Results of Oxygen after calibration

| | mean sat. oxygen | mean simulated | % error in mean | Std Dev sat. Oxygen | Std Dev simulated | Coeff of determination (R ²) |
|-------------------------|------------------|----------------|-----------------|---------------------|-------------------|--|
| Low flow period | | | | | | |
| G1H020 | 8.65 | 8.73 | 0.9 | 0.45 | 0.44 | 0.98 |
| G1H036 | 8.55 | 8.61 | 0.7 | 0.52 | 0.5 | 0.97 |
| G1H013 | 8.4 | 8.5 | 0.6 | 0.52 | 0.53 | 0.98 |
| G1R003 | 8.3 | 8.9 | 7.6 | 0.51 | 0.42 | 0.9 |
| High flow period | | | | | | |
| G1H020 | 10.5 | 10.3 | -1.8 | 0.62 | 0.59 | 0.93 |
| G1H036 | 10.7 | 10.6 | -0.6 | 0.72 | 0.86 | 0.7 |
| G1H013 | 10.8 | 10.7 | -0.2 | 0.79 | 0.76 | 0.88 |
| G1R003 | 10.8 | 10.8 | 0 | 0.83 | 0.82 | 0.85 |
| Yearly | | | | | | |
| G1H020 | 9.6 | 9.55 | -0.6 | 0.95 | 0.96 | 0.98 |
| G1H036 | 9.62 | 9.61 | -0.06 | 1.23 | 1.22 | 0.93 |
| G1H013 | 9.6 | 9.62 | 0.15 | 1.35 | 1.31 | 0.98 |
| G1R003 | 9.55 | 9.8 | 3.3 | 1.42 | 4.14 | 0.94 |

Table 1.4.7: Results of TDS Loads after Verification

| | Total Load measured (tons) | Total Load simulated (tons) | % diff in total load | mean measured g/s | mean simulated (g/s) | Coeff of determination (R ²) | Coeff of efficiency |
|-------------------------|----------------------------|-----------------------------|----------------------|-------------------|----------------------|--|---------------------|
| Low flow period | | | | | | | |
| G1H020 | 2683 | 2669 | -0.5 | 171 | 170 | 0.81 | 0.41 |
| G1H036 | 3738 | 4007 | -7.2 | 238 | 255 | 0.9 | 0.8 |
| G1H013 | 7008 | 6137 | -12 | 446 | 390 | 0.93 | 0.84 |
| G1R003 | 6811 | 6795 | -0.2 | 433 | 432 | 0.92 | 0.75 |
| High flow period | | | | | | | |
| G1H020 | 14132 | 6767 | -52 | 894 | 428 | 0.93 | 0.41 |
| G1H036 | N/A | | | | | | |
| G1H013 | 59589 | 51082 | -14 | 3769 | 3231 | 0.92 | 0.76 |
| G1R003 | 61961 | 70959 | 14.5 | 3919 | 4488 | 0.91 | 0.8 |
| Yearly | | | | | | | |
| G1H020 | 16815 | 12030 | -28 | 533 | 381 | 0.95 | 0.73 |
| G1H036 | N/A | | | | | | |
| G1H013 | 66597 | 57218 | -14 | 2112 | 1814 | 0.92 | 0.82 |
| G1R003 | 68772 | 77756 | 13 | 2181 | 2465 | 0.92 | 0.85 |

Table 1.4.8: Results of TDS Concentration after Verification

| | mean measured (mg/l) | mean simulated (mg/l) | % error in mean | Coeff of determination(R ²) |
|-------------------------|----------------------|-----------------------|-----------------|---|
| Low flow period | | | | |
| G1H020 | 52.3 | 47 | -21 | 0.23 |
| G1H036 | 124 | 96 | -27 | 0.22 |
| G1H013 | 137 | 99 | -27 | 0.3 |
| G1R003 | 191 | 111 | -41 | 0.11 |
| High flow period | | | | |
| G1H020 | 65 | 47 | -27 | 0.04 |
| G1H036 | N/A | | | |
| G1H013 | 148 | 139 | -7 | 0.58 |
| G1R003 | 166 | 147 | -12 | 0.47 |
| Yearly | | | | |
| G1H020 | 62 | 47 | -24 | 0.04 |
| G1H036 | N/A | | | |
| G1H013 | 143 | 119 | -17 | 0.42 |
| G1R003 | 179 | 129 | -27 | 0.22 |

NOTE : For station G1H036 the flow measurements are incomplete from the 3rd of July to end September, and the statistical comparisons have for this reason not been included.

Table 1.4.9: Results of PO₄ Load after Verification

| | Total Load measured (tons) | Total Load simulated (tons) | % diff in total load | mean measured (g/s) | mean simulated (g/s) | Coeff of determination (R ²) | Coeff of efficiency |
|-------------------------|----------------------------|-----------------------------|----------------------|---------------------|----------------------|--|---------------------|
| Low flow period | | | | | | | |
| G1H020 | 1 | 1.1 | 5 | 0.06 | 0.06 | 0.25 | -0.24 |
| G1H036 | 2 | 1.1 | -46 | 0.13 | 0.07 | 0.85 | 0.39 |
| G1H013 | 1.4 | 1.5 | 11 | 0.09 | 0.098 | 0.86 | 0.58 |
| G1R003 | 0.6 | 1.5 | 159 | 0.04 | 0.1 | 0.93 | -4.2 |
| High flow period | | | | | | | |
| G1H020 | 6 | 5.3 | -11 | 0.38 | 0.34 | 0.43 | 0.15 |
| G1H036 | N/A | | | | | | |
| G1H013 | 18.3 | 15.1 | -18 | 1.2 | 0.95 | 0.93 | 0.8 |
| G1R003 | 14.8 | 17.9 | 21 | 0.94 | 1.14 | 0.92 | 0.79 |
| Yearly | | | | | | | |
| G1H020 | 7 | 6.3 | -9 | 0.22 | 0.2 | 0.5 | 0.33 |
| G1H036 | N/A | | | | | | |
| G1H013 | 19.7 | 16.6 | -16 | 0.62 | 0.53 | 0.94 | 0.84 |
| G1R003 | 15.4 | 19.5 | 26.5 | 0.49 | 0.62 | 0.93 | 0.86 |

Table 1.4.10: Results of PO₄ Concentration after Verification

| | mean measured (mg/l) | mean simulated (mg/l) | % error in mean | Coeff of determination (R ²) |
|-------------------------|----------------------|-----------------------|-----------------|--|
| Low flow period | | | | |
| G1H020 | 0.02 | 0.017 | -15 | 0.18 |
| G1H036 | 0.062 | 0.019 | -69 | 0.3 |
| G1H013 | 0.02 | 0.019 | -15 | 0.31 |
| G1R003 | 0.02 | 0.021 | 3.4 | 0.26 |
| High flow period | | | | |
| G1H020 | 0.033 | 0.029 | -8.8 | 0.14 |
| G1H036 | N/A | | | |
| G1H013 | 0.043 | 0.036 | -15 | 0.15 |
| G1R003 | 0.032 | 0.038 | 16 | 0.72 |
| Yearly | | | | |
| G1H020 | 0.026 | 0.024 | -11 | 0.44 |
| G1H036 | N/A | | | |
| G1H013 | 0.031 | 0.028 | -10 | 0.43 |
| G1R003 | 0.026 | 0.029 | 12 | 0.72 |

NOTE : For station G1H036 the flow measurements are incomplete from the 3rd of July to end September, and the statistical comparisons have for this reason not been included.

Table 1.4.11: Results of Temperature after Verification

| | mean measured | mean simulated | % error in mean | Std Dev measured | Std Dev simulated | Coeff of determination (R ²) |
|-------------------------|---------------|----------------|-----------------|------------------|-------------------|--|
| Low flow period | | | | | | |
| G1H020 | 24 | 23.1 | -3.5 | 2.6 | 3 | 0.94 |
| G1H036 | 24.7 | 24.3 | -1.5 | 2.8 | 3.6 | 0.84 |
| G1H013 | 24.2 | 25.7 | 5.9 | 2.6 | 4.2 | 0.75 |
| G1R003 | 25.1 | 27.1 | 8.3 | 2.5 | 4.4 | 0.72 |
| High flow period | | | | | | |
| G1H020 | 14.1 | 13.3 | -5.4 | 2.7 | 2.8 | 0.94 |
| G1H036 | 13.6 | 13.4 | -1.8 | 2.9 | 3.1 | 0.85 |
| G1H013 | 14 | 13.2 | -5.7 | 2.8 | 3.9 | 0.78 |
| G1R003 | 15.2 | 13.1 | -13 | 2.8 | 3.4 | 0.83 |
| Yearly | | | | | | |
| G1H020 | 19 | 18.2 | -4.2 | 5.6 | 5.7 | 0.98 |
| G1H036 | 19.1 | 18.8 | -1.6 | 6.2 | 6.4 | 0.96 |
| G1H013 | 19.1 | 19.4 | 1.6 | 5.8 | 7.5 | 0.93 |
| G1R003 | 20.1 | 20.1 | 0 | 5.6 | 8.6 | 0.94 |

Table 1.4.12: Results of Oxygen after Verification

| | mean saturation oxygen | mean simulated | % error in mean | Std Dev sat. Oxygen | Std Dev simulated | Coeff of Determination (R ²) |
|-------------------------|------------------------|----------------|-----------------|---------------------|-------------------|--|
| Low flow period | | | | | | |
| G1H020 | 8.54 | 8.66 | 1.4 | 0.51 | 0.51 | 0.96 |
| G1H036 | 8.3 | 8.36 | 1 | 0.55 | 0.57 | 0.93 |
| G1H013 | 8.2 | 8.23 | 1.4 | 0.52 | 0.53 | 0.94 |
| G1R003 | 8.3 | 8.2 | 1 | 0.51 | 0.52 | 0.93 |
| High flow period | | | | | | |
| G1H020 | 10.5 | 10.34 | -1.5 | 0.68 | 0.7 | 0.89 |
| G1H036 | 10.45 | 10.4 | -0.4 | 0.79 | 0.82 | 0.79 |
| G1H013 | 10.54 | 10.47 | -0.75 | 0.94 | 0.96 | 0.76 |
| G1R003 | 10.8 | 10.6 | -1.8 | 0.95 | 1.1 | 0.75 |
| Yearly | | | | | | |
| G1H020 | 9.53 | 9.51 | -0.2 | 1.15 | 1.04 | 0.97 |
| G1H036 | 9.37 | 9.39 | 0.2 | 1.3 | 1.25 | 0.95 |
| G1H013 | 9.35 | 9.36 | 0.14 | 1.43 | 1.37 | 0.94 |
| G1R003 | 9.55 | 9.4 | -1.5 | 1.4 | 1.8 | 0.92 |

Table 1.4.13: Results of TDS Loads of simulation run without ungauged TDS

| | Total Load measured (tons) | Total Load simulated (tons) | % diff in total load | mean measured (g/s) | mean simulated (g/s) | Coeff of Determination (R ²) | Coeff of efficiency |
|-------------------------|----------------------------|-----------------------------|----------------------|---------------------|----------------------|--|---------------------|
| Low flow period | | | | | | | |
| G1H020 | 2577 | 1923 | -25 | 164 | 122 | 0.74 | -0.19 |
| G1H036 | 3204 | 2743 | -14 | 204 | 174 | 0.55 | 0.25 |
| G1H013 | 6078 | 3950 | -35 | 386 | 251 | 0.59 | 0.06 |
| G1R003 | 5598 | 4389 | -22 | 356 | 279 | 0.79 | 0.51 |
| High flow period | | | | | | | |
| G1H020 | 13220 | 8555 | -35 | 836 | 541 | 0.98 | 0.85 |
| G1H036 | 39214 | 16254 | -58 | 2480 | 1028 | 0.97 | 0.47 |
| G1H013 | 82042 | 46597 | -43 | 5189 | 2947 | 0.85 | 0.68 |
| G1R003 | 81497 | 76346 | -6 | 5154 | 4828 | 0.9 | 0.41 |
| Yearly | | | | | | | |
| G1H020 | 15798 | 10479 | -34 | 501 | 332 | 0.98 | 0.87 |
| G1H036 | 42419 | 18997 | -55 | 1345 | 602 | 0.98 | 0.57 |
| G1H013 | 88120 | 50471 | -43 | 2794 | 1603 | 0.86 | 0.73 |
| G1R003 | 87097 | 80735 | -7 | 2761 | 2560 | 0.9 | 0.53 |

Table 1.4.14: Results of TDS Concentration of simulation run without ungauged TDS

| | mean measured (mg/l) | mean simulated (mg/l) | % error in mean | Coeff of determination (R ²) |
|-------------------------|----------------------|-----------------------|-----------------|--|
| Low flow period | | | | |
| G1H020 | 62.6 | 40.5 | -35 | 0.1 |
| G1H036 | 120 | 81 | -32 | 0.49 |
| G1H013 | 141 | 85 | -40 | 0.27 |
| G1R003 | 219 | 113 | -51 | 0.21 |
| High flow period | | | | |
| G1H020 | 56.5 | 36 | -36 | 0.38 |
| G1H036 | 123 | 92 | -25 | 0.44 |
| G1H013 | 158 | 121 | -23 | 0.34 |
| G1R003 | 210 | 169 | -19 | 0.28 |
| Yearly | | | | |
| G1H020 | 59.5 | 38 | -36 | 0.07 |
| G1H036 | 121 | 87 | -28 | 0.44 |
| G1H013 | 149 | 103 | -31 | 0.37 |
| G1R003 | 215 | 141 | -36 | 0.12 |

Table 1.4.15: Results of PO₄ Loads of simulation run without ungauged TDS

| | Total Load measured (tons) | Total Load simulated (tons) | % diff in total load | mean measured (g/s) | mean simulated (g/s) | Coeff of determination (R ²) | Coeff of efficiency |
|-------------------------|----------------------------|-----------------------------|----------------------|---------------------|----------------------|--|---------------------|
| Low flow period | | | | | | | |
| G1H020 | 1.02 | 1.02 | -0.8 | 0.065 | 0.064 | 0.31 | 0.09 |
| G1H036 | 1.2 | 0.79 | -34 | 0.076 | 0.05 | 0.6 | 0.1 |
| G1H013 | 1 | 0.96 | -4.6 | 0.06 | 0.06 | 0.5 | 0.24 |
| G1R003 | 0.6 | 0.81 | 35 | 0.04 | 0.05 | 0.61 | 0.26 |
| High flow period | | | | | | | |
| G1H020 | 13.9 | 2.38 | -83 | 0.9 | 0.15 | 0.95 | 0.06 |
| G1H036 | 28.6 | 4.26 | -85 | 1.8 | 0.26 | 0.95 | 0.08 |
| G1H013 | 48.2 | 8.11 | -83 | 3 | 0.51 | 0.95 | 0.18 |
| G1R003 | 25.6 | 10.9 | -58 | 1.6 | 0.69 | 0.94 | 0.61 |
| Yearly | | | | | | | |
| G1H020 | 14.9 | 3.4 | -77 | 0.47 | 0.11 | 0.95 | 0.19 |
| G1H036 | 29.8 | 5 | -83 | 0.95 | 0.16 | 0.96 | 0.2 |
| G1H013 | 49.3 | 9.1 | -82 | 1.56 | 0.29 | 0.96 | 0.22 |
| G1R003 | 26.2 | 11.7 | -56 | 0.83 | 0.37 | 0.94 | 0.63 |

Table 1.4.16: Results of PO₄ Concentrations of simulation run without ungauged TDS

| | mean measured | mean simulated | % error in mean | Coeff of determination (R ²) |
|-------------------------|---------------|----------------|-----------------|--|
| Low flow period | | | | |
| G1H020 | 0.02 | 0.023 | -3.4 | 0.22 |
| G1H036 | 0.04 | 0.022 | -44 | 0.11 |
| G1H013 | 0.024 | 0.019 | -17 | 0.09 |
| G1R003 | 0.024 | 0.02 | -18 | 0.51 |
| High flow period | | | | |
| G1H020 | 0.023 | 0.016 | -55 | 0.76 |
| G1H036 | 0.08 | 0.021 | -74 | 0.25 |
| G1H013 | 0.05 | 0.021 | -58 | 0.46 |
| G1R003 | 0.03 | 0.021 | -31 | 0.39 |
| Yearly | | | | |
| G1H020 | 0.03 | 0.019 | -34 | 0.57 |
| G1H036 | 0.06 | 0.022 | -65 | 0.13 |
| G1H013 | 0.04 | 0.02 | -45 | 0.44 |
| G1R003 | 0.027 | 0.025 | -25 | 0.41 |

TDS Loads for low flows (Calibration)

Figure 1.4.1

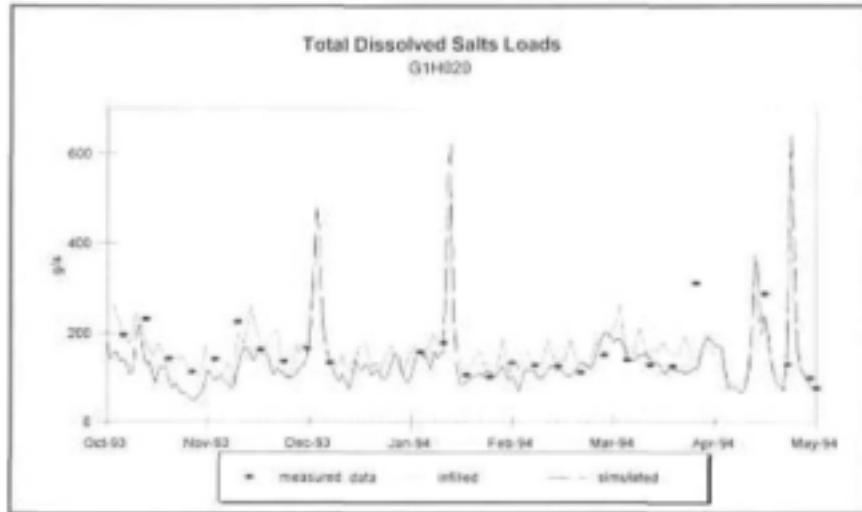


Figure 1.4.3

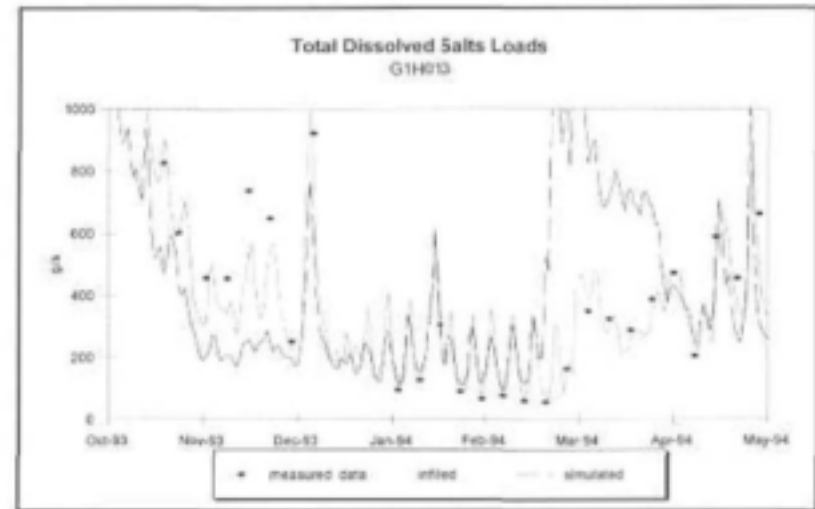
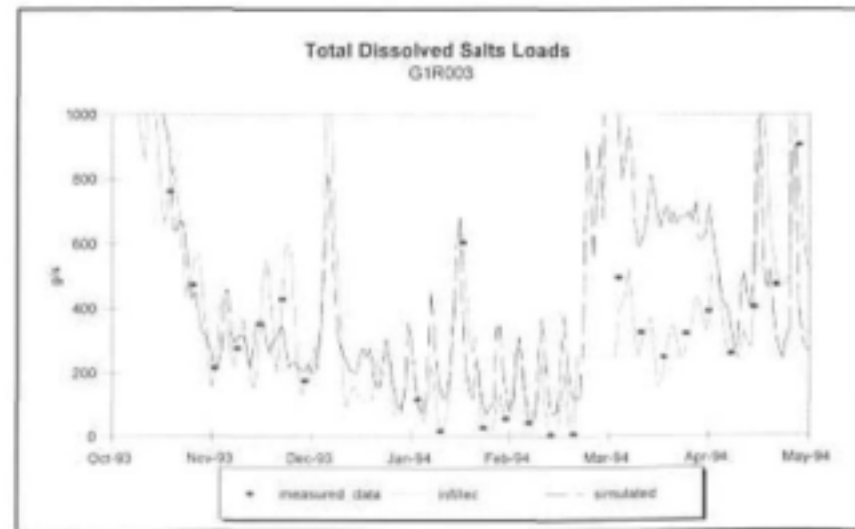
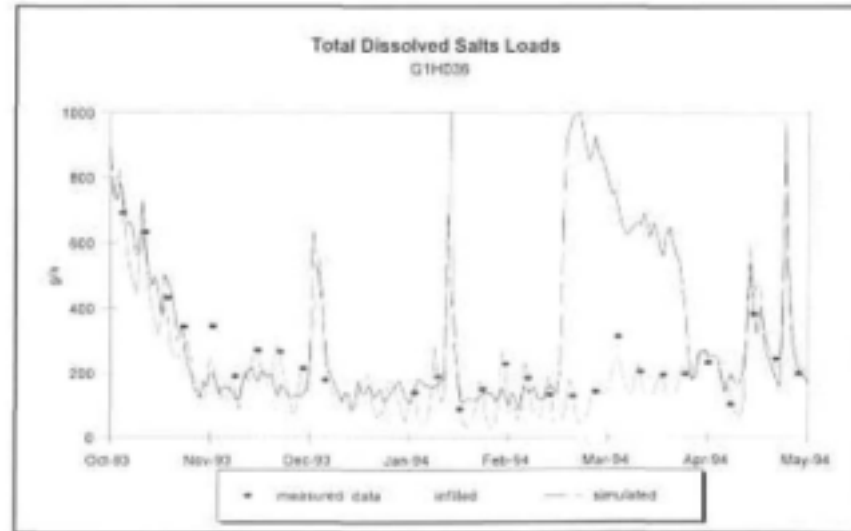


Figure
Figure 1.4.4

1.4.2



A.1.4-9

TDS Loads for high flows (Calibration)

Figure 1.4.5

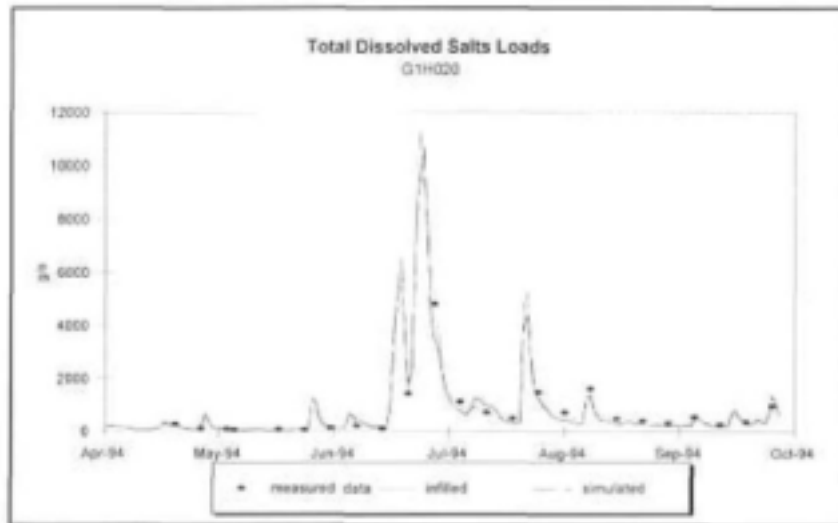


Figure 1.4.7

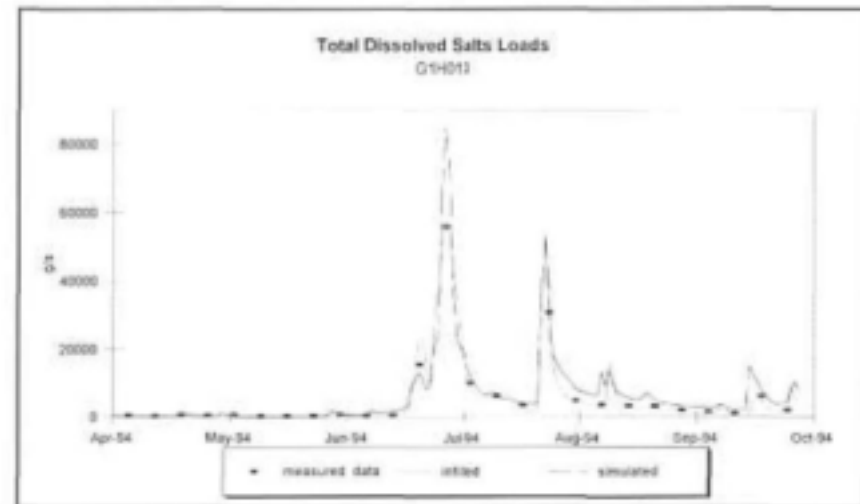


Figure 1.4.6

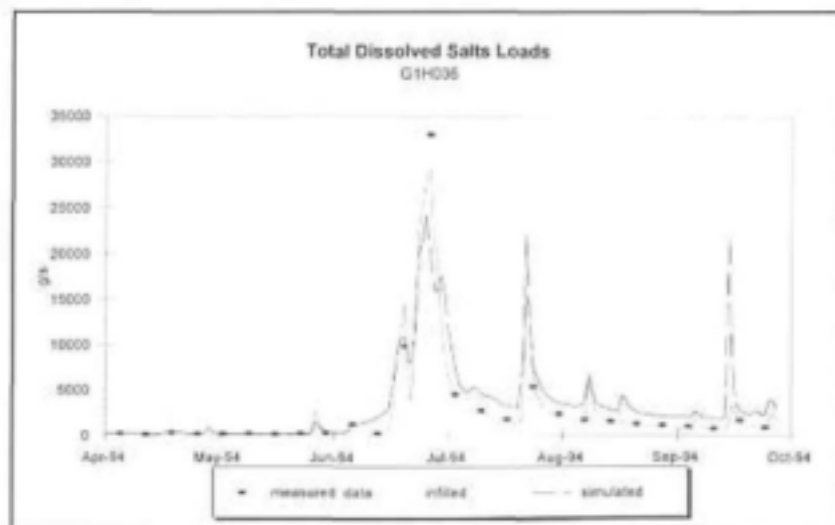
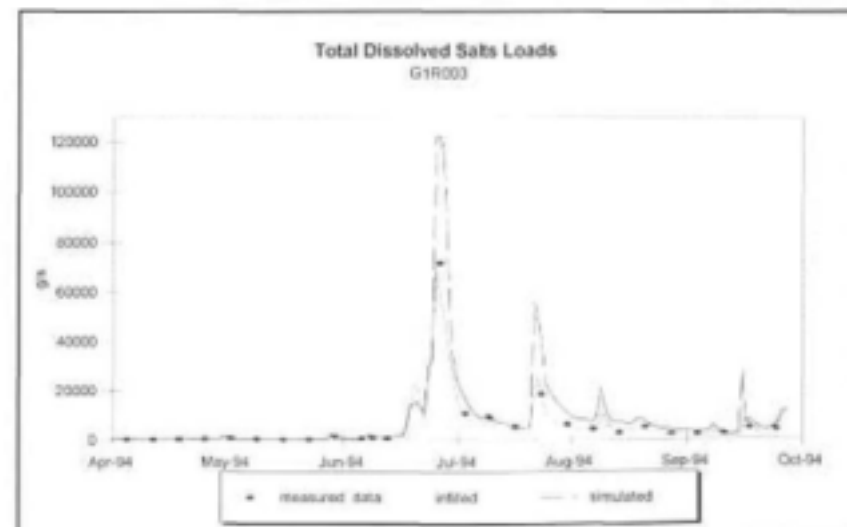


Figure 1.4.8



TDS Concentration (Calibration)

Figure 1.4.9

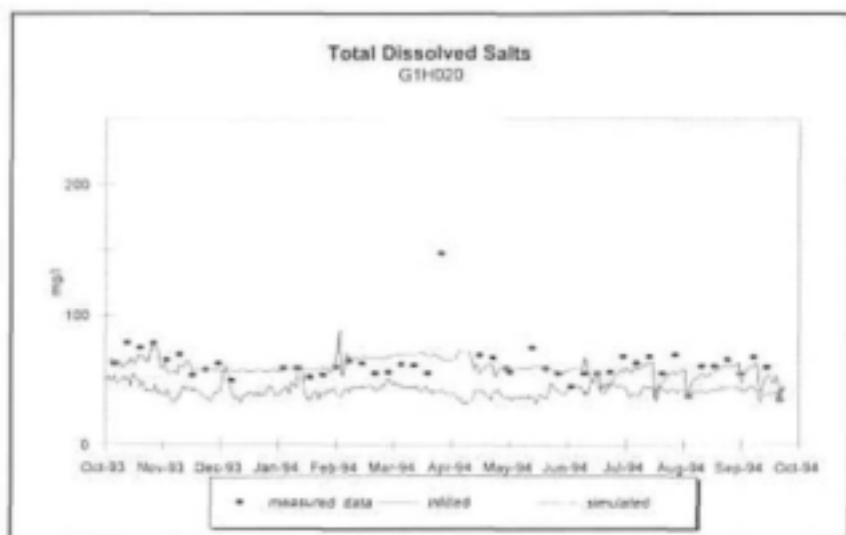


Figure 1.4.11

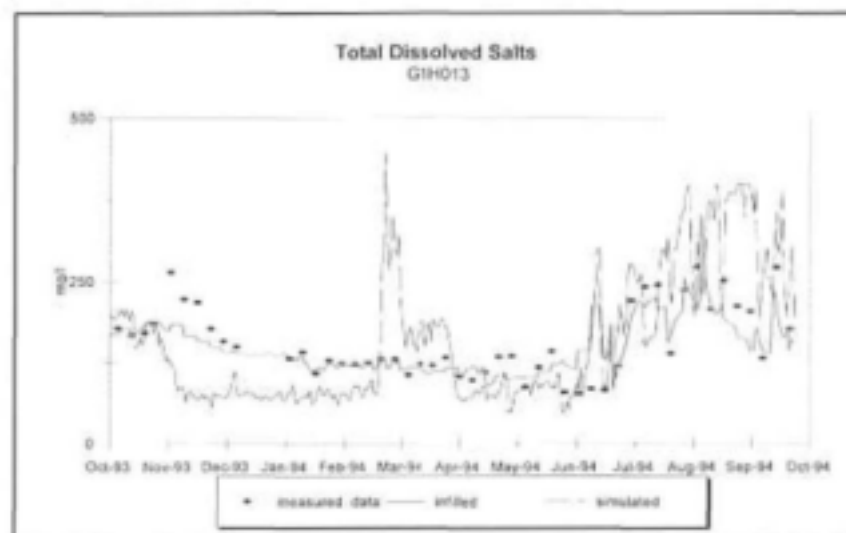


Figure 1.4.10

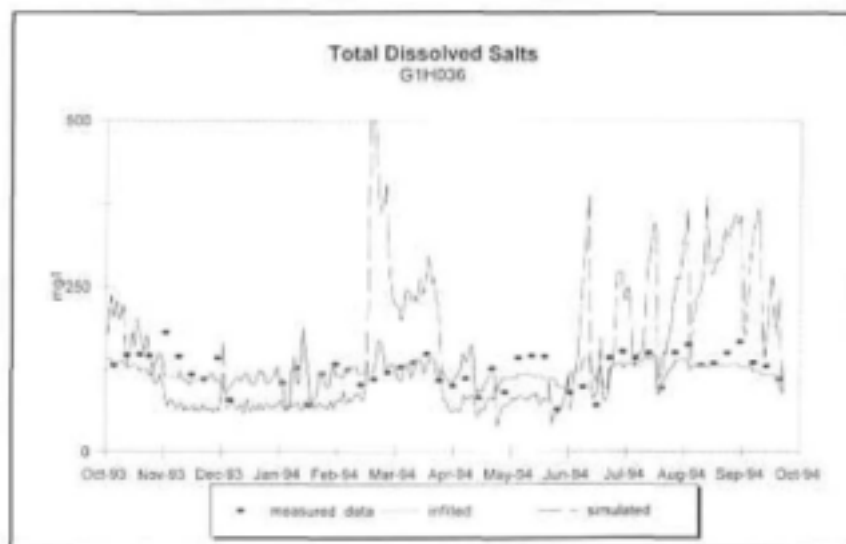
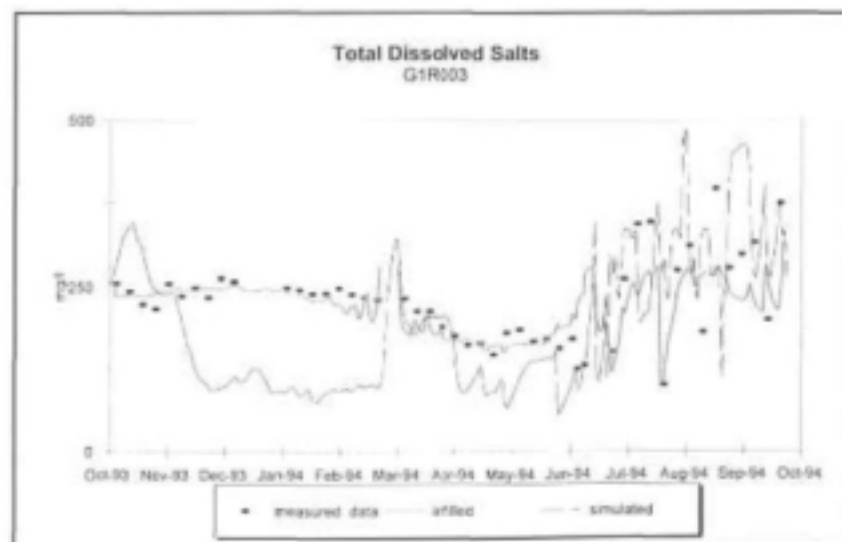


Figure 1.4.12



Phosphate Loads for low flows (Calibration)

Figure 1.4.13

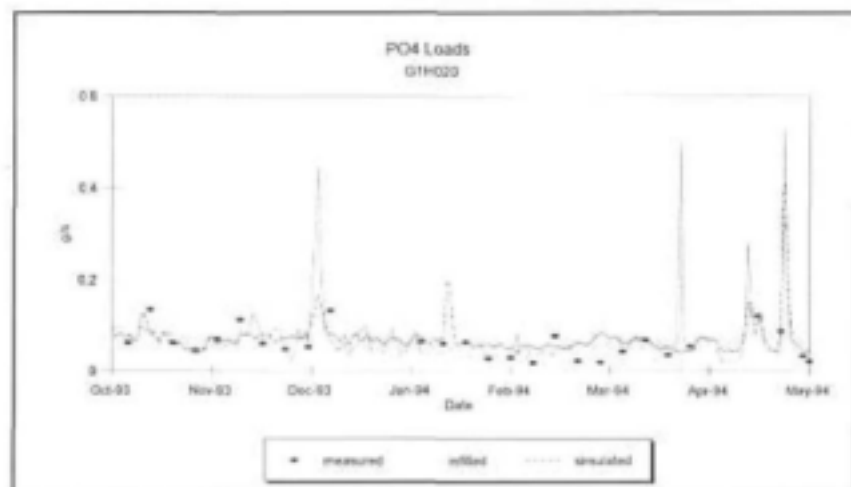


Figure 1.4.15

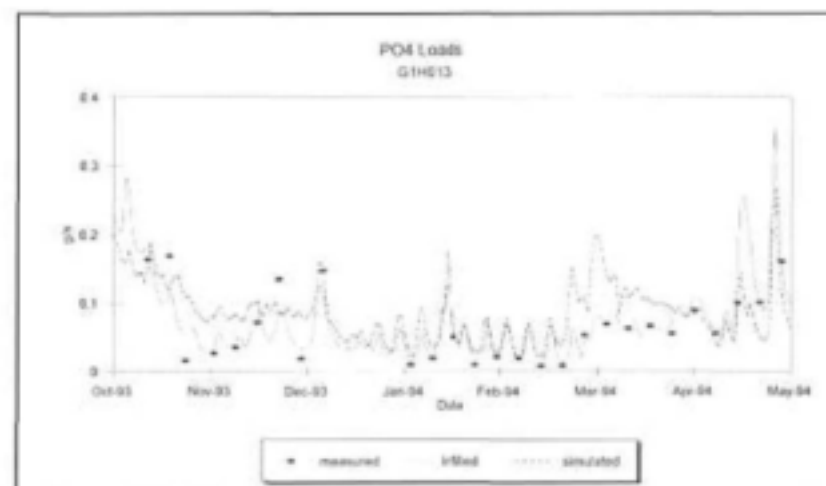


Figure 1.4.14

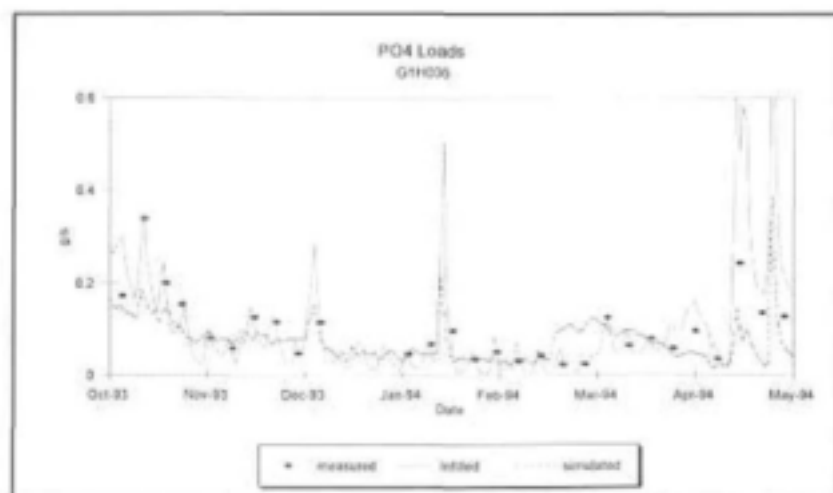
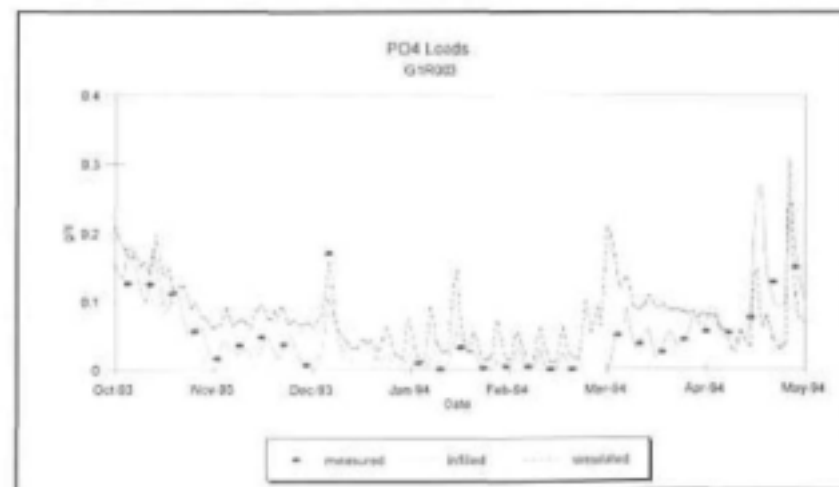


Figure 1.4.16



Phosphate Loads for highflows (Calibration)

Figure 1.4.17

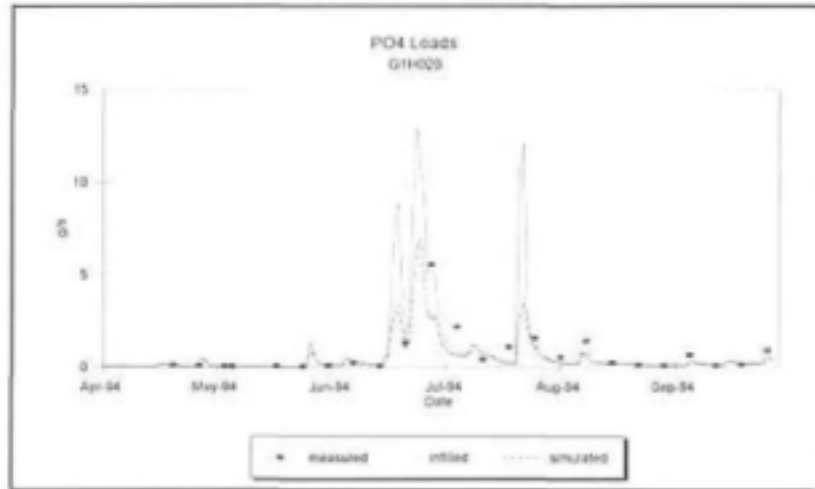


Figure 1.4.19

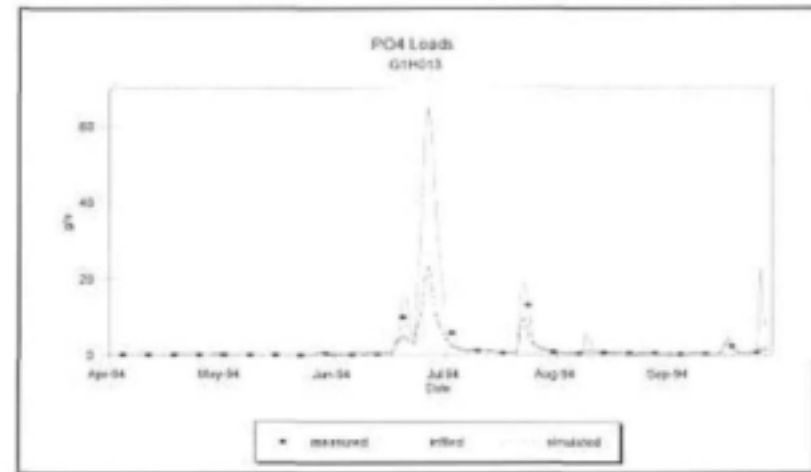


Figure 1.4.18

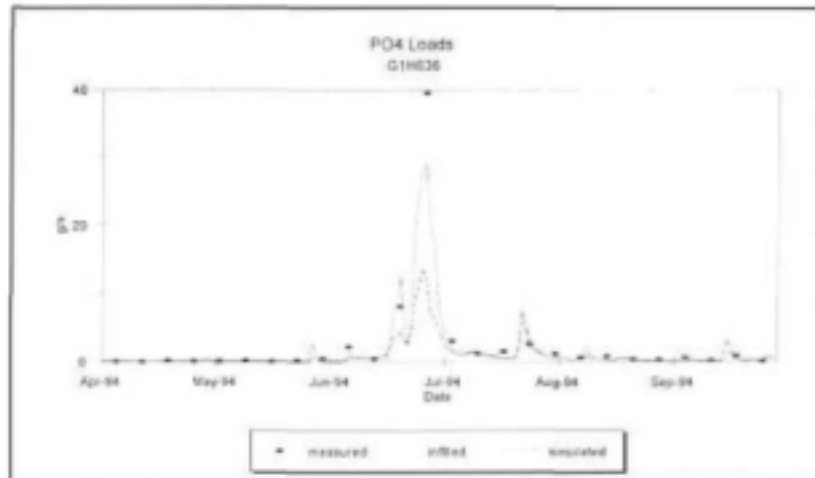
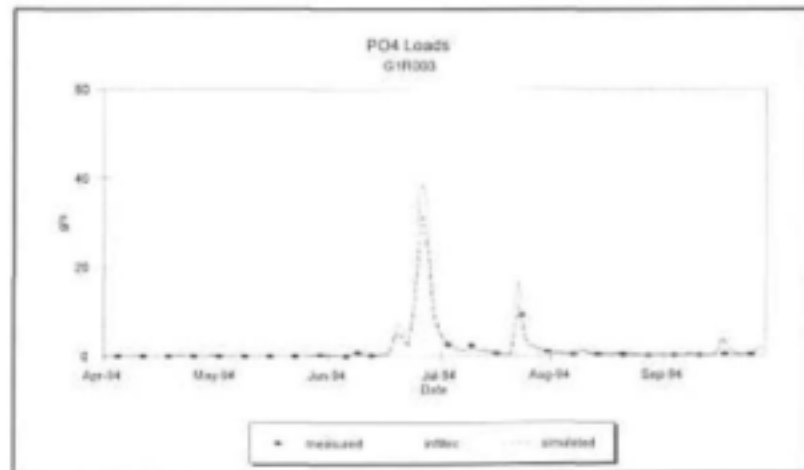


Figure 1.4.20



Phosphate Concentration (Calibration)

Figure 1.4.21

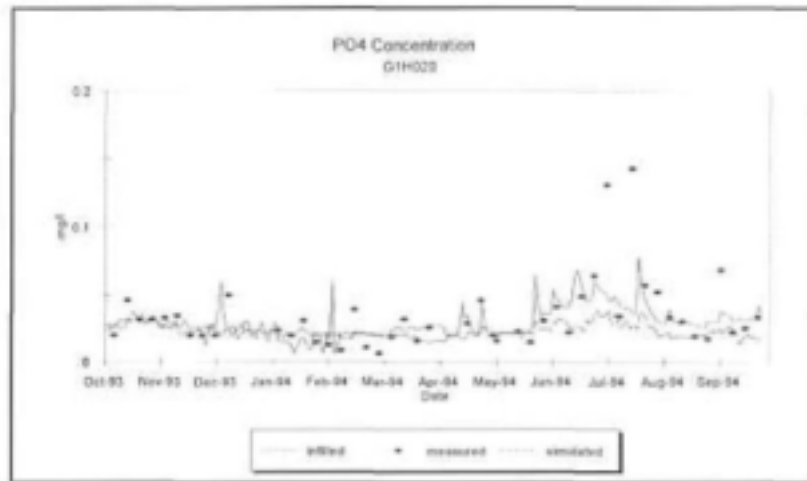


Figure 1.4.23

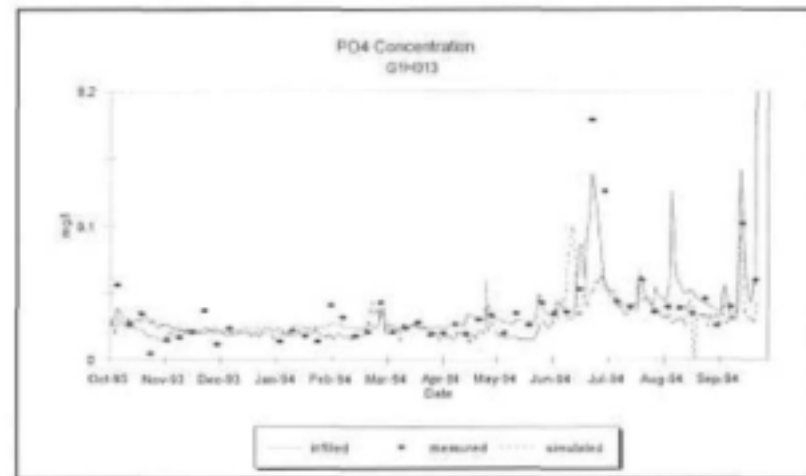


Figure 1.4.22

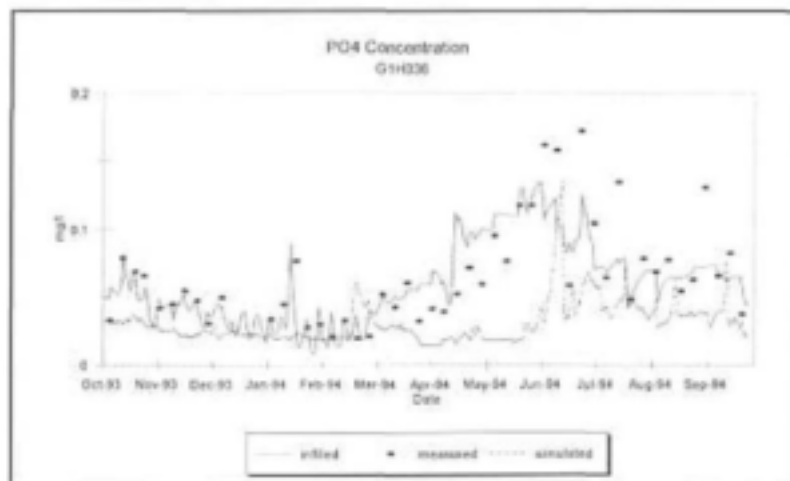
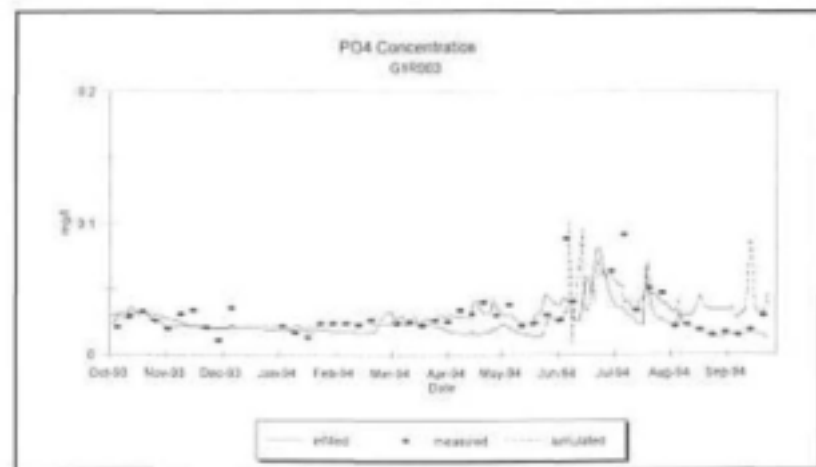


Figure 1.4.24



Temperature (Calibration)

Figure 1.4.25

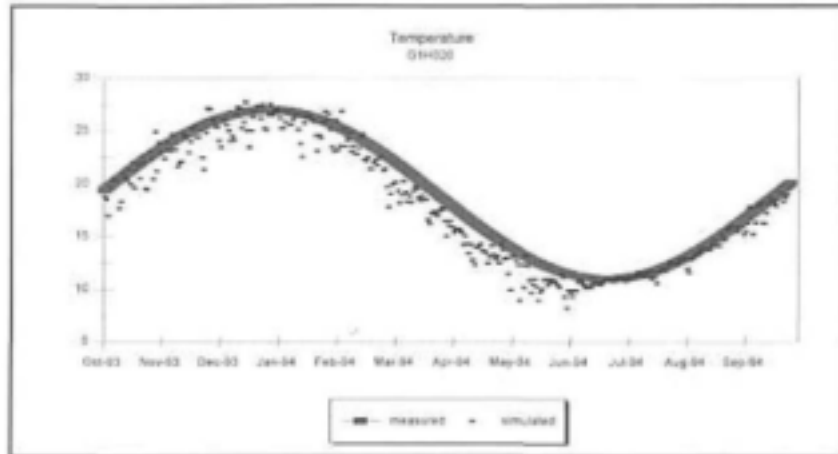


Figure 1.4.27

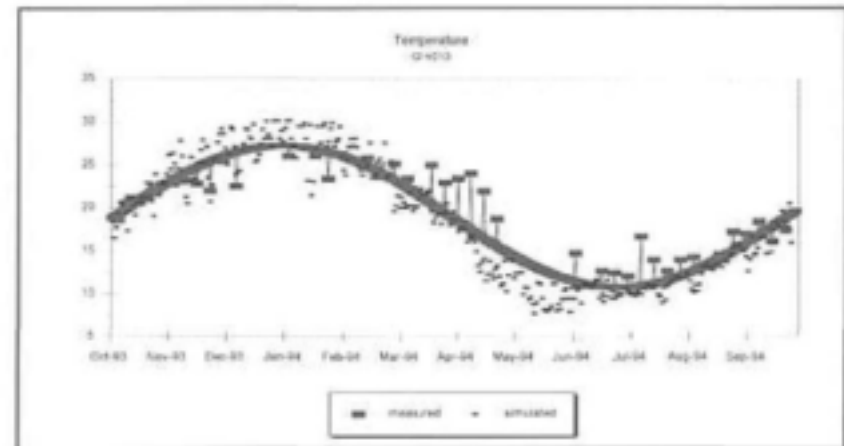


Figure 1.4.26

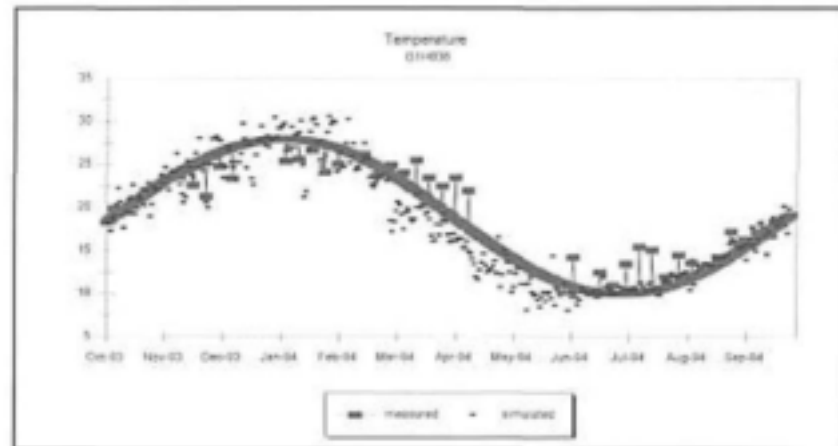
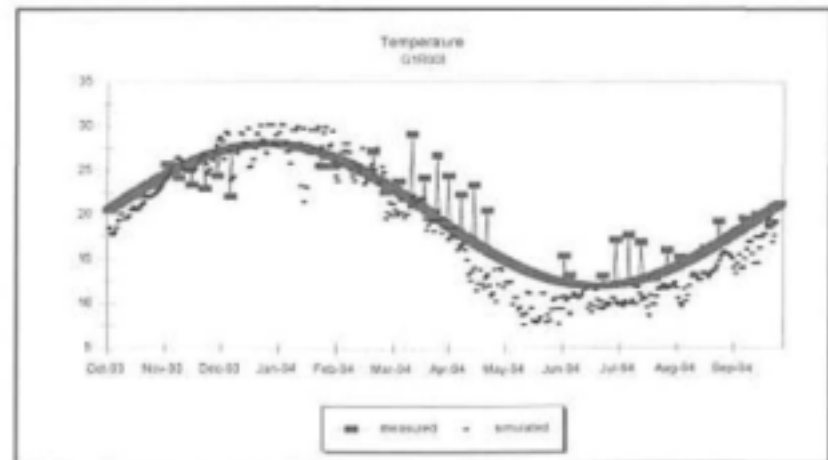


Figure 1.4.28



Oxygen (Calibration)

Figure 1.4.29

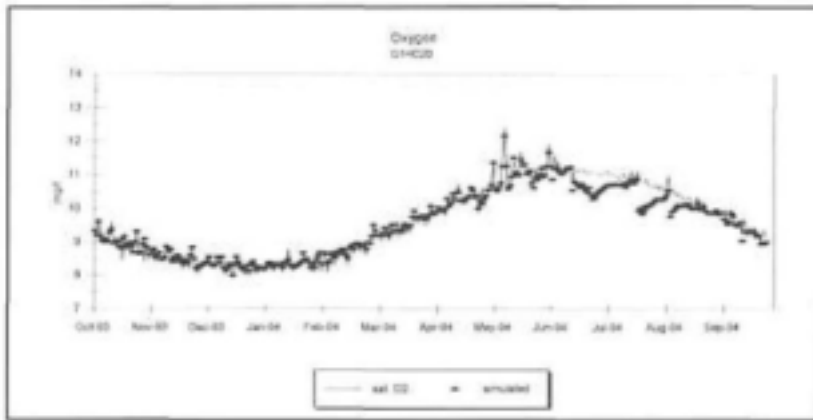


Figure 1.4.31

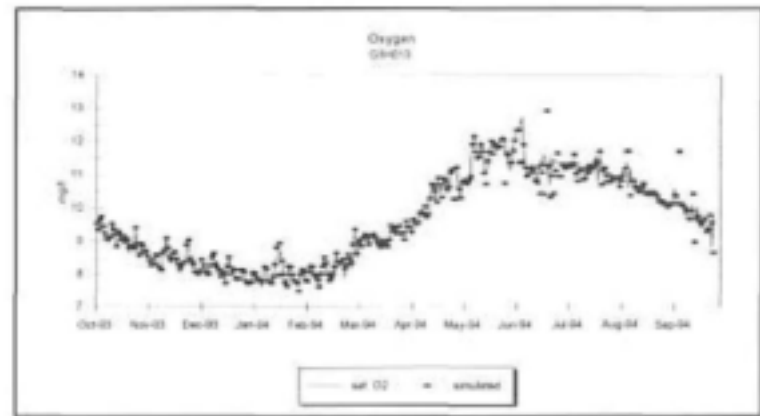


Figure 1.4.30

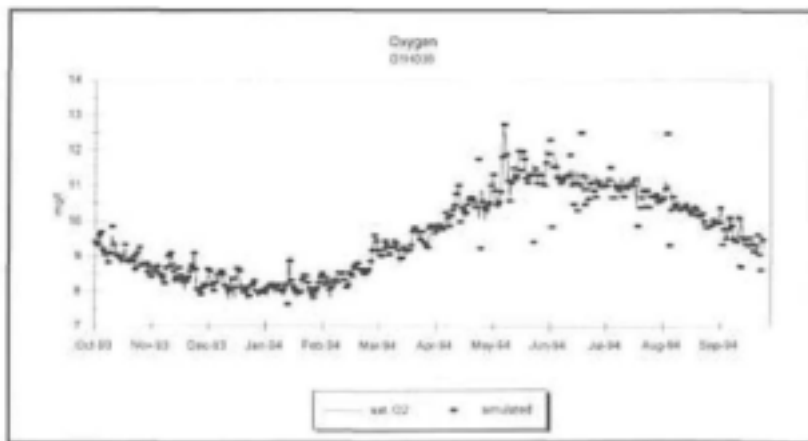
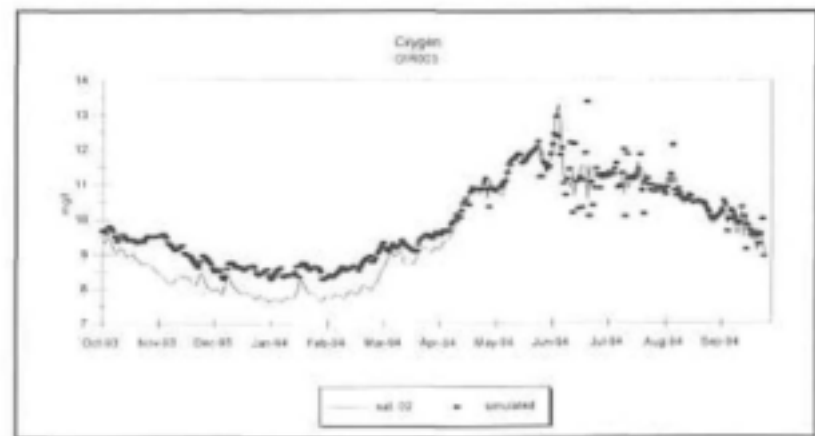


Figure 1.4.32



TDS Loads for low flows (Verification)

Figure 1.4.33

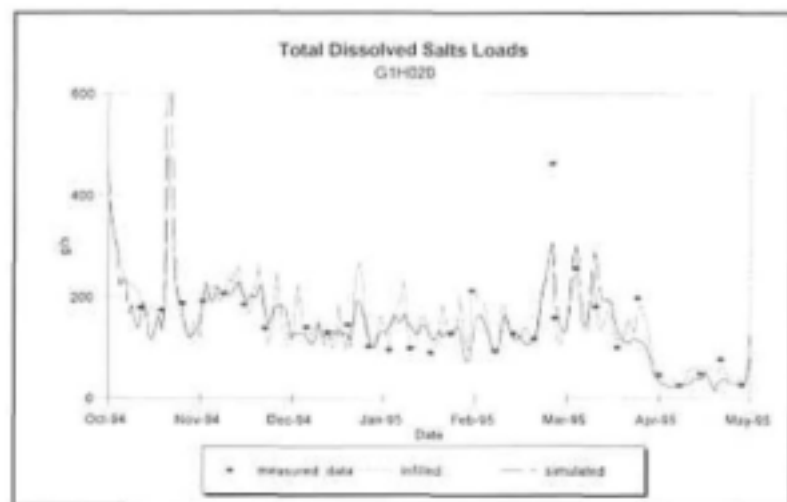


Figure 1.4.35

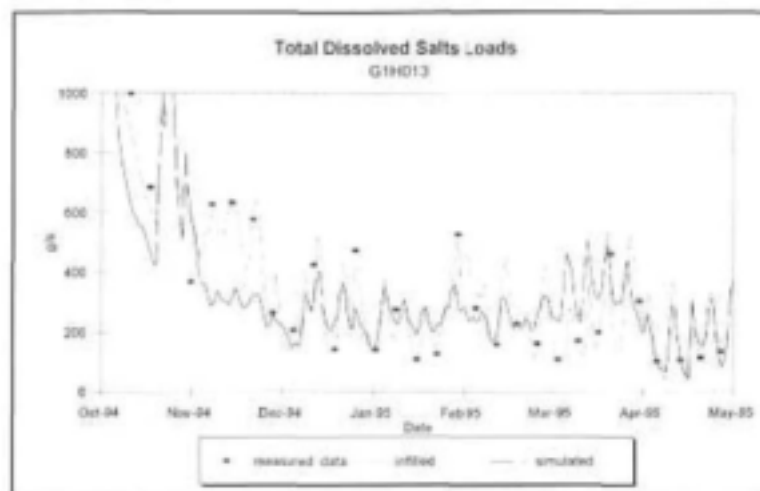


Figure 1.4.34

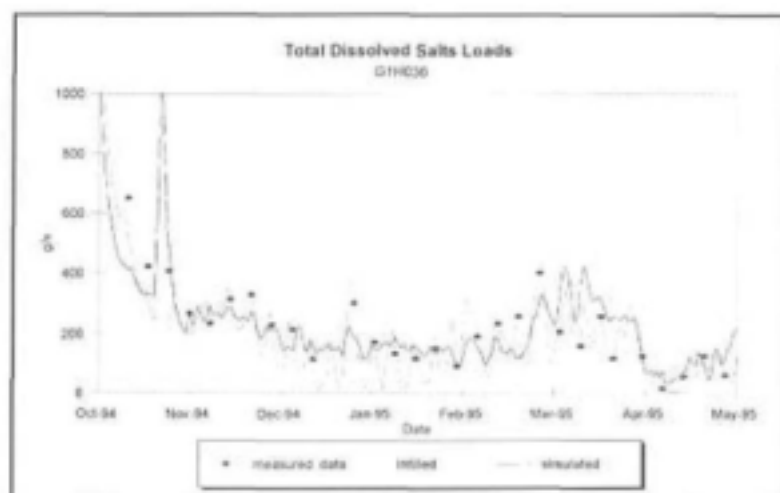
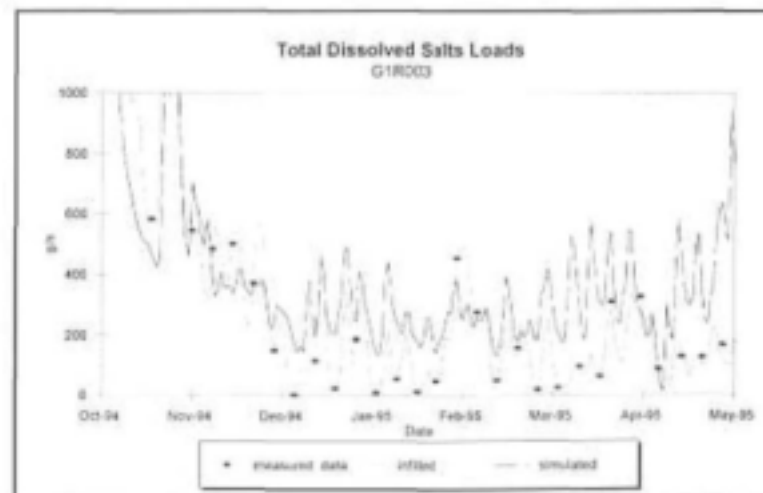


Figure 1.4.36



TDS Loads for high flows (Verification)

Figure 1.4.37

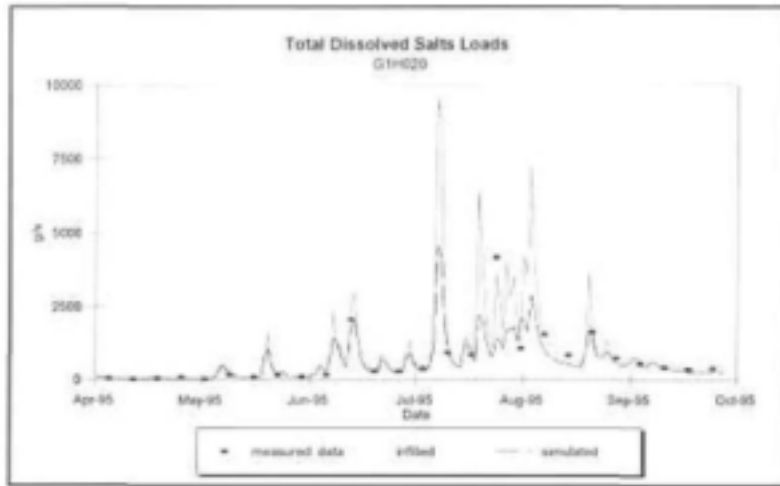


Figure 1.4.39

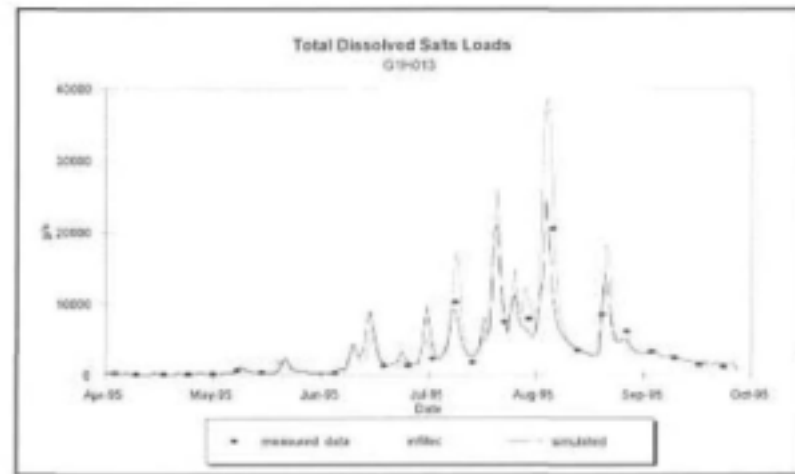


Figure 1.4.38

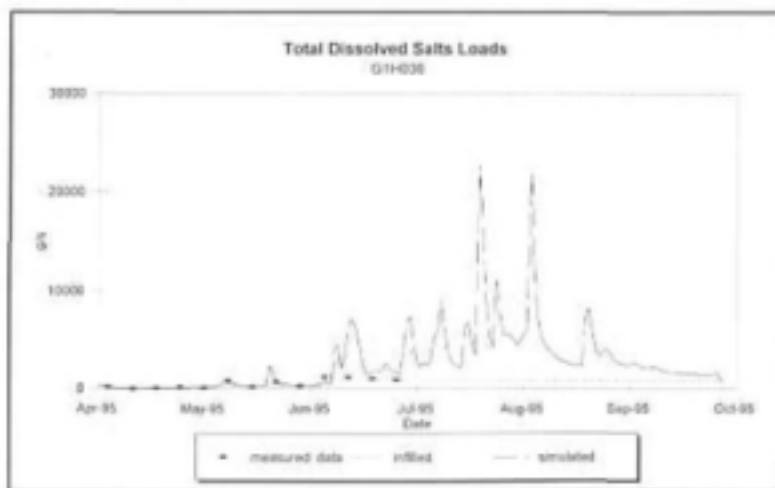
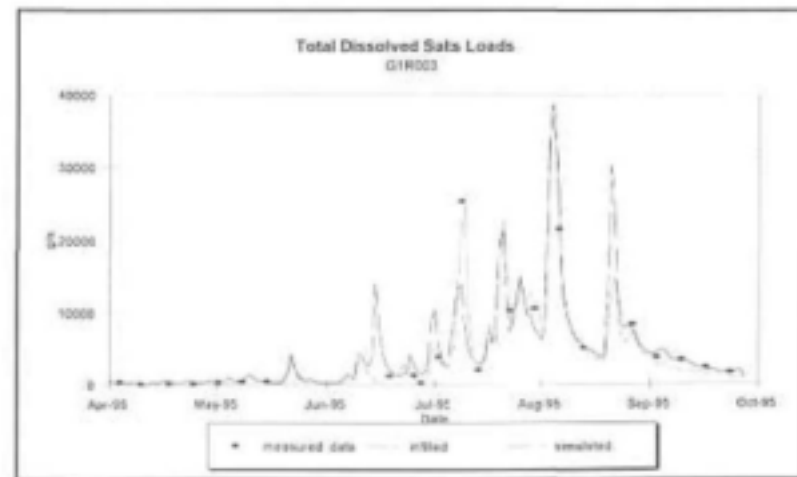


Figure 1.4.40



TDS Concentration (Verification)

Figure 1.4.41

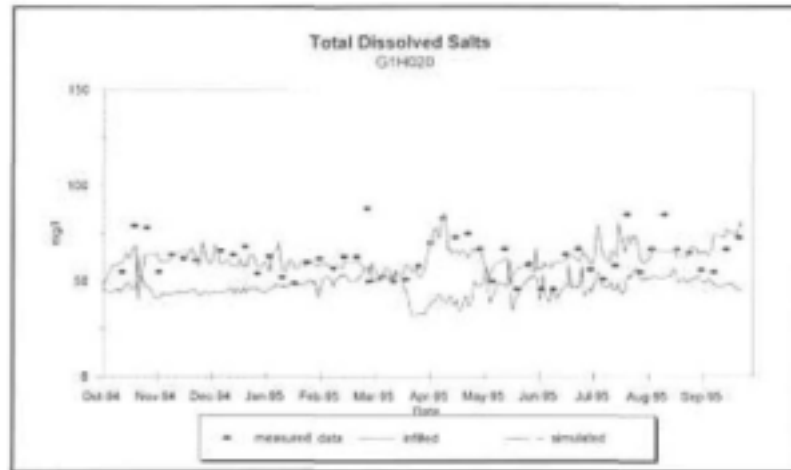


Figure 1.4.43

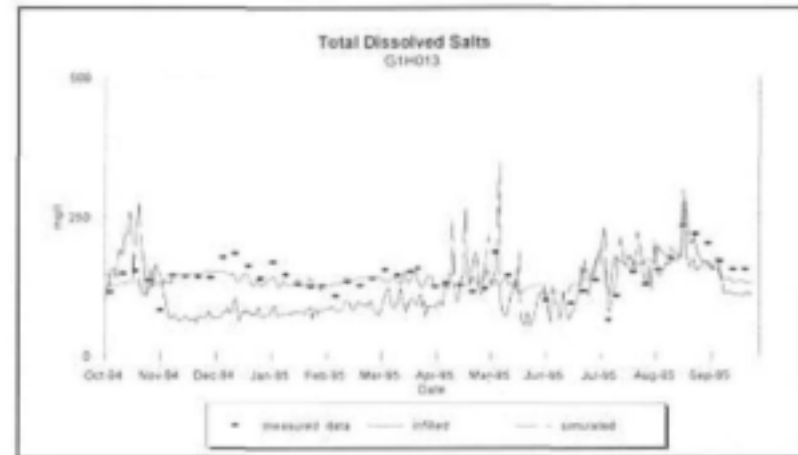


Figure 1.4.42

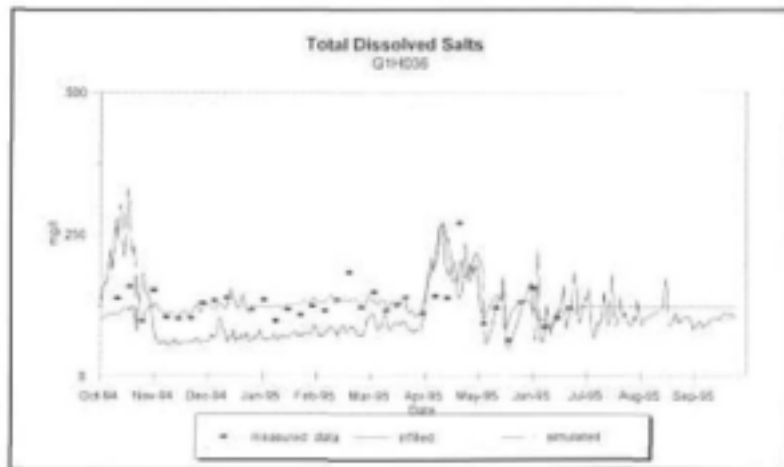
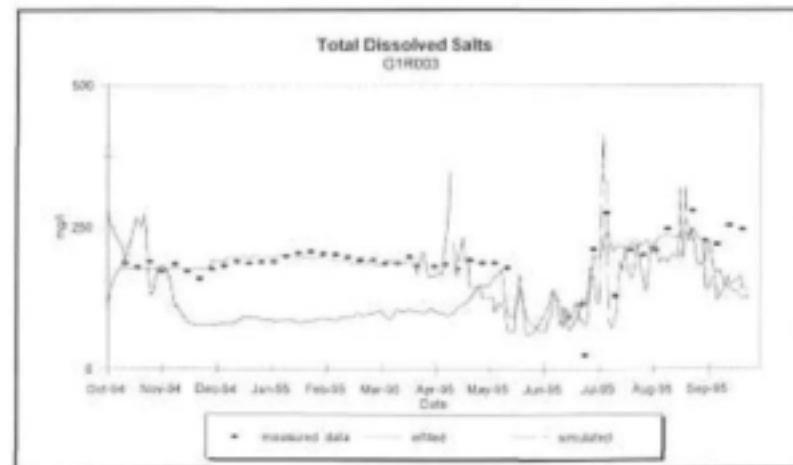


Figure 1.4.44



Phosphate Loads for low flows (Verification)

Figure 1.4.45

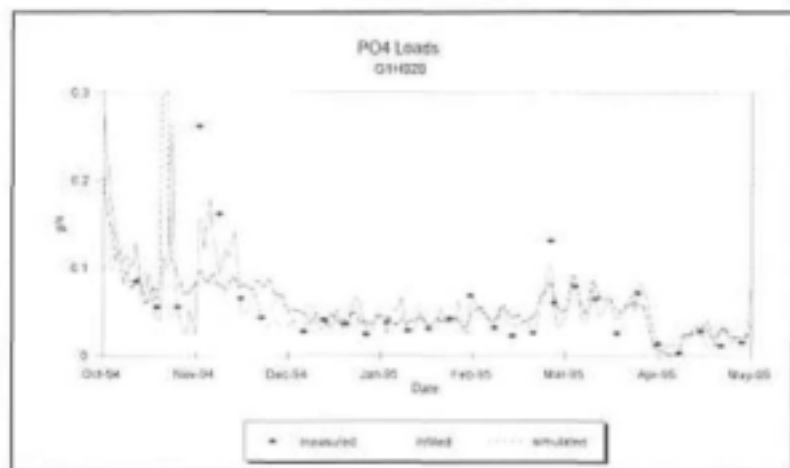


Figure 1.4.47

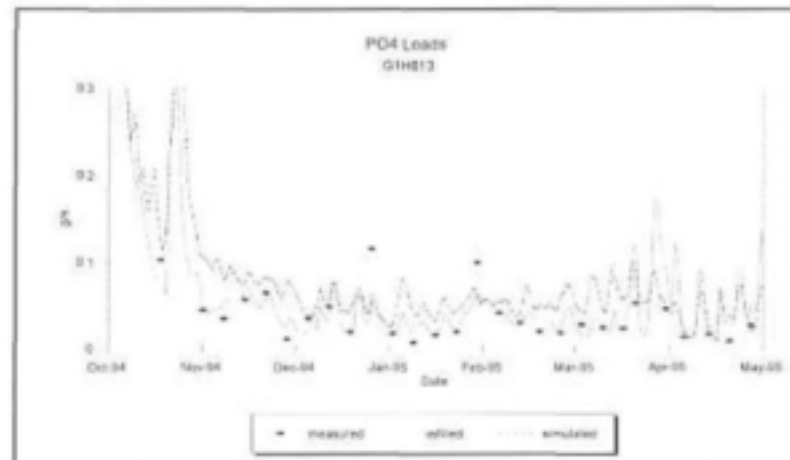


Figure 1.4.46

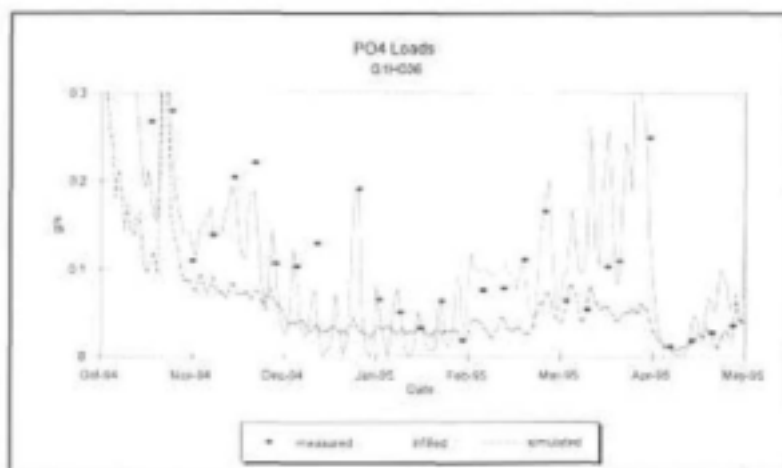
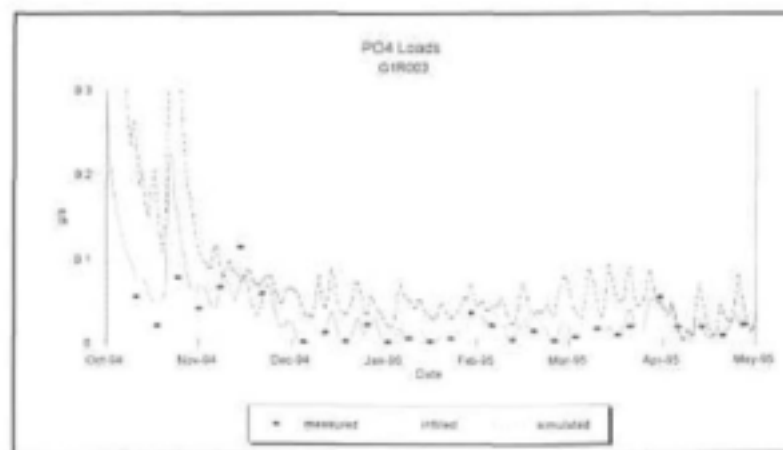


Figure 1.4.48



Phosphate Loads for high flows (Verification)

Figure 1.4.49

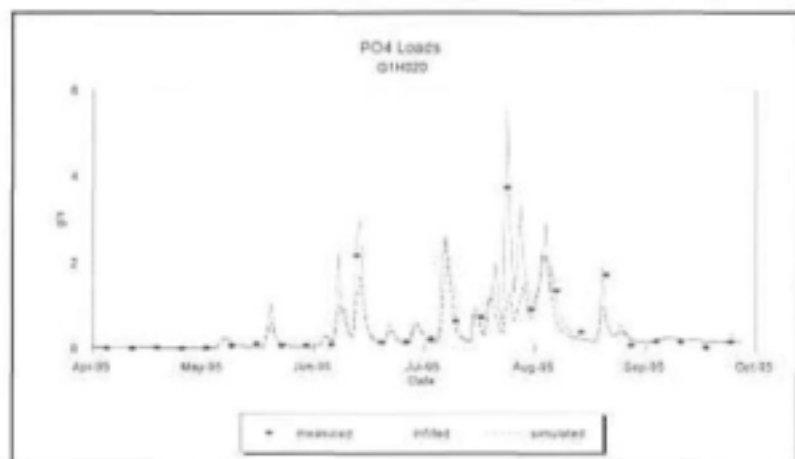


Figure 1.4.51

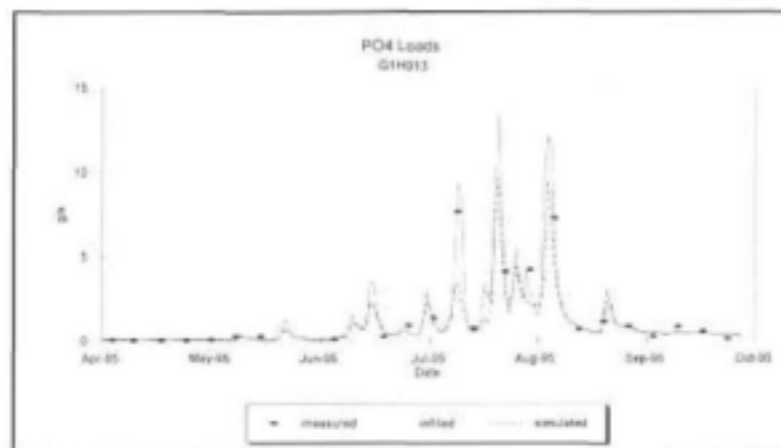


Figure 1.4.50

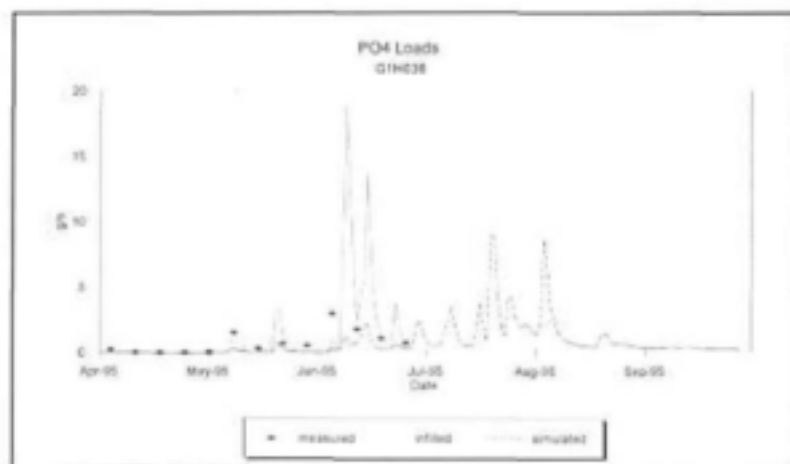
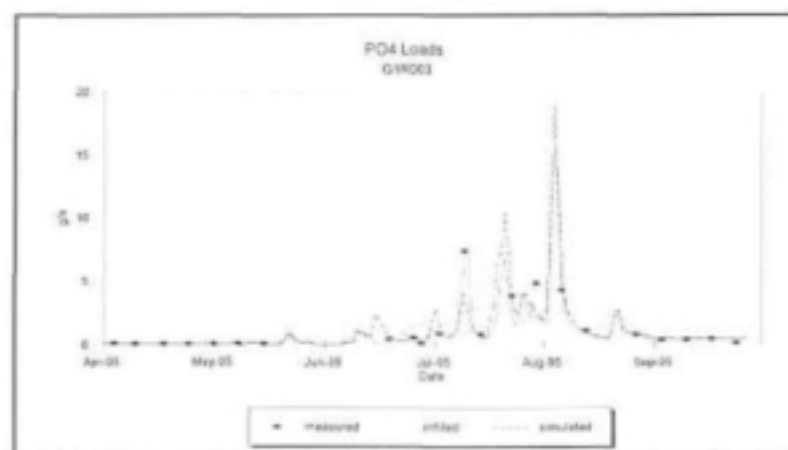


Figure 1.4.52



TDS Concentration (Verification)

Figure 1.4.53

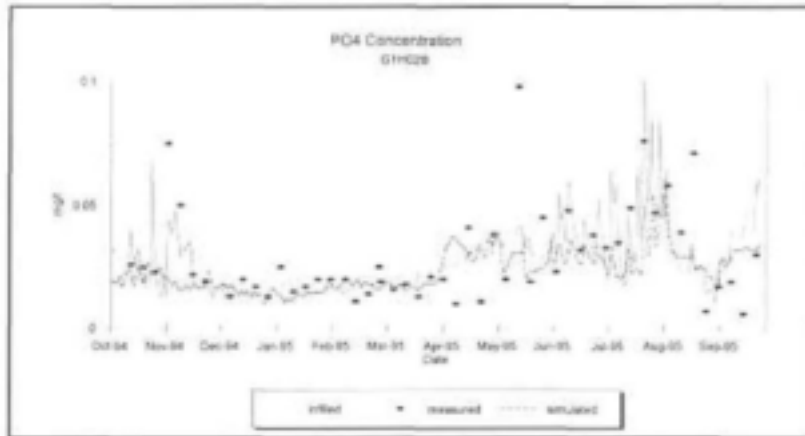


Figure 1.4.55

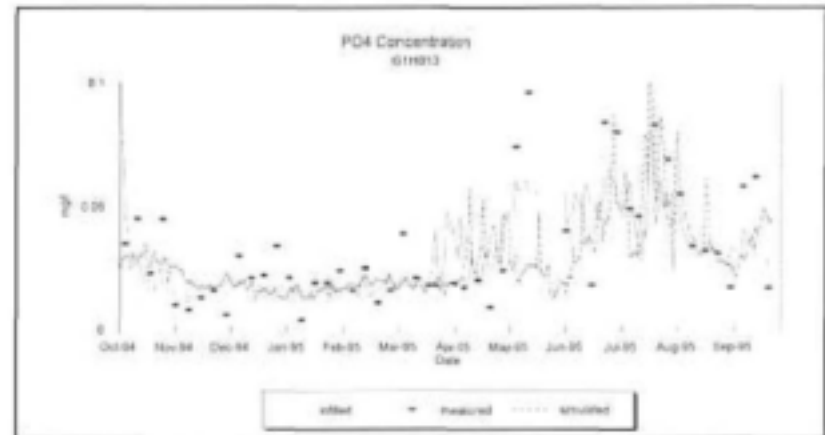


Figure 1.4.54

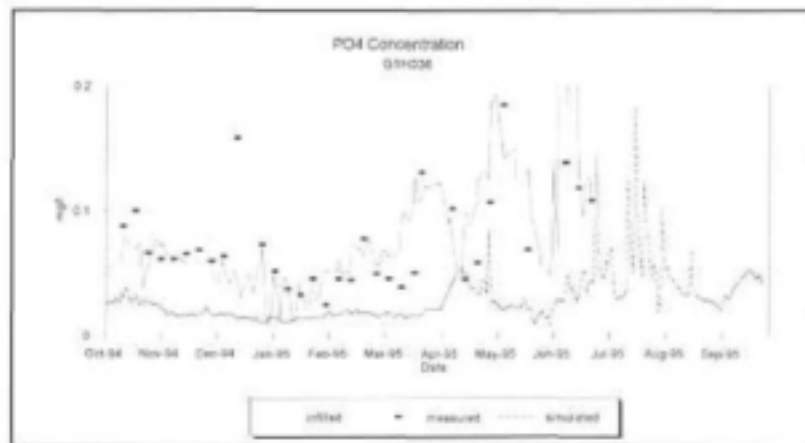
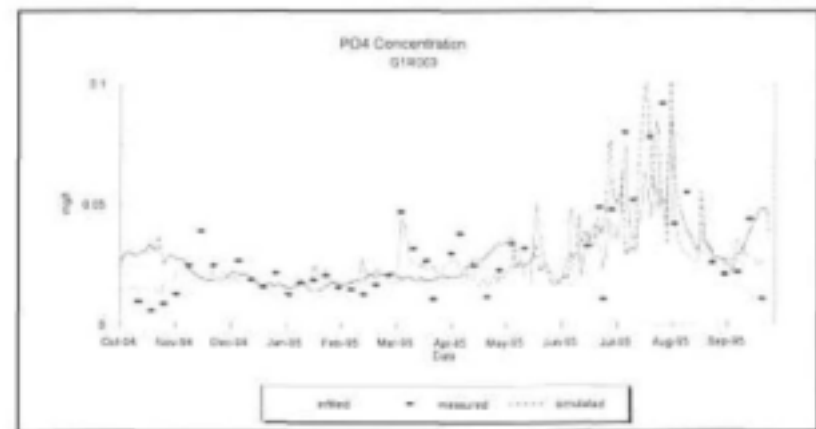


Figure 1.4.56



Temperature (Verification)

Figure 1.4.57

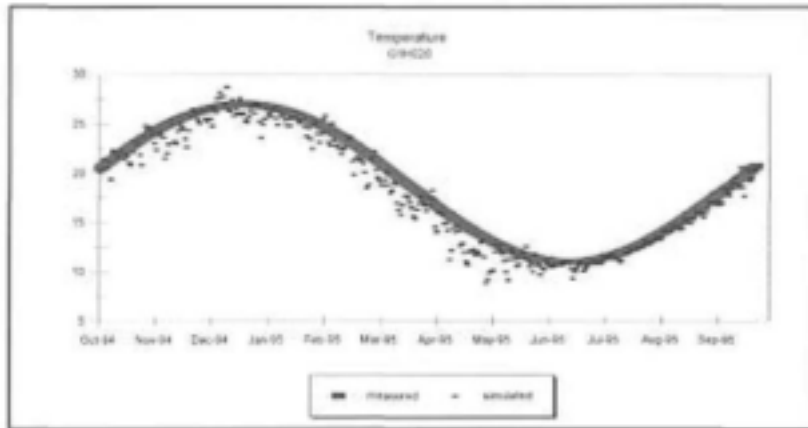


Figure 1.4.59

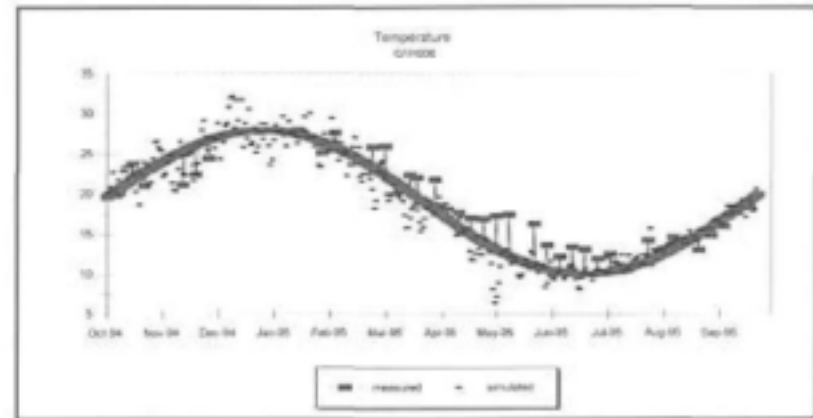


Figure 1.4.58

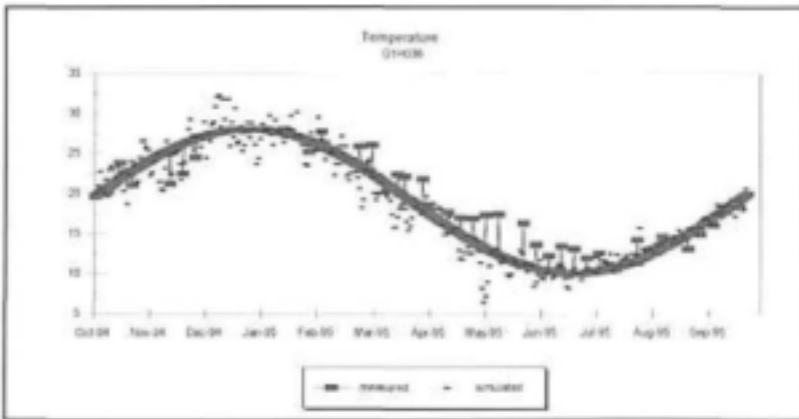
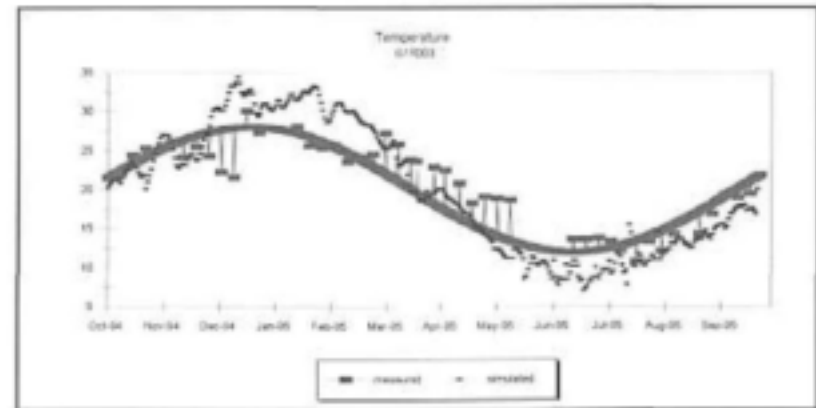


Figure 1.4.60



Oxygen (Verification)

Figure 1.4.61

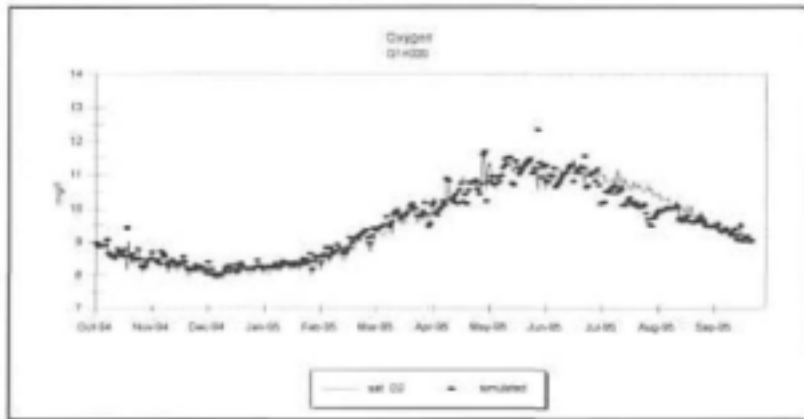


Figure 1.4.63

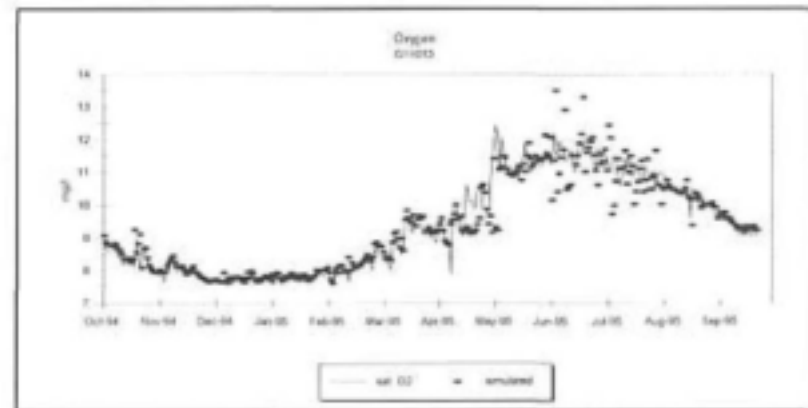


Figure 1.4.62

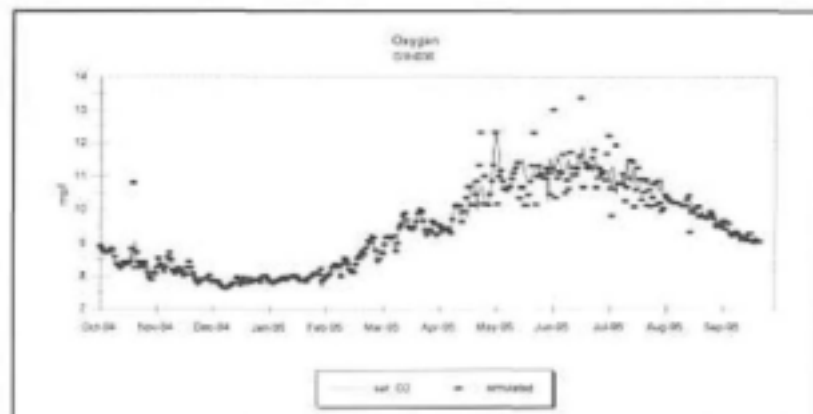
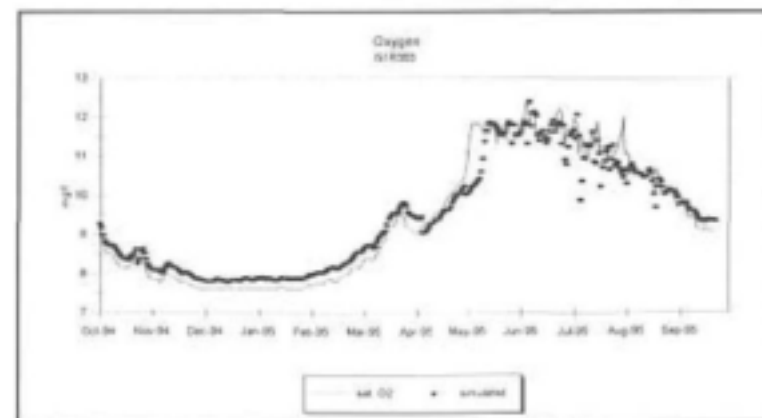


Figure 1.4.64



TDS Loads for low flows (Simulation without ungauged flows)

Figure 1.4.65

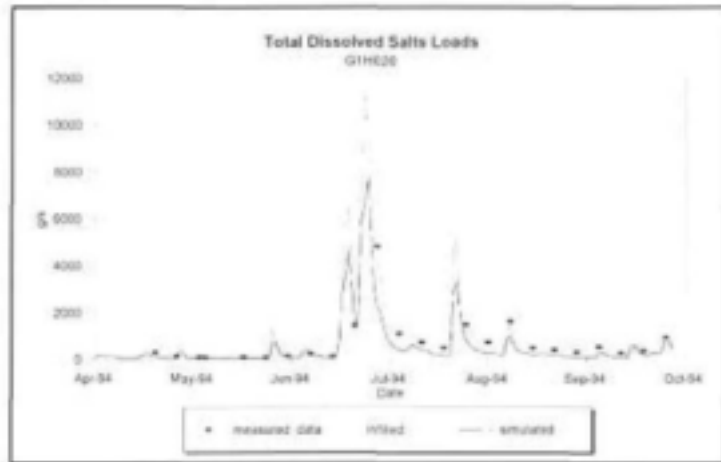


Figure 1.4.67

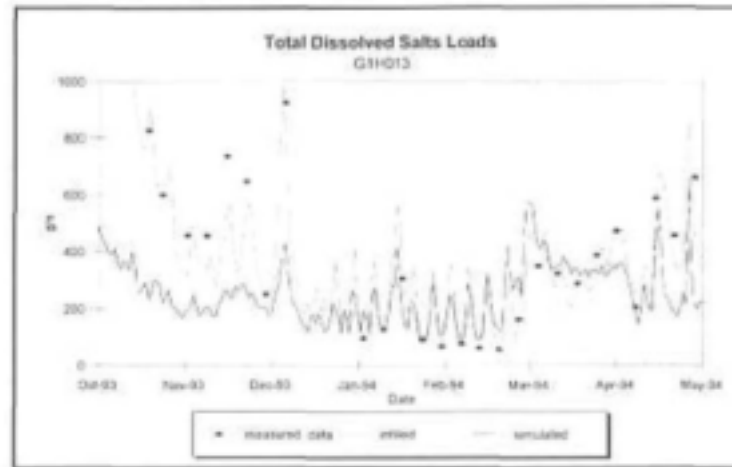


Figure 1.4.66

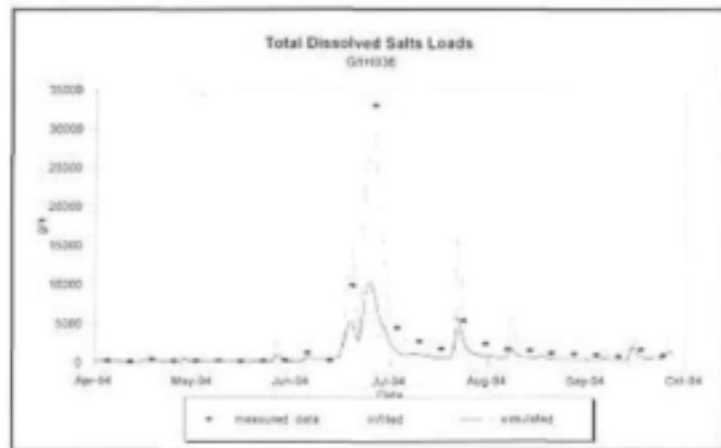
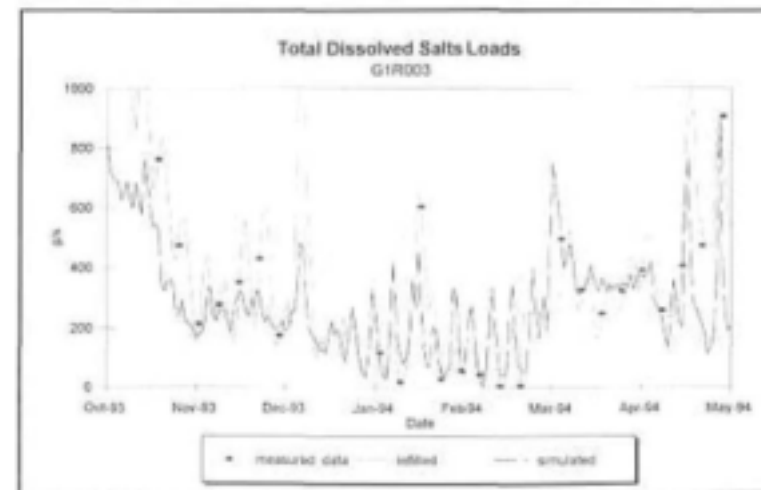


Figure 1.4.68



TDS Loads for high flows (Simulation without ungauged flows)

Figure 1.4.69

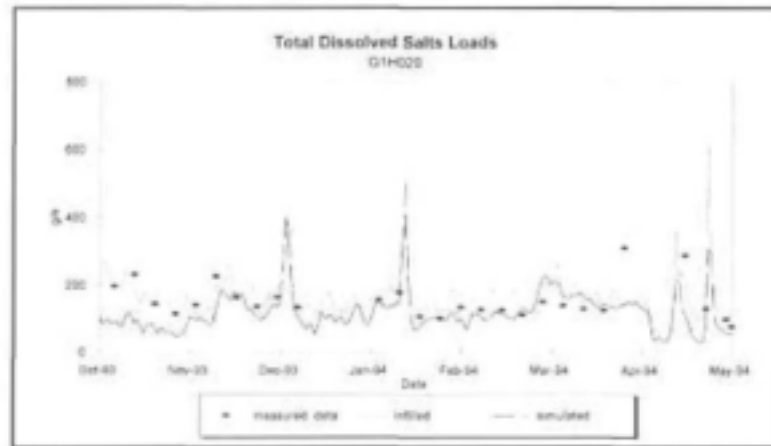


Figure 1.4.71

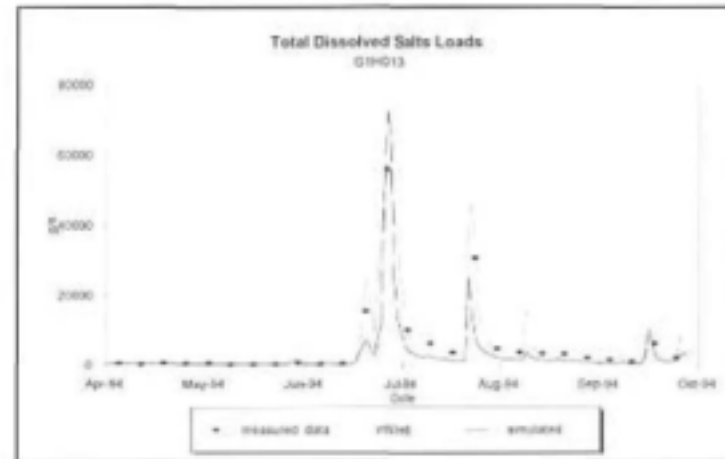


Figure 1.4.70

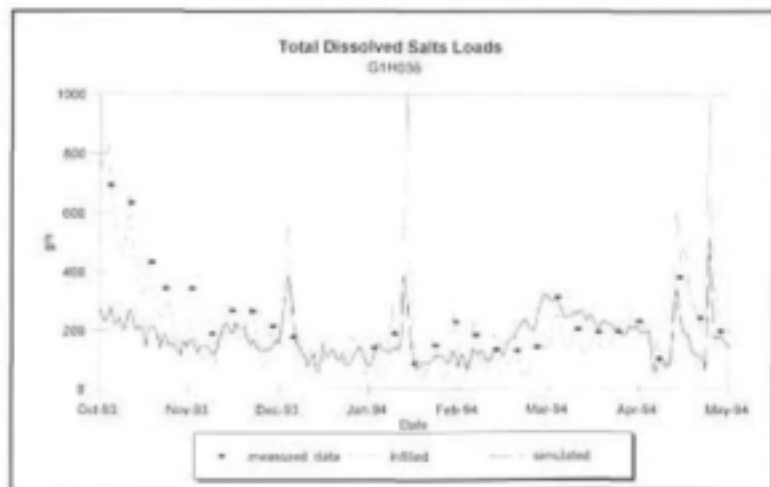
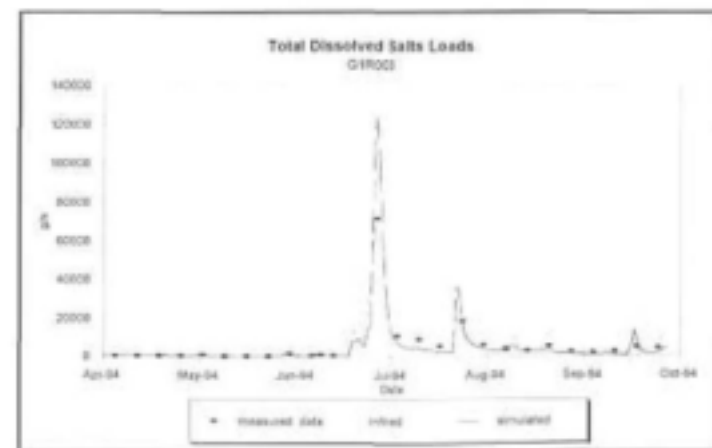


Figure 1.4.72



TDS Concentration (Simulation without ungauged flows)

Figure 1.4.73

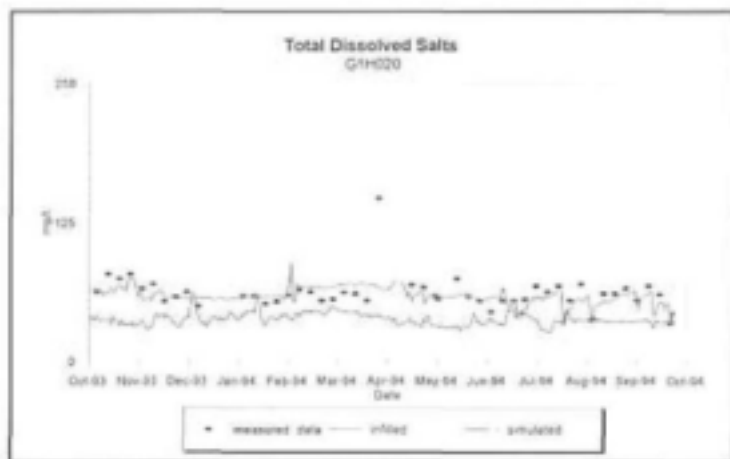


Figure 1.4.75

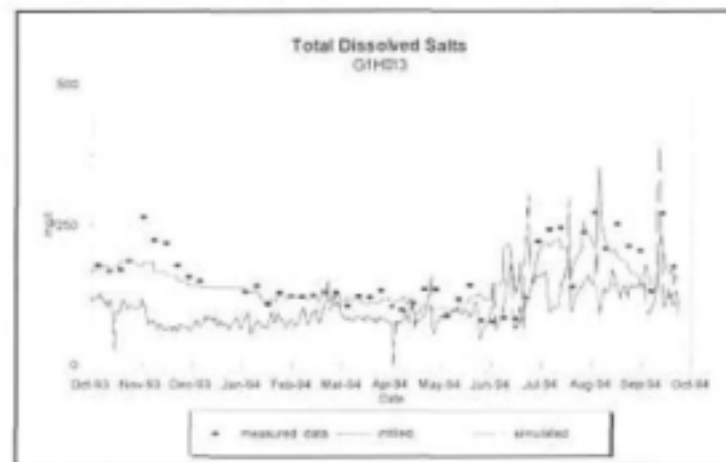


Figure 1.4.74

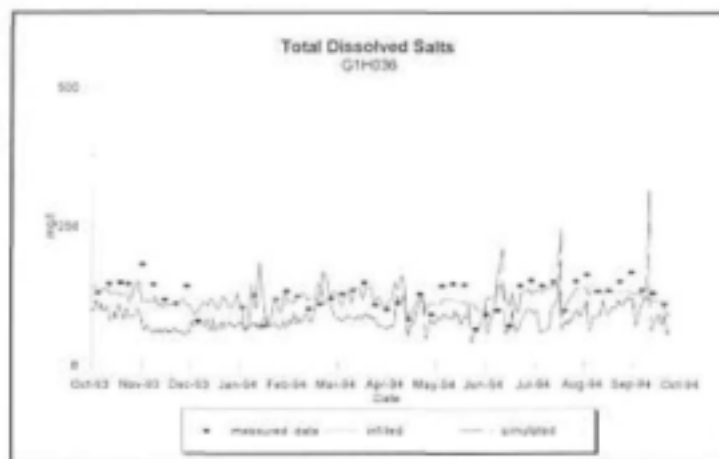
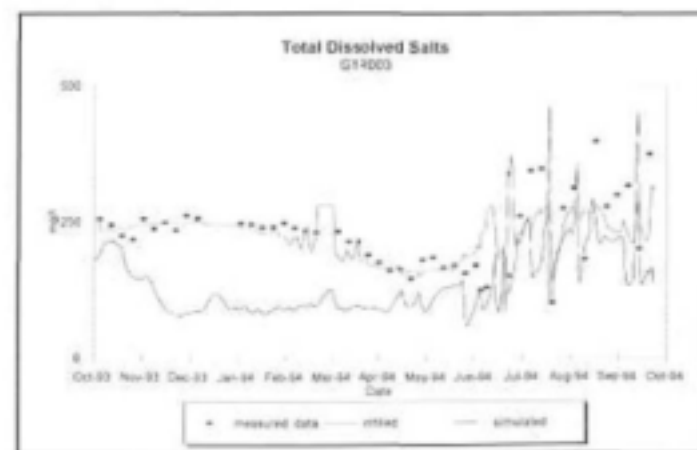


Figure 1.4.76



Phosphate Loads for low flows (Simulation without ungauged flows)

Figure 1.4.77

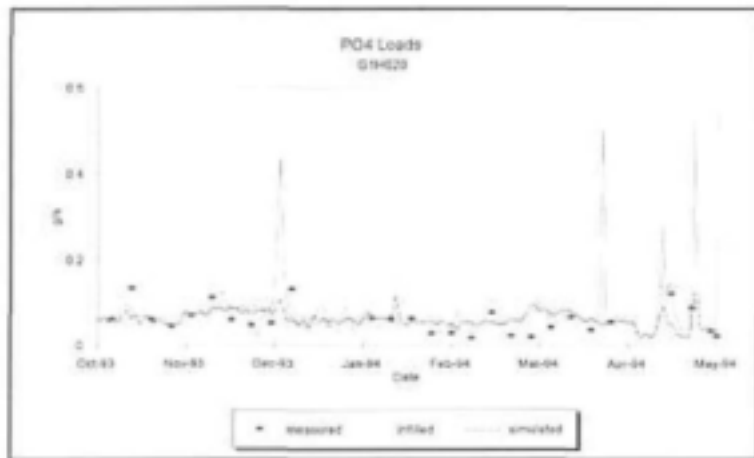


Figure 1.4.79

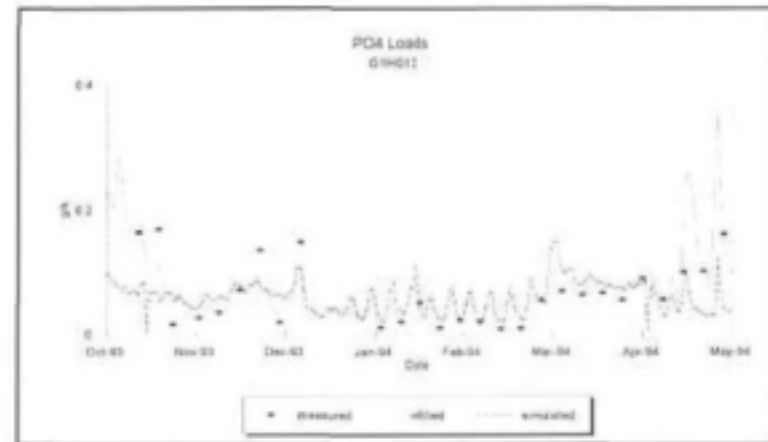


Figure 1.4.78

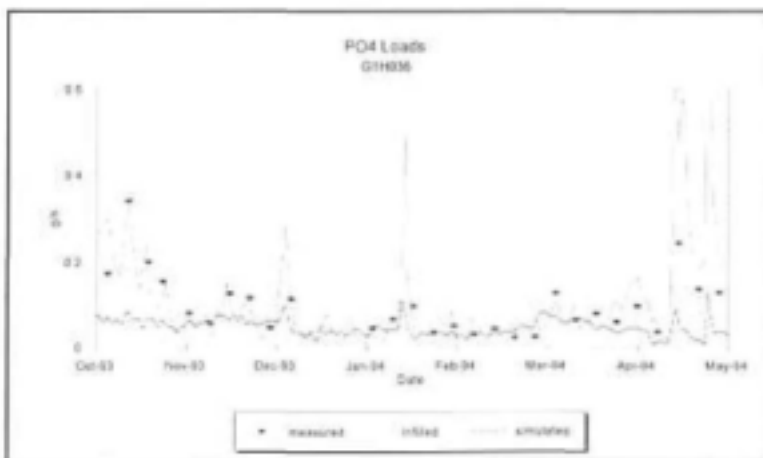
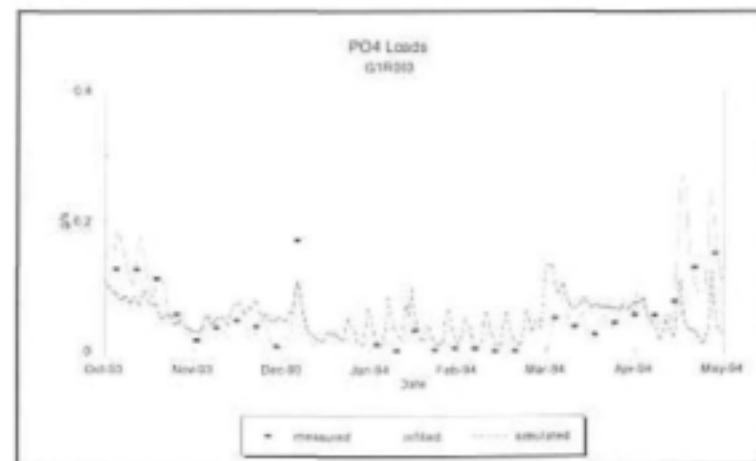


Figure 1.4.80



TDS Loads for high flows (Simulation without ungauged flows)

Figure 1.4.81

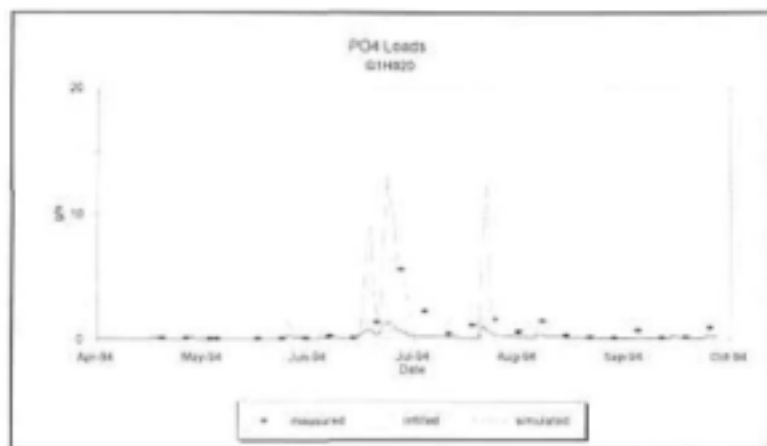


Figure 1.4.83

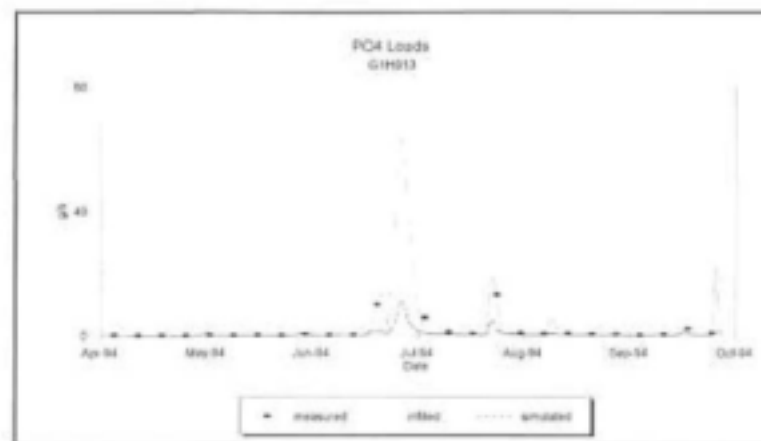


Figure 1.4.82

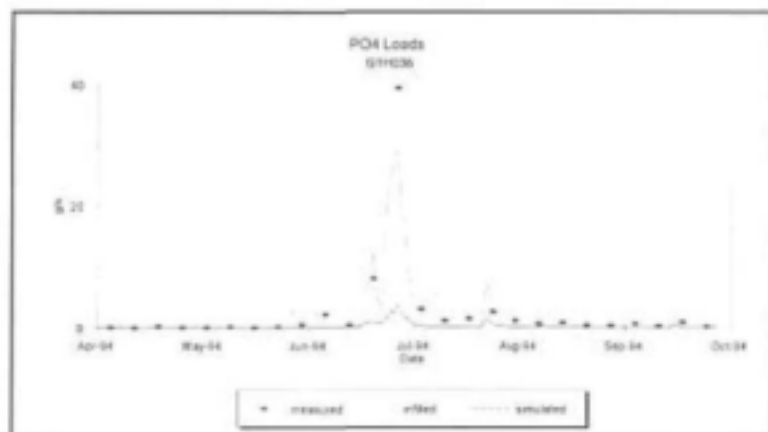
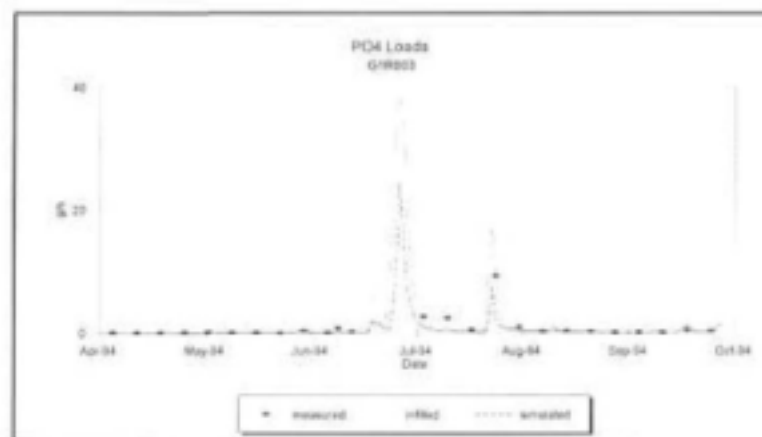


Figure 1.4.84



TDS Concentration (Simulation without ungauged flows)

Figure 1.4.85

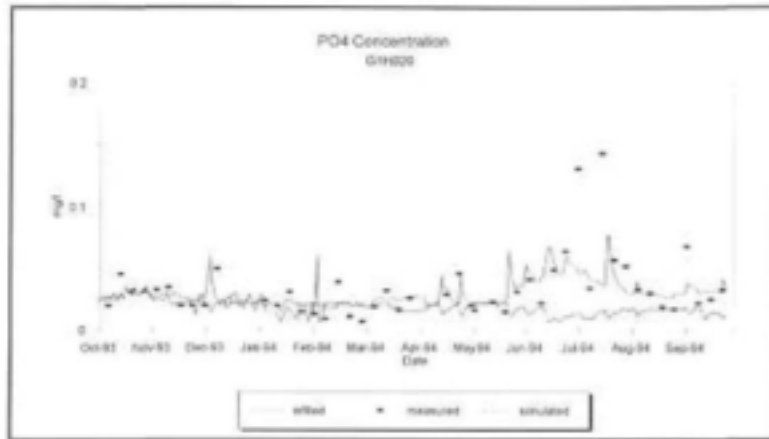


Figure 1.4.87

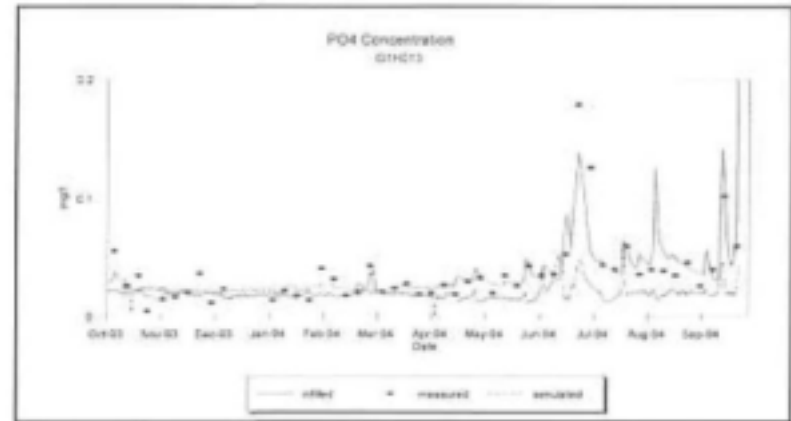


Figure 1.4.86

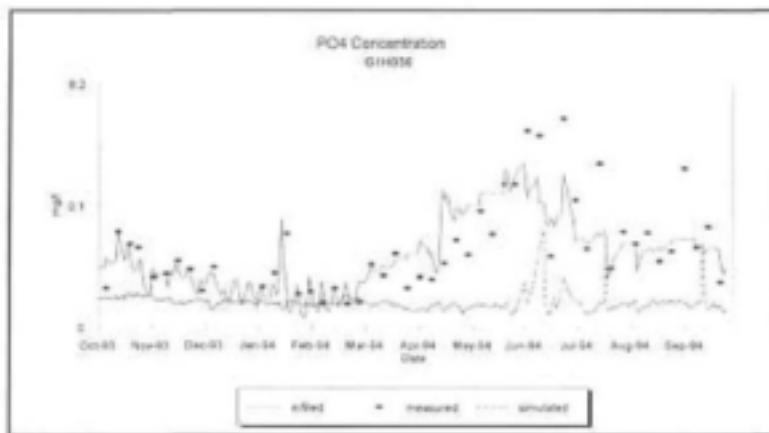
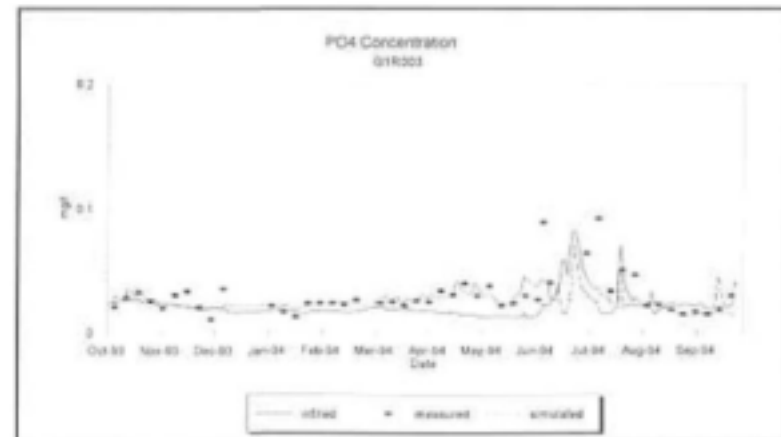


Figure 1.4.88

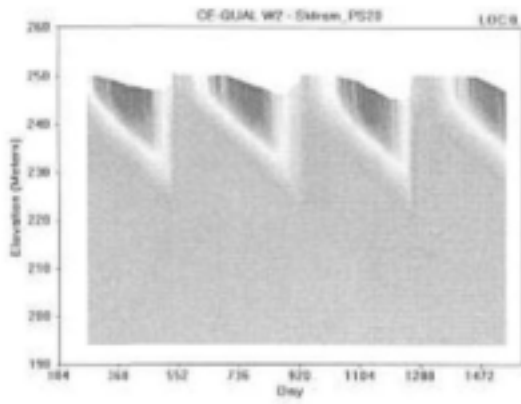


APPENDIX 2.1

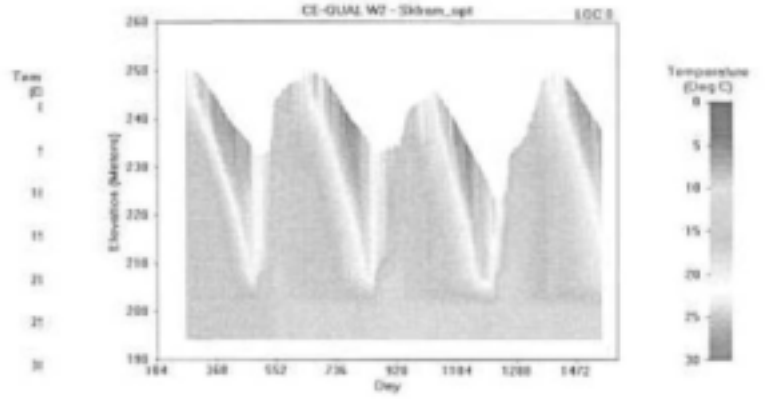
CE-QUAL-W2 : Comparing temperature and dissolved oxygen profiles for the "stratified" and "mixed" scenarios

APPENDIX 2.1 PROPOSED SKUIFRAAM DAM

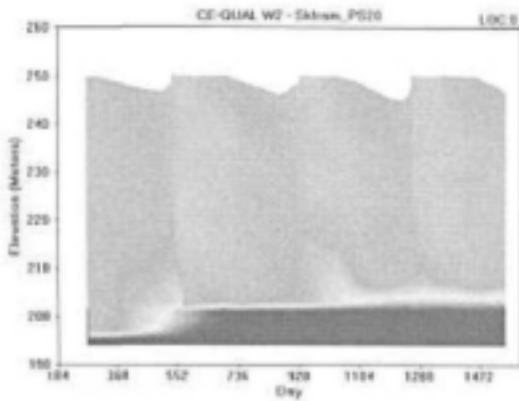
Comparing temperature and dissolved oxygen profiles for the "stratified" and "mixed" scenarios



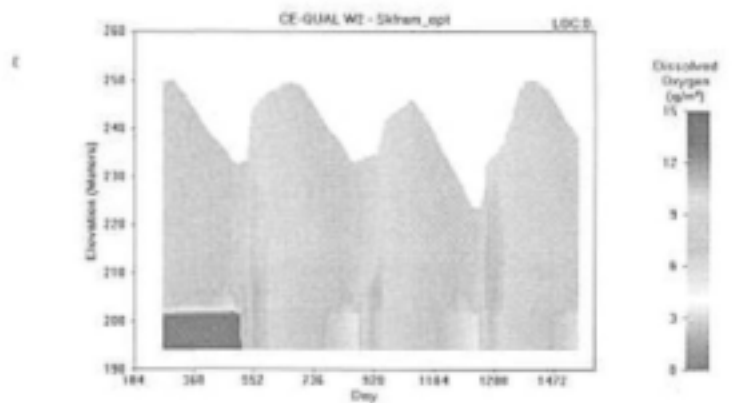
A_s



A_m



B_s



B_m

'Stratified' _s

'Mixed' _m

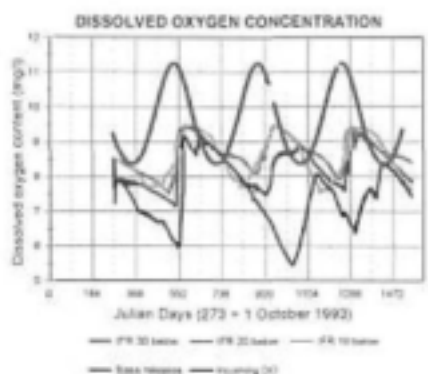
APPENDIX 2.2

CE-QUAL-W2 : Comparing dissolved oxygen and temperature of inflows with that of release

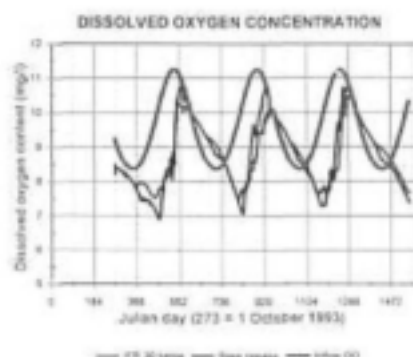
APPENDIX 2.2 PROPOSED SKUIFRAAM DAM

Comparing dissolved oxygen and temperature of inflows with that of the release

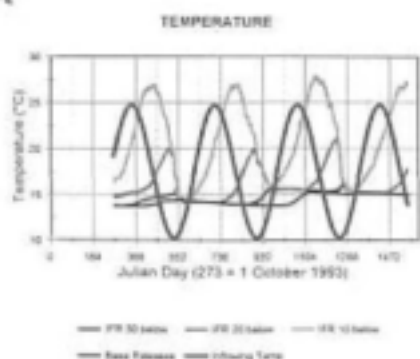
'Stratified' _s



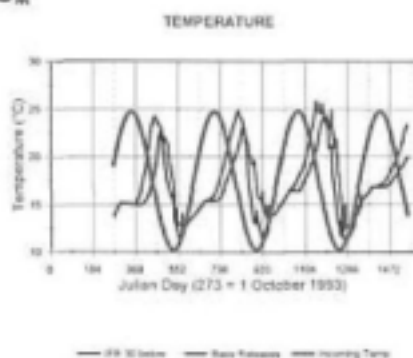
'Mixed' _m



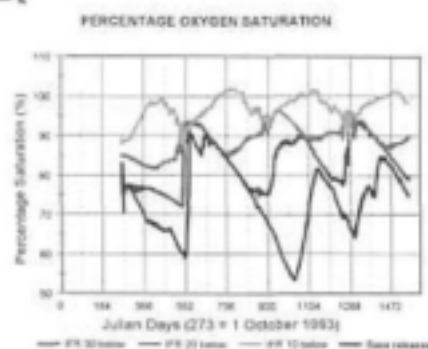
C_s



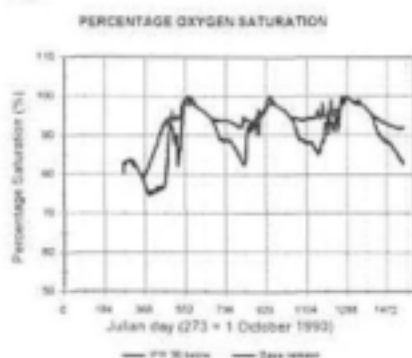
C_m



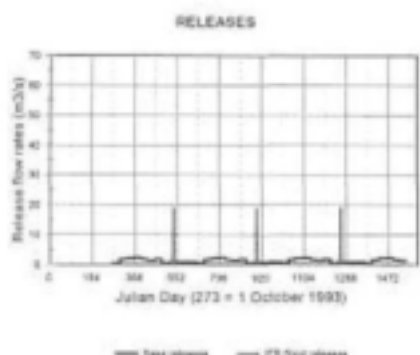
D_s



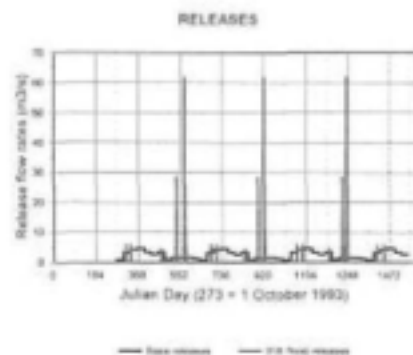
D_m



E_s



E_m



F_s

F_m

APPENDIX 2.3

CE-QUAL-W2 : Operating Rule for the Proposed Skuifraam Scheme

**APPENDIX 2.3
PROPOSED SKUIFRAAM DAM**

**OPERATING RULES FOR THE
PROPOSED SKUIFRAAM SCHEMES**

BASIC OPERATING RULE

To maximise the yield, spillage and evaporation from the system must be minimised. This can be arranged by judicious transfer of water between the Skuifraam and Theewaterskloof Dams. Water can be pumped at a rate of up to 2 m³/s from Skuifraam Dam into Theewaterskloof or released (at the Berg River syphon) at a maximum rate (limited by the valve's capacity) of 6,6 m³/s to flow from Theewaterskloof Dam into Skuifraam Dam.

Skuifraam Dam has a greater propensity to spill than Theewaterskloof, because its storage to MAR ratio is less than that of Theewaterskloof Dam as can be seen in Table 1.

TABLE 1 : STORAGE, MAR CHARACTERISTICS

| DAM | LIVE STORAGE CAPACITY (million m ³) | MAR (million m ³ /a) | STORAGE / MAR RATIO |
|------------------------|---|---------------------------------|---------------------|
| Skuifraam | 122 | 115,6 | 1,1 |
| Skuifraam + Supplement | 122 | 152 * | 0,8 |
| Theewaterskloof | 432 | 265 | 1,6 |

- * Includes a potential transfer of 36,4 million m³/a from the Supplement, although if the Supplement does not pump to spill, then only 25,4 million is actually transferred.

Theewaterskloof can support all the system demands by itself for short periods and it is therefore acceptable for Skuifraam dam to be allowed to become almost empty¹. It was found that maximum yield can be obtained by :

- splitting Theewaterskloof into two operational zones with the lower zone being considered as the "reserve" storage zone. The volume of the upper zone is selected so as to equalise the storage to MAR ratio of Skuifraam and Theewaterskloof's upper zone and then adjusted in order to minimise pumping required whilst not significantly reducing the yield. It was found that a ratio of storage to MAR of 1,1 for Theewaterskloof's upper zone gave the same yield as the case with a storage to MAR of 0,8 and involved less pumping.
- operating the upper zone of Theewaterskloof on an equal drawdown basis with Skuifraam Dam. This means that water is transferred between the two dams with the objective of preserving the integrity of the following equation :

¹ The agricultural releases into the Berg River during January may exceed the syphon's capacity of 6,6 m³/s, so sufficient water to meet the demands should be stored in Skuifraam Dam in the preceding November.

$$\frac{\text{Skuifraam storage volume}}{\text{live storage capacity}} = \frac{\text{Theewaterskloof Upper Zone storage volume}}{\text{live storage capacity}}$$

The volumes and levels associated with the respective zones in Theewaterskloof Dam are as shown in Table 2.

TABLE 2 : ZONES IN THEEWATERSKLOOF DAM

| ZONE | VOLUME OF ZONE (million m ³) | UPPER LEVEL (MSL) | PERCENTAGE OF STORAGE CAPACITY | |
|--------------|---|----------------------|--------------------------------|-------------|
| | | | TOTAL | LIVE |
| Upper | 285 | 308,5 | 59% | 66% |
| Lower | 147 | 301,3 | 31% | 34% |
| Dead storage | 48 | 293,0 | 10% | 0% |
| TOTAL | 480 | | 100% | 100% |